

University of Windsor

Scholarship at UWindor

Electronic Theses and Dissertations

Theses, Dissertations, and Major Papers

2016

Experimental Investigation of Laser Cladding Bead Morphology and Process Parameter Relationship for Additive Manufacturing Process Characterization

Syed Mohammad Saqib
University of Windsor

Follow this and additional works at: <https://scholar.uwindsor.ca/etd>

Recommended Citation

Saqib, Syed Mohammad, "Experimental Investigation of Laser Cladding Bead Morphology and Process Parameter Relationship for Additive Manufacturing Process Characterization" (2016). *Electronic Theses and Dissertations*. 5782.

<https://scholar.uwindsor.ca/etd/5782>

This online database contains the full-text of PhD dissertations and Masters' theses of University of Windsor students from 1954 forward. These documents are made available for personal study and research purposes only, in accordance with the Canadian Copyright Act and the Creative Commons license—CC BY-NC-ND (Attribution, Non-Commercial, No Derivative Works). Under this license, works must always be attributed to the copyright holder (original author), cannot be used for any commercial purposes, and may not be altered. Any other use would require the permission of the copyright holder. Students may inquire about withdrawing their dissertation and/or thesis from this database. For additional inquiries, please contact the repository administrator via email (scholarship@uwindsor.ca) or by telephone at 519-253-3000ext. 3208.

**Experimental Investigation of Laser Cladding Bead Morphology and Process
Parameter Relationship for Additive Manufacturing Process Characterization**

By

Syed Mohammad Saqib

A Dissertation
Submitted to the Faculty of Graduate Studies
through the Department of Industrial and Manufacturing Systems Engineering
in Partial Fulfillment of the Requirements for
the Degree of Doctor of Philosophy
at the University of Windsor

Windsor, Ontario, Canada

2016

© 2016 Syed Mohammad Saqib

**Experimental Investigation of Laser Cladding Bead Morphology and Process
Parameter Relationship for Additive Manufacturing Process Characterization**

by

Syed Mohammad Saqib

APPROVED BY:

Dr. Allan. D. Spence (External Examiner)
Mechanical Engineering
McMaster University, Hamilton, ON, Canada

Dr. Faouzi Ghib (External Reader)
Civil and Environmental Engineering

Dr. Michael Wang
Mechanical, Automotive and Materials Engineering

Dr. Ahmed Ismail Azab
Mechanical, Automotive and Materials Engineering

Dr. Ruth Jill Urbanic, Advisor
Mechanical, Automotive and Materials Engineering

May 27, 2016

DECLARATION OF CO-AUTHORSHIP/PREVIOUS PUBLICATION

I. Co-Authorship Declaration

I hereby declare that this thesis incorporates material that is result of joint research, as follows:

This thesis incorporates the outcome of joint research undertaken in collaboration with Syed Saqib and Kush Aggarwal under the supervision of Dr. Ruth Jill Urbanic. The collaboration with Kush Aggarwal is covered under the sub-section of chapter 5. In the end of the thesis, collaboration with Mohammad Alam and Dr. A. Edrisy was undertaken and is covered in the Summary Section of Chapter 7. In all cases, the key ideas, primary contributions, experimental designs, data analysis and interpretation, were performed by the author. The contribution of co-authors was primarily through the provision of comments, suggestions and recommendations.

I am aware of the University of Windsor senate policy on Authorship and I certify that I have properly acknowledged the contribution of other researchers to my thesis, and have obtained written permission from each of the co-author(s) to include that material(s) in my thesis.

I certify that with the above qualification, this thesis and the research to which it refers to, is the product of my own work.

II. Declaration of Previous Publication

This thesis includes excerpts, citations and partial sections from the papers that have been previously published /submitted for publication in peer reviewed journals, as follows:

Publication title/full citation	Publication Status
S. Saqib, R. J. Urbanic and K. Aggarwal., "Analysis of laser cladding bead morphology for developing additive manufacturing travel paths." Proceedings of the 47 th CIRP conference on Manufacturing Systems. vol. 17, 2014, pp.824-829, DOI: 10.1016/j.procir.2014.01.098	Published
Aggarwal. K, Urbanic. J and Saqib. S., "Development of predictive models for effective process parameter selection for single and overlapping laser clad bead geometry," Rapid Prototyping Journal, RPJ-04-2016—0059.	Submitted
Aggarwal. K, Urbanic. R. J, and Saqib. S., "Identifying relative importance of the input parameters for developing predictive model for laser cladding process." Proceedings of ASME-2014 International Mechanical Engineering Congress and Exposition. Montreal, Canada. 2014, vol. 2A pp. 12 pages. DOI: 10.1115/IMECE2014-37719	Published
Urbanic. R. J, Saqib. S and Aggarwal. K., "Using predictive modeling and classification methods for single and overlapping bead laser cladding to understand bead geometry to process parameter relationships." Journal of Manufacturing Science and Engineering. 2016, 138(5). DOI:10.1115/1.4032117	Published
Saqib. S and Urbanic. R. J., "Investigation of the transient characteristics for laser cladding beads using 420 stainless steel	Submitted

powder.” Journal of Materials Science and Technology.	
Saqib. S and Urbanic. J., “An experimental study to determine geometric and dimensional accuracy impact factors for fused deposition modeled parts.” Proceedings of the 4 th International Conference on Changeable, Agile, Reconfigurable and virtual production (CARV 2011), Montreal, Canada, 2-5 Oct 2014. pp. 293-298. DOI: 10.1007/978-3-642-23860-4	Published
Mohammad. A, Urbanic. J, Saqib. S and Edrisy. A., “Effect of process parameters on the microstructural evaluations of laser clad 420 martensitic stainless steel.” Proceedings on Materials Science & Technology (MS&T-2015), Oct 4-8, OH, USA	Published

I declare that I have obtained written permission from the copy right owner(s) to include the above published material(s) in my thesis in appendix A. I certify that the above material describes work completed during my registration as graduate student at the University of Windsor.

I declare that, to the best of my knowledge, my thesis does not infringe upon anyone’s copyright nor violate any proprietary rights and that any ideas, techniques, quotations, or any other material from the work of other people included in my thesis, published or otherwise, are fully acknowledged in accordance with the standard referencing practices. Furthermore, to the extent that I have included copyrighted material that surpasses the bounds of fair dealing within the meaning of the Canada Copyright Act, I certify that I have obtained a written permission from the copyright owner(s) to include such material(s) in my thesis and have included copies of such copyright clearances to my appendix.

I declare that this is a true copy of my thesis, including any final revisions, as approved by my thesis committee and the Graduate Studies office, and that this thesis has not been submitted for a higher degree to any other University or Institution.

ABSTRACT

During the past two decades, basic and applied research has led to an in-depth understanding of the cladding process as well as to a variety of potential applications. Industry had been reluctant to adopt this technology mainly due to high investment costs, and the unpredictable and nonlinear behavior of the process. However, the repair and refurbishment sector of production engineering is flourishing. Most engineering applications require high strength and corrosion resistant materials for long term reliability and performance of the components; consequently, laser cladding (LC) has been explored as a viable solution for an additive manufacturing (AM) approach.

Laser cladding is one of the material AM processes used to produce a metallurgically well-bonded deposition layer and now it has been integrated into the industrial manufacturing lines to create a quality surface. To obtain a desired-quality resulting part, a deep understanding of the process mechanisms is required since laser cladding is a multiple-parameter-dependent process. Developing a bead shape to process parameter model is challenging due to the nonlinear and dynamic nature of the LC environment. This introduces unique predictive modeling challenges for both single bead and overlapping bead configurations.

A set of cladding experiments have been performed for single and multiple bead scenarios, and the effects of the transient conditions on the bead geometry for these scenarios have been investigated. It is found that the lead-in and lead-out conditions differ, corner geometry influences the bead height, and when changing the input power levels, the geometry values oscillate differently than the input pulses. The dynamic, time varying heating and solidification, for multiple layer scenarios, leads to challenging process planning and real time control strategies.

Models are developed for single and overlapping beads using the analysis of variance (ANOVA) and Generalized reduced gradient (GRG) approach along with regression analysis to determine the process trends and the best modeling approaches. Since laser cladding (LC) process has potential to make 3D components; determination of the fill volume for the ‘near net shape’ and the appropriate fill rate is the primary challenge. Although the additive approach reduces many issues related to process planning, there are still issues related to accuracy, surface finish, and build time that require improvement.

DEDICATION

To my mother and wife,

For their sacrifice, encouragement and patience.

ACKNOWLEDGEMENTS

I would like to thank the one who made this dissertation possible, my sincere appreciation and gratitude to my academic supervisor, Dr. Ruth Jill Urbanic, who provided continuous motivation and support in helping me to successfully finish my research work during my PhD program. A special recognition for her in-depth knowledge, enthusiasm and perfection in my research area. My ambitions grew more to perform this novel work for my dissertation under her supervision. Dr. Urbanic, a mentor and a friend, who was always available for consultation throughout the tenure of this journey.

I express my appreciation to my committee members, Dr. Fouzi Ghrib, Dr. Michael Wang and Dr. Ahmed Azab for their time and patience taken to review my dissertation and provided valuable suggestions time to time. Dr. Wang's design of experiment course was so beneficial and helped me in conducting my experiments efficiently. The essence of 3D modeling and drafting was well understood through Dr. Azab's CAD course, which broadened the concept of model designing with theoretical background.

The final smooth written dissertations may cause to forget the unsmooth passed path of the research behind it, and to forget the role of other people in their generation. With that, I would like to thank and extend my appreciation to Mr. Robert Hedrick, president of Camufacturing, who taught me the programming and tool path generation in CAM environment and his ongoing support to help me. I am grateful to all faculty and staff of Industrial and Manufacturing Systems Engineering Department (IMSE), in particular Dr. Waguih ElMaraghy and Dr. Hoda ElMaraghy for their help and administrative support. I would also like to thank Mohammad Alam, Andy Jenner and Ram Barakat for helping in expediting the experiments.

I would also like to thank the Industrial Partner for using their resources and on-site technical help in conducting the experiments successfully on time. Many thanks to Ontario Center of Excellence (OCE) for financially supporting this research project through the collaborative research funding program.

Lastly, I would like to thank my mother and brother for helping me realizing my own potential and their continuous moral support. Of course, above all, I have received enormous loving support from my immediate family; wife and three children for their day and night motivation, patience and unconditional help.

TABLE OF CONTENTS

DECLARATION OF CO-AUTHORSHIP/PREVIOUS PUBLICATION	iii
ABSTRACT	v
DEDICATION	vi
ACKNOWLEDGEMENTS	vii
LIST OF TABLES	xi
LIST OF FIGURES	xii
LIST OF APPENDICES	xvii
LIST OF ABBREVIATIONS/ACRONYMS	xviii
NOMENCLATURE	xxi
Chapter 1	1
General Introduction	1
1.1 Background	1
1.2 Additive Layered Manufacturing Processes (ALM).....	2
<i>1.2.1 ALM Categories, Processes and Materials</i>	4
1.3 Laser Cladding Process (LC) and Applications	6
<i>1.3.1 Advantages and Dis-advantages of Laser Cladding</i>	8
1.4 Motivation and Research Objectives	9
<i>1.4.1 Motivation</i>	9
<i>1.4.2 Thesis Objective</i>	10
<i>1.4.3 Limitations</i>	12
1.5 Outline of the Dissertation	12
Chapter 2	14
Literature Review	14
2.1 Introduction.....	14
2.2 Rapid Prototyping Methods and Hybrid Approach	15

2.3 Laser Cladding and Other Conventional Methods.....	16
2.4 Mathematical Modeling of Bead Geometry and Build ups	18
2.5 Process Planning in Manufacturing Processes.....	20
2.6 Summary	22
Chapter 3	30
Process Overview: Laser Cladding: State-of-the-Art.....	30
3.1 Laser Cladding Method and Other Laser Surface Treatments.....	30
3.2 Laser Cladding (LC) versus Selective Laser Sintering (SLS)	33
3.3 Effects of Process Parameters on Clad Layer Geometry	34
3.4 Feedback Control System in LC	39
Chapter 4	41
Experimental Methodology	41
4.1 Experimental Design and Methodology	41
4.1.1 <i>Experimental Design Parameters</i>	44
4.1.2 <i>Central Composite Design (CCD)</i>	45
4.1.3 <i>Experimental Design Matrix for Single Bead Experiments</i>	47
4.2 Cladding Material and Measurement Technique	49
4.2.1 <i>Sample Preparation Process and Post-processing</i>	51
4.3 Overlaps Bead Experiments (40 %, 50% and 60% overlaps).....	53
4.4 Multiple Beads and Layers Stacking Conditions.....	56
4.5 Laser Power Step Function Based Transient Heat Conditions	60
4.6 Single Bead Corner Configurations (Acute, Right and Obtuse Angled)	65
4.7 Cladding with Lead-in and Lead-out Situation.....	66
4.8 Building 3D Geometry and CT Scanned the Models	68
Chapter 5	71
Experimental Results and Derived Models	71
5.1 General Observations in Single Bead Experiments	72
5.2 Predictive Models using ANOVA and GRG Approaches	79
5.3 Percentage Overlapping Bead Analysis.....	85
5.3.1 <i>The ANOVA Model for Overlapping Conditions</i>	90

5.3.2 <i>Overlap Results and Modeling using Artificial Neural Network (ANN)</i>	92
5.4 Multilayer Beads Analysis and Modeling.....	95
5.5 Transient Heat Conditions Analysis	103
5.6 Standard Process Transient Condition Analysis	112
5.6.1 <i>Bead Corners Configurations Analysis</i>	112
5.6.2 <i>Lead-in and Lead-out Situation Analysis</i>	114
5.6.3 <i>Analysis of CT Scanned Models</i>	118
Chapter 6	120
Process Planning and Associated Challenges	120
6.1 Process Planning in Additive and Subtractive Manufacturing (Machining).....	121
6.2 Process Planning in Hybrid Manufacturing	124
6.3 Tool Path Planning in Laser Cladding Process.....	126
Chapter 7	131
Summary and Conclusion	131
7.1 Summary	131
7.2 Conclusion	133
Chapter 8	138
Future Work	138
REFERENCES	141
APPENDICES	151
VITA AUCTORIS	173

LIST OF TABLES

Table 1. Critical Literature Review Summary	24
Table 2. Properties of clad layers.....	32
Table 3. Surface modification process.....	32
Table 4a. The static parameters used for the experiments	44
Table 4 b. The experimental design parameters and their levels	44
Table 5. Experimental Configurations generated for sample collection.....	48
Table 6. Equipment used for the experiments.....	51
Table 7. Measurements of each layer (Figure 27) are shown	59
Table 8. Transient heat experiments with the power varying	60
Table 9. Evaluation of the average and standard deviation for each shape parameter using the complete experiment set	72
Table 10. Evaluation of the average values of the observed ‘standard deviations’ for each shape parameter-experiment set.....	75
Table 11. Evaluation of the mean and standard deviations for the shape parameters for the constant mass transfer per unit length experimental conditions (0.033 grams/mm).....	75
Table 12. Significant factors for response variables	83
Table 13. A summary of the modeling results	83
Table 14. Comparison for theoretical and actual bead heights	97
Table 15. Slopes of the single bead shape geometrical values and their differences among their sections.....	106
Table 16. Slopes of the bead heights in 3x4 stacks and their differences among their sections.	109
Table 17. Ranges and Standard Deviations are shown for thickness data	119
Table 18. Comparison in geometry between CAD model and clad models	119
Table 19. Comparison of CAD model and the clad model	130

LIST OF FIGURES

Figure 1. Different methods of additive layered manufacturing processes.....	3
Figure 2. AM categories, processes and material types are shown.....	5
Figure 3. A schematic diagram of the laser cladding process (adapted from [11])	7
Figure 4. Application of laser clad areas [13-14].....	8
Figure 5. Position of RP and CNC process in terms of their characteristics [29].....	16
Figure 6. Trend of publication on process planning over the last 14 years.....	21
Figure 7. A schematic view of the laser cladding process (adapted from [121]).....	31
Figure 8. Inputs, processes and outputs parameters are shown with powder injection laser cladding.....	33
Figure 9. A schematic of Selective Laser Sintering process (SLS)[adapted from[122]	34
Figure 10. Cross section view of a single bead notation.....	35
Figure 11. Cross section view of an experimental sample.....	36
Figure 12. Different bead cross sections showing the impact of varying process parameters.....	36
Figure 13. Schematic cross section of a clad layer	38
Figure 14. Cross section views of the clads a) low dilution (9.0 %) and b) high dilution (48 %) values are shown.....	39
Figure 15. Schematic overview of laser cladding with camera control system	40
Figure 16. General model of a process or system [adapted from (123)].....	41
Figure 17. Flow chart of the experimental plan for this research	43
Figure 18. a) CCD demonstration (8-end points, 6 axial points and 1 center point), b) CCD parameters used for this research (generated by Mini Tab).....	46
Figure 19. Laser Cladding work cell utilized for this research [Courtesy to industrial partner]....	49
Figure 20. a) A coaxial nozzle with a visible laser spot size used for the experiments b) section view of the nozzle [courtesy of the industrial partner]	50
Figure 21. a) Single bead sample is being prepared b) Single bead is shown in 3.0 inches length [Courtesy of the industrial partner].....	50
Figure 22. a) Sample mounting machine b) Three mounted samples at a time	51
Figure 23. Optimal Microscope attached with computer.....	52
Figure 24. Deviation in the height and penetration is shown for a bead with replicates (pixel units)	52

Figure 25. Process flow diagram of samples preparation	53
Figure 26. Sectioned views of 3-passes a) 40 % overlap b) 50% overlap and c) 60% overlap beads	54
Figure 27. Schematic of cross sections of a 3-bead overlap formation	55
Figure 28. Sequence of the multi-layer experiments; characterized with the type of the substrate	56
Figure 29. Cross sectioned views of one, two, three and five layers	57
Figure 30. a) Circular sample of a 10-layers clad b) EDM cut piece-polished and etched c) Macrograph view of 10-layers with individual layer heights are shown in mm.	58
Figure 31. Comparison of heights in 10 layers and 25 layers samples	59
Figure 32. The processing steps used in the transient heat conditions experiments	61
Figure 33. a) Graph shows the variation in bead width over 15 sec period b) Longitudinal section view of the transient bead with 3kW-4kW-3kW power	62
Figure 34. Stepping condition with 3-beads overlap a) Full length clad sample (top view) and cut through the middle b) Cross sectional view of the 50% overlap beads.	63
Figure 35. a) Graph shows the variation in bead width over 15 sec period (6" in length) b) Longitudinal section view of the middle bead of the 3-bead sample.....	63
Figure 36. a) Longitudinal EDM cut of the 3x4 bead stack sample b) Cross section views of all three sections—each view contains four layers of stack--enlarged view is also shown.	64
Figure 37. Single bead samples with different configurations a) Obtuse angled b) Right angled c) Acute angled	65
Figure 38. Three different sectioned views of obtuse angled configuration using Figure 34a.	66
Figure 39. Track in/track out is shown for the circular coating on a round steel substrate [80]....	67
Figure 40. Cross section view of a single bead a) Lead in and b) Lead out situations	68
Figure 41. Models made using laser cladding method a) b) CAD models c) Hollow cone model d) Parabolic shape model	69
Figure 42. CT scanned views of a) The hollow cone and b) The sectioned parabolic model-All dimensions are in mm	70
Figure 43. Data analysis and modeling approaches	71
Figure 44. Experimental data histogram for the height and penetration shape parameters using the complete experimental set.....	73

Figure 45. The 3D graphical representation illustrates the effect of process parameters on the response output. The effect of laser power and the nozzle speed on a) the bead height b) the bead width and c) the penetration. All other factors were kept constant.....	74
Figure 46. Width versus power when there is a constant FR to LS ratio (note: the CTWD and FL values vary).....	76
Figure 47. Width versus FL relationship when there is constant FR to LS ratio (note: the CTWD and power values vary).	76
Figure 48. Width versus FR relationship (note: all parameters vary)	77
Figure 49. Positive bead Area versus CTWD (all other values vary).....	77
Figure 50. Positive bead Area versus laser speed (all other values vary)	78
Figure 51. Height versus Power (all other values vary).....	78
Figure 52. Bead width model results versus observed data a) when applying a Log10 data transformation on the input parameters b) using the ANOVA model	85
Figure 53. Schematic of a 50 % overlap beads	85
Figure 54. (a) Predicted overlapping bead width geometry versus observed bead width geometry, (b) Standard Deviations, and (c) Range	87
Figure 55. The average penetration and height changes with the percentage overlap and representative bead with 60% overlap illustrating the height and penetration variations per bead	87
Figure 56. The average penetration and height changes with the percentage overlap	89
Figure 57. The penetration variations based on the bead deposition order and percentage overlap	89
Figure 58. The R^2 values for the bead width for the overlapping bead experiment set	90
Figure 59. The R^2 values for the bead height for the overlapping bead experiment set	91
Figure 60. The R^2 values for the bead penetration for the overlapping bead experiment set	91
Figure 61. Cross section view of 3-beads with 50% overlap; measurements are also shown	92
Figure 62. Neural network architecture for generating an overlap bead pass model	93
Figure 63. Regression plot for the ANN network.....	94
Figure 64. (a) Width, (b) Height, (c) Penetration, (d) Dilution (red is the experimental data, blue is the predicted/network output data) [119]	95
Figure 65. a) Theoretical height of 10-layers b) Experimental/measured height of 10-layers sample c) Schematic diagram shows that CTWD changes with the bead height d) 25-layers sample shows the total height	96
Figure 66. The height and width of the 10-layer sample	97

Figure 67. Section view of stacked sample (3x4 beads)	98
Figure 68. Bead height vs. CTWD (from the steady state experiments presented in Table 4).....	98
Figure 69. Height difference between the expected and real height of the 10-layer sample	99
Figure 70. Curve fitting between the deposited layers and the corresponding height, residuals are also shown.....	100
Figure 71. Trend in bead height with respect to the individual layers deposited and their residuals are also shown.....	101
Figure 72. Trend in bead height with respect to the 50-layers deposition and their residuals	102
Figure 73. The instantaneous melt pool width variations (10 mm/sec travel speed).	103
Figure 74. Average bead width for the step intervals, where the overall average width for the 2.6kW level = 2.89 mm, and the average width for the 3.6kW power level = 3.95 mm.	104
Figure 75. a) Segmented view of the height and penetration of the single bead transient layer b) Segmented bead width in each section.	105
Figure 76. a) Longitudinal transition sample show the variations in height and penetration in sections, star symbols indicates the average height and penetration in each section b) Segmented bead width.....	107
Figure 77. a) Transition sample of 3x4 stack shows the variations in height and penetration b) Segmented views of the i) First bead ii) Second bead and iii) Third bead of the 3 x 4 bead stack.	109
Figure 78 . Bead width is shown for 12 beads (3x4 stack) in different stable regions	110
Figure 79. Width comparison of 50% overlap beads and 3x4 bead stack	111
Figure 80. Height comparison between theoretical and actual bead heights	112
Figure 81. The bead geometry variations a) height b) width and c) penetration) based on the bead deposition flow direction and different cornering configurations.....	113
Figure 82. Standard deviations in single bead height, width and penetration are shown	114
Figure 83. Deposited bead profile in the beginning (lead-in) and in the end (lead-out) of a single track	115
Figure 84. Bead heights varies in lead-in and lead-out situations a) Single bead b) overlap bead c) 1st bead section of 3x4 stack d) 2nd bead section of 3x4 stack and e) 3rd bead section of 3x4 stack.	117
Figure 85. Thickness variation (bottom to top) for a) The cone and b) The parabolic model is shown.....	118
Figure 86. Cladded models made with layer by layers	120

Figure 87. Flow of the additive and subtractive manufacturing processes	122
Figure 88. Subtractive manufacturing process and associated machining operations are shown on a CAD model (2 hr-22 min).....	123
Figure 89. A stack of 2D is shown for CAD model (shown in Fig. 88)	124
Figure 90. a) b) Models made using metal bead deposition process [128-129] c) A cladded componenet with half machined	125
Figure 91. CAD model shown (in extruded layers) using commercial CAD program.....	126
Figure 92. Process planning process flow for laser cladding process [1]	127
Figure 93. a) A rectangular block is build up with bottom up layers, Note the ‘dish’ in the center region. b) Start-stop phenomenon encircled and cornering condition boxed in the cladded model [6].....	128
Figure 94. i) A CAD model ii) Tool path is being generated iii) The Cladded model	129
Figure 95. a) Measurement of micro hardness of a bead b) Variation in micro hardness in four different zones of the bead with three power levels [130]	133
Figure 96. A cladded solid block, note the sloped corners	136
Figure 97. a) Schematic view of 40 degree angular deposition b) A sample made with 40 degree tilt	137
Figure 98. Four different cladded models with angular deposition	137
Figure 99. FFT for the single bead, 2 sec. step intervals, showing dominate frequencies at 0.23, 0.69, and 1.22 Hz or 4.35, 1.45, and 0.82 sec., respectively. The mean value is recorded at the 0 Hz point.....	139
Figure 100. Laser cladded models with different filling strategies a) Raster type filling with no contour b) Contour the square and then filling with 50% overlap c) A small square in a big square, contour and filling. The problematic corner is encircled d) Filling with 50% overlap and e) f) Solid cladded blocks, bulging is visible	140

LIST OF APPENDICES

Appendix A: Published papers-acceptance letters	149
Appendix B: Response variables measured against five process parameters	152
Appendix C: Experimental design matrix of 50 % overlap bead configuration	155
Appendix D: Different cornering configurations with numbers shown on them	157
Appendix E: Screen shot of the hollow cone	160
Appendix F: Screen shot of hollow parabolic cone	160
Appendix G: Single bead experiments-- No overlaps	161
Appendix H: Response output--40 % overlap	164
Appendix I: Response output--50 % overlap	166
Appendix J: Response output--60 % overlap	168
Appendix K: The3D representation shows the effect on the positive bead area by varying the laser power, CTWD and the focal length, while the other factors were remained constant.....	172

LIST OF ABBREVIATIONS/ACRONYMS

Abbreviations

2D	Two dimensional
3D	Three dimensional
3DMW	3-Dimensional micro welding
420 power	A stainless steel powder with 12~13 % chromium
ABB	Robot manufacturer
ALM	Additive layered manufacturing
ANN	Artificial neural network
ANOVA	Analysis of variance
CAD	Computer aided design
CCD	Central composite design
CCD Camera	Charged couple device
CNC	Computerized numerical control
CAM	Computer aided manufacturing
CT	Computerized tomography
CTWD	Contact tip to work piece distance
DOE	Design of experiment
DMD	Direct metal deposition
EDM	Electrical discharge machine
FDM	Fused deposition modeling
FEA	Finite element analysis
FR	Feed rate of the clad powder
FL	Focal length of the lens
GA	Genetic algorithm
GMAW	Gas metal arc welding
GRG	General reduced gradient
HAZ	Heat affected zone
HLM	Hybrid layered manufacturing
HPDM	Hybrid plasma deposition and milling
Hz	Hertz
H13 powder	A stainless steel powder with 4~5 % chromium

I	In (lead in situation)
LC	Laser cladding
LM	Layered manufacturing
LOM	Layered object manufacturing
LENS	Laser-engineered net shaping
LBAM	Laser based additive manufacturing
LS	Laser speed of the nozzle
MIG	Metal inert gas welding
MLP	Multi-layer perception
MRA	Multi regression analysis
O	Out (lead-out situation)
OEM	Original equipment manufacturer
PW	Laser power
RP	Rapid prototyping
RH	Reinforcement height
RM	Rapid manufacturing
RT	Rapid tooling
RSM	Response surface methodology
S _i C	Silicon carbide
SLS	Selective laser sintering
SLA	Stereo lithography
SDM	Shape deposition manufacturing
STD Dev	Standard deviation
SM	Subtractive manufacturing
STL	Standard tessellation language
TIG	Tungsten inert gas welding

Symbols for Laser Cladding Process

A_n	Negative bead area
A_p	Positive bead area
D	Dilution %
H	Bead height 'mm'
P	Bead penetration or depth 'mm'
W	Bead width 'mm'

NOMENCLATURE

DF_{error}	Degree of freedom error
F	Total number of factors
H_0	Null hypothesis
H_1	Alternate hypothesis
L	Total number of levels
MS_{error}	Mean square error
N	Total numbers of experiments
r	Replicates of the experiments
SS_{error}	Sum of squares error
W_c	Calculated width-mm
W_s	Average width for all single bead experiments
X_i	Experimental value
X_i'	Ratio of experimental value and min or max value
X_{min}	Minimum value of the experimental data
X_{max}	Maximum value of the experimental data
Y	Response variable or objective function
β_0	Free term or constant of the regression equation
β_i	Coefficients of linear terms
β_{ii}	Coefficients of square terms
β_{ij}	Coefficients of quadratic terms
ϵ	Noise or error observed in the response

Chapter 1

General Introduction

1.1 Background

To improve the surface properties of metallic mechanical parts, such as the resistance against wear and corrosion, several thermal surface treatments are available; for instance, plasma spraying, arc welding are established techniques. Depending upon the applied technique, common problems are the occurrence of porosity, a combination of a poor bonding of the applied surface layer to the base material, and the thermal distortion of the work piece.

One of the techniques that overcome these problems is laser cladding, which is a process of protecting one metal by bonding or adding a second metal to its surface. Well known applications include the enhancement of the corrosion resistance of gas turbine blades and the repair of dies and molds. The clad material, which could be powdered metal or wire and can possess similar or dissimilar metallurgical properties, is applied to the substrate material to achieve enhanced strength, resistance or abrasion characteristics. There are several static and dynamic process parameters which can be varied between builds and these parameters all influence the bead shape. The bead width, height, penetration depth and the bead cross sectional area are all interlinked and depend on the optimum selection of process parameters.

Unlike the other commercial additive manufacturing processes such as fused deposition modeling (FDM) and selective laser sintering (SLS), which have original equipment manufacturer (OEM) software with process planning modules defined, no comprehensive process planning software solution exists for bead deposition process of laser cladding [1]. Prior research [2-5] has been performed to be able to select process parameters with confidence that will generate the desired bead geometry for a single bead. However, to facilitate process planning, the process parameters that have the most influence on each geometry parameter and valid bead geometry combinations parameter need to be determined.

1.2 Additive Layered Manufacturing Processes (ALM)

Additive layered manufacturing (ALM) has its root in the development of rapid prototyping in the 1980's. In all layered manufacturing (LM) processes, the three dimensional (3D) CAD model is sliced in to horizontal layers of uniform thickness. Each cross sectional layer is successfully deposited, hardened, fused, or cut, depending on the particular process, and attach to the layer beneath it. The stacked layers form the final part. ALM is a tool less process that is capable of producing complex geometries with minimal human intervention. A 3D component is created in the virtual domain is realized in the physical domain by layering two dimensional (2D) cross sections successively to create final part [6].

There are several competing technologies which are commercially available to make the parts in layers. All of the available systems differ mainly in the way the layers are built to create parts [7]. Some systems include melting or softening material to produce layers such as selective laser sintering (SLS) and fused deposition modeling (FDM). Another approach is to lay liquid material thermosets layers which are cured using an ultra violet laser i.e. steriolithography (SLA). In the case of laminated object manufacturing (LOM), thin layers of adhesive backed solid materials are cut to shape and joined together (i.e. paper, polymer or metal).

All these technologies reduce the process planning time as they are all based on the 2D layering concept, although there are limitations with the available build materials and the fabrication size. There are various technologies available and those are widely used are highlighted in color, as illustrated in Figure 1. Among those, the FDM process is one of the most widely used layered manufacturing process [7].

The foremost advantage of LM is the ability to make a prototype; hence the term rapid prototyping (RP) is also applied to this technology. In fact, it is in the area of RP that the technology has seen most commercialization. Layered manufacturing is gaining ground for rapid prototypes, rapid tools (RT) and rapid manufacturing (RM) for production of functional parts. A few of the fundamental challenges in materials processing confronting the manufacturers are as follows:

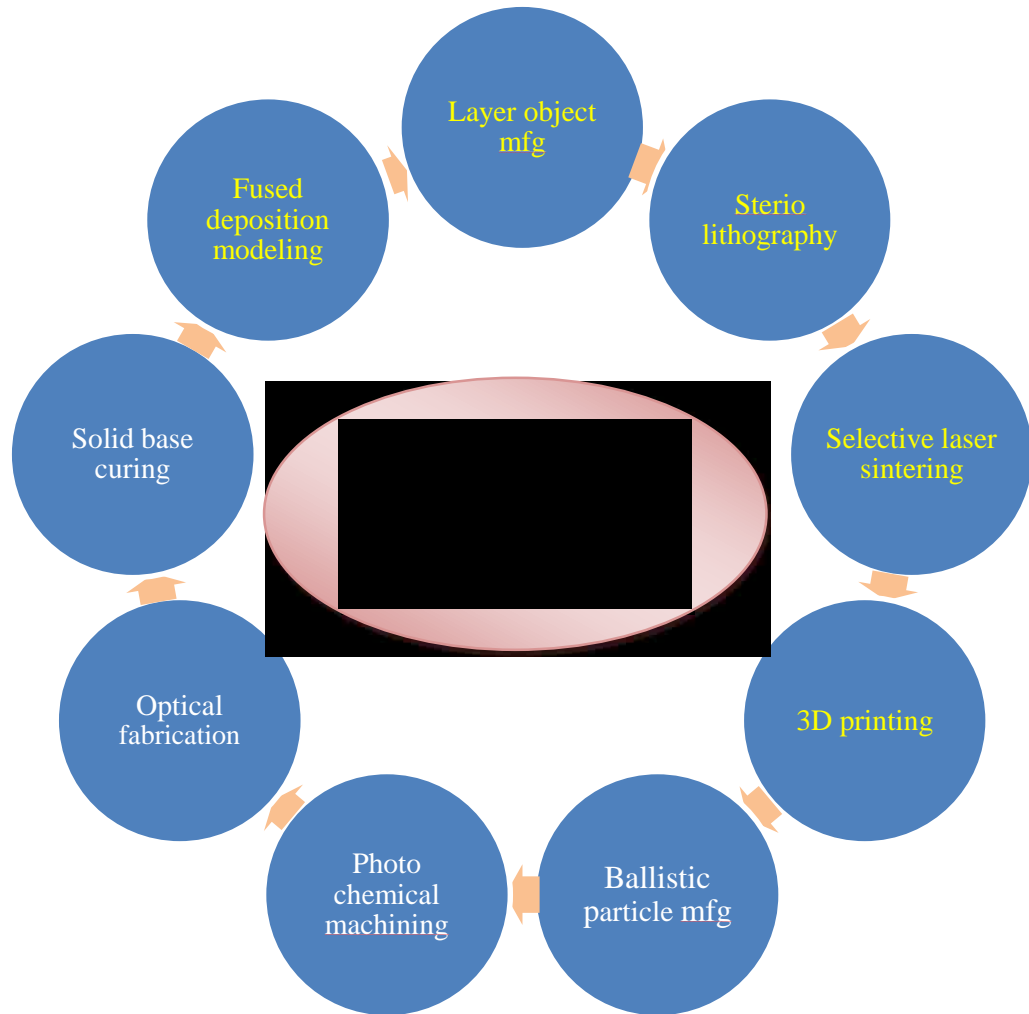


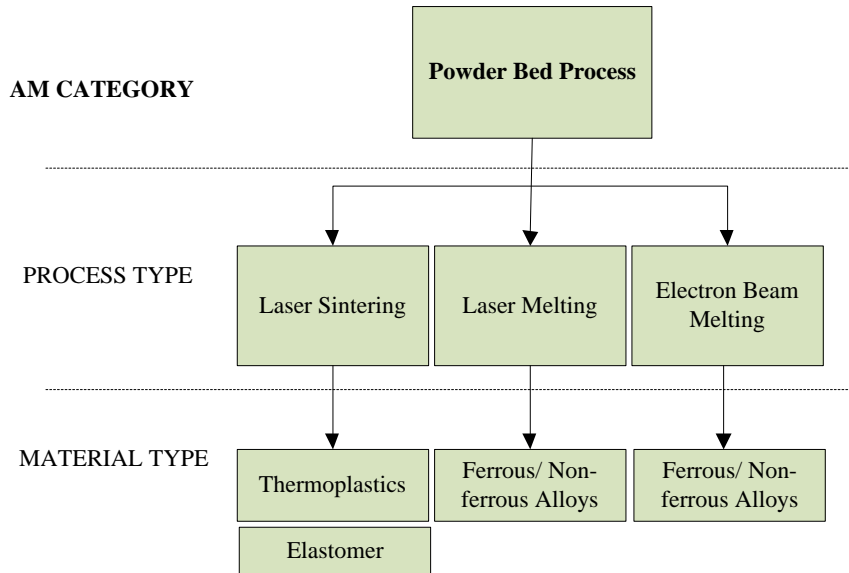
Figure 1. Different methods of additive layered manufacturing processes

- i. improving the quality of the surface finish,
- ii. eliminating residual stress,
- iii. understand local compositions and microstructures,
- iv. achieving fine feature sizes and dimensional tolerance [8]
- v. accelerating the fabrication speed. and
- vi. understanding of anisotropic properties

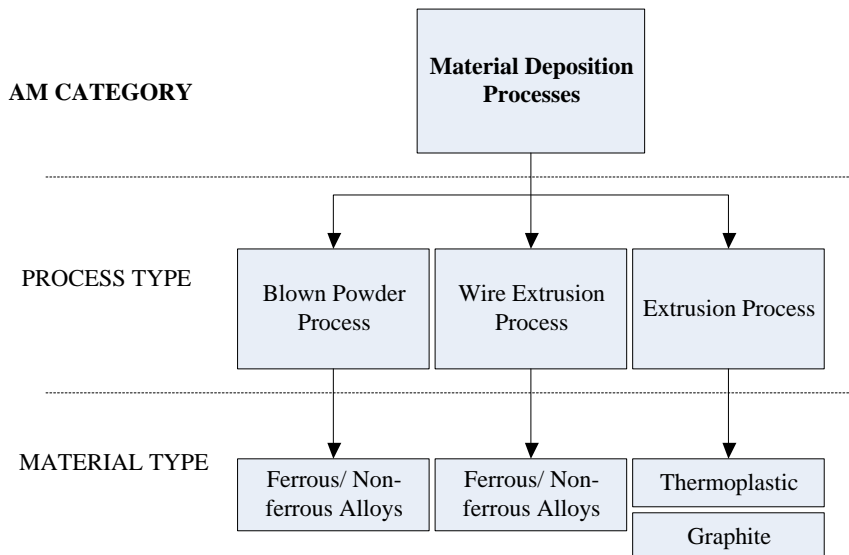
Until these challenges are met, the applicability of LM and its commercialization is restricted.

1.2.1 ALM Categories, Processes and Materials

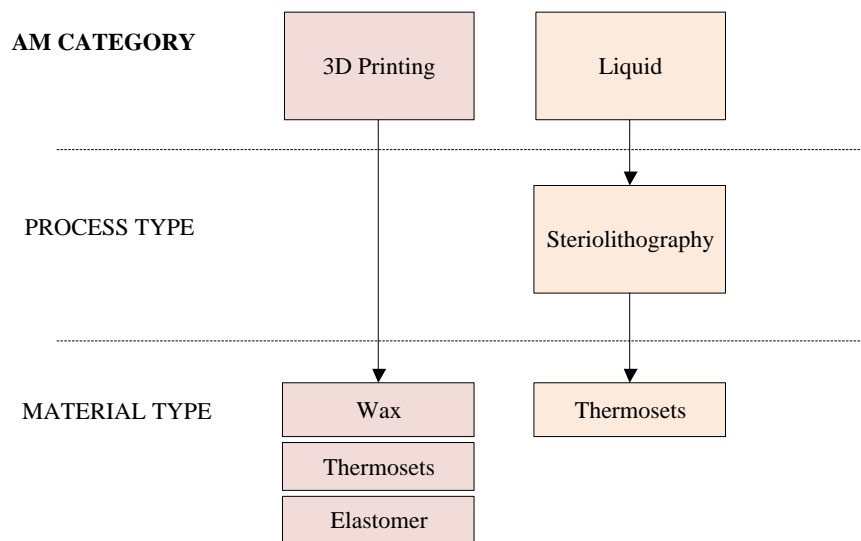
There are several different categories and processes of additive layered manufacturing available, each appropriate for different materials and requirements. These are detailed in the following Figure 2 a, b, c.



- a) **Powder bed** processes consolidate thin layers of powder using a laser or electron beam to fuse scans of the sliced CAD data to create the geometry



b) **Material Deposition/** Extrusion processes work by heating the material through an extrusion nozzle which follows a predefined deposition path, layering on top of a platform, depositing material on top of previous layers to create the 3-dimensional geometry. For metallic, blown powder and /or wire extrusion is used; however, the material is melted at using a laser or electron beam at source



c) **3D Printing** works by laying down thin layers of heated material on to a platform. Either the head or platform will continuously be moving to deposit more material on top of each other to form the 3D object. Binders and powder can also be used to form 3D objects.

The **liquid** vat process solidifies thin layer together, using an ultraviolet (UV) curable thermoset polymer liquid with a laser to create the required geometry layer by layer.

Figure 2. AM categories, processes and material types are shown

For this research, blown powder process type is chosen, as mentioned in Figure 2b which works with laser heat. Details of this process are described in the next section.

1.3 Laser Cladding Process (LC) and Applications

One of the pressing problems of modern engineering is the production of durable coatings on surfaces of materials. Laser technology not only provides a unique way to modify the surface of materials such as transformation hardening, alloying, cladding etc., and achieve desired surface properties [8]. These are all established techniques. Characteristic for these techniques is the application of a surface layer with the required properties on top of another material.

One of the techniques that is used in the industry is laser cladding (LC). It has been defined as “a process which is used to fuse with a laser beam another material which has different metallurgical properties on a substrate, whereby only a very thin layer of the substrate is melted in order to achieve metallurgical bonding with minimal dilution of added material and substrate in order to maintain the original properties of the coating material” [10].

Laser cladding is a technique in which a laser beam is used as the heating source to melt the alloy powder or wire to be deposited on the surface of the substrate. The LC process using off-axis powder injection material is shown in Figure 3. The focal length of the lens and the contact tip to work piece distance (CTWD) can also be seen. Both of these parameters play an important role in achieving good quality clad, which is discussed in chapter 5. The metallic powder is injected into the molten pool through a coaxial or off-axis nozzle while simultaneously a high power laser beam melts the cladding material over the substrate or base metal.

It has been observed that different properties are often required at different locations on the products. For instance, wear and corrosion resistance are only required at the surfaces of the products. Laser cladding is a superior coating technique, which manifest a metallic bonding of substrate and coating [9]. It has become an important surface modification technique in today's industry and continues to gain market.

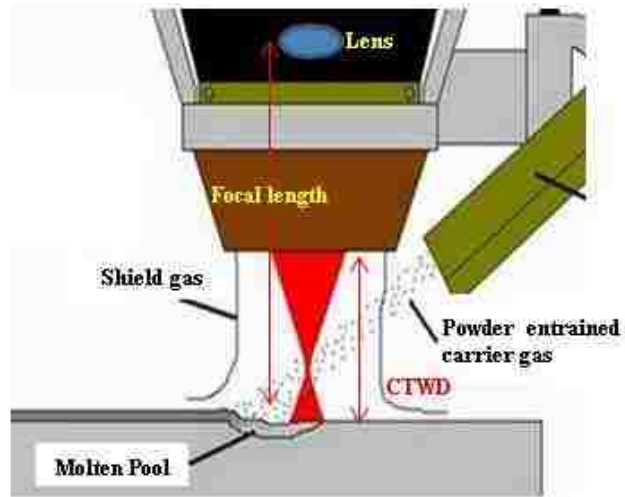
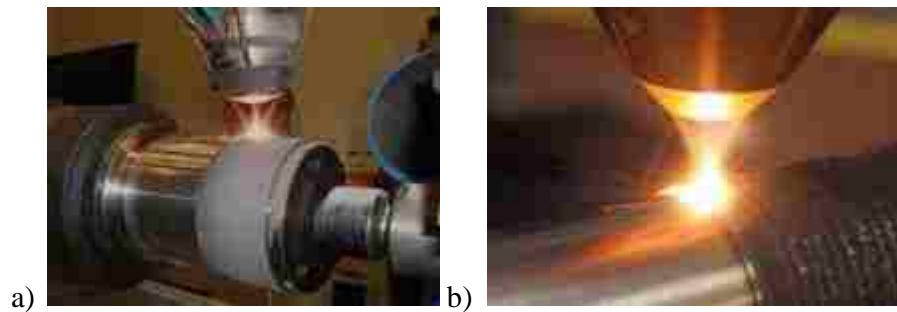


Figure 3. A schematic diagram of the laser cladding process (adapted from [11])

LC is not only applied for coating but also for repair and refurbishment as well as for rapid prototyping [12]. In these applications, the aim is to have the minimum dilution of the added material by the substrate.

A major application of laser cladding is in repair and refurbishment of high-value components such as tools, turbine blades, gas turbine and internal combustion engine parts (Figure 4). In addition, there are many other applications of laser-based direct material deposition, such as functional coatings, repair depositions, rapid design changes and finally the direct generation of 3D parts made from ferrous/nonferrous material.



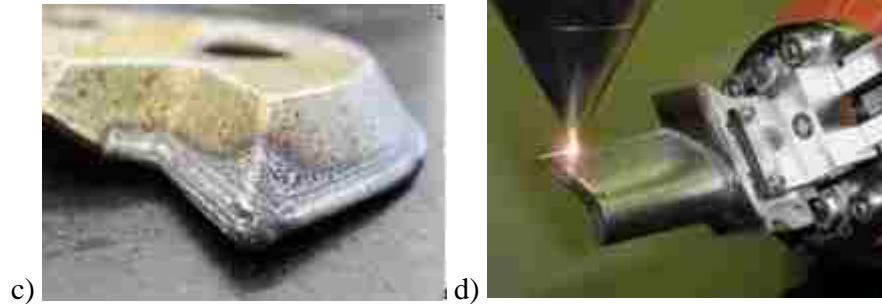


Figure 4. Application of laser clad areas [13-14]

The state-of-art laser cladding process along with other surface treatment methods are presented in detailed in chapter-3.

1.3.1 Advantages and Dis-advantages of Laser Cladding

Currently there is a growing interest in the industry for using this technology for making large, metallic functional components. Most engineering applications require high strength and corrosion resistant materials for long-term reliability and performance [12]; consequently, laser cladding is being explored as a viable solution for it. The advantages of this process are:

- Capability of mixing two or more types of powders and the feed rate control of each powder make laser cladding a flexible process to fabricate functionally-graded materials.
- Material thus can be tailored in a flexible way for their functional performance in particular application.
- It enhances the performance of components such as hardness, yield strength and fatigue strength.[15]
- The beam of energy from laser can be focused and concentrated to a very small area and keeps the heat effected zone (HAZ) of the substrate very shallow. [16]
- The shallow HAZ minimizes the chance of cracking, distorting or changing the metallurgy of the substrate.

In addition to surface cladding, near net shape components could be built in a layer by layer fashion which would only require some machining, as enough research have been performed for the bead behavior in different scenarios. This would be a great advantage for sectors such as mold

and die industries, where integration of this process could reduce the high amount of waste material in the form of chips. Moreover cooling rate during laser cladding is more rapid and this enhances mechanical properties of the component [16]. Other sector in which this process is becoming of interest is the aeronautical, where it is feasible alternative to conventional welding processes such as TIG or plasma welding.

High investment cost, low efficiency of the laser sources and lack of control over cladding process parameters and skilled operator required are disadvantages of the use of this technology. Since this process has the potential to fabricate 3D components; however, foundational work related to establishing process planning parameters, rules, and use of different materials needs to be conducted.

1.4 Motivation and Research Objectives

Since the development of high power laser, the cladding has become a major research topic. Over the past fifteen years, basic and applied research has provided an in-depth understanding of the cladding process, as well as variety of potential applications. But initial investment and running cost is high to have this system. In recent years, LC has gained momentum due to the diversity of its potential applications: metallic coatings, high-value mechanical component repairs, rapid prototyping, layered metal deposition and nano-scale manufacturing [15]. Unlike conventional methods, laser cladding is fast and precise; at the same time, it has a small heat-affected zone (HAZ). In order to obtain a strong fusion bond, the process requires the formation of the melt pool on the substrate. For a better coating, the depth of the melt pool must be as small as possible; hence a minimal dilution in the substrate. Since the dilution and clad geometry vary with different process parameters, it is essential to understand the relationship of these parameter to the required product quality.

1.4.1 Motivation

It is evident from the information presented in the previous section that many aspects of the laser cladding (LC) process have already been investigated. Due to its additive nature, LC can be applied in a variety of ways to parts, tools and advanced manufacturing to overcome the limitations of existing metal fabrication technologies. Despite its benefits, LC is not yet widely utilized in metallic coating or prototyping applications because of high investment cost, low efficiency of the laser sources and lack of control over the cladding process and its associated parameters.

The laser cladding process is highly complex and very sensitive to its internal and external factors. The internal factors such as manufacturing process parameters like laser power, deposited nozzle speed, powder feed rate etc. Nevertheless, there are areas that require attention in order to make the process more productive and diverse for industrial applications. The different physical aspects of this process, for instance laser-substrate interactions, laser-powder interactions and melt pool flow phenomena are basically understood and well investigated by the researchers.

Several researchers have developed experiments and predictive models for various configurations to extract information relevant to their environment typically for steady state conditions. The non-linear coupled nature of the LC process introduces predictive modeling challenges. The influence of the manufacturing process parameters and non-linear trend shows a great impact on the resulting bead geometry and the bead characteristics are varied for single and overlapping bead conditions. The main problem faced in cladding is the selection of optimum combinations of process parameters for achieving good clad bead geometry. To successfully deposit powder material employing the cladding process, the influence of many process parameters need to be understood to be able to generate the desired bead geometry and predict probable shape related variations.

In this thesis, several of these aspects such as the impact of these internal factors on the clad bead geometry in different deposition scenarios are investigated. It is therefore of great interest to establish a good correlation and develop some predictive models between the input and output factors of the LC process. Estimation of the resulting clad would allow the process planners to program for layer-by-layer structures without previous measuring the clad geometry. Both single track and overlap cladding experiments needs to be conducted to determine the influence of the process settings on the clad characteristics.

1.4.2 Thesis Objective

The objective of this research is to develop quantifiable relationships of the laser cladding process to its manufacturing parameters and their effects on the clad bead geometry. Realistic scenarios, which investigate overlapping and stacking, are investigated, since this process has potential to fabricate some large solid components in layers. Characterizing key geometric features for each deposited layer either is laid down side by side or overlapped is not trivial unless an in-depth study in different scenarios is performed on this highly coupled and multi-parameter process. The subsequent bead not only transfers the heat rather impacts the preceding bead geometry as well. An extensive set of experiments is to be performed with single bead,

overlapping beads, multiple layer beads, and stack ups. Having experimental data for realistic manufacturing scenarios will help to establish a foundation for process planning data. The objective of this research work is divided in to two categories i.e. primary and secondary objective. To achieve the primary goals, some assumptions are made, which are described in the following paragraph. The impact of the laser heat on the melt pool dimensions and HAZ are evident but beyond the scope of this research.

It is hypothesized that:

- i. Small variations in the manufacturing process parameters leads to variations in all the general bead shape parameters and the relationships are nonlinear.
- ii. The overlap and stacked layers bead geometry will not be the direct multiples of a single deposited bead. It is anticipated that difference exists due to changing boundary conditions as heat transfer is occurring among the layers and the deposited bead's physical mass changes the deposition surface area.
- iii. There are transient conditions that influence the bead geometry both in single and multiple layer conditions. Deposition scenarios such as lead-in, lead-out and corner configurations do impact the bead geometry.
- iv. Changing the power level would impact the melt pool width. Insight into the transient heat phenomenon and system dynamics can be determined by varying the laser power level during the deposition process.

The secondary objective is to strategize the experimental plan for data collection. It is hypothesized that a structured experimental approach can be employed to reduce the data set yet still generate robust predictive models. To achieve this goal, the following methodology is adopted for this research:

- i. To conduct the experiments, the conventional factorial design method for five levels and five factors with replicates would require thousands of experiments to perform. To set up this huge number of experiments is very expensive and time consuming. A formal design of experiment (DOE) utilizing the response surface methodology (RSM) approaches with a central composite design (CCD) is applied to develop the experimental plan.

Laser cladding is a multi-variable, nonlinear process with possibility of significant interactions among its parameters. These factors need to be explored using the analysis of

variance (ANOVA) technique. By identifying the significant factors that impact dimensional quality in this bead deposition process, hybrid manufacturing method can be made an alternate manufacturing process. The additive and subtractive manufacturing processes complement each other; therefore the idea of the hybrid approach has potential to build prototypes or even functional parts.

1.4.3 Limitations

This thesis focuses on laser cladding. The research work is limited in defining and analyzing clad bead geometry for selected conditions, as defined in section 3.3. The melt pool region, heat affected zone (HAZ) and temperature monitoring/controlling during the cladding process are important but not considered in the research. Similarly the effect of external factors such as ambient temperature, powder shielding gas, and varying laser spot size are also beyond the scope of this work.

Most of the practical work and experiments are conducted at the facility of the industrial partner. The 420 stainless steel powder was chosen as cladding material for all single and all overlap configuration experiments. One of the reasons to have this powder is less expensive than other types of stainless steel and carbide powders. The overlap configurations are limited to 40%, 50% and 60% overlaps with a three bead pass formation. The industrial partner facility is used to conduct all experimental work. The facility contains a robotic arm equipped with a nozzle assembly which provides the laser spot size of 4.3 mm only. Other materials from stainless steel class such as H13 and the material from carbide family such as tungsten carbide may be used with different spot size to find any consistencies between these types of materials.

1.5 Outline of the Dissertation

Chapter 1 provides the general information and different categories of additive manufacturing methods used in the industry. In particular, the laser cladding process is defined with its advantages and disadvantages. Research objective and its motivation are also presented here.

In chapter 2, a literature review is presented which covers the use and development of laser cladding system in different areas. The lack of models contributes to the necessity to perform expensive series of experiments with different materials and input conditions (laser spot size, power levels, etc.) for new applications. Many aspects of laser cladding are already understood and described in this section.

In chapter 3, the state of art, the laser cladding technique is presented and compared with other laser surface treatment methods. The significance of the static and dynamic process parameters and their effects on bead geometry are also discussed. Based on this state of the art process, the objectives of this thesis are formulated.

The experimental methodology and set up that is adopted throughout in this research is mentioned in chapter 4. This section also contains the information related to the sample preparation, measurement techniques and data collection for single and overlapping beads. The multiple bead, stacking, transient heat conditions and lead-in and lead-out scenarios are also presented in this section.

In chapter 5, the results of all the experiments and general observations for the different deposited scenarios are discussed. The effects of the process parameters on the bead geometry are graphically presented. Predictive models for single bead, stack up layers etc. are developed using multiple approaches. The fitness of the best fit model is also explored with these approaches. The analysis of the transient conditions with different power levels and its impact on bead width and height are also investigated and illustrated graphically in this chapter.

The process planning challenges associated with the deposition of laser track are evident and discussed in chapter 6. A single bead model provides insight with respect to the process characteristics but an overlap model is relevant for process planning and travel path generation for surface cladding operations. A hybrid approach, which constitutes both additive and subtractive manufacturing processes, is also discussed in this chapter. Tool path generations and filling strategies for 'near net shape' model is also explored in this section.

In chapter 7, the overview of the thesis is reviewed and conclusions are stated. The significance of the laser cladding process in different scenarios is also discussed.

Finally, in chapter 8, future work is presented. More experiments need to be conducted with multi beads, stack ups and some angular depositions in order to understand the effect of laser heat and its parameters on the geometric shapes of the cladded models. Other interesting topics such as the heat effected zone, microstructure and hardness of the deposited bead are not investigated in this work, so this area should be investigated.

Chapter 2

Literature Review

This section provides primarily a review of the literature with respect to laser cladding process and associated process planning issues. It also shows the significance of this process especially in tool and die industry and how the researchers are eagerly investigating the process using the criteria with the selection of optimum parameters, modeling of the bead, effects of heat on the substrate, heat effected zone, clad geometry, and the clad mechanical properties. Over the past fifteen years, basic and applied research has provided an in-depth understanding of the cladding process, as well as a variety of potential applications of it. In the following sections, not only the review of the previous work is mentioned but also critics and gaps of the research are highlighted as well.

2.1 Introduction

The potential of this technology is massive, with research groups around the world continuing to contribute to its growth through research programs and industrial applications. From the literature review it is evident that many approaches have been taken to collect and model bead deposition data, and there is no unified approach, although the majority of researchers focused on the travel speed, power levels, and material feed rate.

There are several experimental approaches that have been used in the past by researchers for sample preparation and data collection. The L9 Taguchi approach [17] and factorial design technique (DOE) [18] are mostly used by researchers to analyze the collected data. Ermurat et al. 2013 [17] used both the methods to investigate the effect of process parameters of single clad for minimum size. Taguchi optimization method which was developed by Genichi Taguchi, is used to find out optimum parameter levels of a system by least number of design evaluations. Orthogonal design arrays are used in this method in which all design parameters can be analyzed rapidly.

The design of experiments (DOE) approach and some statistical analysis techniques are commonly used to achieve optimum solution at some various targets. The DOE factorial strategy is helpful in generating mathematical models that can help in predicting the shape parameters. One of the most effective and widely used DOE approaches is a response surface methodology

(RSM) technique which uses a central composite design (CCD) to define an experimental data set. The CCD design, which is a robust design is used in this research for developing the experimental plan by studying the interactions of quadratic and squared terms along with linear terms.

The literature contains information on several laser cladding models, but it also shows the absence of a model for the prediction of the clad geometry in the transient and dynamic period of the process. A literature review matrix is presented at the end of this chapter which summarizes the in-depth review and which methods have been used by researchers in laser cladding process.

2.2 Rapid Prototyping Methods and Hybrid Approach

Rapid prototyping (RP) draws its appeal from its ability to allow parts to be built directly from CAD descriptions without any tooling and this ability has reduced the need for skilled worker for process planning and fabrication. RP is a mold-less process and has proven to be an effective tool for reducing the time and cost involved in it. As RP was introduced as design visualization tool, the early focus of the research was on the physical realization of the shape rather than its functionality. Thus most of the existing RP processes produce objects using resin and other non-metals, limiting their applications. In comparison, metallic prototypes have a larger domain of applications [19]. Thus efforts have been going on for extending RP for manufacture of metallic objects.

Several techniques like laser-engineered net shaping (LENS), 3D welding, direct metal deposition (DMD), shape deposition manufacturing (SDM), laser based additive manufacturing (LBAM), 3D micro-welding (3DMW) and electron beam melting capable of producing metallic prototypes have been developed by different research groups [20–26]. These techniques generally use an arc, laser or electron beam as the energy source for metal deposition and all of them produce only rough surfaces and cannot be directly used for high precision applications such as in tooling where around 1 μm accuracy is required.

Some researchers [27-29] developed hybrid layered manufacturing processes, which combine the advantages of both additive and subtractive manufacturing. Karunakaran et al. 2010 [30] presented hybrid layered manufacturing process which possesses best features of both of these approaches. The near-net shape of the object is first built using weld deposition and is then finish machined subsequently. Near-net shape building and finish machining at the same station is the unique feature of their work. Hur et al. 2002 [29] proposed a system of material deposition and

material removal (CNC) at the process planning and manufacturing level. They believed that their system incorporates a combined RP concept, and offers an optimum manufacturing solution by adopting the advantages of the RP and CNC systems (Figure 5).

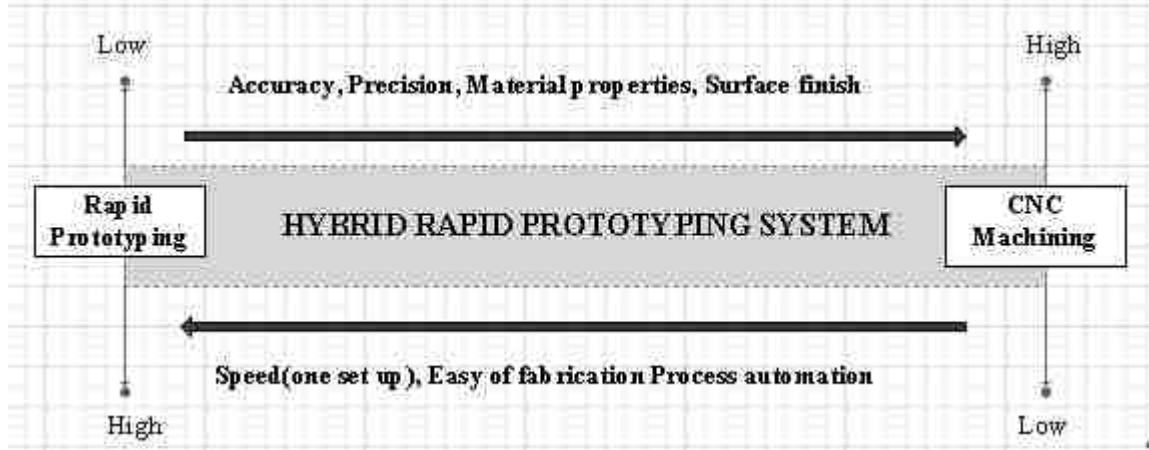


Figure 5. Position of RP and CNC process in terms of their characteristics [29]

They proposed a unique approach in their research and confident that their method would solve the issues arises in hybrid-RP system such as the stair-case effect, handling hidden and complex geometry, shrinkage problem especially when large amounts of melting material is deposited and efficiently combining deposition and machining in a station etc.

2.3 Laser Cladding and Other Conventional Methods

Laser cladding is traditionally employed for component repairing and re-conditioning and laser heat can be used for hardening localized surfaces. The experiments at various laboratories and some universities are currently exploiting the commercial viability of the developed process, while some other researchers are augmenting the technology with the process modeling using analytical and numerical tools. The main problem faced in cladding is the selection of optimum combinations of process parameters for achieving good clad bead geometry. Many studies have been conducted in which a specific process parameter, the material properties of a particular product, or physical phenomena associated with the process is studied.

The research groups of Kovacevic, Merz and Dickens are some of the early contributors to this area [31-33]. A systematic investigation of the effect of each process parameters on the deposition geometry has been reported by Li et al. 2005 [34] and Qi al. 2005 [35]. They investigated evaluation of metallurgical micro structures and mechanical properties of laser deposited Inconel 718 powder as well. They also proved by conducting design of experiments (DOE) that the main factors effecting the deposition bead width are laser power; travel speed and the beam defocus distance. By changing these parameters during laser deposition, variable bead widths can be produced. Huan et al. 2007 [36] considered bead height a constant parameter and bead width as an output variable in the generation of tool path design. They conducted full factorial central composite design (CCD) experiment with the following four parameters, i.e. laser power, travel speed, beam defocus distance and layer height.

Several authors [37-40], when reporting on laser cladding, have shown that the processing parameters have an essential impact on the geometric form of clad. Recently, Davim et al. 2008 [41] presented a study that evaluates the processing parameters (laser power, scanning velocity and powder mass flow rate) under the form of single-cladding layer (clad height, clad width and depth penetration into the substrate) and hardness of coating. A plan of experiments, based on the orthogonal arrays, was established by them considering laser cladding with prefixed processing parameters. An analysis of variance (ANOVA) was performed to investigate the influence of the processing parameters in the form of single-cladding layer. In addition, these authors presented a study for prediction of the geometric form of clad in laser cladding by powder using a multiple regression analysis (MRA). Onwubolu et al. 2007 [42] investigated the prediction of the clad angle in laser cladding by powder using response surface methodology and a scatter search optimization technique.

Various materials and experimental configurations are explored, and no constant approach is taken in order to develop a predictive model for clad geometry. Researchers acknowledge that it is challenging to develop an analytical model; consequently, other methods need to be utilized. Various methods of modeling are explored in this thesis/research to determine the best fit of the experimental data.

Some researchers used gas metal arc welding instead of laser heat for their research. Contemporary work done on arc-based hybrid layered manufacturing (HLM) at Indian Institute of Technology and hybrid plasmas deposition and milling (HPDM) at Huazhong University, China. HLM integrates gas metal arc welding (GMAW) for near net shape layer deposition with CNC

machining for net shaping and finishing to manufacture metallic parts. Xinhong et al. 2010 [43] have successfully demonstrated HPDM's ability to build aero engine double helix integral impeller made of a super alloy. GMAW, another approach of additive manufacturing besides laser cladding, is also very popular among researchers. Significant research has been done using the GMAW process where Sreeraj et al. [44] conducted experiments using GMAW, to optimize various input process parameters such as the welding current, welding speed, contact tip to work piece distance and the gun tilt angle. A five level five factor full factorial design matrix based on central composite rotatable design technique was used for the mathematical development of model to predict clad bead geometry using GMAW. In their study, two models, an artificial neural network (ANN) and genetic algorithm (GA) are developed for prediction and optimization of bead geometry. The authors aimed for getting low percentage of dilution which is a universal criterion of a good clad quality.

Several models have been developed and used in predicting the process for different parameters. An accurate model can significantly reduce the development cost of automated laser cladding system. Chande and Mazumdar, 1985 [45] developed a numerical model which solves a two-dimensional transient equation of convection diffusion in the melt pool. The model developed by Jouvard et al. 1997 [46] predicts the power limits for generating good quality clad. Their model takes in to account the interaction between the powder and the laser beam. Picasso et al. 1994 [47] also developed a simple geometrical model for the laser cladding. Their model calculates the laser-beam velocity and the powder feed rate when the laser power, beam radius, powder jet geometry and clad height and width are known. Some researchers (Kim and Peng 2000), [48] used metallic wire instead of powder to model the melt pool of laser cladding using a two-dimensional, transient finite element technique.

2.4 Mathematical Modeling of Bead Geometry and Build ups

Due to the importance of the laser cladding process, numerous analytical and numerical models of the LC process have been developed in past years. Kar and Mazumder, 1987 [49] described a one-dimensional conduction model to determine the composition of the alloys and cooling process. Hoadley and Rappaz, 1992 [50] developed a two-dimensional model to calculate the temperature in steady state. In their model, the influence of laser power and processing speed on dilution and thickness was considered. Some researchers have developed bead shape prediction models using finite element method (FEM) like Amara et al., 2005 [51], Toyserkani and Khajepour, 2004 [52], analysis of variance techniques (Davim et al., 2008 [53], Song et al.,

2005 [54]), and artificial intelligence approaches using fuzzy logic (Zeinali, 2010 [55]), or neural network techniques (Toyserkani et al., 2002 [9], Liu, 2012 [56], Mahapatra, 2008 [57], Song et al., 2008 [58]).

Many researchers such as Liu and Lin, 2003 [58] have investigated the laser power interaction phenomenon and analyzed the powder heating process for a single spherical powder particle in coaxial LC. Picasso and Rappaz, 1994 [60] established a finite-element model to compute the shape of the melt pool. Their model took into account the interactions among the powder particles, and analyzed the effect of the laser beam properties and the change of absorption on the shape of the melt pool. Recently, a three-dimensional transient finite-element model was proposed by Toyserkani et al. 2004 [52] for laser cladding with a powder injection process. They decoupled the interaction between the powder and melt pool to simplify the thermal analysis and melt pool boundary calculation.

Tabernaro et al, 2014 [16] used three different sub- models for the geometric modeling of clads. Their sub-models predict the particle flow, the attenuation of laser power, and the geometry of the melt pool by applying a heat balance on the substrate. They assumed that the clad height at each surface point depends on the powder mass concentration in this point at that particular instant. The core of their model is based on a mass balance between injected powder material at each point of the melt pool and the mass of the resulting clad, using the following equation 1:

$$m_{injected} = m_{clad} \tag{1}$$

Later on in their work, they calculated the height of the clad using the mass balance equation (eq-1). Similarly, Hofman, 2009 [12] presented a model for the determination of the clad geometry and dilution in LC process. He investigated the correlation between observed melt pool characteristics and dilution using the model. He also compared the simulation results with the experimental results and found that melt pool width is the perfect indicator of the dilution level and also argued that when the melt pool width is smaller than $W_{critical}$, i.e. about 90% of the laser beam diameter, the dilution levels are small and this critical value is independent of the cladding speed and the temperature of the substrate.

Han et al. 2004 [61] developed a mathematical model to simulate the LC process and interactions between their parameters. They predicted the influences of the powder injection on the melt pool shape, penetration and flow pattern through the comparison for the cases with

powder injection and without powder injection. Their results indicate that the particle injection has a significant effect on melt pool flow pattern and penetration but they did not consider the effect of heat on the bead profile. They also simulated the dynamic behavior of the melt pool and the formation of the clad. Contrary to numerical models in the literature, which made some oversimplified assumptions, their model does not require a prior knowledge of the melt pool shape or the decoupling of some interaction processes.

2.5 Process Planning in Manufacturing Processes

Process planning and especially automated process plan has been the goal of researchers for years and many computer aided process planning systems have been developed, also reported by Maropoulos, 1999 [62] and Kiritsis, 1995 [63]. Process planning is the interface between design and manufacturing. It translates the design specifications into process and operations sheet. It has two distinguished levels, Macro and Micro-level planning (ElMaraghy, 1993)[64].

In the literature, process planning is often approached with a set of goals driven by high volume components that is, a set of plans that strives for cost effectiveness through maximizing feeds and speeds and create repeatable setups. Process planners should be capable of querying all geometric and functional information about the product (Azab, 2008)[65]. He argued that macro-level process planning is difficult because of its dependency on declarative process knowledge including part geometry, tools, machine tools, fixtures and technological requirement. Azab et al [66] also worked on reconfigurable process plan with the objective to determine the best location to insert the new features in the existing sequence without violating constraints.

The planning time can be long, as on some occasion, fixtures need to be designed for various in-process orientations, tools selected, and decisions with respect to the travel path type, step over, lead in/lead out, stock removal, etc. is required. When a component is designed, all detailed information with respect to the shape, tolerances, surface finish and engineering specifics are used as the foundation for developing a process plan. Process planning involves defining a set of workable instructions to transform raw material into the final part. The challenge related to the complexity of process planning is evident in the literature, as the research in this field continues to grow (Figure 6).

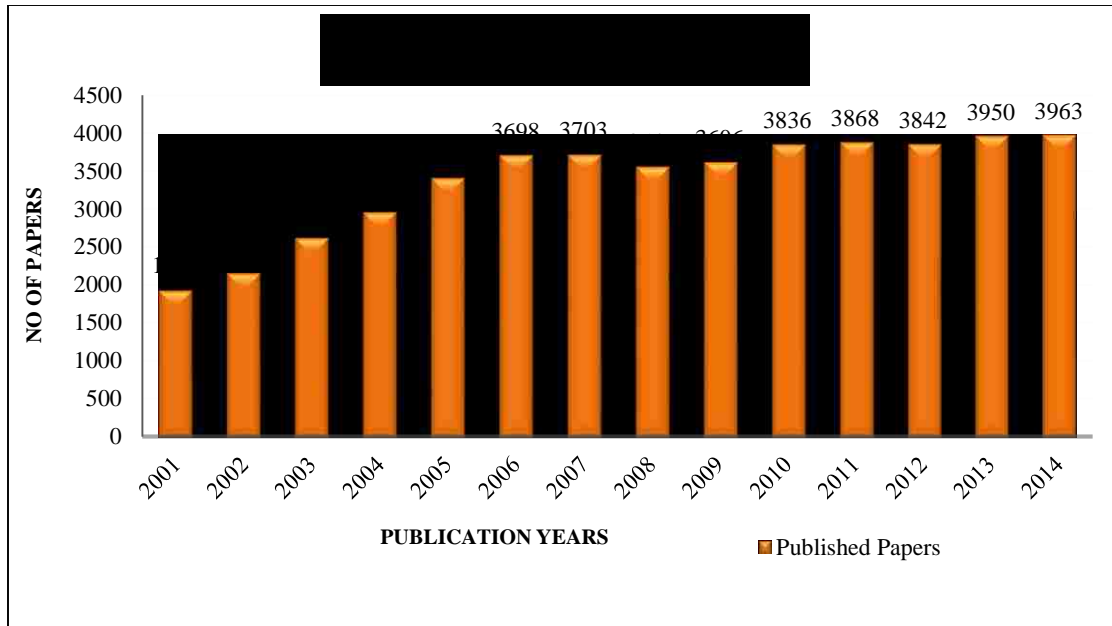


Figure 6. Trend of publication on process planning over the last 14 years

Koulmans, 1993 [67] considered the problem of determining the sequence and cutting speeds for the operations performed using the same tool with the objective of minimizing the sum of machining costs and machining speed change costs. They formulated the problem with a continuous nonlinear mathematical program and suggest an optimal solution algorithm based on heuristic algorithm.

Many researchers have also been applied the local search techniques to various operation-sequencing problems. Vancza and Markus, 1991 [68] presented a genetic algorithm for the problem with the objective of minimizing the number of set-ups, the variety of tools, and operation processing costs. Usher and Bowden, 1996 [69] suggested a genetic algorithm in which different coding schemes are suggested to reduce the size of the solution space. Ma et al. 2000 [70] reported a simulated annealing algorithm for the operation selection and sequencing problem with the objective of minimizing the sum of operation processing costs and change costs. Kim et al. 2001 [71] proposed a feature recognition based method to generate machining precedence relations systematically, based on the geometric information of the part. Limaiem and ElMaraghy, 1995 [72], Yut and Chang, 1995 [73], Irani et al. 1995 [74], Yip-Hoi and Dutta, 1996 [75], Morad and Zazala, 1999 [76] and a few other researchers reported similar models and

approaches for the process planning problems. Several researchers have explored the uses of CNC machines for rapid prototyping.

However, the use of CNC machines is hindered by complex process planning for the generation of tool path and fixturing issues. Sun et al, 2001 [77] presented an approach and algorithm to decompose the overall task especially the finishing operations in to small operations and to further decompose in to sub-operations. They presented the approaches to select the optimal decomposition values (tool diameter, surface slopes) that minimizing the machine time. Recently Gupta et al. 2011 [78] formulated a model to find the minimum cost (based on predefined data bases for speed, feed and depth of cut) for machining cylindrical parts with turning and cylindrical grinding process. Their model was able to develop all the possible sequences and generated more options by combining one or more sections during the turning process but the problem is their model has not reach the optimal solution and is dependent on the selection criteria built in the model, the user is also burdened with a lot of computations and other process inputs. Spence et al. 2014 [79] developed an environment with a higher level of intelligence and decision making ability for machining under variable geometry conditions. They believed that the fixture set up is one of the essential requirements in machining and later on the authors used the touch probe and laser scanner measurement for CNC machining.

2.6 Summary

Different techniques have been used by researchers for experimental design for the analysis of laser cladding process such as Taguchi method and design of experiments (DOE). The finite element analysis (FEA) and models are employed by many researchers for the development of bead shape prediction. The artificial neural network (ANN) and fuzzy logic techniques are also used for the predictive model development. Overlapping and stacking of the beads are the areas which have not been investigated and need predictive models to be developed in order to get better understanding and relationship of the process and its parameters and to make some 3D components as well using this additive manufacturing approach.

Some researchers like Huan et al. 2007 [36] performed quadratic regression on the measured bead width and obtained 99.2% R-square value from the regression indicating a good statistical fitting on the measured data. They also generated bead width prediction equation which provides a good reference for tool path design and a ballpark for multi-pass deposition where parameters can be fine-tuned to obtain high quality deposition. Toyserkani et al. 2004 [52] introduced a 3D

transient finite element model of LC to investigate the effect of laser pulse shaping (frequency and energy) in the process. Their model can predict the clad geometry as function of time and process parameters. Oceleik et al. 2012 [80] considered beginning and ending of the clad track and analyzed that best methods to ensure a good clad in the start/stop zone are the gradient power and the variable defocus set ups. Both methods show an increase in height of the track, where the start and end of the laser track overlaps and later on it would be machined in post-finishing procedure. Their aim was to eliminate geometrical and microstructural defects formed inside the Start/Stop zone. The defect elimination in Start/Stop zone is especially required, when a closed loop of laser clad track is desired.

A fundamental understanding of how process variables relate to deposit characteristics is essential for controlling the cladding process, and this was the goal of almost every researcher. Prediction of the power limits and other parameters to generate good quality clad such as maximum height, minimal dilution percentage and surface roughness was also the aim of many researchers. Different techniques and methods were adopted to achieve these targets. No unified experimental approach is evident, but using a design of experiments methods to develop a physical testing strategy and form a basis for subsequent analysis has been done by many researchers. Consequently, this strategy has been employed as described in detail in Chapter 4. Some researchers investigated in how to obtain a consistent and desirable microstructure and resulting mechanical properties. This research is recommended as an extension of the work performed here.

Although the literature contains several models, still there is significant lack in more accurate numerical models for single and overlapping beads which takes in to account the effects of laser heat on the clad track, temperature dependencies of material properties, melt pool geometry and laser pulse characteristics.

The review of the literature is summarized and the research gap is shown in Table 1.

Table 1. Critical Literature Review Summary

S.No	Authors	LASER CLADDING (LC) PROCESS											Comments (Methods Used)	
		Additive Manufacturing Process-AM	Laser Assisted-AM Process	Optimization of Process Parameters	Experimentation Analysis / methods	Single bead clad geometry / modeling	Overlapping bead clad -- analysis / modeling	Multiple layers and Stack ups	Modeling using various techniques	Transient heat conditions analysis	Metal deposition/repair Work	Tool Path Planning for buildups		3D build ups -LC
1	Zheng et al, 2011[81]		X			X			X					Deformation/ FEA
2	BenYounis et al,2008 [82]	X		X	X									DOE/RSM
3	Dev. V et al, 2008 [83]	X		X	X									DOE/RSM
4	Davim et al, 2008 [41]	X			X					X				DOE
5	Liao et al, 2007 [84]	X		X	X									Taguchi
6	Song et al, 2005[54]	X			X					X				Taguchi
7	Cardosa et al, 2008 [53]		X		X					X				Factorial
8	Giuliani et al, 2008 [85]	X				X				X				
9	Gangxian et al, 2011 [86]		X		X	X								DOE
10	Pinkerton et al, 2004 [87]		X				X				X			Thermal
11	Oliveira et al,2004[37]		X			X								Thermal
12	Mehmat et al, 2013 [17]		X	X	X									Taguchi
13	Alireza et al,2006 [88]		X		X	X								DOE , Taguchi

		LASER CLADDING (LC) PROCESS												
S.No	Authors	Additive Manufacturing Process-AM	Laser Assisted-AM Process	Optimization of Process Parameters	Experimentation Analysis / methods	Single bead clad geometry / modeling	Overlapping bead clad -- analysis / modeling	Multiple layers and Stack ups	Modeling using various techniques	Transient heat conditions analysis	Metal deposition/repair Work	Tool Path Planning for buildups	3D build ups -LC	Comments (Methods Used)
14	Mondol et al, 2013 [89]		X		X									DOE, Taguchi
15	XingHong et al,2010 [90]				X						X			FEA
16	Edoardo et al, 2006 [91]		X		X									DOE, RSM
17	Benjamin et al, 2013 [92]		X		X				X					Factorial, DOE
18	Karunakaran et al, 2009 [93]	X			X									FEA
19	Jeng et al, 2000 [94]		X		X						X			SLS
20	Lalas et al, 2007[95]		X		X				X					Analytical
21	Vijay et al, 2013[96]		X			X					X			
22	Glardon et al. 2001[97]		X		X	X								Bead surface, thermal
23	Mazumdar et al,2010 [98]		X			X					X			Thermal
24	Levy et al, 2003[99]	X									X			
25	Shepeleva et al, 2000 [100]		X								X			
26	Liou et al,2005[61]		X											Heat transfer
27	Suryakumar et al, 2011 [101]		X	X	X	X								DOE

		LASER CLADDING (LC) PROCESS												
S.No	Authors	Additive Manufacturing Process-AM	Laser Assisted-AM Process	Optimization of Process Parameters	Experimentation Analysis / methods	Single bead clad geometry / modeling	Overlapping bead clad -- analysis / modeling	Multiple layers and Stack ups	Modeling using various techniques	Transient heat conditions analysis	Metal deposition/repair Work	Tool Path Planning for buildups	3D build ups -LC	Comments (Methods Used)
28	Griffith et al, 1996 [102]		X					X				X		
29	Yuwen Sun et al, 2012 [103]		X		X	X								DOE, Taguchi
30	Qi et al, 2007[36]		X		X						X	X		Factorial
31	Onwobolu et al,2007 [42]		X		X						X			RSM, Scatter
32	Sreeraj et al, 2013 [44]	X		X	X	X			X		X			RSM,ANN, GA
33	Xinhong et al, 2010 [43]	X									X	X	X	CAM
34	Chande et al, 1985[45]	X									X			
35	Jouvard et al, 1996[46]		X	X	X									Heat Analysis
36	Picasso e al, 1995[47]		X		X	X								FEA/Melt pool
37	Mazumder et al. 1988[49]		X			X								Heat transfer
38	Hoadley et al.1992[50]		X			X								Thermal analysis
39	Picasso et al, 1994[47]		X			X								FEA
40	Liu & Lin et al, 2005[40]		X			X								Thermal analysis
41	Han et al, 2004 [61]		X			X								Thermal analysis

S.No	Authors	LASER CLADDING (LC) PROCESS										Comments (Methods Used)	
		Additive Manufacturing Process-AM	Laser Assisted-AM Process	Optimization of Process Parameters	Experimentation Analysis / methods	Single bead clad geometry / modeling	Overlapping bead clad -- analysis / modeling	Multiple layers and Stack ups	Modeling using various techniques	Transient heat conditions analysis	Metal deposition/repair Work		Tool Path Planning for buildups
42	Tabernaro et al, 2014[16]		X			X			X	X			Thermal analysis
43	Hofman et al. 2011[104]		X			X			X				FEA, Thermal
44	Amara et al, 2005[51]		X			X				X			FEA, Thermal
45	Toyserkani et al, 2004 [52]		X			X			X				FEA, Thermal
46	Davim et al, 2008 [53]		X		X	X			X				Regression
47	Zeinali et al, 2010 [55]		X		X	X							Fuzzy logic
48	Toyserkani et al, 2002 [9]		X		X	X							ANN
49	Liu et al, 2012 [56]		X		X	X							ANN
50	Mahapatra et al, 2008 [57]		X		X	X							ANN
51	Song et al,2008 [58]	X	X		X	X							ANN, Taguchi
52	H-K Lee, 2008 [4]		X	X	X	X			X				Taguchi
53	Kim et al, 2005 [105]	X		X	X	X							ANN, Regression
54	Nagesh et al, 2002 [106]	X		X	X	X							ANN
55	Jendrzewski, 2004 [107]		X		X	X							Thermal, crack analysis

		LASER CLADDING (LC) PROCESS												
S.No	Authors	Additive Manufacturing Process-AM	Laser Assisted-AM Process	Optimization of Process Parameters	Experimentation Analysis / methods	Single bead clad geometry / modeling	Overlapping bead clad -- analysis / modeling	Multiple layers and Stack ups	Modeling using various techniques	Transient heat conditions analysis	Metal deposition/repair Work	Tool Path Planning for buildups	3D build ups -LC	Comments (Methods Used)
56	Paul et al, 2008 [108]	X	X		X		X	X					X	SEM, X-ray
57	Ding et al, 2015 [109]	X			X	X	X		X		X			Tangent model
58	Xing J et al, 2013 [110]	X			X	X	X		X					Parabola/cosine
59	Aiyiti et al, 2006 [111]	X			X	X	X		X					Tensile test
60	Zoran et.al, 2015 [112]		X	X	X	X			X					DOE, GA
61	Gangxian et al, 2011 [113]	X	X		X	X	X	X					X	Nozzle distance
62	Shojjin et al. 2004[114]		X		X	X			X					Thermal
63	Victor et al. 2008 [115]	X			X			X		X				FEA, Thermal
64	Bi et al. 2013[116]		X		X	X		X						Temp monitor
65	Cheikh et al. 2012 [117]		X		X	X			X					Analytical
	TOTAL	20	47	11	44	39	6	5	15	1	18	4	3	

It is evident from the summary matrix Table-1 that researchers have used the cladding process for additive manufacturing and contributed significantly in analyzing and modeling of the single beads using different approaches. Mostly, Factorial and Taguchi methods have been employed for setting the experimental plan, and the data has been collected in steady state conditions.

A research gap is identified in the areas of multiple beads in overlapping and stack up conditions, as well as investigating transient heat conditions, which is the focus of this research. This research will provide a foundation for the generation of tool path planning when multiple layers and solid blocks components are to be building up. Transient heat conditions, where any of the parameter values vary during the deposition need to be further explored in different deposition scenarios.

Chapter 3

Process Overview: Laser Cladding: State-of-the-Art

3.1 Laser Cladding Method and Other Laser Surface Treatments

Laser cladding is a melting process uses a high power laser beam to melt a cladding material and a thin layer of the substrate to form a pore and crack free coating with low dilution and the process ensure a metallurgical bonding between layer and substrate. Coating thickness may vary from 0.05 mm to 3.0 mm depending upon laser spot size. The aim of laser cladding process is to deposit a clad layer onto surfaces of work pieces in order to generate functional layers or to regenerate the natural shape of parts. The material can be deposited in three different ways:

- I. by powder injection
- II. by pre-placing the powder
- III. by wire feeding

A laser beam generates a melt pool in the substrate and allows the additional material to be melted. By moving the laser beam over the surface, a solid layer is formed immediately after the laser has passed. Some researchers [118-120] believe that laser cladding by powder injection is superior to alternative processes because it is more energy efficient and it allows for better process control and reproducibility. A great variety of materials can be deposited on a substrate by powder injection. Also multi-layer cladding of the same or different materials is possible to achieve better mechanical properties or higher cladding thicknesses. Details of single and multi-layer experiments and their results are presented in chapter 5. The process is schematically shown in Figure 7.

The laser cladding process starts with the introduction of the powdered clad material through the powder feeder (pneumatic flow, gravity flow or hybrid i.e. pneumatic and vibrational). The next step involves the injection of the powder onto the substrate through a lateral or co-axial nozzle (Figure 6). In both cases the powder travels some distance through the laser beam causing the particles to be preheated or to be melted before they reach the melt pool. Once the powder is introduced with the carrier gas onto the substrate (base metal), the laser interacts (fusion reaction) with the clad powder resulting in formation of a melt pool.

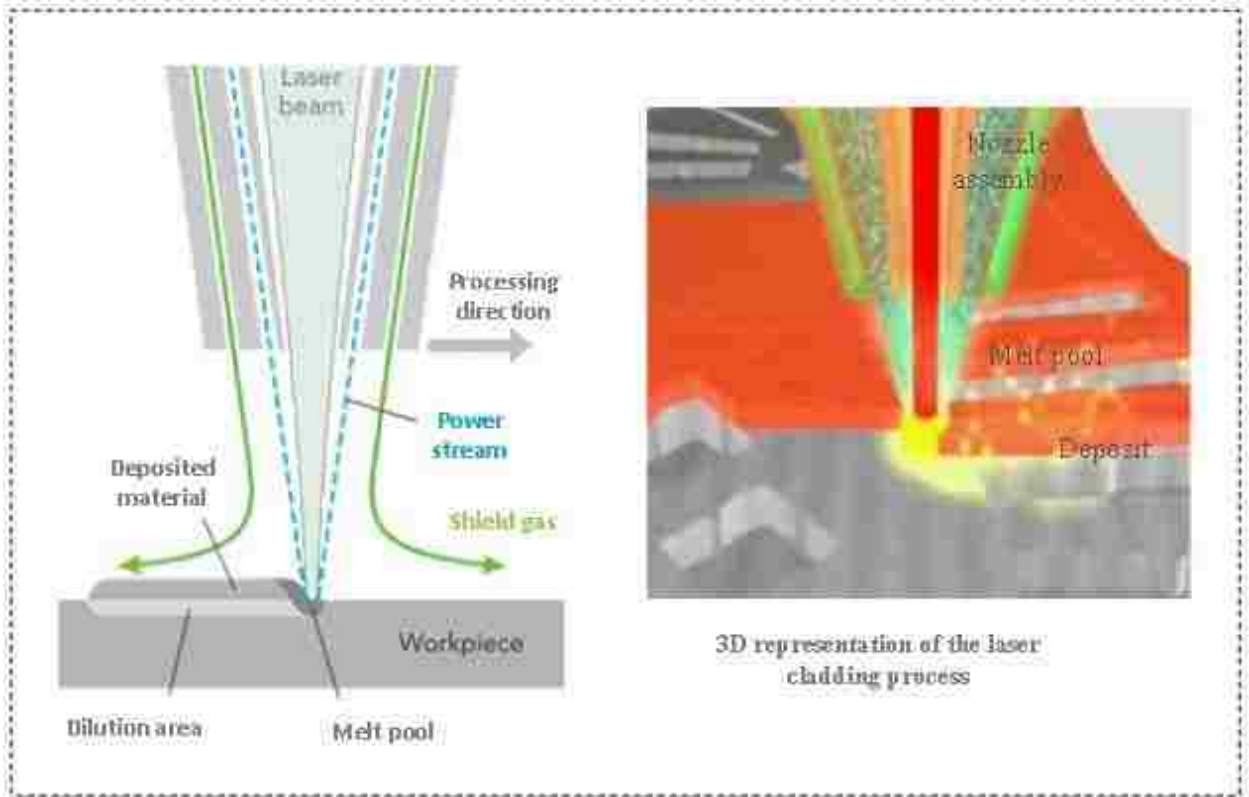


Figure 7. A schematic view of the laser cladding process (adapted from [121])

To protect the melt pool (clad area) from interacting with various atmospheric gases, a shielding gas is introduced in the system which is injected along with the powdered clad material. Thus a melt pool is created onto the substrate metal, and the metal clad track is created via the robotic arm (or other motion control system) onto which the laser system, focusing optics and nozzle are mounted. This metal clad track (single pass) is a result of the melt pool solidification along its movement. Along with melt pool, a heat affected zone (HAZ) is formed. The heat affected zone (HAZ) refers to the area of the substrate metal that has had its microstructure and properties altered due to the heat addition, but has not melted.

The clad interface usually has small dilution zone of substrate and clad material. In order to realize such a small dilution zone, the process parameters and characteristics of deposited material need to be understood. Dilution or penetration is discussed in section 3.5.1. The success of laser cladding relies on the quality of the obtained clad layer and the quality depends on a large variety of input and process parameters. Section 3.5 contains the detail of process parameters and

its effects on the geometrical shape of the clad layer. The quality of a clad layer is classified into four groups [118], as illustrated in Table 2.

Table 2. Properties of clad layers

Mechanical Properties	Metallurgical Properties	Geometrical Properties	Qualitative Properties
Residual stresses	Microstructure	Clad dimensions	Porosity
Hardness distribution	Dilution	Roughness	Crack
Wear resistance	Grain size	Dilution	
Tensile strength	Corrosion resistance		

The main problem faced in the cladding is the selection of optimum combinations of process parameters for achieving desired clad bead geometry. Cladding is a multi-input/ multi-output, nonlinear, highly coupled process. There are significantly more process inputs than the outputs. Some of the major associated parameters with this process are mentioned in Figure 8.

Infact, it is the true combination of parameters and properties (table 1) which makes the laser cladding process unique from other laser surface treatments. The different surface modifications techniques which are currently being used in the industry are briefly summarized in Table 3. Each of the techniques has some advantages over other processes and sometimes they are used on a large scale.

Table 3. Surface modification process

Surface Modification Process	Process Characteristics
Laser	-Low heat input, thin layers, low dilution and porosity, high hardness, small HAZ, high initial equipment investment
Welding	-MIG/TIG- reasonable bond, medium heat input -Submerged arc -Oxyacetylene –liquid/solid bond, high heat input --- Shielded metal arc -Plasma arc –thick layers, high deposition rates, low equipment cost, covers large areas ,high heat input and part distortion
Spraying	-Flame powder-no dilution, no deformation to base metal
Physical vapor deposition	- Sputtering - Vacuum coating

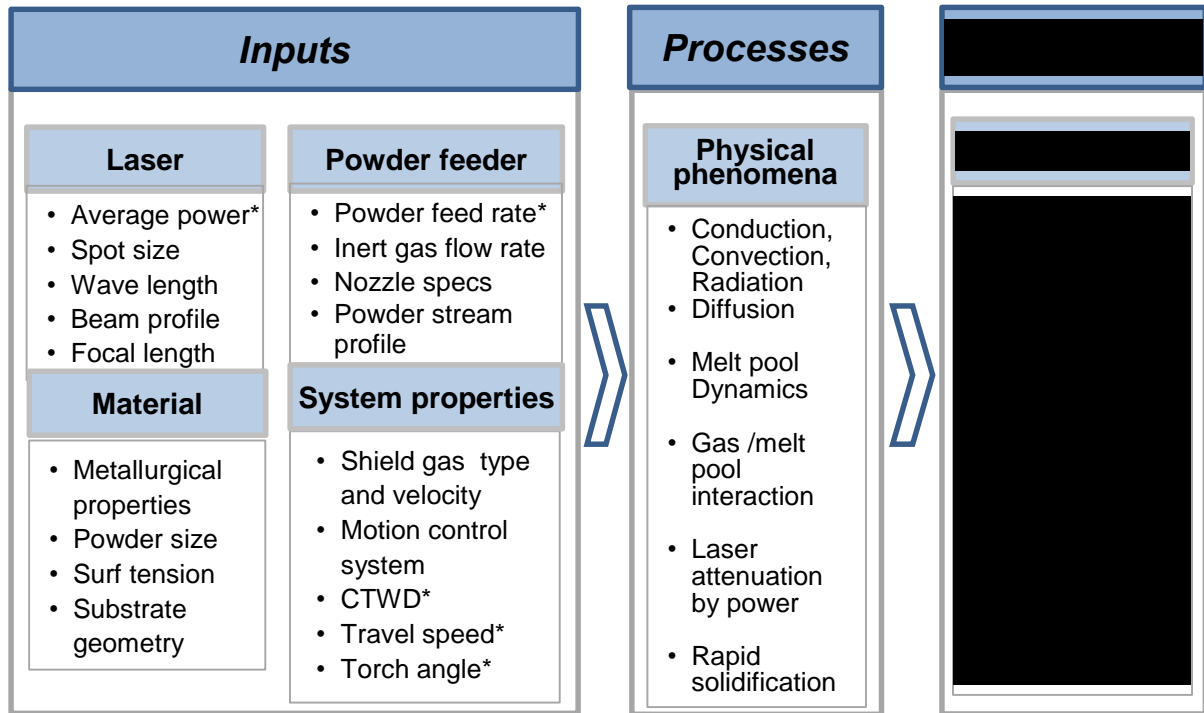


Figure 8. Inputs, processes and outputs parameters are shown with powder injection laser cladding.

The research scope for this work targets the laser cladding process specifically for the 420 stainless steel powder, using a fiber optic laser with a 4.3 mm spot size, Argon shielding gas, and a co-axial nozzle in a robot cell (ABB robot). Experiments were performed with single beads and multiple beads and with different depositing scenarios. Single beads are used in repair works of mold and die sets where the width of the bead is mainly correlated to the diameter of the laser beam while the overlapping beads are generally used to coat a surface of a metal to enhance the metallurgical properties. Chapter 4 describes the experimentation process in detail.

3.2 Laser Cladding (LC) versus Selective Laser Sintering (SLS)

The laser cladding and selective laser sintering considers as a layered additive manufacturing methods. Laser cladding is a blown powder while selective laser sintering (SLS) is a powder-bed system technique that also uses a high power laser to fuse small particles of plastic, metal and ceramics in to a mass representing a desired 3D object. The SLS fuses powdered material by scanning cross sections generated from a 3-D digital description of the part (for example from

CAD file or scan data) on the surface of the powder bed. After each cross section is scanned, the powder bed is lowered by one layer thickness, a new layer of material is applied on top, and the process is repeated until the part is completed. SLS (Fig. 9) does not require binders or support structures due to the fact that the part being constructed is surrounded by unsintered powder at all times. SLS relies on higher-powered lasers to compact and sinter metal powders.

Compared to other rapid manufacturing methods, SLS can produce parts from a relatively wide range of commercially available powder materials, including polymers and polystyrene, as such there is no or very little waste in this process.

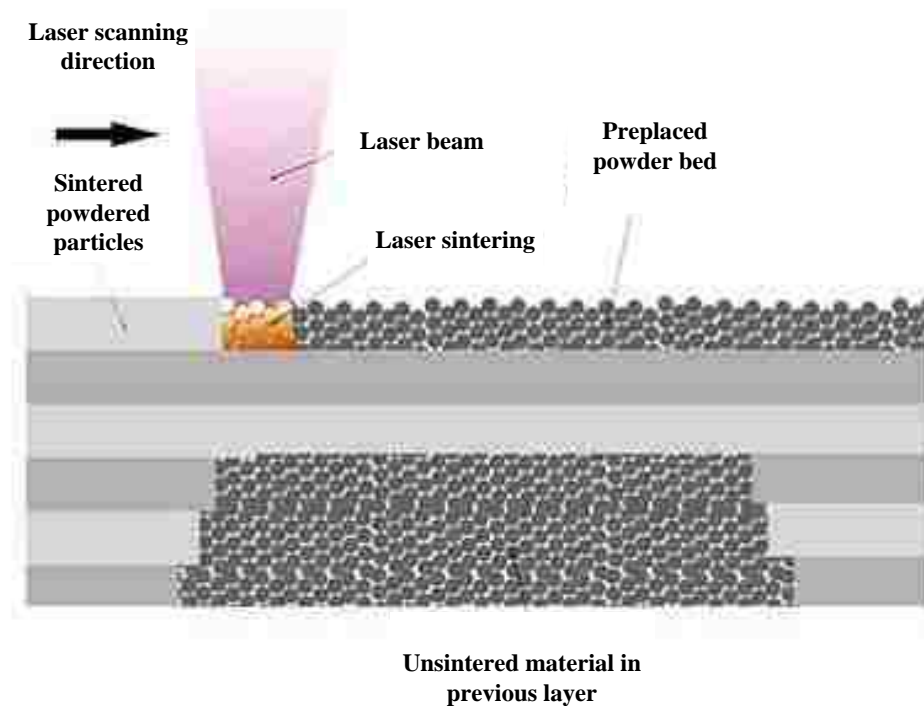


Figure 9. A schematic of Selective Laser Sintering process (SLS)[adapted from[122]

3.3 Effects of Process Parameters on Clad Layer Geometry

Laser cladding is a complex environment and selection of input process parameters is the key to obtain the desired clad track. The effects of these parameters on clad bead quality characteristics have been studied by many researchers [2, 9, 15-16]. Many process parameters

influence the bead geometry non-linearly, and the bead characteristics are varying for single bead and also in overlap bead conditions.

The process parameters or input variables investigated in this work are the:

1. Powder feed rate
2. Laser power
3. Travel speed
4. Focal length of the lens, and
5. Contact tip to work piece distance (CTWD).

These five input independent variables are varied to explore their impact on the bead height, width, penetration depth, dilution area, and the bead shape. The geometric shape nomenclature and an experimental sample for the single bead are illustrated in Figure 10 and Figure 11 respectively.

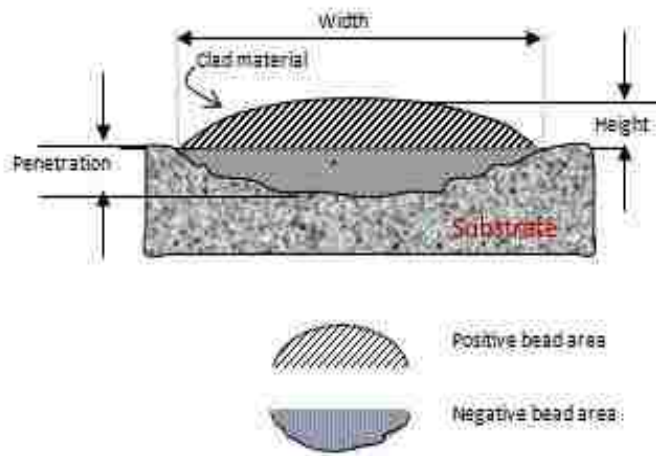


Figure 10. Cross section view of a single bead notation

The Figure 10 shows the scheme with typical cross section of a laser clad bead and defines the main geometrical quantities usually used for laser track characterization: clad width (W), clad height (H), clad penetration (P), the positive bead area A_p , and the ‘negative’ bead area A_n , which is the melt pool region, also seen in Figure 9.

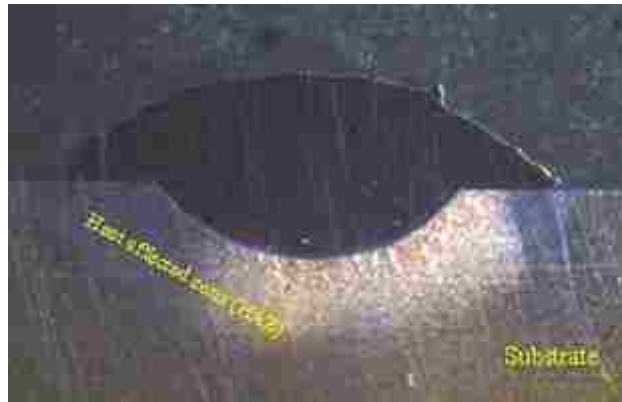


Figure 11. Cross section view of an experimental sample

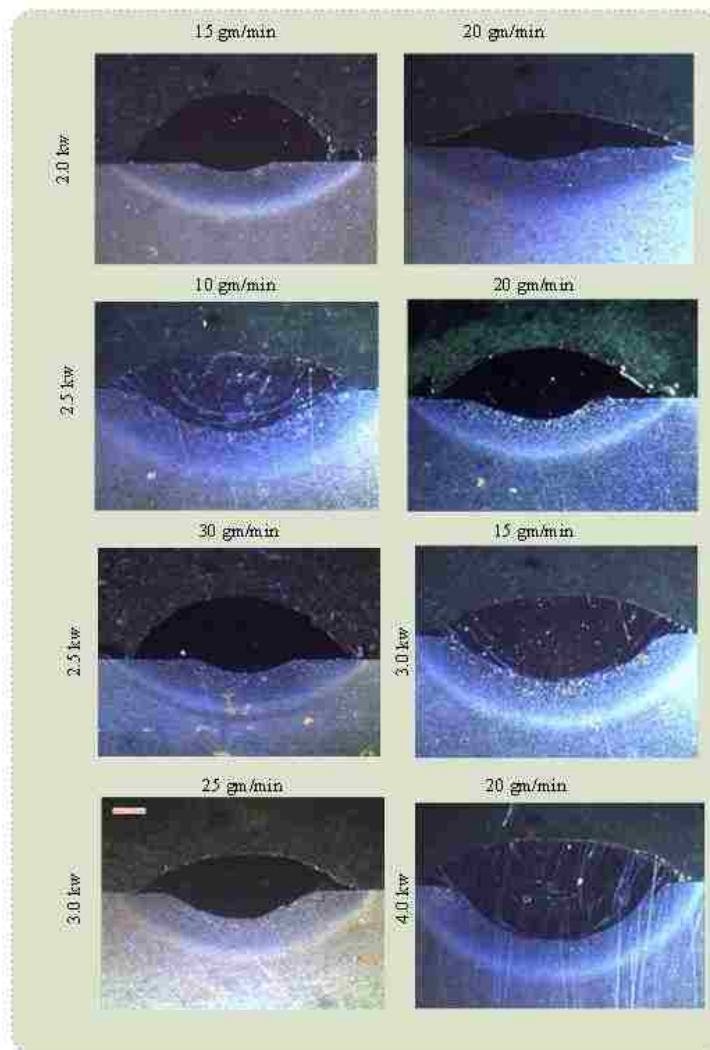


Figure 12. Different bead cross sections showing the impact of varying process parameters on the bead shape

Changing the travel speed will obviously change the bead width, height, and penetration characteristics, but is the rate of change for each linear? What is the impact of the contact tip to work piece distance (CTWD) on the resulting geometry? This area is unattended so far by the researchers and these questions need to be answered. For a desired bead shape, process parameters need to be set. The experimental plan was formulated to capture the impact of these parameters on single and overlapping beads, are presented in chapter 4. The results of the experiments have identified the extent of the contribution of each input variable and key interactions and their impact on the output. The bead shape to process parameter relationships are explored and predictive models are developed using analysis of variance, a 'lumped parameter model, and artificial neural network (ANN) approaches, are described in chapter 5. Figure 12 is a snap shot of bead cross sections which represents the impact on bead shape by using different process parameters settings.

3.3.1 Effects on Penetration or Dilution of the Base Metal

With laser cladding, the clad interface usually has a small dilution zone of substrate and clad material. In order to realize such a small dilution zone, the process parameters and material combinations have to be adapted to the geometrical boundary conditions of the work piece. The basic difference between cladding and welding is the percentage of dilution [15]. The properties of cladding are significantly influenced by dilution obtained. Hence control of dilution is important in cladding. The clad layer is characterized by several geometrical quantities. The quantities h_c , w_c and A_p and A_n (Figure 13) are defined as:

h_c -----clad height (mm)

w_c ----- clad width (mm)

A_p -----Positive bead area

A_n -----Negative bead area

The areas of A_p and A_n are the clad material and molten base material area respectively. An important quality measure is the dilution (D_c) of the individual clad layer. Salehi, 2005 [119] used the iron content to determine the dilution using the concentrations of a specific element in the layer, the supplied clad material and the substrate material.

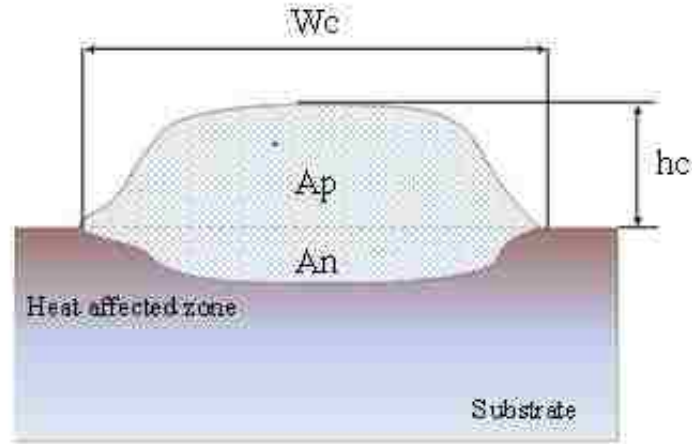


Figure 13. Schematic cross section of a clad layer

The following equation-2 is used to calculate the dilution:

$$D_C = \frac{L_{Fe} - P_{Fe}}{S_{Fe} - P_{Fe}} \quad (2)$$

Where,

P_{Fe} , L_{Fe} and S_{Fe} are the iron concentration in the supplied powder, the clad layer and the substrate material respectively.

Most of the researchers have used the bead geometrical area to calculate the percentage dilution, which is the relation between the area of the molten substrate material and the total area (eq-3) of the molten layer.

$$D = \frac{A_n}{(A_p + A_n)} \times 100 \quad (3)$$

In order to obtain a surface layer which is hardly diluted by the substrate material, this ratio has to be as small as possible. However if the ratio is zero, there is the risk of no fusion bonding between cladding material and substrate. Therefore a dilution between 2% and 10% is generally accepted. A low dilution value of 9% and a high dilution value of 48 % are observed during the experiments and illustrated in Figure 14.

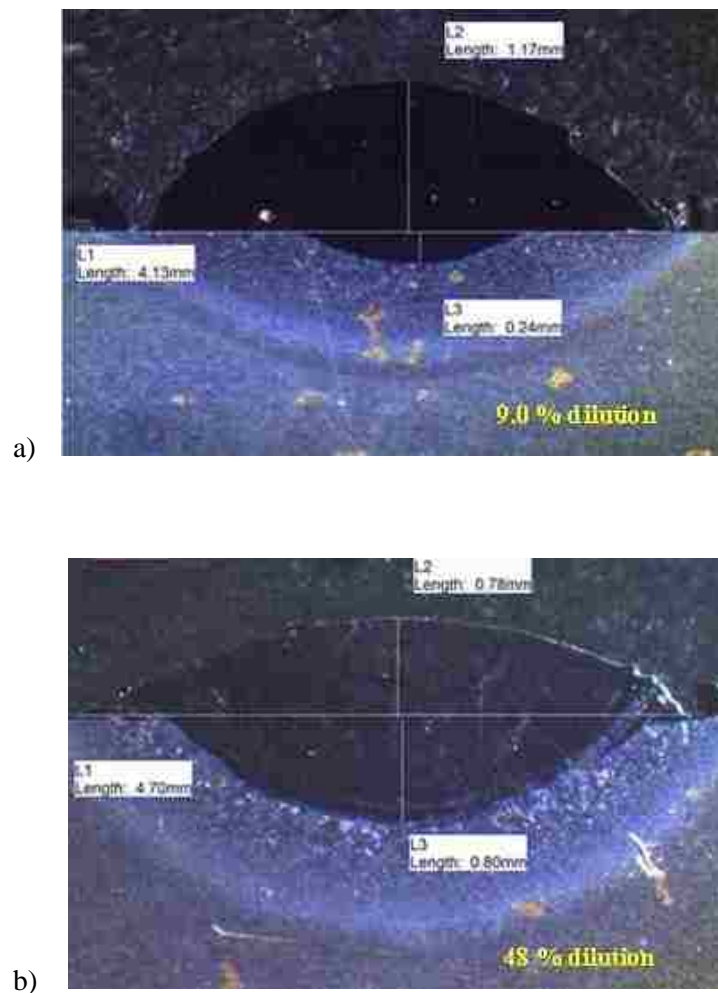


Figure 14. Cross section views of the clads a) low dilution (9.0 %) and b) high dilution (48 %) values are shown

3.4 Feedback Control System in LC

The feedback control system within the industrial partner's system uses an online camera to detect the melt pool width, using in-house developed control software. The melt pool dimensions are determined in real time from the digital images of the melt pool using the developed software. The idea of decreasing/increasing power during cladding has appeared in the work of Mazumder et al. [24] with the aim to control the overall height of overlapped laser tracks in metal deposition process.

In this research work, for some experimental samples, an online camera was used to monitor the variation in melt pool width during the cladding process and graphs are generated for the bead

width through the feedback system but no adjustment to laser power was made based on the feedback because that work is beyond the scope of this research. The details and the illustrations are mentioned in section 4.5 (transient beads).

The system works in a way that an optical fiber cable (600 μm) transports the beam to an optical system which is mounted on six-degrees of freedom industrial robot, enabling the cladding of complicated three dimensional surfaces. The beam is focused on to the work piece. This system consists of a lens which converts the diverging beam to a parallel beam. A focus lens focuses the beam imaging the fiber end on the work piece. A mirror is placed at an angle of 45° to the optical axis in the parallel beam. This mirror is transparent for the laser radiation, but reflects visible light. In this way, a camera or sensor system can view the cladding process coaxially with the laser beam, as illustrated in Figure15.

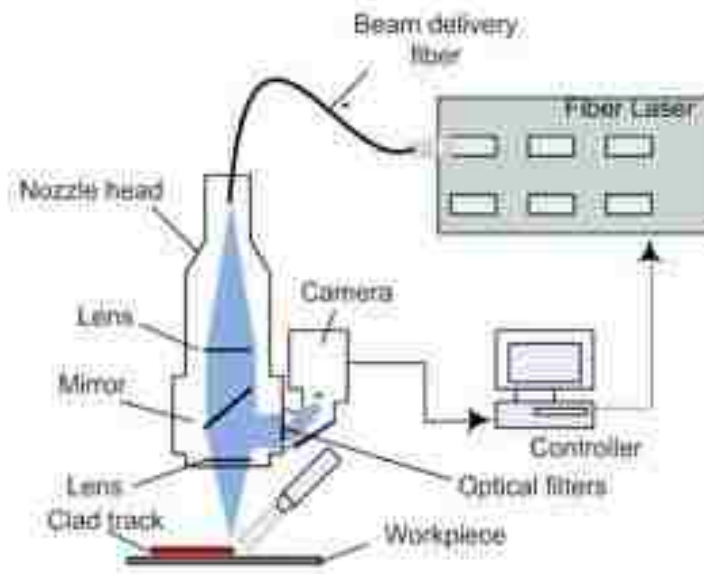


Figure 15. Schematic overview of laser cladding with camera control system

Images from the melt pool are transferred from the camera to the computer at a frame rate of about 200Hz. The LC process is complex and numerous input and output parameters are involved. Besides, the process is extremely sensitive to small changes in the operating conditions. Additionally, some of the parameters are not inherently measurable or the measurement is not practical. So the control of clad width or height has a great impact on the improvement of the produced clad and in turn, of the final part.

Chapter 4

Experimental Methodology

4.1 Experimental Design and Methodology

In general, experiments are conducted to study the performance of processes and systems. A well-designed experiment is important because the results and conclusions that can be drawn from the experiment depend to a large extent on the manner in which the data are collected. Well-designed experiments can often lead to a model of system performance. It can usually visualize the process as a combination of operations, machines, methods and other resources that transform some input into an output that has one or more observable response variables. Some of the process variables are controllable and some are uncontrollable as illustrated in Figure 16.

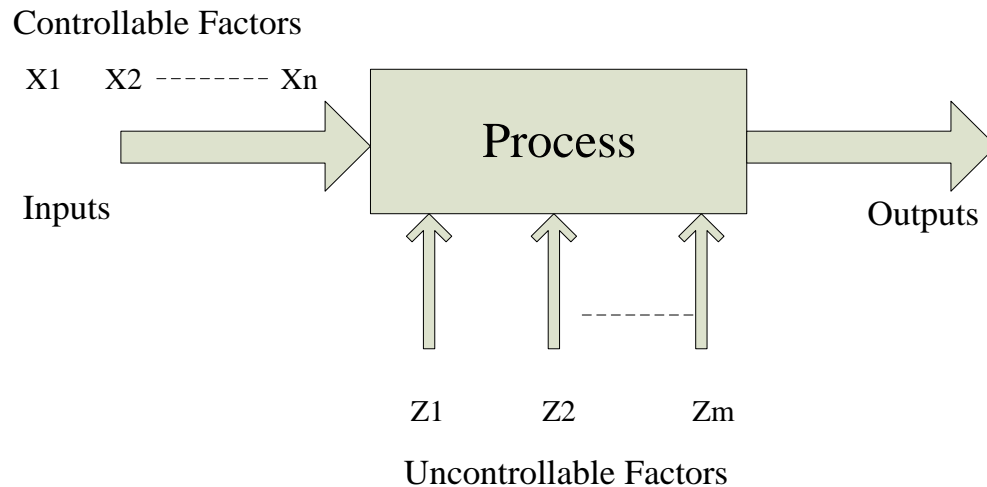


Figure 16. General model of a process or system [adapted from (123)]

The objectives of the experiment may include the following:

1. Determining which variables are most influential on the response output
2. Determining where to set the influential factors (controllable factors) so that output is always near the desired value
3. Determine to set the input factors so that variability in response is small

4. Determine where to set the controllable factors so that the effects of the uncontrollable factors are minimized.

Prior to the design of experiments, the process parameters in laser cladding process and their ranges should be determined based on the equipment conditions and preliminary studies. In this research, facility of an industrial partner is used to conduct the experiments. Due to the equipment limitation, the laser spot size was fixed but the laser power, scanning speed and powder federate etc. are selected as adjustable process parameters, which can be seen in Table 4. For the research purpose, an experimental plan was derived that covers single bead, multiple beads and some stack up cladded models experiments, as shown in Figure 17.

Typically, factorial experiments are used in designing of an experiment technique (DOE), where multiple variable are grouped together instead of one variable at a time. A full factorial designed experiment provides possible combinations of its process and factors to constructs an approximation model that captures interactions between various variables. In a factorial design, the total experimental runs are defined using the following mathematical expression:

$$N = L^F \tag{4}$$

Where,

N= total number of experiments

L= Total number of Levels (in process parameters)

F= Total number of factors (ranges of factor level)

For this research, five levels of process parameters and five levels of factors are chosen to conduct the experiments. If equation-4 is used, the total number of experiments would be $N= 5^5$ (i.e.3125 experiments), which is practically impossible to conduct that many numbers of experiments because of time restriction and money constraint. Determining alternative approaches or best practices is necessary as there are many other approaches that have been used in the past by various researchers in setting up experimental plan for the data collection. Researchers have utilized design of experiments (DOE) approaches such as response surface methodology (RSM), Taguchi methods and fractional factorial approaches for a variety of metal deposition processes. This research work uses Central Composite Design (CCD), which is one of the kinds of the response surface methodology in order to reduce number of experiments and to get the desired output. Sub-section 4.1.2 describes the CCD in detail and the remaining sub-

sections follow the experimental plan as mentioned in Figure 17. Some preliminary work for building a symmetric thick walled shell (cone and parabolic model) has been done and discussed in section 4.8.

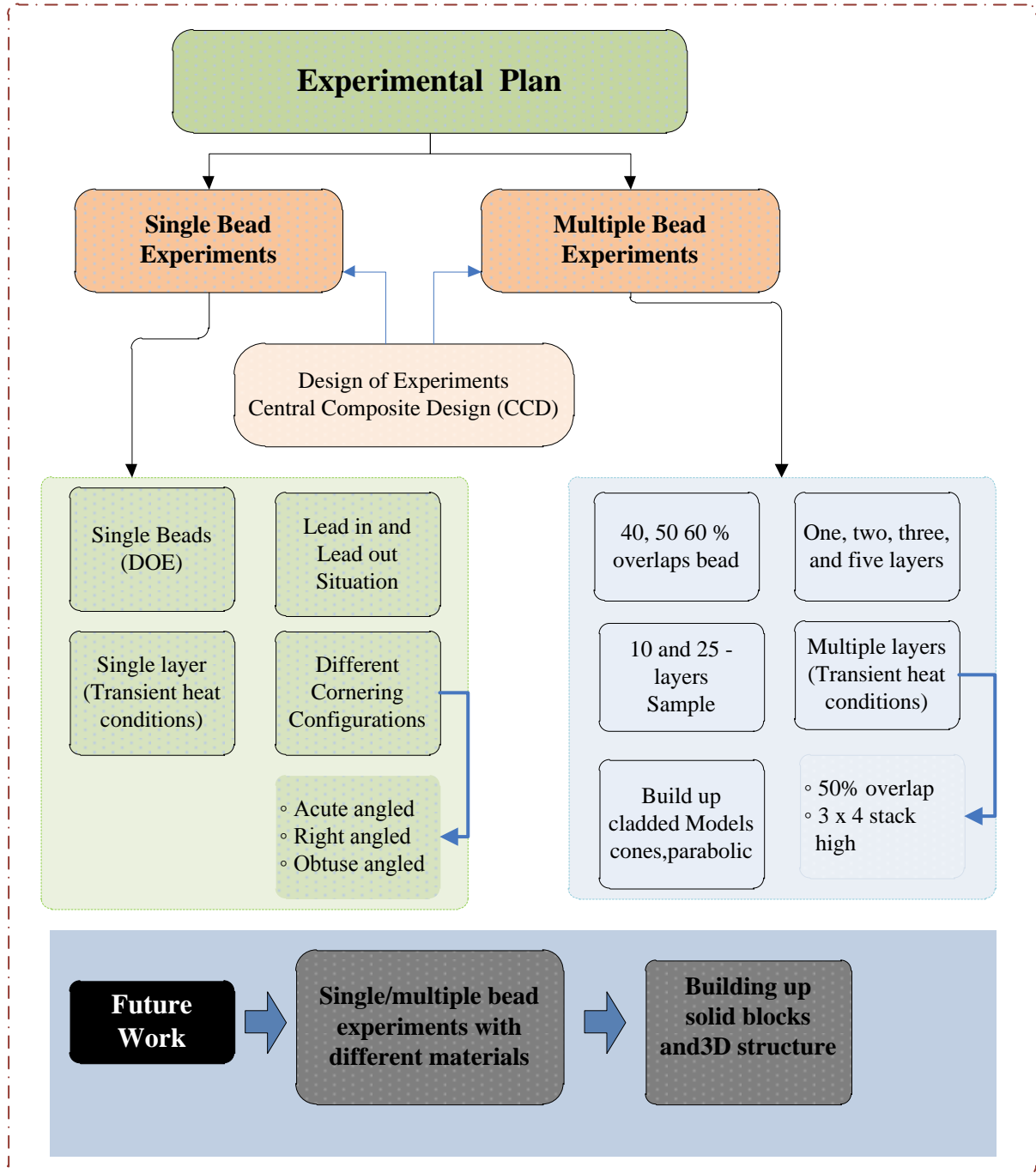


Figure 17. Flow chart of the experimental plan for this research

4.1.1 Experimental Design Parameters

To set up the experiments, some factors were kept as static parameters (Table 4a) for all single beads and multiple beads samples. It is evident from the literature review that majority of researchers focused on the travel speed, power levels and powder/wire feed rate. The following five process parameters (independent variables) (Table 4b) and their five ranges or levels are considered for the experiments based on previous researchers work and the experience of the industrial partner:

Table 4a. The static parameters used for the experiments

Constant Factors	Specification
Workbench angle	0 (degrees)
Laser torch angle	90 (degrees)
Shielding gas	100 % Argon gas
Base material (Substrate)	Cold rolled structural steel
Powdered material (Clad)	420 Steel powder
Nozzle type	Co- Axial nozzle
Tip- Size (diameter)	4.3 (mm)
Grain size	55 ~ 160 μm

Table 4b. The experimental design parameters and their levels

Parameters	Units	Notations	Factor Levels				
			-2	-1	0	1	2
Laser power	kW	PW	1	2	2.5	3	4
Powder feed rate	grams / min	FR	10	15	20	25	30
Laser speed	mm/sec	LS	5	7.5	10	12.5	15
Focal length of lens	mm	FL	380	390	400	410	420
Contact tip to work piece distance	mm	CTWD	21	22	23	24	25

The factors chosen for evaluations (section 3.3.1), also known as dependent variables are mentioned below:

1. Bead width

2. Bead height
3. Bead depth (penetration)
4. Positive bead area
5. Negative bead area
6. Dilution

The design of experiments (DOE) approach is utilized to develop an experimental plan to identify key parameters and interdependencies with a minimal amount of data. Still the data collection is extensive due to the number of parameters and their ranges, where each factor is varied over five levels. A thorough analysis of the bead shapes and the shape errors are explored with respect to the process parameters. In this work, the statistical analysis technique (analysis of variance, ANOVA) is applied to investigate the correlation between the cladding geometry and process parameters. To investigate the effect of these parameters, the central composite design (CCD), the most popular experimental design with a fractional factorial, is developed using the statistical software, Mini Tab 16. The next sub-section highlights the features of the central composite design.

The predictive models are also developed by assessing the observed effects of the process parameters on the bead shapes. These models development are explained in detailed in chapter 5.

4.1.2 Central Composite Design (CCD)

A central composite design is used to find the optimal setting of the variables and also plot the response surfaces. It is one of the types of the response surface design or methodology (RSM), which is an advanced DOE technique that helps better understand and optimize experiment's responses. RSM is often used to refine the models after important factors are determined using factorial designs especially when a curvature is suspected in response surface. It is a set of techniques used in the study of relationships between one or more responses and a group of variables. It is also referred to as the process of identifying and fitting an appropriate response surface model from the given experimental data. This surface can be nonlinear.

A CCD design is considered the most superior class of design for fitting a second order model [123]. It consists of end points or cube, axial points and center points. The axial points are mathematically calculated as $2 \cdot F$, i.e. twice the number of factor levels. The center points should always be selected between 3 and 6 to maintain maximum stability of the system. The remaining points out of the total experimental runs are the end points. A system of F factors for a first order

system produces a 2^F experimentation runs. In case of second order model systems, an alternative 3^F design is also available. The benefit of such a design is that the total numbers of experimental runs (N) are way less than that of full factorial approach. Visualization of this technique is illustrated in Figure 18 (a) and the CCD for this work is shown in Figure 17 (b).

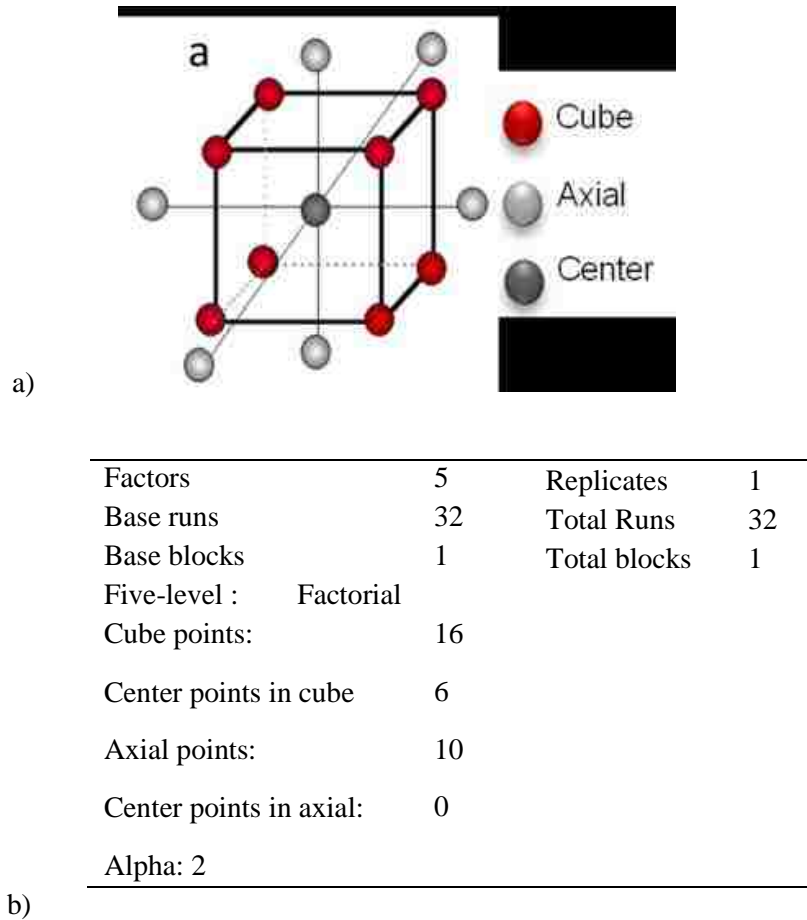


Figure 18. a) CCD demonstration (8-end points, 6 axial points and 1 center point), b) CCD parameters used for this research (generated by Mini Tab)

In a CCD, each factor has five levels (extremely high, high, center, low, and extreme low) which can be coded between the ranges of -2 to +2. The total number of experimental runs for a CCD is defined by the following equation:

$$N = r \cdot 2^F \quad (5)$$

Where, N= Total number of experiments, r = Replicates, F= Levels of factors

So, for this research, the experiments are replicated 3-times to reduce the experimental noise with 5-levels of factors, so the equation-5 would become:

$$N = 3 * 2^5 \quad (6)$$

N = 96 experiments

Hence, the totals of 96 experiments were performed (32 experiments with 3- replicates) for the single bead experiment only.

4.1.3 Experimental Design Matrix for Single Bead Experiments

From the literature, it is apparent that DOE techniques have been successfully utilized in laser cladding methods and even in welding applications as well, although the parameters being assessed, their setting and the evaluation techniques vary. Once the experimental outputs are chosen and the factors are selected (Table 4) and coded between [-2, +2], the next step is to develop a design matrix.

As mentioned earlier, the CCD design is selected for this work which contains two important parameters, one is alpha (α) and the other is numbers of center points in the cube. The value of alpha is computed as the fourth root of the total experiments i.e. approximately 2 (using 32 experiments). The number of center points that are used in constructing a stable design is 6, as mentioned Figure 18 b.

Lastly, a statistical software Mini Tab 16 environment is used along with a central composite design approach to define the experimental runs, as illustrated in Table 5. It shows the different combination of experimental runs. The experiment number 13, 17, 22, 23, 24 and 29 are all set a midpoint runs or center point of the design to increase the stability of the overall design. These 32-experimental runs are combinations of manufacturing process parameters which are used to collect four bead shape parameters for single bead configuration. This experimental design matrix is also used for overlap bead configurations as well, details of which are mentioned in section 4.3.

Once the experimental design matrix is set up, the next step is the sample preparation and the measurement techniques. The following sub-section describes the material selection, assumptions, the apparatus requirement etc. for the data collection.

Table 5. Experimental Configurations generated for sample collection

Runs	FR	PW	FL	LS	CTD
1	-1	-1	-1	-1	1
2	2	0	0	0	0
3	1	1	-1	-1	1
4	0	0	0	0	-2
5	1	-1	-1	-1	-1
6	1	1	-1	1	-1
7	-1	-1	-1	1	-1
8	-1	1	1	-1	1
9	0	0	0	0	2
10	0	0	-2	0	0
11	0	0	0	-2	0
12	1	-1	1	1	-1
13	0	0	0	0	0
14	1	1	1	1	1
15	0	2	0	0	0
16	-1	-1	1	1	1
17	0	0	0	0	0
18	1	-1	-1	1	1
19	1	1	1	-1	-1
20	-2	0	0	0	0
21	-1	-1	1	-1	-1
22	0	0	0	0	0
23	0	0	0	0	0
24	0	0	0	0	0
25	-1	1	1	1	-1
26	-1	1	-1	-1	-1
27	-1	1	-1	1	1
28	1	-1	1	-1	1
29	0	0	0	0	0
30	0	0	0	2	0
31	0	0	2	0	0
32	0	-2	0	0	0

4.2 Cladding Material and Measurement Technique

The experiments are conducted on low carbon structural steel plates also known as coupon (plates size vary depending on the experiment type) where 420 stainless steel powder (a steel alloy commonly used in injection molding) is deposited on it using the coaxial powder flow laser cladding method. A robotic based laser cladding cell, equipped with a rotary table is employed for this research and is illustrated in Figure 19.



Figure 19. Laser Cladding work cell utilized for this research [Courtesy to industrial partner]

The experiments are performed based on Table 4 and Table 5 with 3-replicates of each run. For this purpose, a maximum of 4.0 kW diode laser power is used and laser spot size is kept at 4.3 mm through the experiments. The 420 powder steel is delivered through a concentric nozzle (Figure 20) with the argon gas. The nozzle assembly is a part of the laser beam delivery head and is mounted on the Z-axis, while the work piece stays stationary.

To avoid potential time lag between powder hopper and the molten pool, the powder feeder is turned on 5 s before the laser deposition begins. Argon gas is also used as carrier and shielding gas in order to ensure powder conveyance and to limit oxidation. The single bead experiment set up is shown in Figure 21 where the sample coupon can be seen and is mounted with F-clamp. The 3-inch single bead is marked with “I” and “O” which represents the lead-in and lead-out direction respectively.

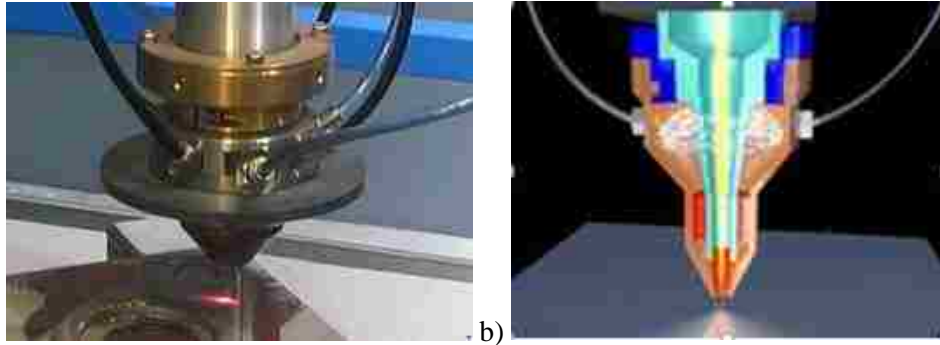


Figure 20. a) A coaxial nozzle with a visible laser spot size used for the experiments b) section view of the nozzle [courtesy of the industrial partner]

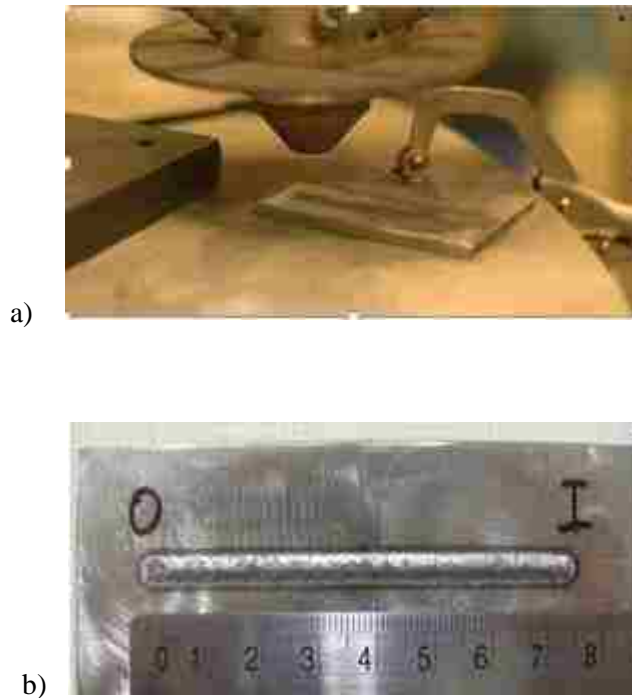


Figure 21. a) Single bead sample is being prepared b) Single bead is shown in 3.0 inches length [Courtesy of the industrial partner]

The Table 6 incorporates a list of equipment that is used for all the experiments. Once the experiments are set up and all the samples/coupons have been prepared; the next step is to process them and to collect the desired bead shape parameters. The following sub-section mentions the details of the process needed to perform the post processing on generated samples.

Table 6. Equipment used for the experiments

Constant Factors	Specifications
Microscope (Imaging)	Olympus SZX12
Abrasive Cutter	Buehler, Oscillamet
Mounting Press	Leco, PR-32
Flush Mount Variable	Buehler, Ecomet 12
Polisher/ Grinder	Speed Grinder & Polisher with Automet 3000 Power head
Etching Solution	Nitric hydrochloric glycerol (10 ml HNO ₃ , 20-40 ml HCL and 30 ml glycerol)
Gas Mask	Gas respirator face mask
Fume Hood	Lincoln electric mobiflex 200-M fume extractor

4.2.1 Sample Preparation Process and Post-processing

Majority of the specimens developed for this research are sectioned from the center (where the clad shape reaches its steady state) using a manual 16"-abrasive cutter and/or electric discharge machine (EDM) and then mounted on sample mounting machine. Some of the samples that are made with transient heat conditions are processed in a different way because of their size, which is explained in section 4.5. An illustration of mounted samples (three in number) is shown in Figure 22.

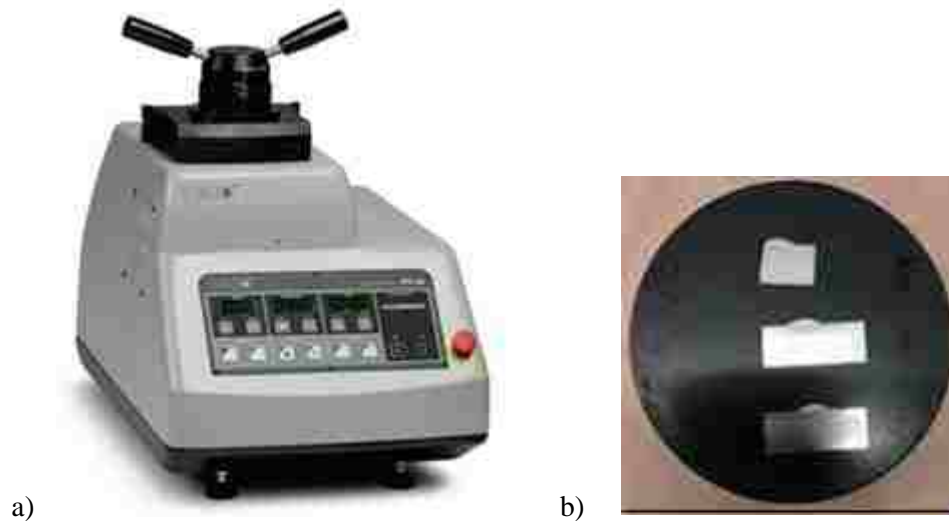


Figure 22. a) Sample mounting machine b) Three mounted samples at a time

Before putting under the microscope, all samples are grinded with Si C abrasive grinding paper with common grit size ranging 120 to 600 microns. The deposition heights, widths and dilution depths are measured with Image J-software equipped with the optical microscope (Fig. 23), and data are collected.



Figure 23. Optimal Microscope attached with computer

The response variables or the outputs of these experiments are mentioned in Appendix B. There are many factors that affect the quality of the deposited clad such as amount of material deposited, heat absorbed by the substrate and also the dynamics of the molten metal etc. Three replicates of a bead section are illustrated in Figure 24; deviations are clearly seen between these beads. Therefore numerical modeling can give some insight to this cladding process. This is explained in chapter 5.

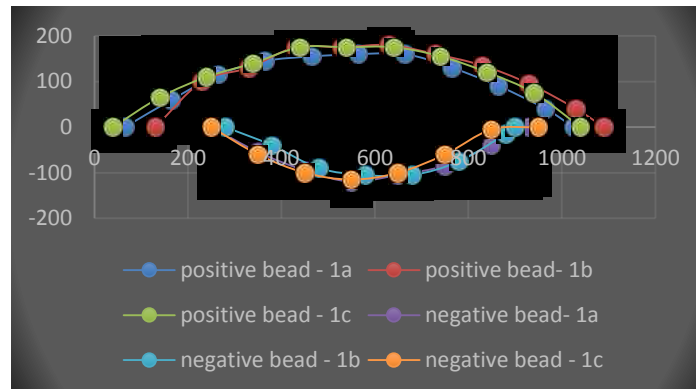


Figure 24. Deviation in the height and penetration is shown for a bead with replicates (pixel units)

The processing flow chart for sample preparations is shown in Figure 25.

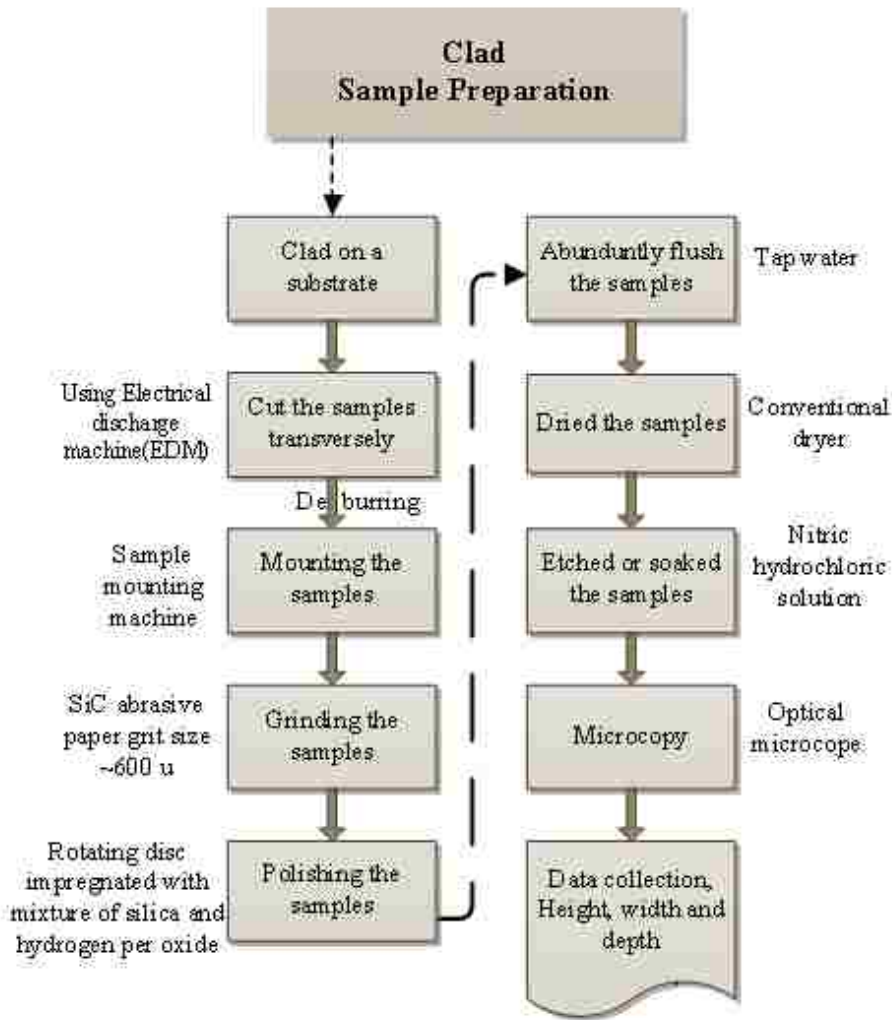


Figure 25. Process flow diagram of samples preparation

4.3 Overlaps Bead Experiments (40 %, 50% and 60% overlaps)

Single bead followed with stacking of beads are generally used in repair work of mold and die sets, whereas overlapping beads are used to coat a surface of a metal to enhance the metallurgical properties of a substrate. The bead overlap configurations experiments are planned to set at 40%, 50% and 60% overlaps with a three pass bead formation but those are replicated twice because of the time and cost constraint. The sample preparation for the overlap configurations follows the same method and process parameters as described for the single bead

experiments. The 50% overlap configuration design matrix is shown in Appendix C. Figure 26 shows the cross sections of the 3-bead formation with different percentages of overlaps. The geometric shape nomenclature for the overlapping beads is illustrated in Figure 27.

Once the samples are prepared, they are analyzed under an optical microscope to determine the bead geometrical measurements. Depending on the size and profile of the bead, a certain magnification is set in the microscope to get the shape parameters, and these are briefly described below:

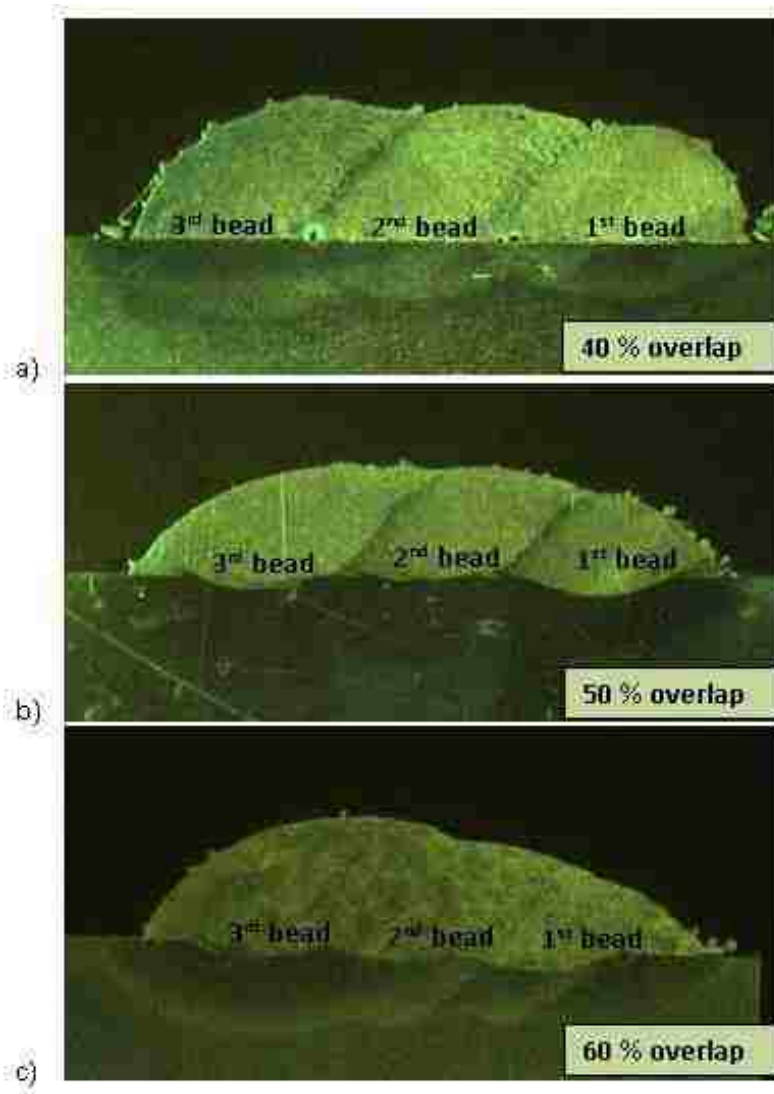


Figure 26. Sectioned views of 3-passes a) 40 % overlap b) 50% overlap and c) 60% overlap beads

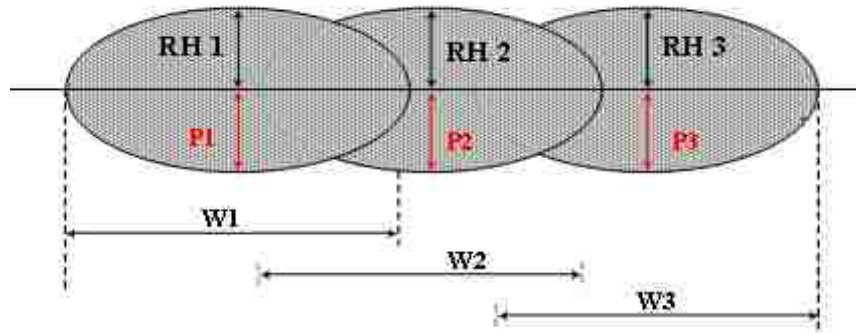


Figure 27. Schematic of cross sections of a 3-bead overlap formation

- 1) Reinforcement height of the bead (RH) ----- the reinforcement height is the maximum vertical distance between the substrate metal and the deposited clad material of the bead or it a maximum longitudinal measurement from the top of the base metal to the outer boundary of the cross sectional bead in the positive Y direction. The reinforcement height is also known to determine the strength of the clad bead and is highly dependent on the feed rate of the clad powder material.
- 2) Width of the bead (W) ----- the clad bead width is the maximum width of the clad metal deposited or it is also a maximum latitudinal distance of the cross-sectional bead in positive X direction.
- 3) Penetration or depth of the bead (P) ----- the penetration is the maximum vertical distance between the outer boundary of the substrate material and the boundary of the fusion reaction inside the substrate. It is also known as the maximum longitudinal distance between the top of the base plate to the boundary of the cross sectional bead created by fusion reaction of the laser heat,, i.e. the boundary just before the starting of the heat effected zone (HAZ) in the negative Y direction. According to the literature, penetration depth is increases with the increase of laser heat and decreases with the high travel speed and nozzle diameter [53].

- 4) Area of the positive bead (A_p) (Fig 12) ----- this is the enclosed space between the top boundary of the base metal and the extent to which clad material is deposited. It is generally affected and depends by the width and height of the deposited clad.
- 5) Area of the negative bead (A_n) (Fig 12) ----- this is the enclosed space between the top boundary of the base metal and the extent to which fusion reaction occurs within the base metal. It is generally affected by the clad width and its penetration.

There are only 3-sets of bead width (W_1, W_2, W_3), reinforcement heights (H_1, H_2, H_3) and penetration (P_1, P_2, P_3) in all configurations of overlap i.e. 40%, 50% and 60 %, since the overlapping experiments are restricted to a single pass 3-bead formation. Hence the above mentioned parameters are studied and modeled for this work with respect to five process parameters and are presented in section 5.2.

4.4 Multiple Beads and Layers Stacking Conditions

Generally, the laser clad cross section shape represents a half-moon shape and can be characterized with the width and height, but it is also common to find some irregular geometries as the layers are deposited on top of each other based on selected parameters. After conducting experiments in single bead and percentage overlapping beads; their results and findings are explained in chapter 5. To understand and model the effect of heat on multiple layers; bead stacking experiments (Figure 28) are performed on circular substrate and rests of them are prepared on rectangular substrate.

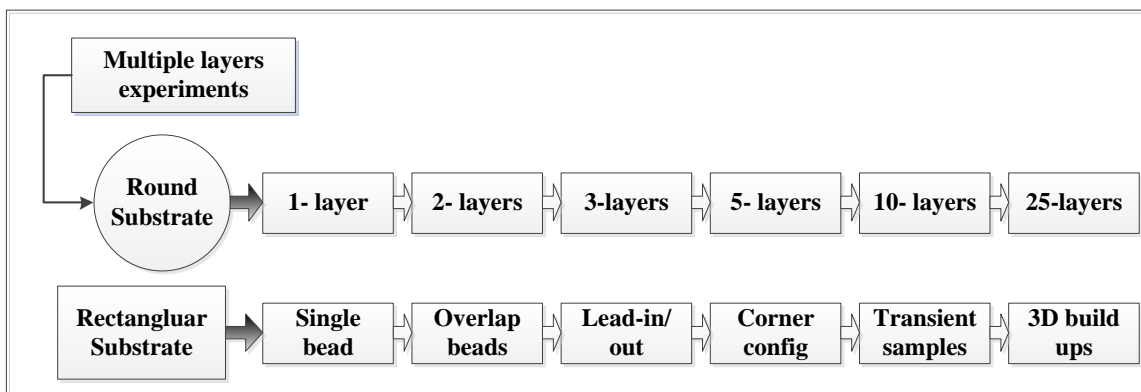


Figure 28. Sequence of the multi-layer experiments; characterized with the type of the substrate

The process parameters chosen for this set of experiments are acquired from the expertise of industrial partner as mentioned in Table 4b (bolded values). The Figure 29 illustrates the cross sections of one layer, two layers, three layers and five layers.

It can be seen that the bead heights are not in direct proportion with the number of layers. Since the laser cladding environment is very noisy and highly coupled, it is difficult to understand the real cause of anomalous variations in bead height and width. This observation is strengthened by further exploration of making cladding samples of 10-layers and 25-layers on a substrate with 420 powder steel. The process parameters are kept constant throughout the experiments. Figure 30 illustrates the 10-layer sample. Although the same parameter was set for this multiple bead stack and each layer is deposited with the same set up, despite that individual layer heights are measured differently and appeared to be 'm' shape, especially the first 4-layers which are prominent (highlighted in red color) in Figure 30.

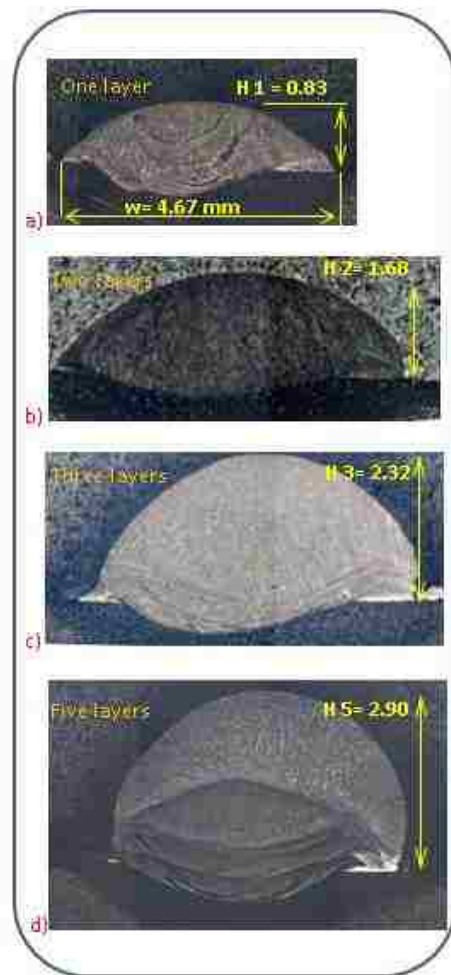


Figure 29. Cross sectioned views of one, two, three and five layers

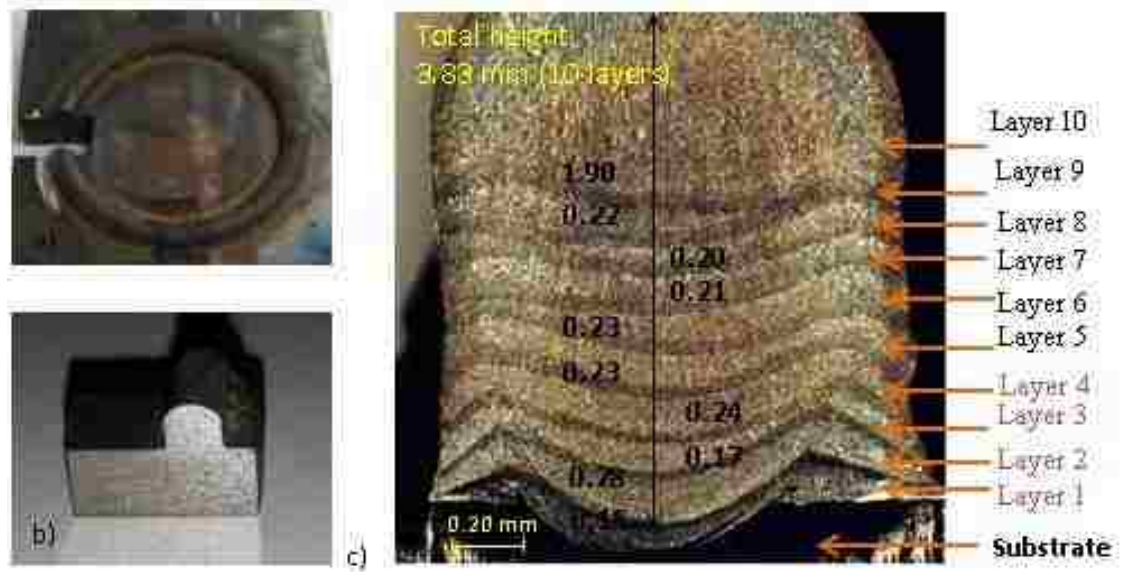


Figure 30. a) Circular sample of a 10-layers clad b) EDM cut piece-polished and etched c) Macrograph view of 10-layers with individual layer heights are shown in mm.

In the analysis of Figure 29 and Figure 30, it is believed that in a single layer deposition, the deposited layer boundary is placed on a planer surface of the substrate which is normal to the +Z –coordinate, whereas in multilayer deposition the same does not deposit on the planar surface instead it is deposited on the previous layer which has an irregular surface. This difference requires the development of a new methodology or understanding for incorporating the additive material for the second, third and subsequent layers.

One of the reasons for having this ‘m’ shape could be that melting and solidification takes place simultaneously in a small area and every next layer is deposited on previous layer in an earlier time. The first few layers constituted ‘m’ shape with spikes on both sides and then happened to be flattened in rest of the build ups. The measurements of this 10-layer sample are mentioned in Table 7. These values are graphed to see the trend of layer heights and area of each deposited layer, which are discussed in results section. To get further from this multiple layer sample, another sample is prepared with 25-layers and compared with the 10-layers sample.

The Figure 31 shows the two multi-layers samples and found the difference in height of:

$$5.90 \text{ mm} - 3.83 \text{ mm} = 2.07 \text{ mm (at the end of 10}^{\text{th}} \text{ layer deposition)}$$

Table 7. Measurements of each layer (Figure 27) are shown

Layer Number	1	2	3	4	5	6	7	8	9	10
Bead height (mm)	0.15	0.28	0.17	0.24	0.23	0.23	0.21	0.20	0.22	1.90
Bead width (mm)	3.80	3.72	3.65	3.60	3.57	3.48	3.49	3.49	3.50	3.53
Area of layer (mm ²)	0.58	0.74	0.64	0.93	0.89	0.72	0.75	0.69	0.76	5.15

In all buildups, there is heat, followed by solidification of previous layers that leads to process planning and real time strategies a challenge to address this phenomenon. Significant interactions may also exist between the manufacturing process parameters and the final bead geometry. In this situation, it is essential in developing and manipulating predictive models for the desired results, which are explained in chapter 5.

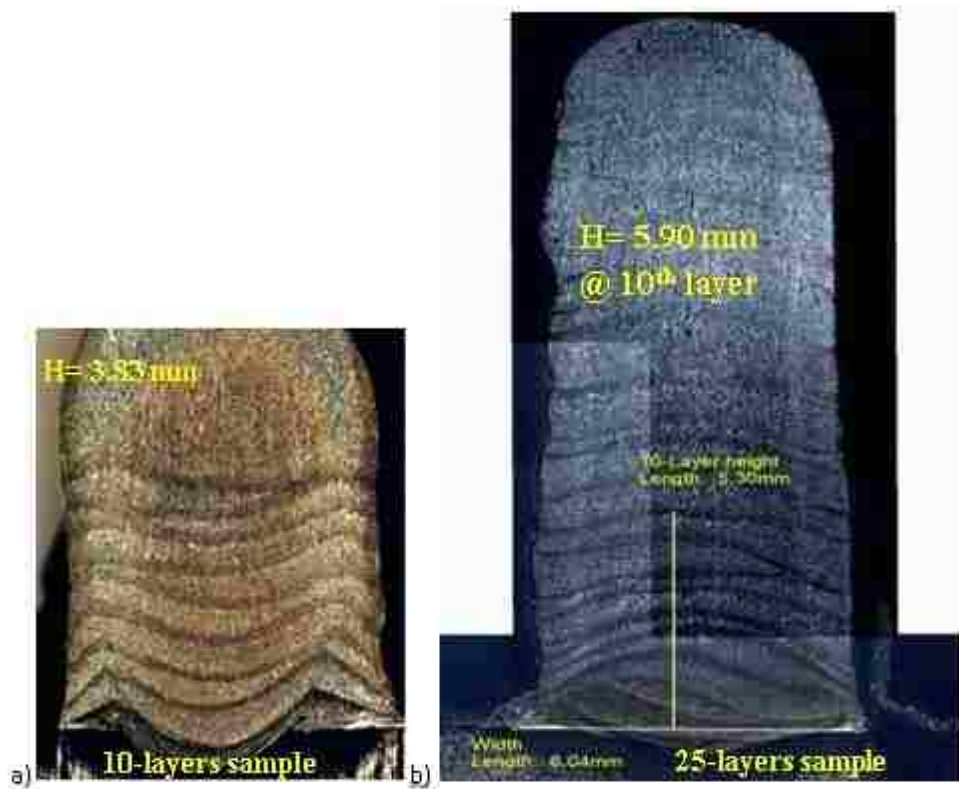


Figure 31. Comparison of heights in 10 layers and 25 layers samples

4.5 Laser Power Step Function Based Transient Heat Conditions

The laser cladding is a typical quasi-state thermal process, in which the process is considered to be steady along the scanning direction of the laser beam [124]. In order to understand the effect of heat during the deposition process; another set of experiments is performed to understand the transient heat conditions with the variation in laser power. The system response time for changing the power level is fast; whereas there are significant system lags when varying the powder feed rate and the focal length of the lens.

A single bead of 6.0 inch in length (~160 mm) was produced while ramping the laser power levels from 3kW-4kW-3kW via a step function. The bead was deposited for 5- seconds at each power levels for a total deposition time of 15 seconds. The experimental approach is shown in (Table 8).

Table 8. Transient heat experiments with the varying power

Sample description	Sample length (mm)	Power variation (kW)			Time interval for each power level (seconds)	Total deposition time (seconds)
		3	4	3		
Single bead	160	3	4	3	5	15
3-beads overlap	160	3	4	3	5	15
3 x 4 beads stack	160	3	4	3	5	15

The transient experiments are planned (Figure 32) based on Table 8 to get some insight that how the heat progresses and the geometrical shape of the current bead and the following bead gets effected when the second layer and the subsequent layers are deposited. There is an increasing relationship between the heat and the bead width is observed [110, 113, and 118].

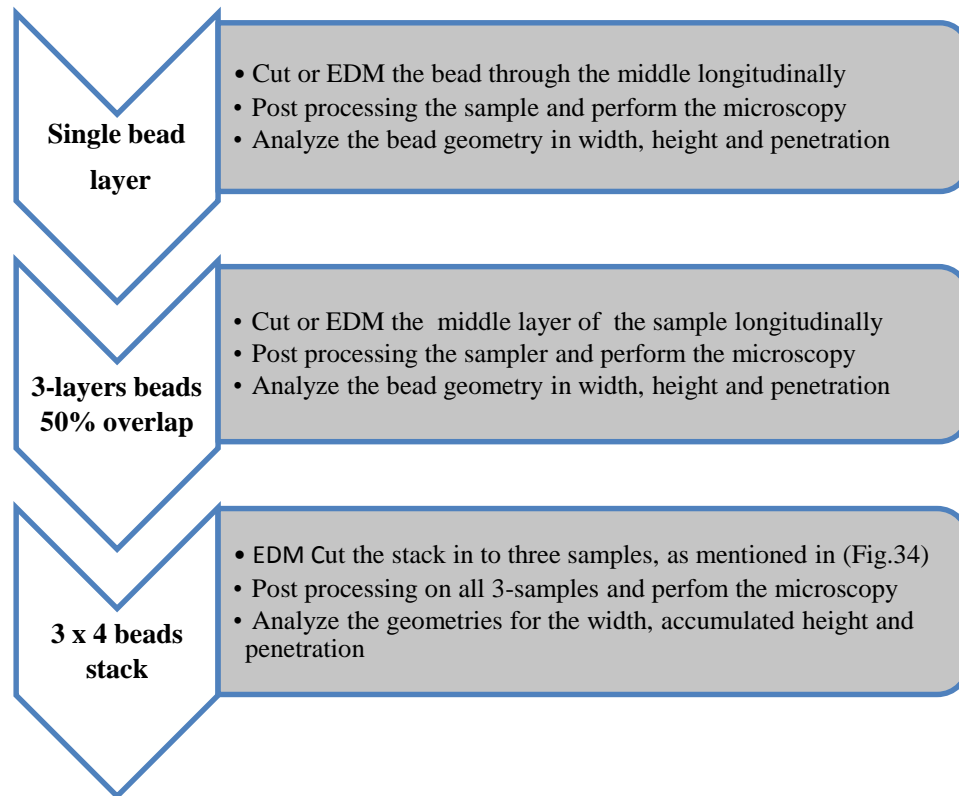
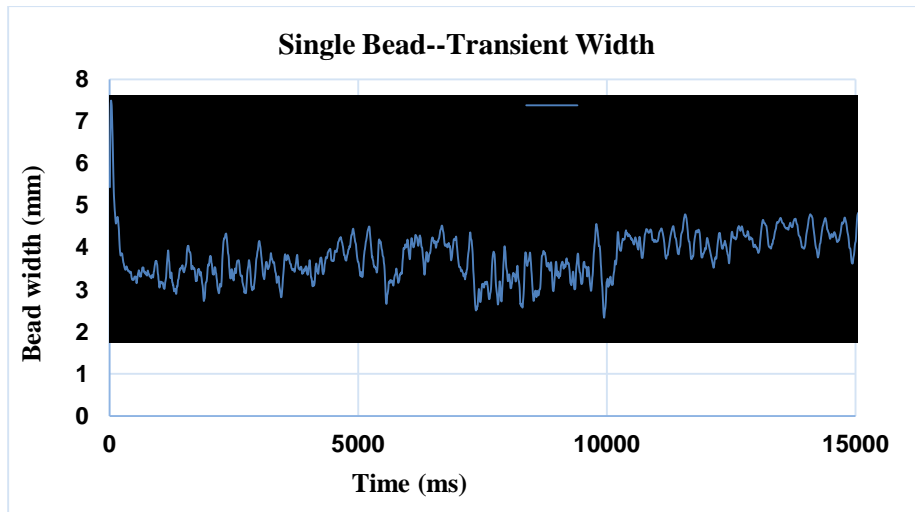


Figure 32. The processing steps used in the transient heat conditions experiments

Prior to these experiments, a hypothesis is developed that changing the power level would impact the melt pool width. For this reason, a sample is produced with 2.6-3.6-2.6 kW over the period of 15 seconds. Each power level is varied for 2-seconds interval. The results are presented in section 5.5.

The bead width data is also recorded for all experimental approaches (Fig. 32) while the material is being deposited. 160 images per second (2447 images in 15.7 seconds) are recorded to analyze the trend of heat and its effect on the bead width. The recorded bead width data over the entire length of deposition and the longitudinal section of the single bead is illustrated in Figure 33.

This work is extended by introducing multiple overlapping layers along with the transient heat conditions in order to see the effect of heat variations when dealing with build-up conditions. Total of 3-layers with 50% overlap are cladded with the same transient heat conditions such as 3kW-4kW-3kW, is shown in Figure 34.



a)

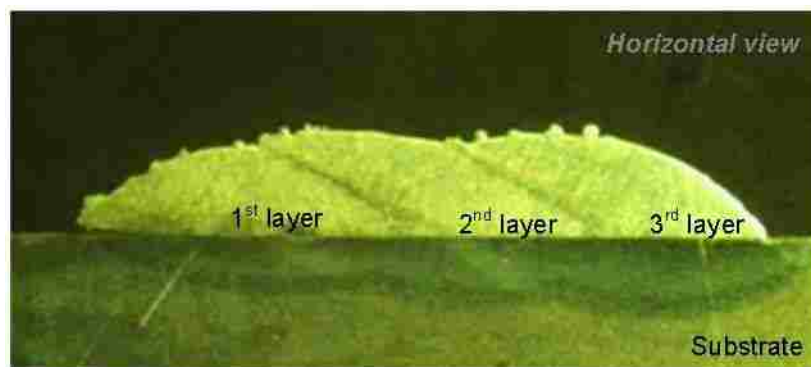


b)

Figure 33. a) Graph shows the variation in bead width over 15 sec period b) Longitudinal section view of the transient bead with 3kW-4kW-3kW power



a)



b)

Figure 34. Stepping condition with 3-beads overlap a) Full length cladded sample (top view) and cut through the middle b) Cross sectional view of the 50% overlap beads.

Data is collected along the center line for all beads. The recorded bead width data over the entire length of deposition is illustrated in Figure 35 a. The 3-bead sample (Fig. 34 (a) is cut using an EDM along the center of the middle bead; its longitudinal sectioned view is shown in Figure 35. Deposited bead is shown with the red dotted line.

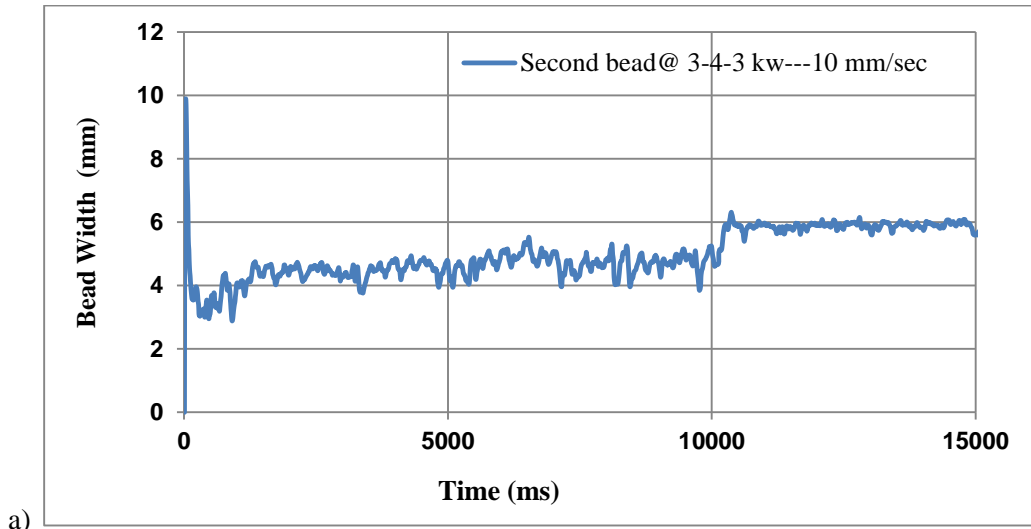


Figure 35. a) Graph shows the variation in bead width over 15 sec period (6" in length) b) Longitudinal section view of the middle bead of the 3-bead sample

The final transient heat experiment considers both overlapping and stacking conditions. A 3 x 4 bead (12 beads) stack is cladded with the same conditions as described in the previous section. This stack is first longitudinally EDM cut through the stack center line (Figure 36 a-- section 2), and then microscopy is performed. The stack is cut again twice, which is named as section 1 and section 3 respectively. All three samples (section 1, 2 and 3) went through the same post processing method (Fig. 25). The longitudinal sectioned views of them are shown in Figure 36b.



Figure 36. a) Longitudinal EDM cut of the 3x4 bead stack sample b) Cross section views of all three sections—each view contains four layers of stack--enlarged view is also shown.

The obvious variations in the bead width, height and penetration are due to the power variations during deposition. Detailed analysis of the transient conditions for single and multi-layers are presented in section 5.5.

4.6 Single Bead Corner Configurations (Acute, Right and Obtuse Angled)

The uniformity of the clad thickness could be one of the measures for quality of the clad, but this is influenced by the travel path requirements. An abrupt change in clad thickness is undesirable. To understand the variations in the bead geometry while depositing with different angles configuration, three corner configurations are explored, as shown in Figure 37. There are challenges in these situations regarding the process planning; deposition in these scenarios is not smooth because of the system's slow response time. These travel path generation strategies is the realistic geometric challenge for the process planners in corner configurations.

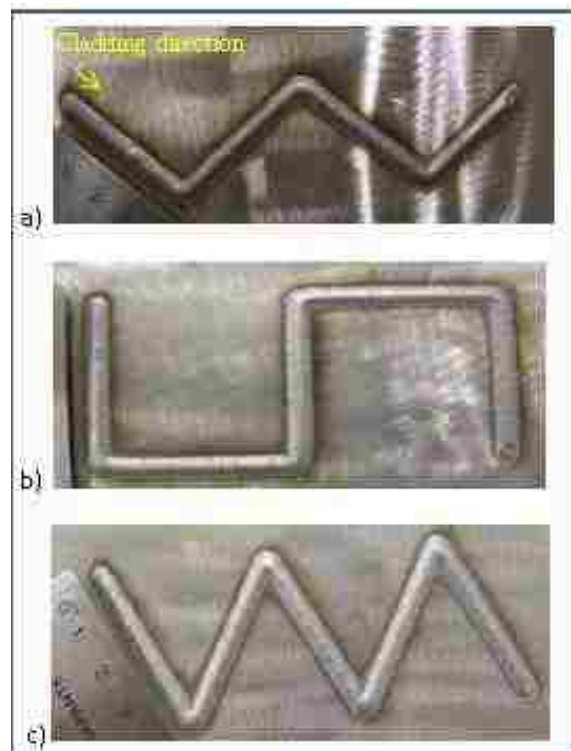


Figure 37. Single bead samples with different configurations a) Obtuse angled b) Right angled c) Acute angled

All the samples are cut at the joints and numbers are assigned in respect to the direction of cladding and processed. Three cross sectioned views of only obtuse angled configuration are shown in Figure 38, rest of them are shown in Appendix D.

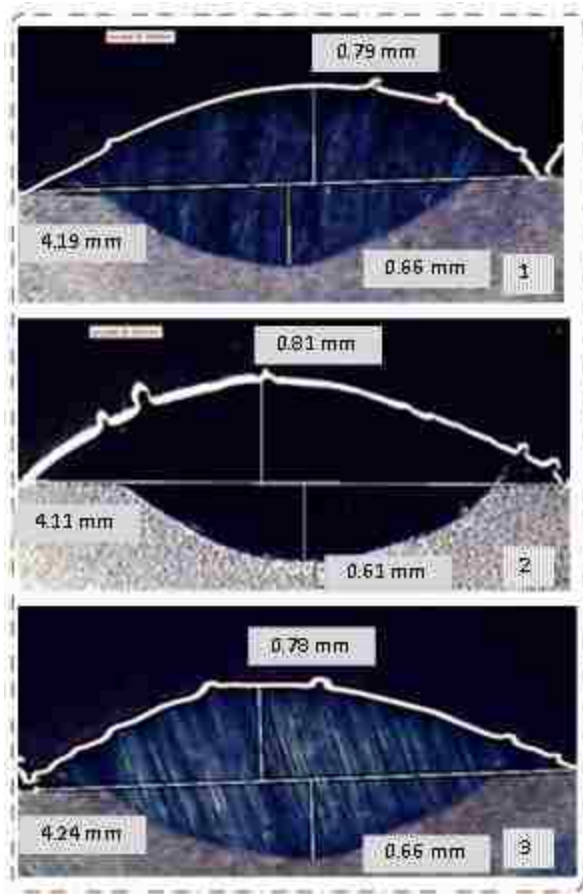


Figure 38. Three different sectioned views of obtuse angled configuration using Figure 34a.

Sometimes the laser cladding on the edges of circular openings or flanges is required. In that case, not only the side overlapping of individual laser tracks is required but also understanding of the lead-in and lead-out situations (section 4.7) is essential as well. The side overlapping of individual laser track is widely studied in literature [19] not only for laser cladding but also for laser hardening and laser melt injection process. The analysis of beads in all these configurations is discussed in chapter 5.

4.7 Cladding with Lead-in and Lead-out Situation

This experiment is aimed at evaluating the lead in/lead out situation to understand its effect on the geometrical shape of the clad. It is understood that the melt pool formation, as well as the transient associated with the motion control system, influence the lead-in and lead-out results. Typical imperfections occurred in cladding process could be in the bead shape and/or microstructural defects. Defects in cladding could be porosity, lack of fusion and cracks. Some

researchers (Ocelik et. al) [80] worked on track in/track out method (Fig. 39) but they only considered hardness and strength of the deposited alloy and did not consider the geometrical shape of the bead.

Defects elimination is required especially when a closed loop of the laser track is needed. These authors also considered start and stop zone where the bead overlaps, and found that this could be controlled either with gradient power, if this parameter is easy to be controlled otherwise adjusting the focal length of the nozzle. Changing in to the desired focal length or introducing different spot size are the options to minimize the clad overlap defects but it would take time for the system to respond. In the event of overlapping of beads in start/stop zone, that causes more height than required in that area; machining would be performed in post processing procedure [80].

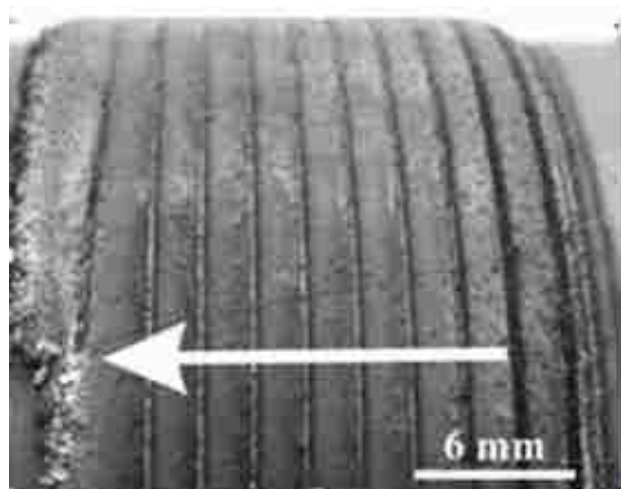


Figure 39. Track in/track out is shown for the circular coating on a round steel substrate [80]

For this research, a 75 mm (3-inch) clad sample is produced on a steel substrate and then cut using an EDM along the center line, and the transient height and penetration data collected. The starting point and ending of the clad, also known as lead-in and lead-out is shown in Figure 40. The measurements at different locations can also be seen.

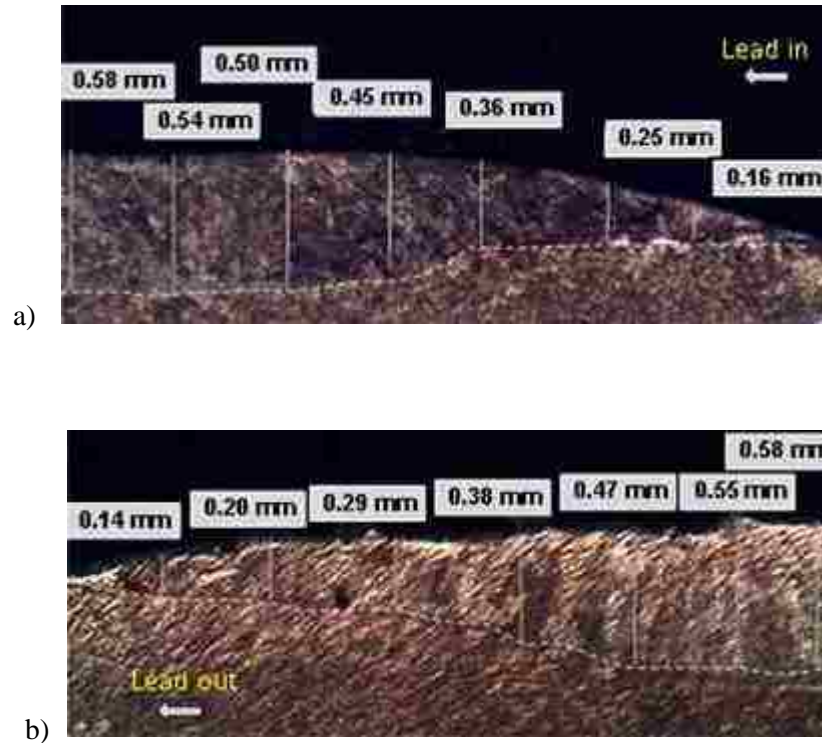


Figure 40. Cross section view of a single bead a) Lead in and b) Lead out situations

In a cladding process, lead-in is a situation where nozzle starts depositing the material and takes little time and distance on the base metal to get the desired or stabilized height, same is the situation with lead-out as well. The analysis of this situation is described in results section.

4.8 Building 3D Geometry and CT Scanned the Models

Deposition process through laser is usually performed by overlapping tracks resulting on layers, which means it could be used for building a 3D geometry. If the desired geometry is high enough, deposition would be performed in layer-by-layer process. The CAD/CAM system or G-codes would be required for programming the overlapping of the beads. The information required for this system such as overlapping distance or percentage between clads, feed rate, laser powder, height between layers etc.

For the research purposes, an attempt was made to build some 3D models with deposition of layers by layers and later on they are compared with the original CAD models. For this purpose, two different types of CAD models are created in CAD software, one is the hollow cone shell and the other is thin wall parabolic shape (Fig. 41).



Figure 41. Models made using laser cladding method a) b) CAD models c) Hollow cone model d) Parabolic shape model

The material deposition travel path is generated for these CAD models which are very similar to machine tool path contour. Travel path generation is a complex job especially there is heat buildup on subsequent deposited layers; this makes a challenge to the process planner. For the comparison purposes, these cladded models are CT (Computerized Tomography) scanned using X-ray diffraction method for which the facility of an in-town company is employed. The results of the CT scanned are shown in Figure 42.

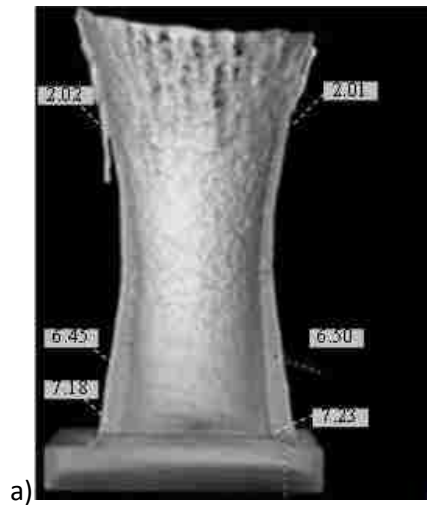
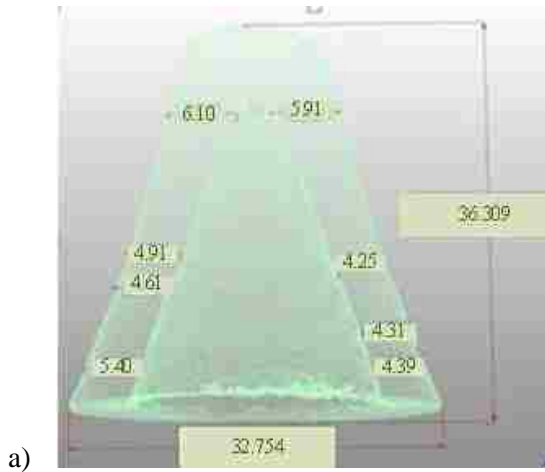


Figure 42. CT scanned views of a) The hollow cone and b) The sectioned parabolic model-All dimensions are in mm

Again the facility of the industrial partner is used and these models are created using robotic arm from bottom to up approach and layers are deposited on top of each other. The parameter used for building these models is mentioned in Table 4b (bolded values). During the experiment, the camera control was off and the table tilt angle was set at 0 degree which means only the nozzle assembly was moving in positive Z-direction while the work piece was stationary. Due to the complexity of the models, it was difficult for the operator to control or maintain the thickness throughout the deposition phase since the diameter of the CAD models are getting smaller and smaller as the build proceeds to upward. Using computerized tomography (CT) scan technology, the variations in thicknesses of the hollow cone and the parabolic cone is identified; the results are graphed and discussed in results section 5.6.3.

Chapter 5

Experimental Results and Derived Models

Three approaches for developing a predictive model from the data are explored: (i) an analysis of variance (ANOVA) approach (ii) an artificial neural network (ANN), and (iii) a ‘lumped parameter’ model based on physics and observed data trends. There are three stages when to consider refining a developed ANN: training, validation, and testing. Another research partner Mr. Aggarwal worked on the ANN method and developed the predictive models using the same data but the details of the model is not mentioned here only the results are presented in section 5.3.2.

However, Minitab™ is used for the ANOVA analysis and to investigate the linear regression models for predicting geometry for a set of process parameters. The lumped parameter model considers factors such as the material deposition and the heat per unit length, as these elements relate directly to the physical domain. The general reduced gradient nonlinear solver (GRG) in Excel is used to determine the coefficients for the lumped parameter models. The modeling approach is summarized in Figure 43.

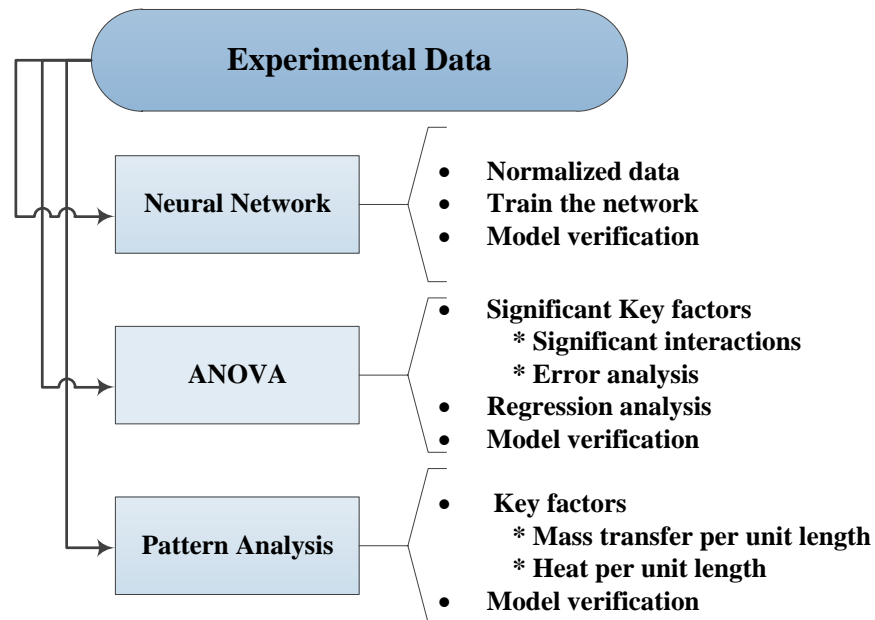


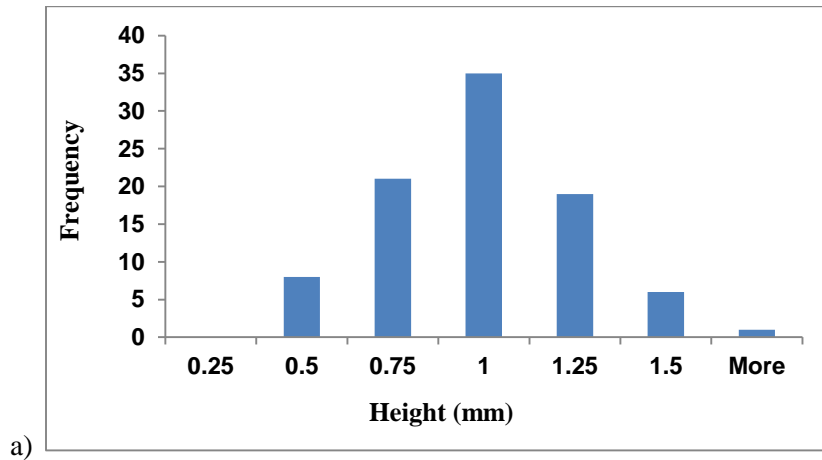
Figure 43. Data analysis and modeling approaches

5.1 General Observations in Single Bead Experiments

General observations are plotted to determine whether the process parameters generate linear or nonlinear response characteristics with respect to the shape parameters, and to provide insight with respect to the noise or process variations. First, a base line assessment is done to compare the average and standard deviation (Table 9) using all of the experimental data to determine which shape parameters have the greatest variations. Interestingly, the variation for the height and penetration is noticeably less compared to the other shape parameters (which is consistent when performing the subsequent analyses). The average width is 4.16 mm, which is approx. 3.3% smaller than the nozzle utilized for this research. The range for the height and penetration is bounded by 0. The height variations still follow a normal distribution, but some skew is evident for the observed penetration results (Fig. 44).

Table 9. Evaluation of the average and standard deviation for each shape parameter using the complete experiment set

	Width (mm)	Height (mm)	Penetration (mm)	Area_p (mm²)	Area_n (mm²)	D (%)
Average	4.16	0.86	0.43	2.51	0.76	21.46
Range	2.17	1.08	1.04	4.24	2.58	47.46
STD	0.44	0.26	0.25	0.91	0.65	13.98



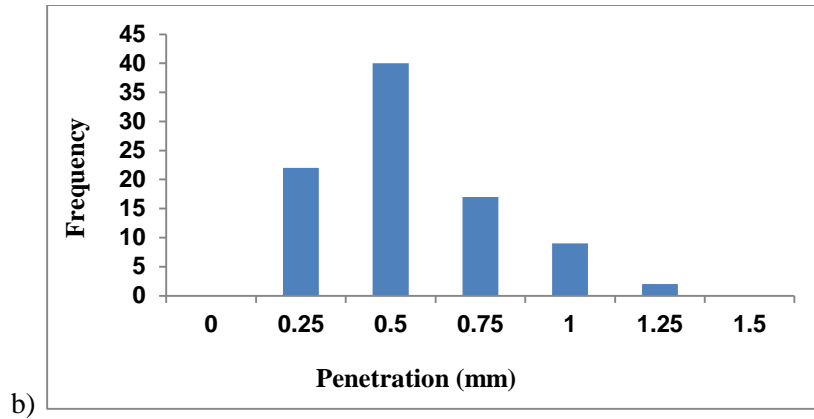
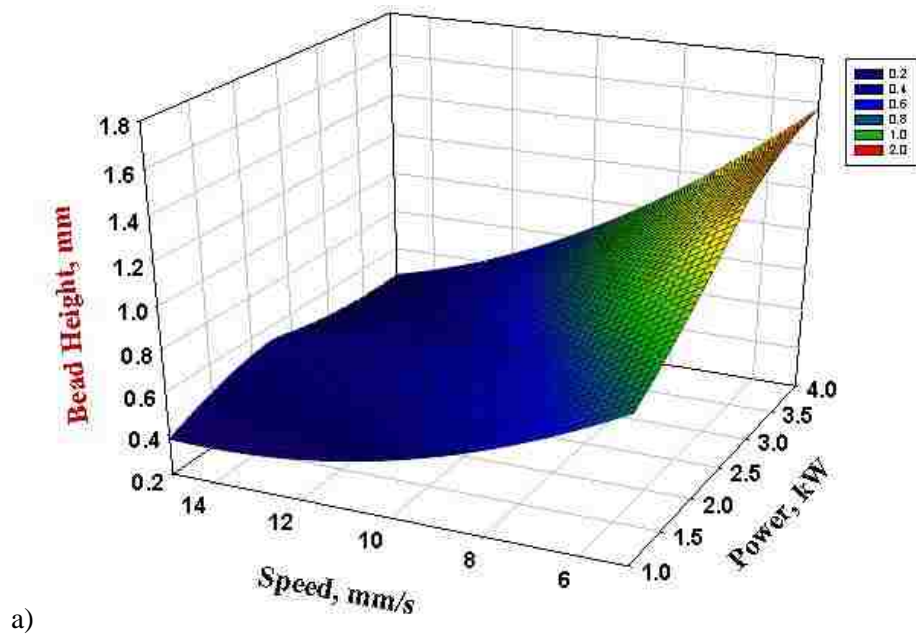
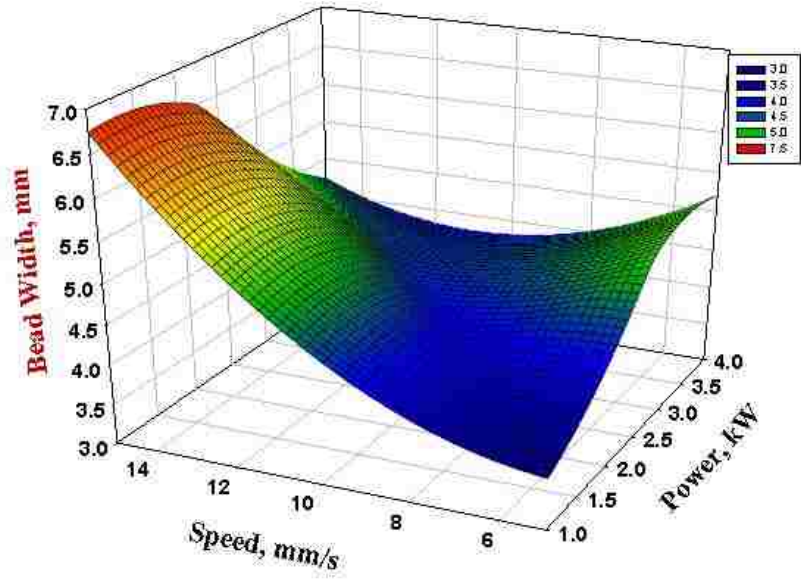


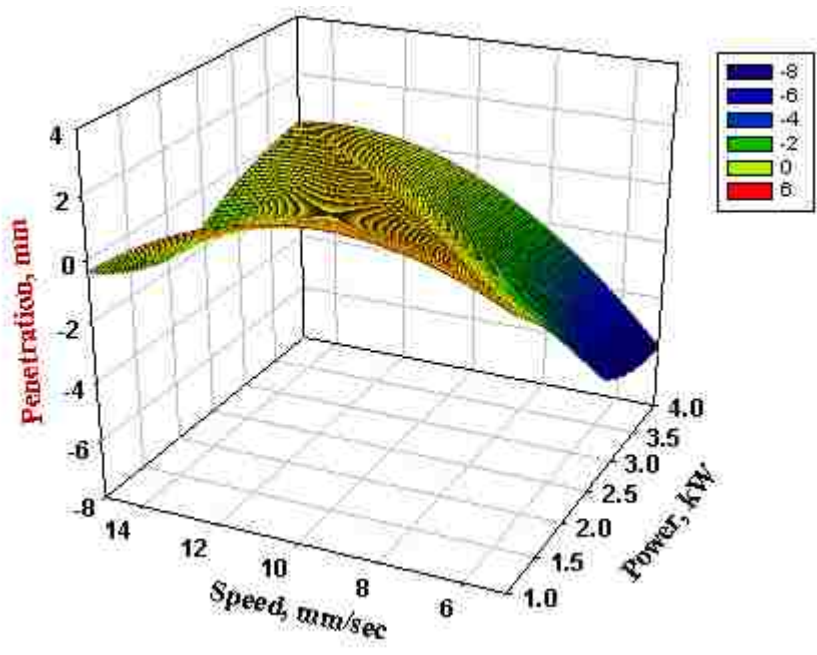
Figure 44. Experimental data histogram for the height and penetration shape parameters using the complete experimental set

The effect of the process parameters and their nonlinear relationship with the bead shape geometry can be seen in Figure 45.





b)



c)

Figure 45. The 3D graphical representation illustrates the effect of process parameters on the response output. The effect of laser power and the nozzle speed on a) the bead height b) the bead width and c) the penetration. All other factors were kept constant.

As mentioned previously, the experiments are replicated three times with the CCD experiment set. The standard deviation is calculated to gain insight with respect to the noise. When assessing the ‘average’ standard deviation for each experiment set-shape parameter, it is found that the average standard deviation for the width is the greatest, whereas the bead height, penetration, area measurements, and dilution (a percentage) indicates little variation between the runs (Table 10).

Table 10. Evaluation of the average values of the observed ‘standard deviations’ for each shape parameter-experiment set

Width (mm)	Height (mm)	Penetration (mm)	Area_p (mm²)	Area_n (mm²)	D (%)
0.18	0.04	0.05	0.12	0.04	1.27

Eighteen experiments (3 replicates) have a constant mass transfer per unit distance (0.033 gram/mm), although individual powder feed rate (FR) and laser travel speed (LS) parameters vary:

$$\frac{\text{Mass } xfer}{\text{unit length}} (\text{grams/mm}) = \frac{FR (\text{grams/min})}{LS (\text{mm/sec}) * 60} \quad (7)$$

Although the mass transfer per unit length is constant, the width and the two area measurements vary considerably (Table 11).

Table 11. Evaluation of the mean and standard deviations for the shape parameters for the constant mass transfer per unit length experimental conditions (0.033 grams/mm)

	Width (mm)	Height (mm)	Penetration (mm)	Area_p (mm²)	Area_n (mm²)	D (%)
Average	4.13	0.88	0.44	2.52	0.80	21.23
Std. Dev.	0.40	0.13	0.26	0.45	0.71	13.00

For the constant mass transfer per unit length data set, the influence of the laser power and the focal length on the bead width is shown in Figures 46 and Figure 47. It appears the power

influences the width as a logarithmic or square root function, where as the focal length (and the contact tip to work piece distance as well) to width relationship appears as inverted parabolic shapes.

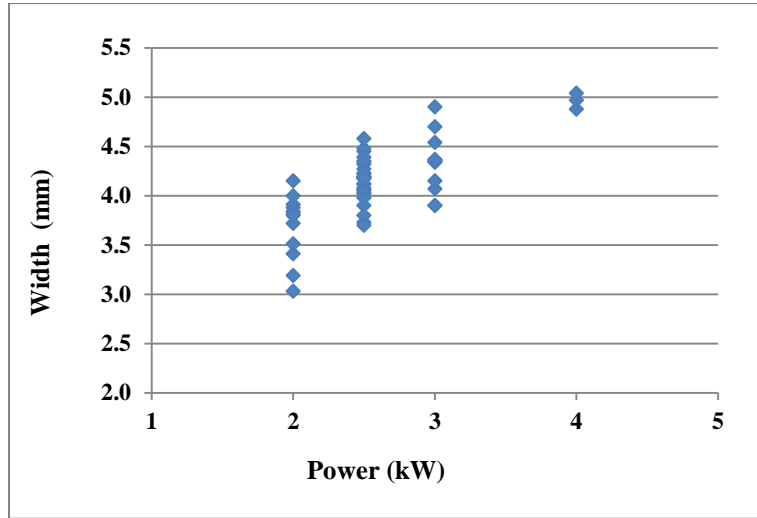


Figure 46. Width versus power when there is a constant FR to LS ratio (note: the CTWD and FL values vary).

An interesting phenomenon with respect to the material feed rate (FR) and its relation to width is illustrated in Figure 48. The width reaches a plateau @ approximately the 20 gram/minute setting. The maximum observed width at this point is: 5.13mm.

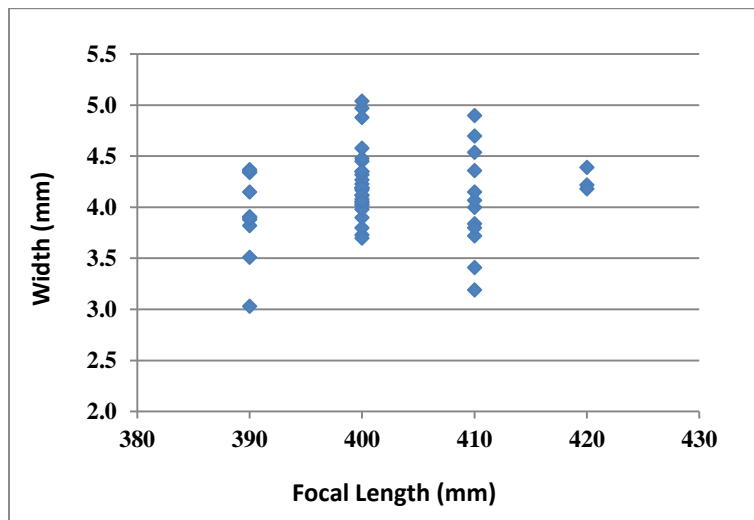


Figure 47. Width versus FL relationship when there is constant FR to LS ratio (note: the CTWD and power values vary).

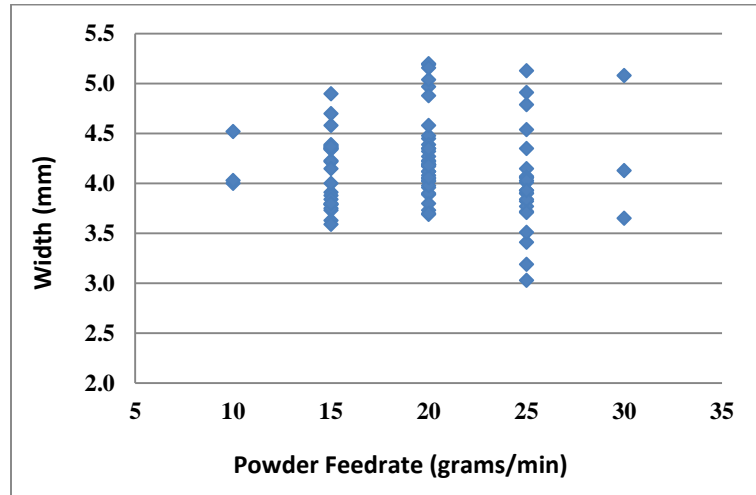


Figure 48. Width versus FR relationship (note: all parameters vary)

For all experiments set, the positive area ($Area_p$) versus the contact tip to work piece distance follows the same observed ‘inverted parabolic’ pattern although the data appears to be mapped around an inflection point (Fig. 49). The 3D representations of such responses are shown in Appendix K. The laser travel speed to the $Area_p$ relationship is linear (Fig. 50). The reflection point also occurs with the height versus power results, as shown in Figure 51.

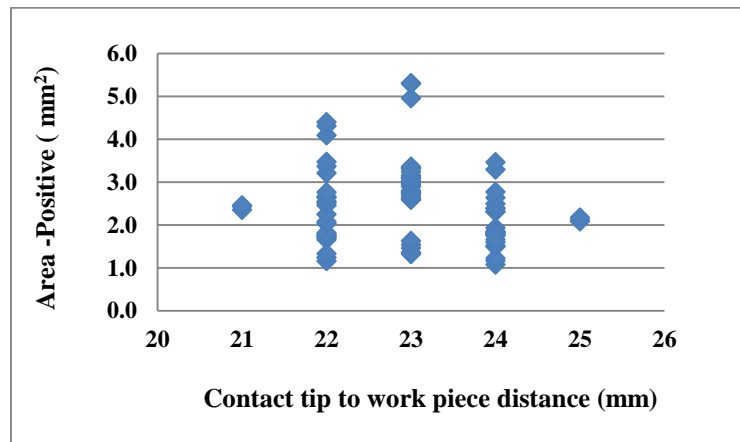


Figure 49. Positive bead Area versus CTWD (all other values vary)

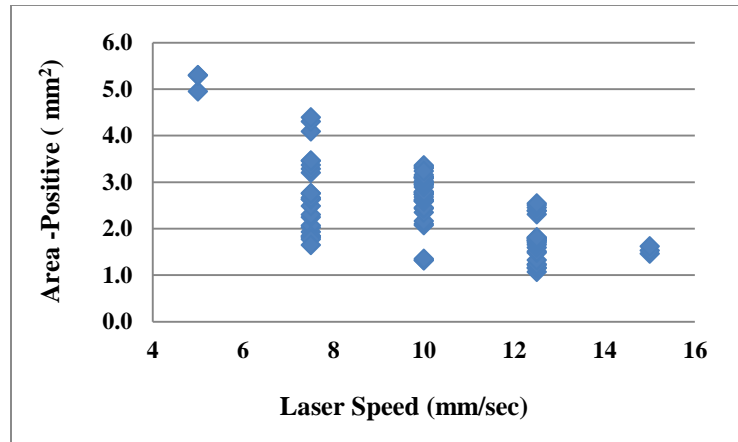


Figure 50. Positive bead Area versus laser speed (all other values vary)

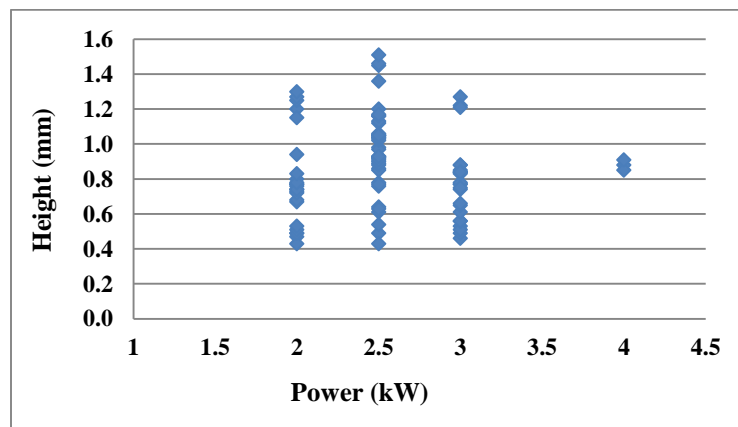


Figure 51. Height versus Power (all other values vary)

These nonlinear responses illustrate the challenges associated with developing a predictive model. Each process parameter impacts the geometry differently. The observed inflection points for the focal length and the contact tip to work piece distance implies that the width (area) will increase to a certain point, and then start decreasing. The power and powder feed rate levels impact width until an upper limit is reached. The impact of the process parameters on the other bead geometry parameters are not as extreme, but they also influence the observed bead height, penetration, and dilution results in a nonlinear fashion.

5.2 Predictive Models using ANOVA and GRG Approaches

While defining an RSM experiment set, the relationship between a response and a response variable contained in the system is unknown. Hence, the first step is to determine an approximation for a true functional relationship between the objective function(y) and the response variables. The response function representing any of the clad bead geometry can be expressed as:

$$Y = f(A, B, C, D, E) + \epsilon \quad (8)$$

Where, Y= Response variable or objective function

f is a function of the manufacturing parameters (input variables)

ϵ is a noise or error observed in the response

A, B, C, D, E are the powder feed rate, laser power, focal length of the lens, laser travelling speed, and the contact tip-to work piece distance respectively.

The ANOVA analysis is employed for the single and the overlap bead configurations using a general linear model based on the following equation:

$$Y = \beta_0 + \sum_{i=0}^5 \beta_i X_i + \sum_{i=0}^5 \beta_{ii} X_i^2 + \sum_{i=0}^5 \beta_{ij} X_i X_j \quad (9)$$

Where,

β_0 = free term (constant) of the regression equation

β_i = Coefficients of linear terms

β_{ii} = Coefficients of square terms

β_{ij} = Coefficients of quadratic terms

by expanding the above equation-9, it becomes:

$$\begin{aligned} Y = & \beta_0 + \beta_1 \cdot FR + \beta_2 \cdot PW + \beta_3 \cdot FL + \beta_4 \cdot LS + \beta_5 \cdot CTWD + \beta_{11} \cdot FR^2 + \beta_{22} \cdot PW^2 \\ & + \beta_{33} \cdot LS^2 + \beta_{44} \cdot FL^2 + \beta_{55} \cdot CTWD^2 + \beta_{12} \cdot FR * PW + \beta_{13} \cdot FR * FL \\ & + \beta_{14} \cdot FR * LS + \beta_{15} \cdot FR * CTWD + \beta_{23} \cdot PW * FL + \beta_{24} \cdot PW * LS \\ & + \beta_{25} \cdot PW * CTWD + \beta_{34} \cdot FL * LS + \beta_{35} \cdot FL * CTWD + \beta_{45} \cdot LS * CTWD \end{aligned}$$

(10)

This generalized mathematical model has square and interaction terms as well as linear terms, with twenty coefficients needing to be determined. Not all terms in the equation are significant, and the significant factors / interactions may vary based on the experimental scenario. The coefficients (β values) are calculated using statistical software, Minitab 16 and the following equations 11-14 are generated for response variables to the single bead deposition.

$$\begin{aligned}
 \text{Clad bead width (W)} = & 4.15694 - 0.0368056 \text{ FR} + 0.332077 \text{ PW} + 0.129577 \text{ FL} - 0.205139 \text{ LS} \\
 & - 0.00625 \text{ CTWD} - 0.00401882 \text{ FR*FR} + 0.00395833 \text{ FR*PW} + 0.060625 \text{ FR*FL} - \\
 & 0.0502083 \text{ FR*LS} - 0.053125 \text{ FR*CTWD} - 0.0115087 \text{ PW*PW} + 0.0989583 \text{ PW*FL} + \\
 & 0.0289583 \text{ PW*LS} - 0.0572917 \text{ PW*CTWD} - 0.0852587 \text{ FL*FL} - 0.061875 \text{ FL*LS} + \\
 & 0.0110417 \text{ FL*CTWD} + 0.0659812 \text{ LS*LS} + 0.0302083 \text{ LS*CTWD} - 0.0169355 \\
 & \text{CTWD*CTWD}
 \end{aligned}
 \tag{11}$$

$$\begin{aligned}
 \text{Clad bead height (H)} = & 1.02419 + 0.161111 \text{ FR} + 0.000228495 \text{ PW} + 0.0360618 \text{ FL} - \\
 & 0.158611 \text{ LS} - 0.0566667 \text{ TWD} - 0.0508602 \text{ FR*FR} - 0.03375 \text{ FR*PW} + 0.0229167 \\
 & \text{FR*FL} + 6.87733\text{e-}017 \text{ FR*LS} - 0.0345833 \text{ FR*TWD} - 0.0582863 \text{ PW*PW} + \\
 & 0.0358333 \text{ PW*FL} + 0.03625 \text{ PW*LS} - 0.0316667 \text{ PW*TWD} - 0.048703 \text{ FL*FL} - \\
 & 0.0329167 \text{ FL*LS} + 0.0433333 \text{ FL*TWD} - 0.00461022 \text{ LS*LS} + 0.0454167 \text{ LS*TWD} - \\
 & 0.0579435 \text{ TWD*TWD}
 \end{aligned}
 \tag{12}$$

$$\begin{aligned}
 \text{Penetration depth (P)} = & 0.362742 - 0.120417 \text{ FR} + 0.208931 \text{ PW} + 0.00893145 \text{ FL} - 0.112361 \\
 & \text{LS} - 0.01375 \text{ TWD} + 0.00975806 \text{ FR*FR} - 0.011875 \text{ FR*PW} + 0.020625 \text{ FR*FL} + \\
 & 0.0289583 \text{ FR*LS} - 0.0227083 \text{ FR*TWD} + 0.0424026 \text{ PW*PW} - 0.006875 \text{ PW*FL} - \\
 & 0.0127083 \text{ PW*LS} - 0.034375 \text{ PW*TWD} - 0.0334308 \text{ FL*FL} - 0.0135417 \text{ FL*LS} - \\
 & 0.0110417 \text{ FL*TWD} + 0.0293414 \text{ LS*LS} + 0.0289583 \text{ LS*TWD} + 0.0172581 \\
 & \text{CTWD*CTWD}
 \end{aligned}
 \tag{13}$$

$$\begin{aligned}
\text{Dilution \% (D)} = & 14.5993 - 9.67762 \text{ FR} + 11.5384 \text{ PW} - 0.85895 \text{ FL} - 2.45166 \text{ LS} + 0.830953 \\
& \text{CTWD} + 2.7882 \text{ FR*FR} - 1.16533 \text{ FR*PW} + 0.0506338 \text{ FR*FL} + 1.17665 \text{ FR*LS} - \\
& 0.682811 \text{ FR*CTWD} + 1.86097 \text{ PW*PW} - 1.04513 \text{ PW*FL} + 1.21214 \text{ PW*LS} - \\
& 0.0112684 \text{ PW*CTWD} + 0.352878 \text{ FL*FL} + 0.142178 \text{ FL*LS} - 2.12907 \text{ FL*CTWD} + \\
& 1.16394 \text{ LS*LS} + 0.448634 \text{ LS*CTWD} + 1.89456 \text{ CTWD*CTWD}
\end{aligned}
\tag{14}$$

The mean is defined as the overall average of the response variables for each model and the standard deviation is defined as the root mean square error (square root of the pure experimental error) and is mathematically calculated as:

$$\text{Std Dev} = \sqrt{MS_{error}} \tag{15}$$

Whereas,

$$MS_{error} = \frac{SS_{error}}{DF_{error}} \tag{16}$$

Where,

MS = Mean square

SS = Sum of squares

DF = Degree of freedom

The ANOVA test is performed to evaluate the statistical significance of the fitted quadratic model and the factors (responses) involved such as bead height, bead width, penetration and the percentage dilution.

The hypothesis set up for the ANOVA model is as follows:

H₀ = There is no interaction between the process parameters and shape parameters

H₁ = There is significant interaction between process parameters and shape parameters

If the F-ratio values of the developed model do not exceed the standard tabulated values for a desired level of confidence (95%) then the models are said to be adequate within the confidence limit or if P-value is found to be less than 0.05 (alpha=5 %) then the observed factor is significant in the model and vice versa. After performing ANOVA analysis for all responses, it has been seen that the null hypothesis (H₀) has been rejected due to the significant interaction resulting from linear, square and interaction terms in the model equation. The results are presented in Table 12 and detailed ANOVA analysis is mentioned in Appendix G.

Since there is magnitude variation in the process setting that impacted the square and interaction terms significantly. Hence model variations are also explored using a ratio (equation 17) and a log₁₀ transformation (equation 18) as follows:

$$X'_i = \frac{X_i}{X(\min)} \text{ or } X'_i = \frac{X_i}{X(\max)} \quad (17)$$

$$X'_i = \log_{10} (X_i) \quad (18)$$

The model fit statistics are summarized in Table 13. The model fit is the poorest when using the raw parameter settings for the width using GRG method. The width predictive model has the poorest overall fit independent of the modeling approach. The best fit graph comparing the observed width to the modeled width data is illustrated in Figure 52a. The predictive width is also calculated and compared with observed width using ANOVA model with a fit of R²=0.71, is shown in Figure 52b.

Table 12. Significant factors for response variables

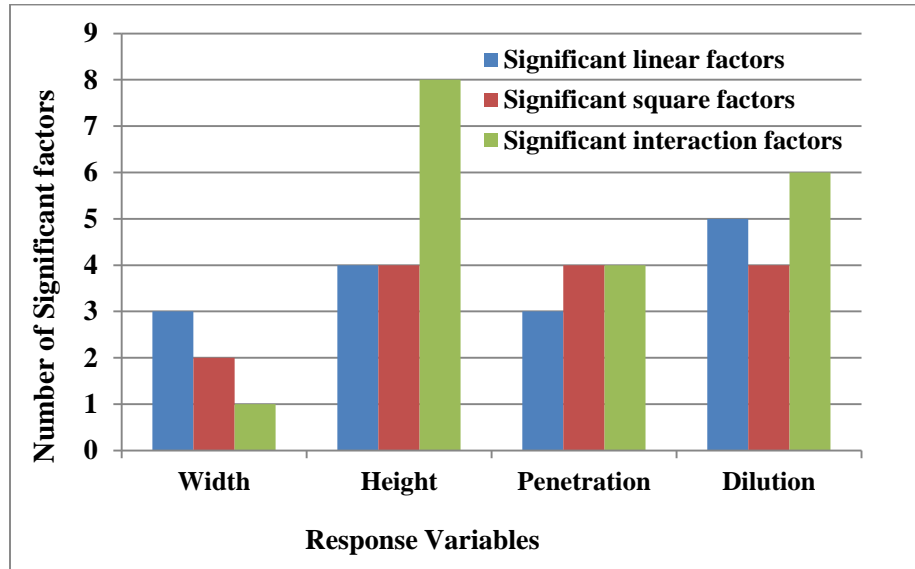


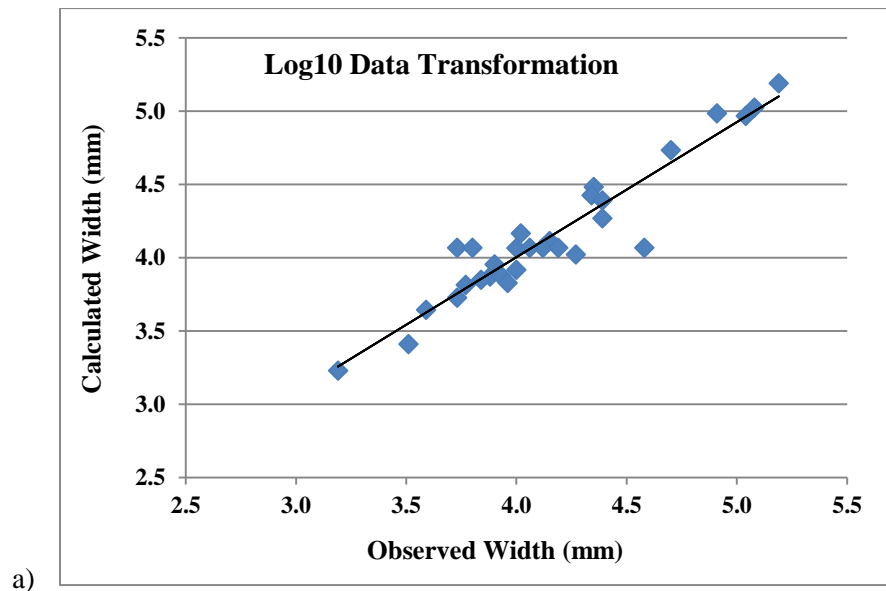
Table 13. A summary of the modeling results

Model Summary: Bead Width (W)				
Raw data (ANOVA - coded)	R ²	0.71	Std Dev.	0.27
Raw data GRG	R ²	0.59	Std Dev.	0.22
Normalized (Xmin) GRG	R ²	0.84	Std Dev.	0.15
Normalized (Xmax) GRG	R ²	0.86	Std Dev.	0.14
Log ₁₀ (X) GRG	R ²	0.90	Std Dev.	0.11
Bead Reinforcement Height (RH)				
Raw data (ANOVA - coded)	R ²	0.91	Std Dev.	0.09
Raw data GRG	R ²	0.90	Std Dev.	0.10
Normalized (Xmin) GRG	R ²	0.98	Std Dev.	0.05
Normalized (Xmax) GRG	R ²	0.97	Std Dev.	0.06
Log ₁₀ (X) GRG	R ²	0.99(2)	Std Dev.	0.03
Bead Penetration (P)				
Raw data (ANOVA - coded)	R ²	0.94	Std Dev.	0.06
Raw data GRG	R ²	0.89	Std Dev.	0.12
Normalized (Xmin) GRG	R ²	0.90	Std Dev.	0.13
Normalized (Xmax) GRG	R ²	0.91	Std Dev.	0.12
Log ₁₀ (X) GRG	R ²	0.94	Std Dev.	0.08
Bead Percentage Dilution (%D)				

Raw data (ANOVA - coded)	R ²	0.98	Std Dev.	2.22
Raw data GRG	R ²	0.91	Std Dev.	2.99
Normalized (Xmin) GRG	R ²	0.91	Std Dev.	3.09
Normalized (Xmax) GRG	R ²	0.91	Std Dev.	3.02
Log ₁₀ (X) GRG	R ²	0.98	Std Dev.	1.49

For the other shape parameters, the overall model fit varies between R² = 0.89 for the bead penetration, to R² = 0.99 for the reinforcement height. Overall, using coded process parameter data provided models with a reasonable fit. Transforming the process parameter data improved the fit statistics, especially when using the log10 transformation.

For the laser cladding process, dilution is a key design parameter, as there needs to be bonding to the substrate, but a minimal amount of material mixing is desired; consequently, predicting this shape parameter is essential. This research illustrates good predictive models can be generated for this parameter using multiple approaches.



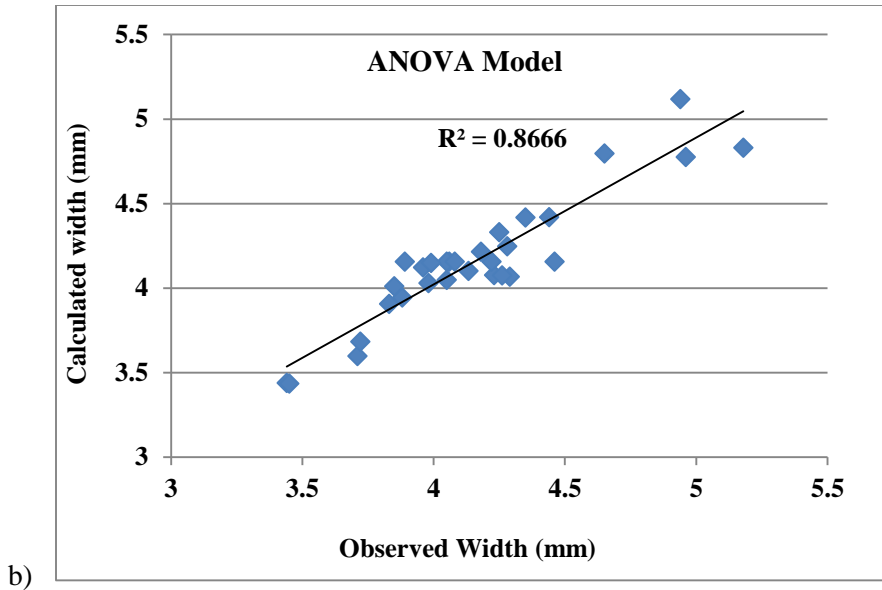


Figure 52. Bead width model results versus observed data a) when applying a Log10 data transformation on the input parameters b) using the ANOVA model

5.3 Percentage Overlapping Bead Analysis

The overlapping bead geometry (Fig. 53) width data is averaged for each complete experiment set, and compared to a calculated average width using the observed average single bead width as a reference:

$$W_c = W_s(3 - 2 * \%overlap) \tag{19}$$

Where, W_c is the calculated width

W_s is the average width for all the single bead experiments

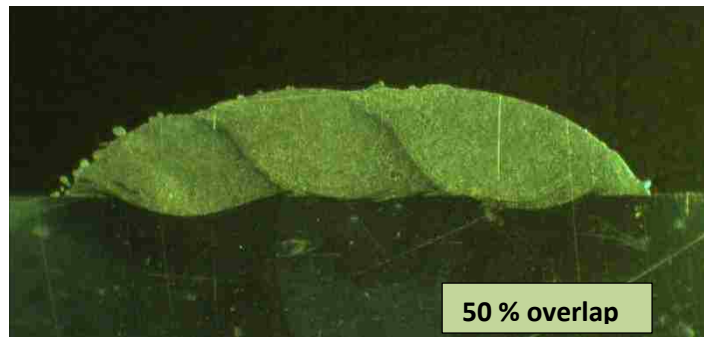
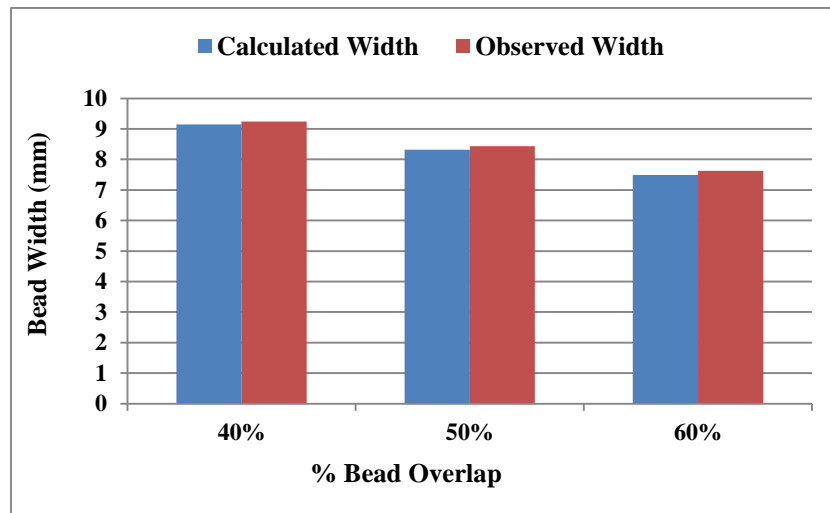
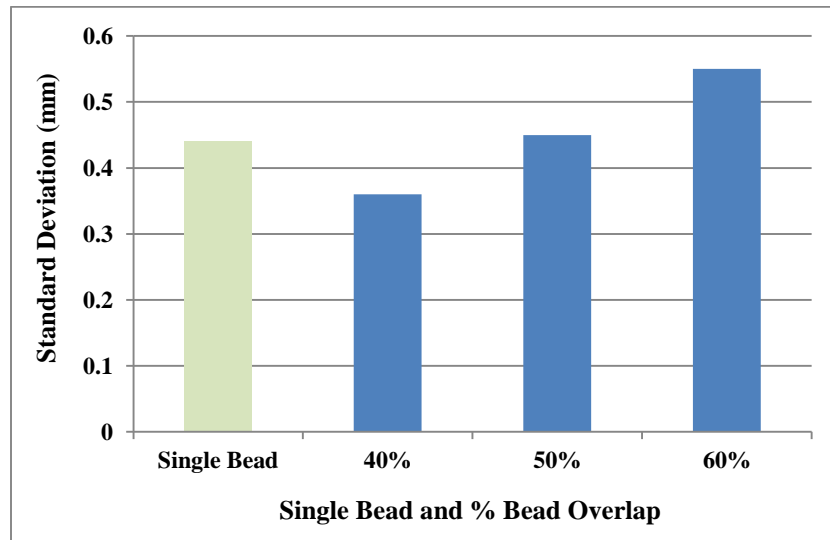


Figure 53. Schematic of a 50 % overlap beads

The calculated and observed bead widths correlate well, as shown in Figure 54 (a). The standard deviations and ranges are also similar in magnitude, but increase with the overlap percentage. This could be due to the melt pool being created over previously deposited material. Unique bead geometry variations are exhibited when changing the overlap penetration and height geometry (Fig. 55). The penetration decreases as the overlap increases, but the observed standard deviations and ranges are very close in value to the single bead deposition scenario (Fig. 56 (a) and (b)). The bead height standard deviations and ranges are very noisy as compared to the single bead configuration (Figure 56 (c) and (d)).



a)



b)

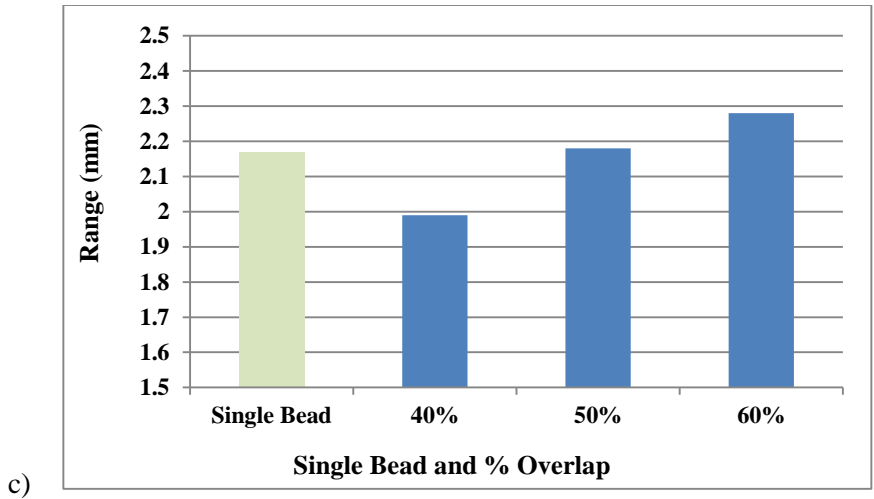


Figure 54. (a) Predicted overlapping bead width geometry versus observed bead width geometry, (b) Standard Deviations, and (c) Range

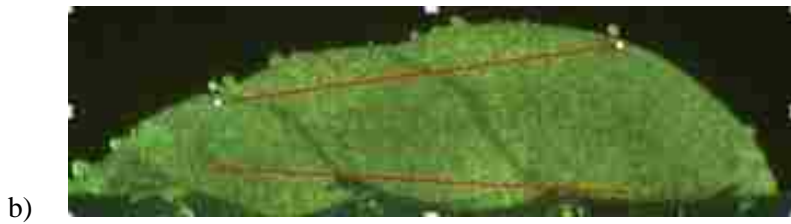
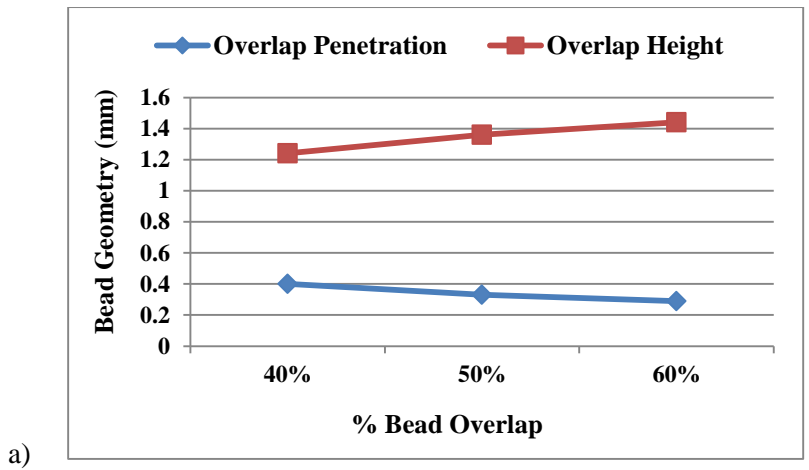
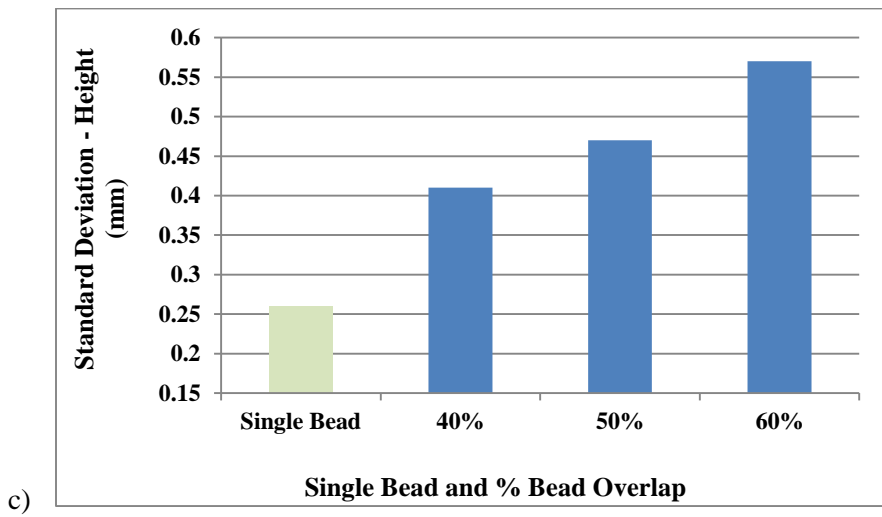
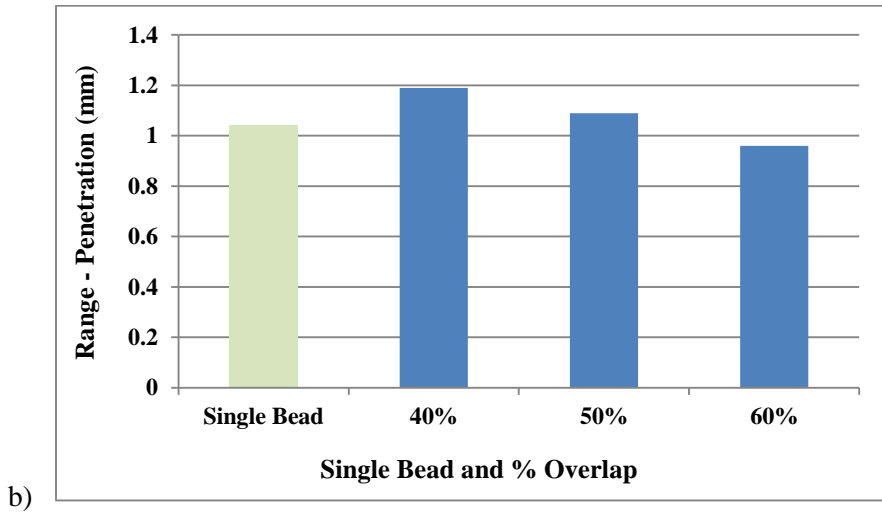
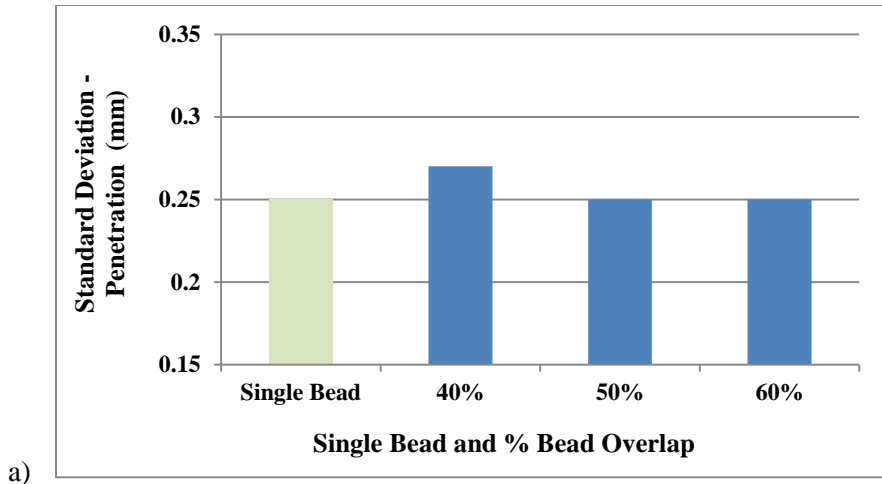


Figure 55. The average penetration and height changes with the percentage overlap and representative bead with 60% overlap illustrating the height and penetration variations per bead



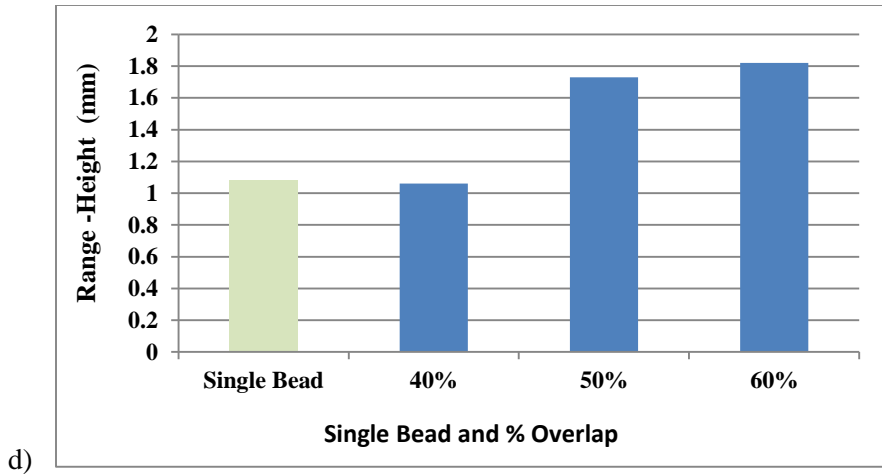


Figure 56. The average penetration and height changes with the percentage overlap

The change in the penetration depth is evident within each overlap experiment, as shown in Figure 57. The percent magnitude of change in the penetration between the first and third beads is essentially equivalent for the 50% and 60% overlap conditions. The average change between the 1st and 2nd beads is ~ 22%, and the average change between the 1st and 3rd beads is 30%.

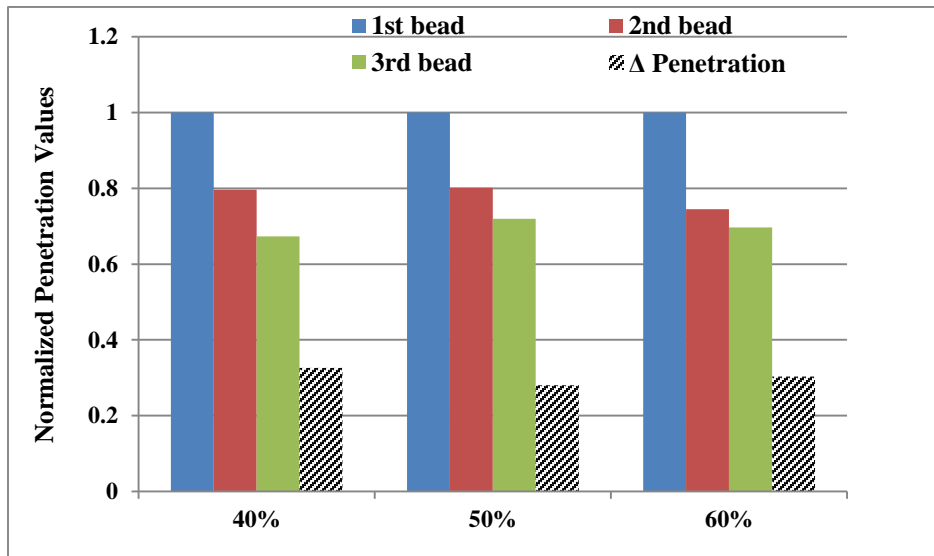


Figure 57. The penetration variations based on the bead deposition order and percentage overlap

5.3.1 The ANOVA Model for Overlapping Conditions

The ANOVA model fits for the various bead parameters and overlap settings are illustrated in Figures 58-60. The goodness of fit varies significantly for the individual entities when assessing the overlap width, which may be due to interpretation of the bead width data where there are unclear boundaries (i.e., for all the second bead width). This may also be the case for the first bead height H1 with the 60% overlap. However, the bead penetration R² values are all greater than 0.90, indicating that the trends are consistent for each condition, although the penetration depth is varies between the first and subsequent beads (Fig. 55). Where the bead data boundaries are well defined, the goodness of the predictive model fits are in line with the single bead data.

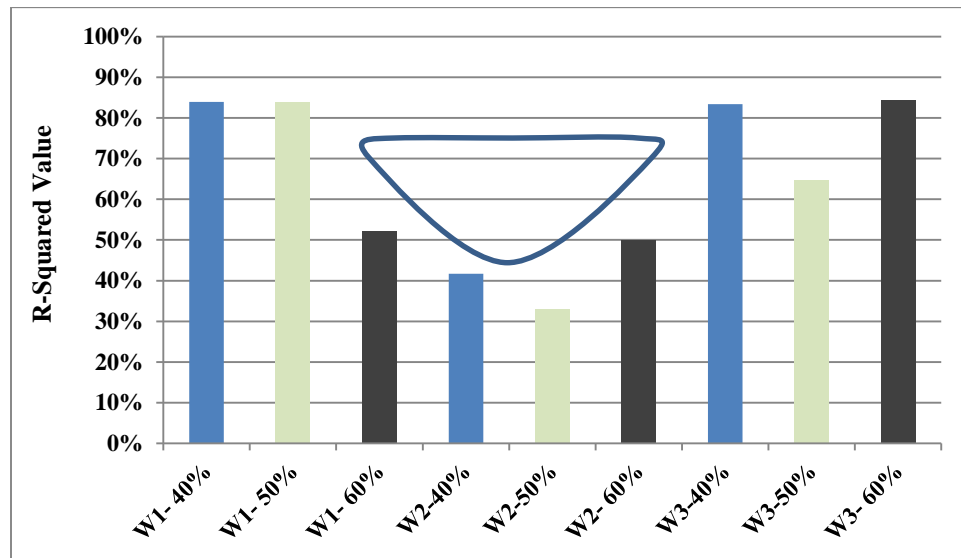


Figure 58. The R² values for the bead width for the overlapping bead experiment set

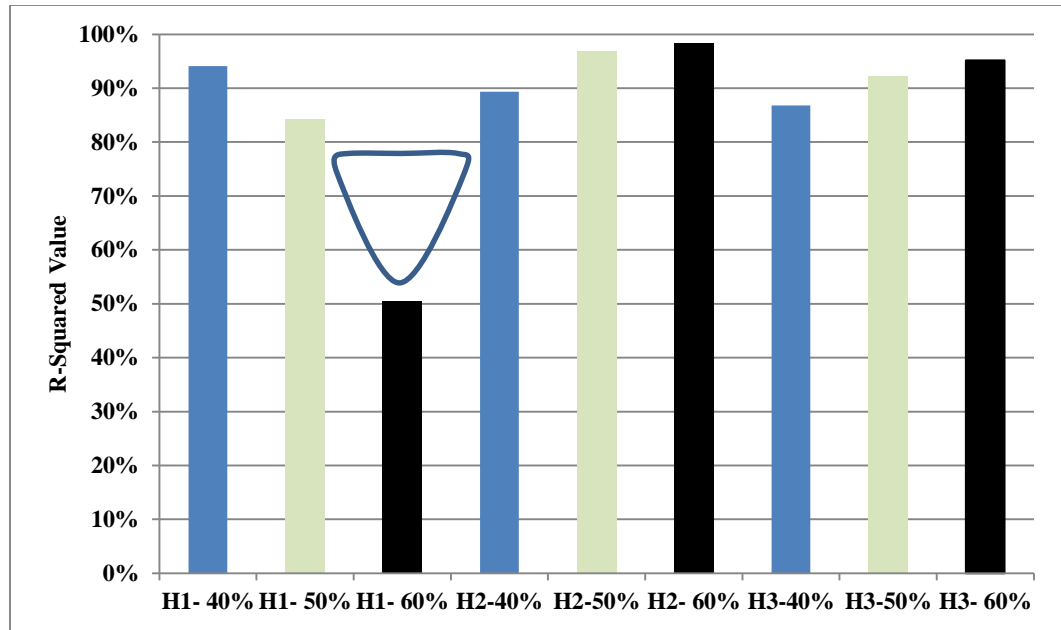


Figure 59. The R^2 values for the bead height for the overlapping bead experiment set

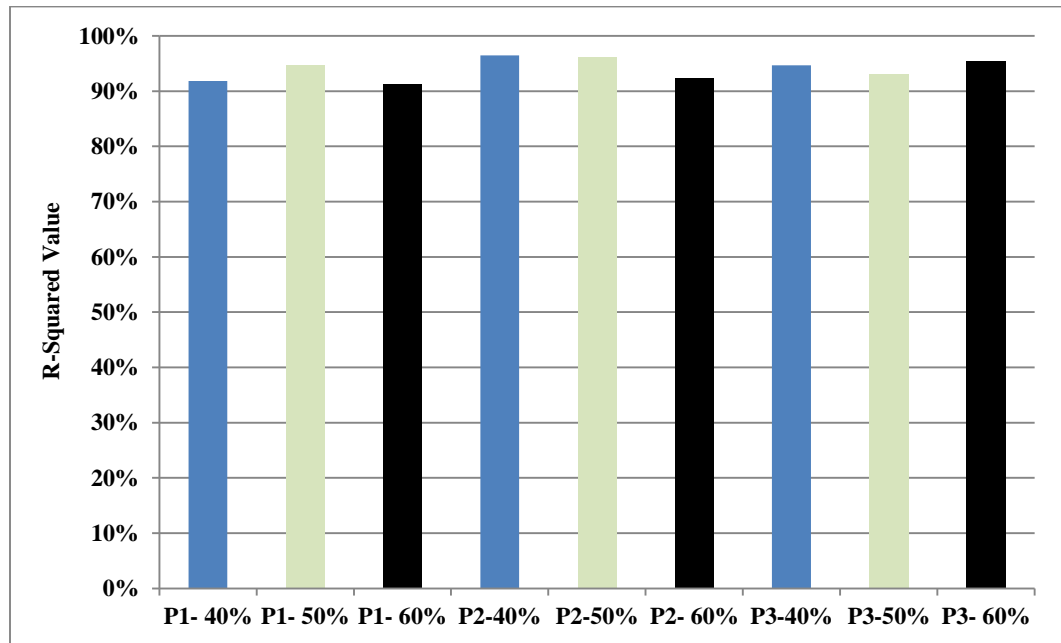


Figure 60. The R^2 values for the bead penetration for the overlapping bead experiment set

5.3.2 Overlap Results and Modeling using Artificial Neural Network (ANN)

Neural networks are an emerging and evolving field that has its origin from the science of neurobiology. It imitates the basic information processing mechanism or path carried out by a human brain. In other words neural network are the mathematical models that perform similar functions as human brain to process information. A human brain consists of various neurons that help in processing information from one to another. Similarly, a neural network consists of various perceptions that help transfer numerical data from one to another. Hence, NN are designed to perform complex tasks just like the brain. [125]

One of the research fellows of this project (Mr. Aggarwal) has worked on this bead overlapping model using the artificial neural network (ANN) technique and jointly a journal paper is published [126]. These results are presented for completeness.

As the ANN has proven to generate the best predictive model, a similar approach for developing predictive model for overlapping beads is performed. The experimental methodology is kept constant i.e., the response surface methodology (RSM) approach is employed with $2^5 = 32$ experiments. The overlap model is generated for '3 pass' bead geometry sets for 40%, 50% and 60% bead overlap. There are 2 replicates for each experiment. Figure 61, shows one such typical example of an overlap bead experiments generated at pre-set configurations of: PW=2.5 kW, FR=25g/min, LS=10 mm/sec, FL= 400 mm and CTWD= 23 mm.

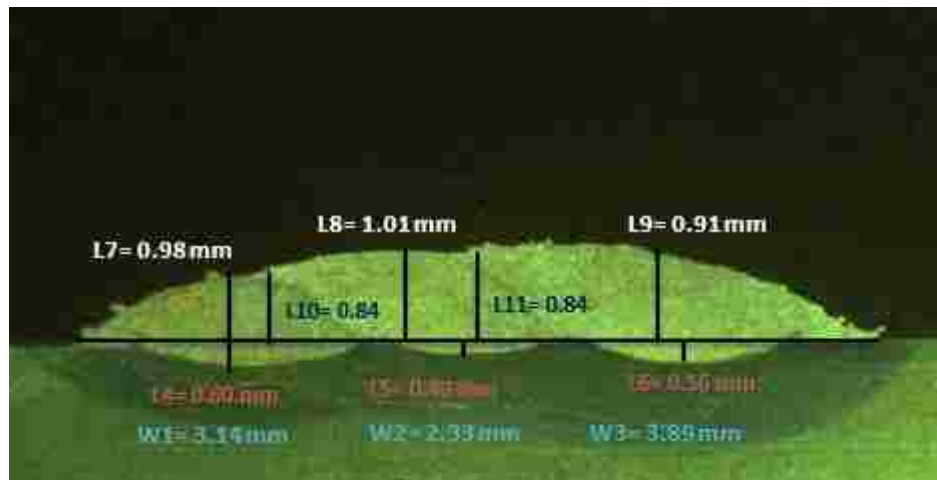


Figure 61. Cross section view of 3-beads with 50% overlap; measurements are also shown

The architecture of the ANN (Fig. 62) for modeling the overlapping beads is briefly described as follows. A multi-layer perceptron (MLP) neural network is devised with a feed forward back propagation approach. This network consists of 5 input parameters i.e. the pre-set configurations established with RSM approach, 40 neurons in the hidden layer, 12 neurons in the output layer (Linear activation function) and 11 outputs (prediction values of overlap bead geometry characteristics shown in Figure 61-L1- L11).

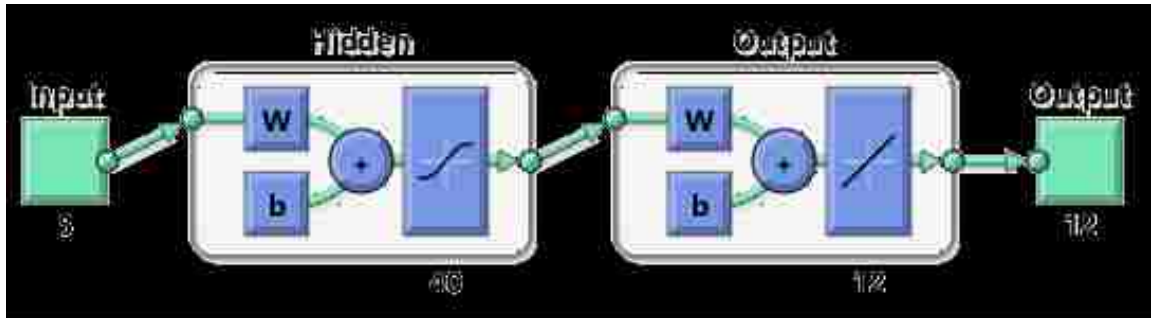


Figure 62. Neural network architecture for generating an overlap bead pass model

The data is entered in the MATLAB environment and the output is shown in Figure 63. It can be seen that the network devised is successfully trained with an accuracy of 95th percentile (94.7%); indicating that the network can make successful predictions with 95% confidence. This complements the bead prediction model. The actual versus the predicted width, height, penetration (for one individual parameter/ pass out of 3 passes) and dilution plots are illustrated in Figure 64 after the completion of the simulation phase.

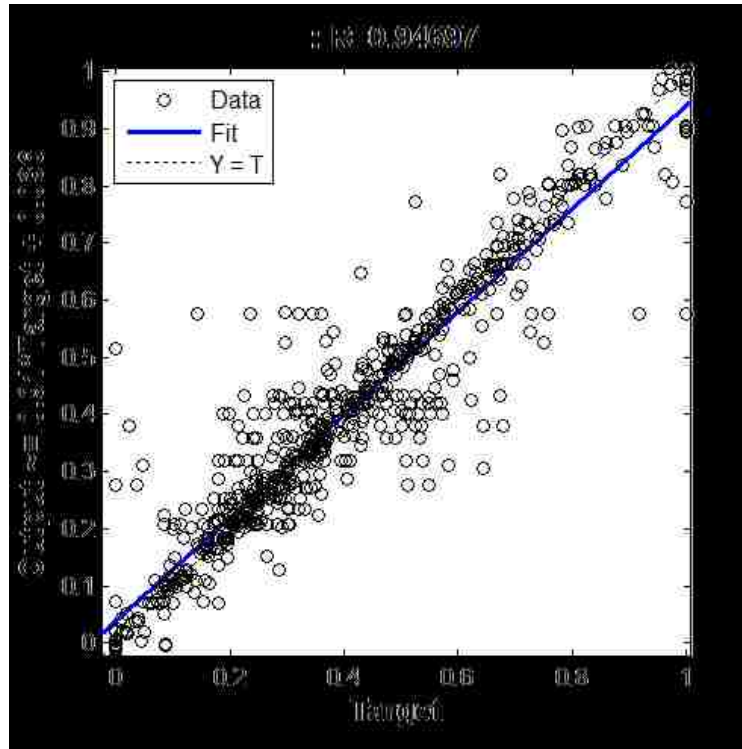
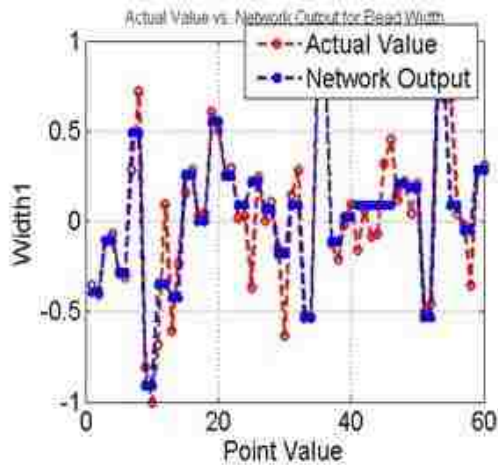
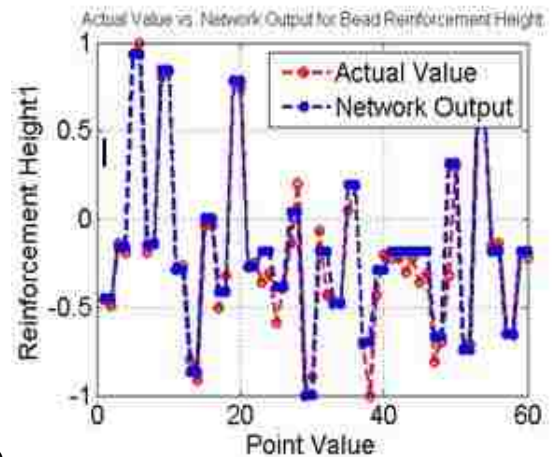


Figure 63. Regression plot for the ANN network

Using the ANN approach, the prediction results are similar for the single bead and overlapping bead geometry [126], providing confidence in the approach for selecting parameters for surface cladding travel paths. The future goal directly related to the single layer clad paths will include investigating approaches to vary the width while maintaining a fixed height to reduce surface waviness and voids for complex shapes, and minimizing the dilution percentages. The expandability of the ANN approach needs to be determined, as well the viability of this approach in a commercial additive manufacturing application.



a)



b)

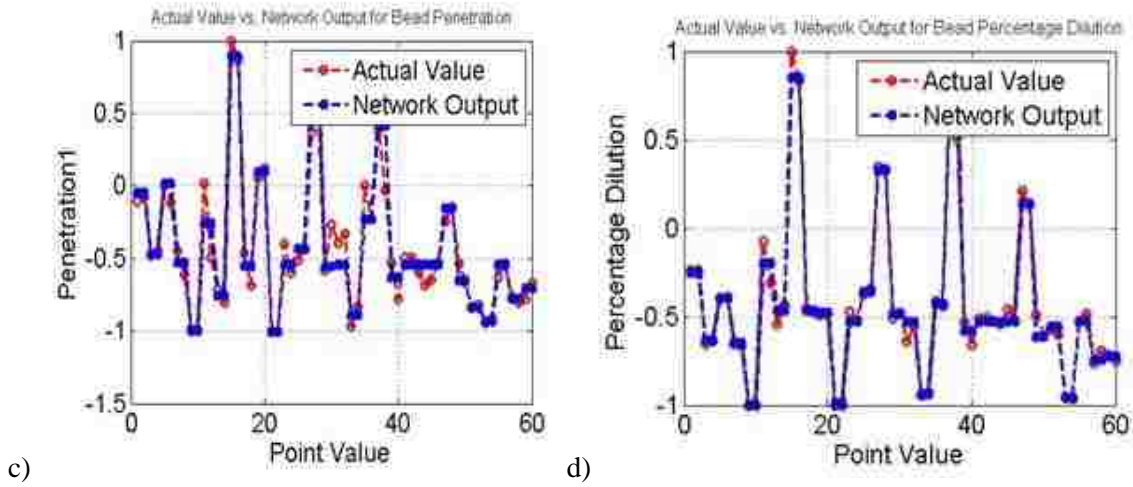


Figure 64. (a) Width, (b) Height, (c) Penetration, (d) Dilution (red is the experimental data, blue is the predicted/network output data) [119]

5.4 Multilayer Beads Analysis and Modeling

Before modeling any situation, it is necessary to define the domain of analysis. In this research, it consists of the substrate and the bead. While the dimensions of the substrate are known prior to the deposition, the bead is created on the substrate and its geometry depends on the combined effects of many process parameters. Some of them which are not considered here such as surface tension and melt pool gravity etc. Predicting the bead geometry on the basis of these effects is out of the scope of this work.

Referring to multiple-beads experiments (Fig. 29), an interesting phenomenon is noticed that the height of a single bead is 0.83 mm and if continued to build up the 10-layers in the same way, the total theoretical height would be 8.30 mm (0.83×10) (Fig. 65a). But the total height measured actually in a 10-layer sample is 3.83 mm and same is the case with 25-layer sample where the total measured height is 17.38 mm (Fig 65 b).

The reason is the contact tip to work piece distance (CTWD), a distance from the top of the each layer to the nozzle to be maintained at 23 mm every time when a new layer gets deposited. The effect of the CTWD on height and width of the bead is found anomalous as investigated by the authors [119]. In all experiments, the CTWD was maintained at 23 mm and after each layer

the deposition nozzle would move in negative Z-direction equal to the amount of first bead height to maintain the desired height. Theoretically it repeats the same incremental height that is fed to the controller and deposits the subsequent layers by maintaining the distance of 23 mm. But in reality, this is not the case; 2nd, 3rd, 4th and subsequent beads (Fig 65 c) constitute lesser height than the 1st bead, so in reality CTWD increases on every layer equal to the difference of the amount of previous two layers and not able to maintain the desired distance, as a result height is not maintained in proportion with the number of layers. The difference in theoretical and actual bead heights is shown in Table 14. The individual height and width of a 10-layer sample is graphically shown in Figure 66.

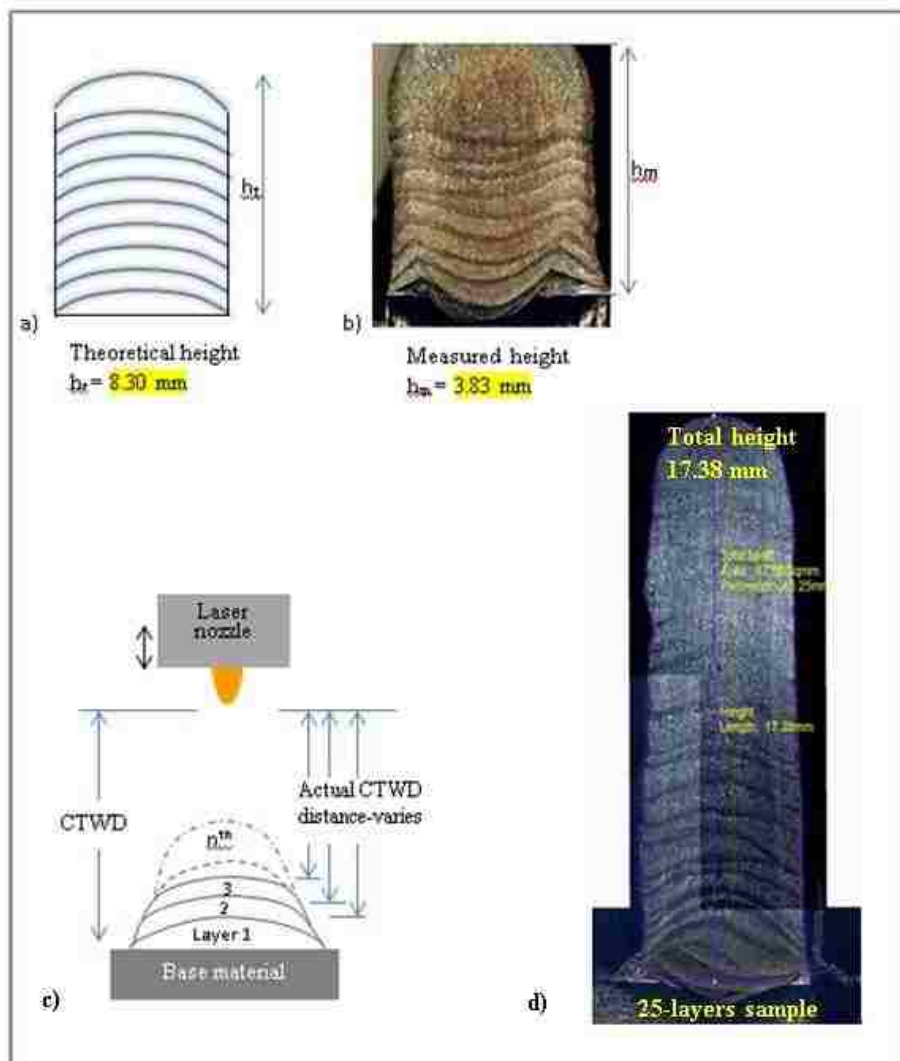


Figure 65. a) Theoretical height of 10-layers b) Experimental/measured height of 10-layers sample c) Schematic diagram shows that CTWD changes with the bead height d) 25-layers sample shows the total height

Table 14. Comparison for theoretical and actual bead heights

Sample	Theoretical bead height	Actual bead height	Difference in height
10-layer	8.30 mm	3.83 mm	4.47 mm
25-layer	20.75 mm	17.38 mm	3.37 mm

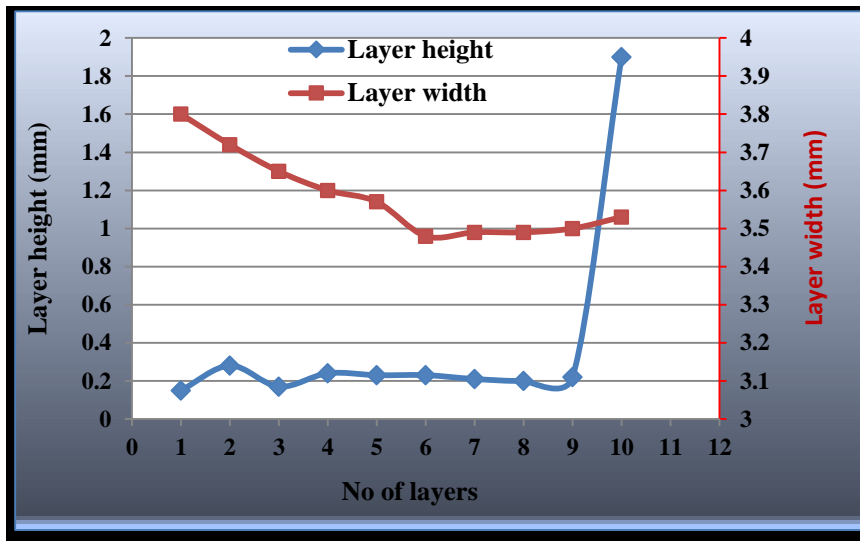


Figure 66. The height and width of the 10-layer sample

It is evident from the graph that the bead width is keep decreasing till the deposition of 6th layer and then it gets stabilized for the remaining layers. The individual bead heights are almost consistent except the last layer. Similarly the bead height varies between 0.15 mm to 0.28 mm till the second last layer but it is exceptionally high of 1.90 mm in the 10th layer and this phenomenon of the height of the top layer is always found higher than the height of the previous layers regardless of number of layers gets deposited, even in the stack ups, as it can be seen in Figure 67. It is noted that in the stack sample (4-layers high), the 4th layer is exceptionally higher than the other three layers.



Figure 67. Section view of stacked sample (3x4 beads)

This type of uncontrolled height creates challenge in achieving the total desired height of the model. From the steady state experiments of single beads conducted by Saqib et al. 2014 [127], it was shown to have a non-linear effect of CTWD on the bead height (Fig. 68). The maximum bead height of 1.5 mm is achieved at 23 mm of CTWD. These types of non-linear responses illustrate the challenges associated with developing a predictive model as each parameter impacts the bead geometry differently.

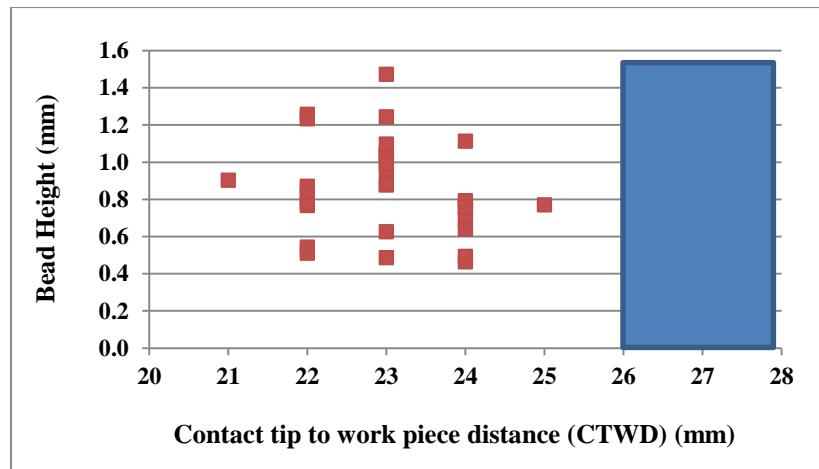


Figure 68. Bead height vs. CTWD (from the steady state experiments presented in Table 4)

The theoretical height and the actual height of the 10-layer sample is shown in Figure 69. The difference of 4.5 mm in both the heights can be seen. The CTWD of 23 mm is not able to maintain on each layer, instead this distance is getting bigger and bigger as the deposition progresses. By the time when 10th layer is being deposited, the CTWD becomes 27.5 mm (23 mm + 4.5 mm) and the actual value would be somewhere in the blue region as marked on Figure 68.

The blue region (from 26 mm to 28 mm), reflects for 10 layers stack, is the area where the CTWD value lies but this region will move to the right and the CTWD value would increase depending on the number of layers gets deposited. Especially when building a solid model where hundreds of layers are being deposited and it is challenge to find and maintain the exact value of CTWD for the model.

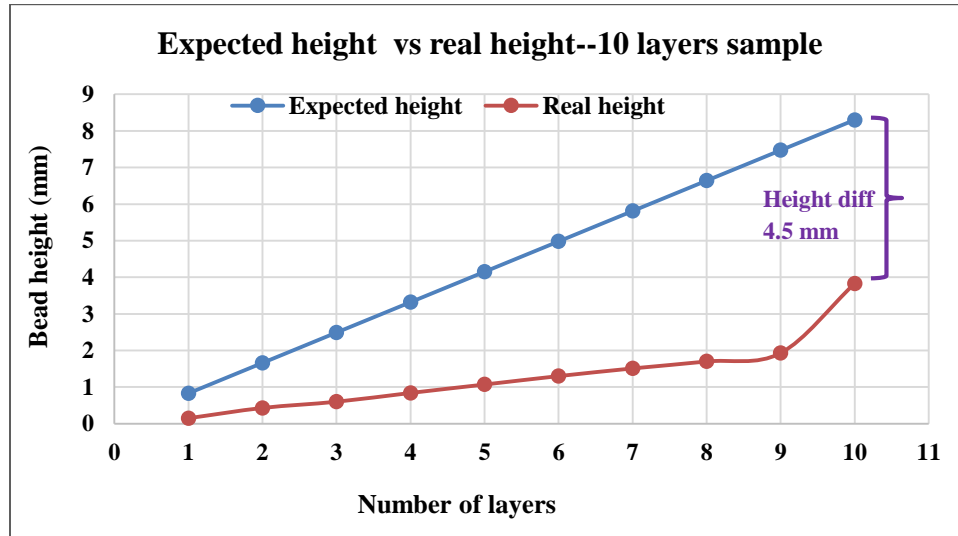


Figure 69. Height difference between the expected and real height of the 10-layer sample

Using the information of bead heights from each an individual layer, a graph is generated in the Mat lab environment to understand the trend in height, which gives the best fit (cubic) with the following model:

$$Y = 0.0032 X^3 - 0.093 X^2 + 0.98 X + 0.0096 \text{ ----- (20)}$$

All the experimental values (height) of layers 1, 2, 3, 5, 10, and layer 25 are plotted and curve fitting is shown in Figure 70. Residuals can also be seen with a norm of 0.179 mm.

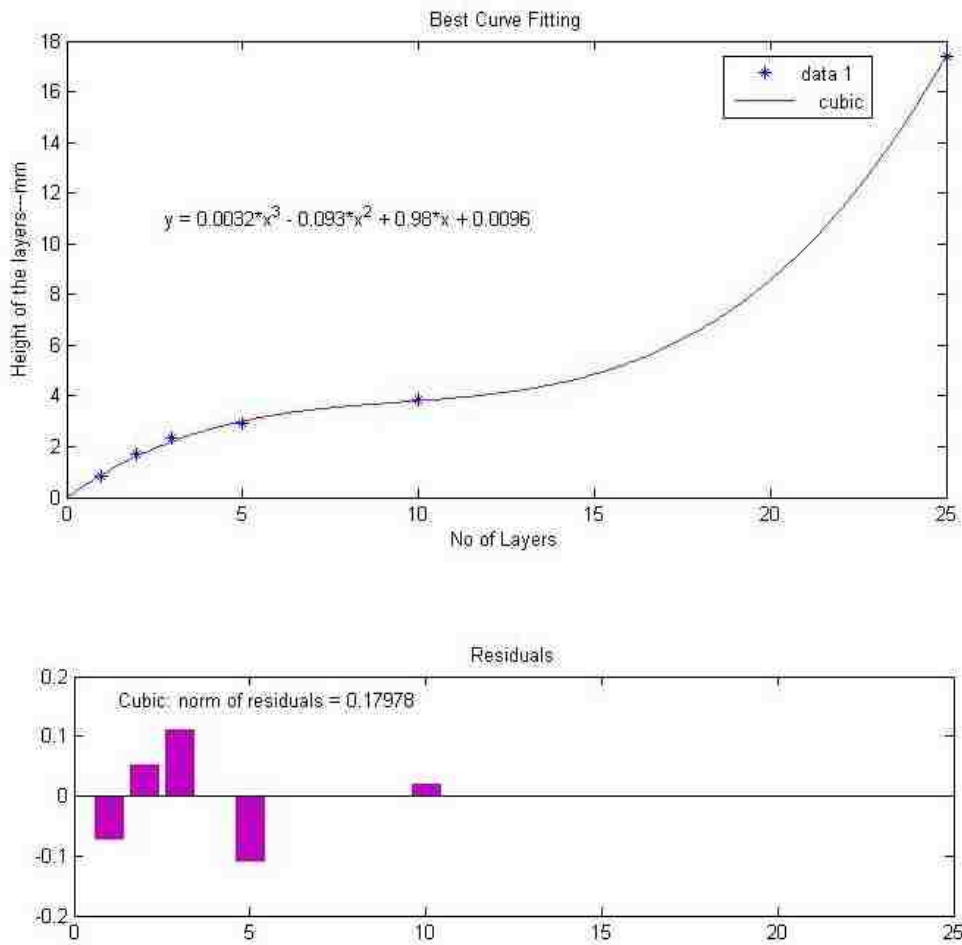


Figure 70. Curve fitting between the deposited layers and the corresponding height, residuals are also shown

Using the model equation-20, a visual representation between the number of layers (from layer 1 to layer 25) and the bead heights with their individual differences in height measurement is illustrated in Figure 71. Similarly the trend in bead height if deposited layers are exceeded to 50 layers is illustrated in Figure 72. The norms of residuals are 0.0014.

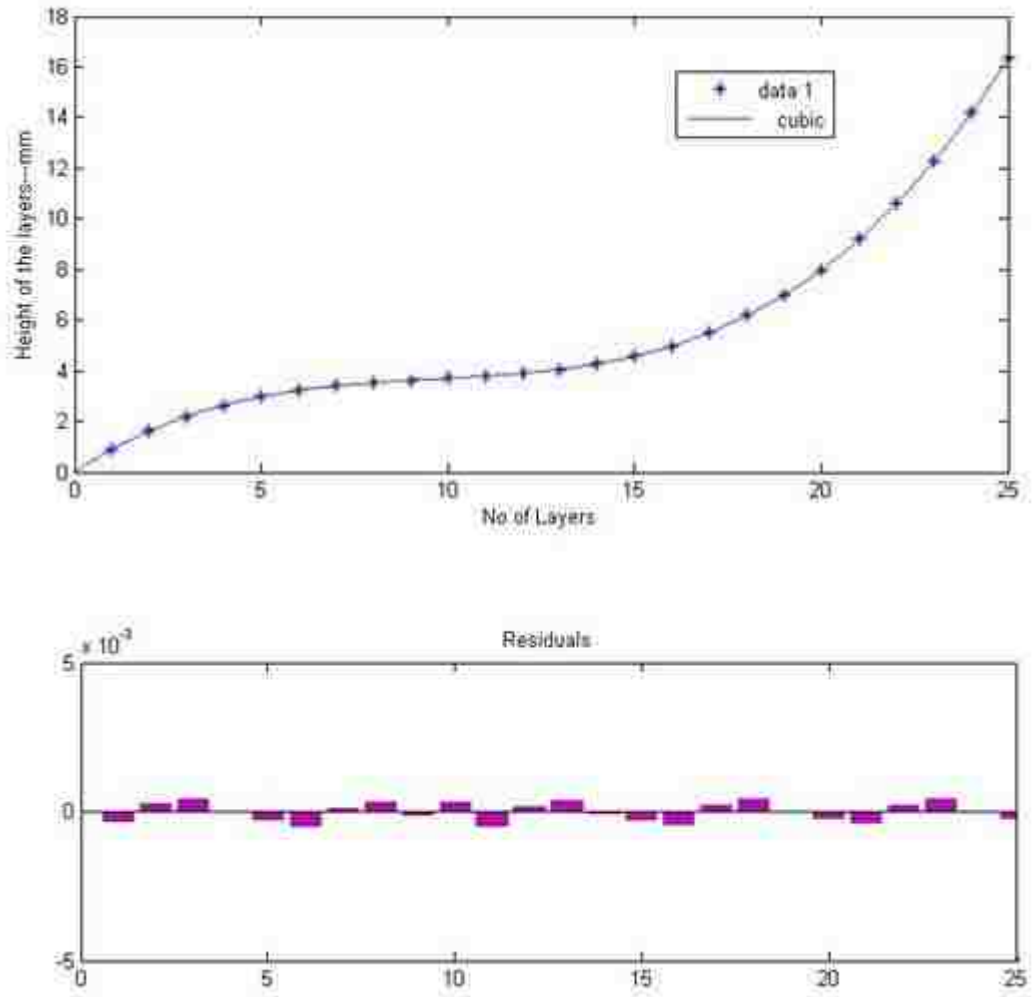


Figure 71. Trend in bead height with respect to the individual layers deposited and their residuals are also shown

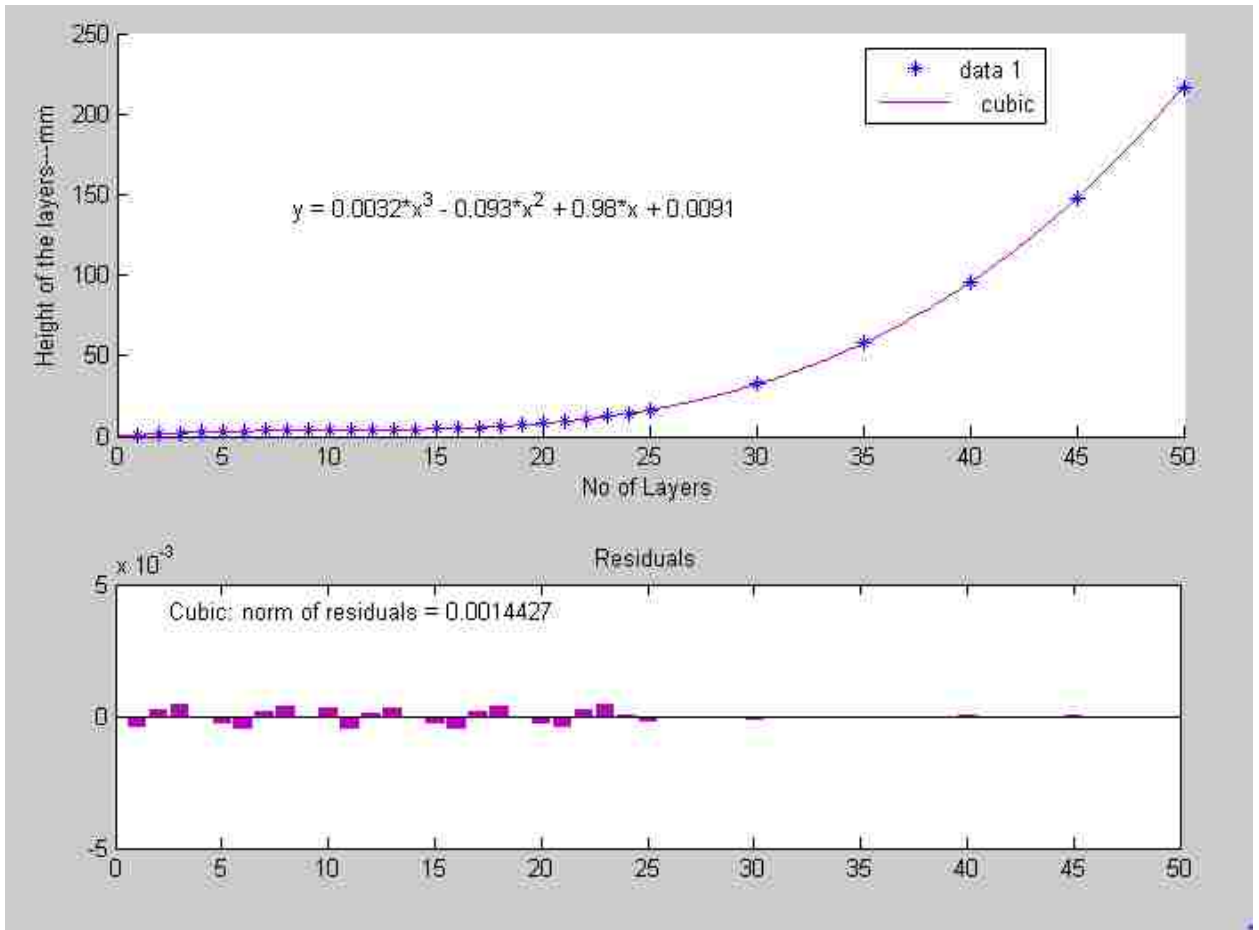


Figure 72. Trend in bead height with respect to the 50-layers deposition and their residuals

5.5 Transient Heat Conditions Analysis

From the experimental work of transient heat conditions, a clear correlation between the heat (laser power) and the width/height of the clad was found. This correlation was found to be independent of the substrate temperature, enabling real time control of the clad height by adjusting the laser power but this is beyond the scope of this research. The melting point of the substrate must preferably be higher than that of the deposited powder material. If this is not the case, then it is possible that during solidification and subsequent cooling of the clad layer, the substrate region just underneath the first layer can be heated to a temperature over the melting point which may lead to porosity and uneven clad along the interface.

To test the developed hypothesis (section 4.5); changing the power level would impact the melt pool width. A single bead sample is prepared with 2.6-3.6-2.6 kW, as each power level varied for 2-second intervals. The real time width data is shown in Figure 73. It can be seen that the melt pool width changes are synchronized with the power level changes; hence, the hypothesis change in the power level would result in an immediate change in the melt pool is validated.

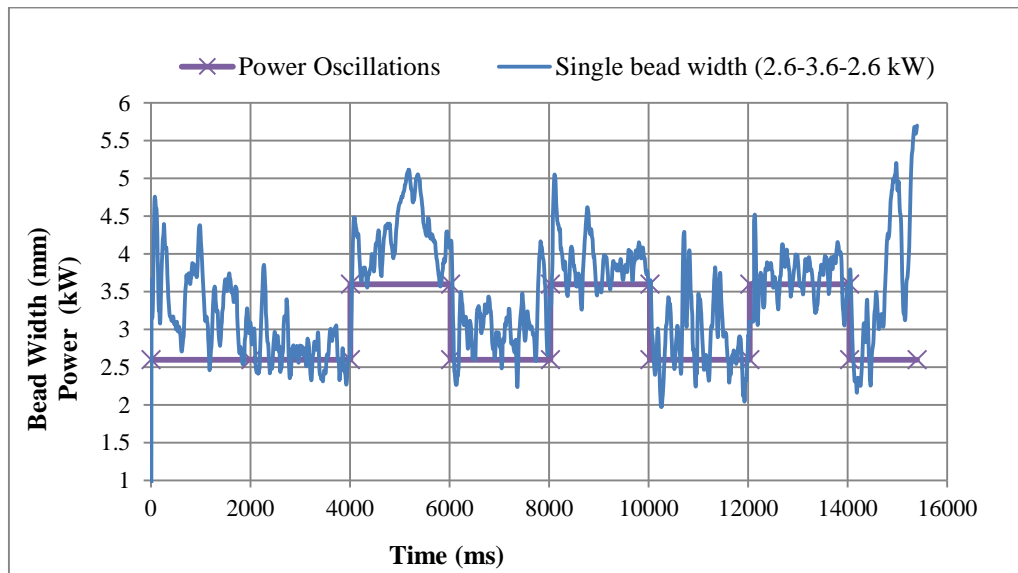


Figure 73. The instantaneous melt pool width variations (10 mm/sec travel speed).

As shown in Figure 72, the real time melt pool width responds to the power level changes. The average width for selected time intervals is shown in Figure 74. It is evident that the bead width is varying, although the process settings are equivalent for three 2.6 kW and 3.6kW intervals respectively.

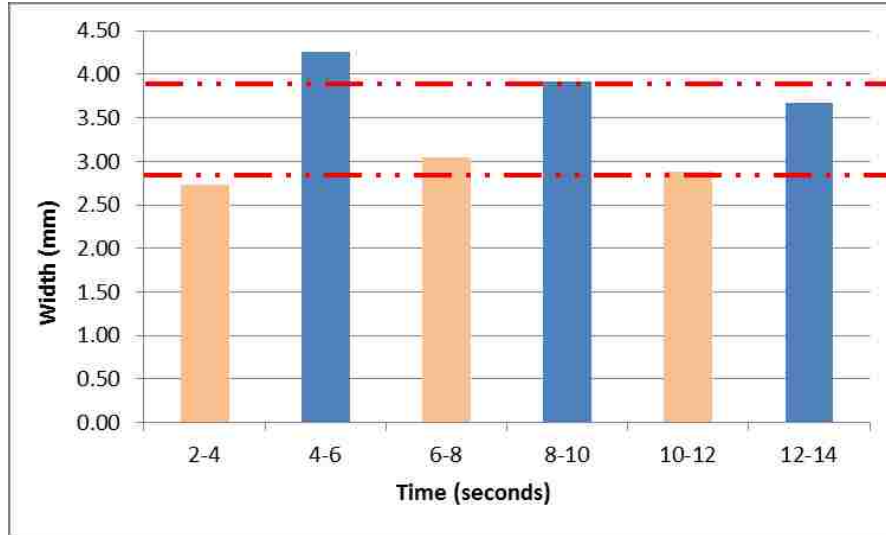
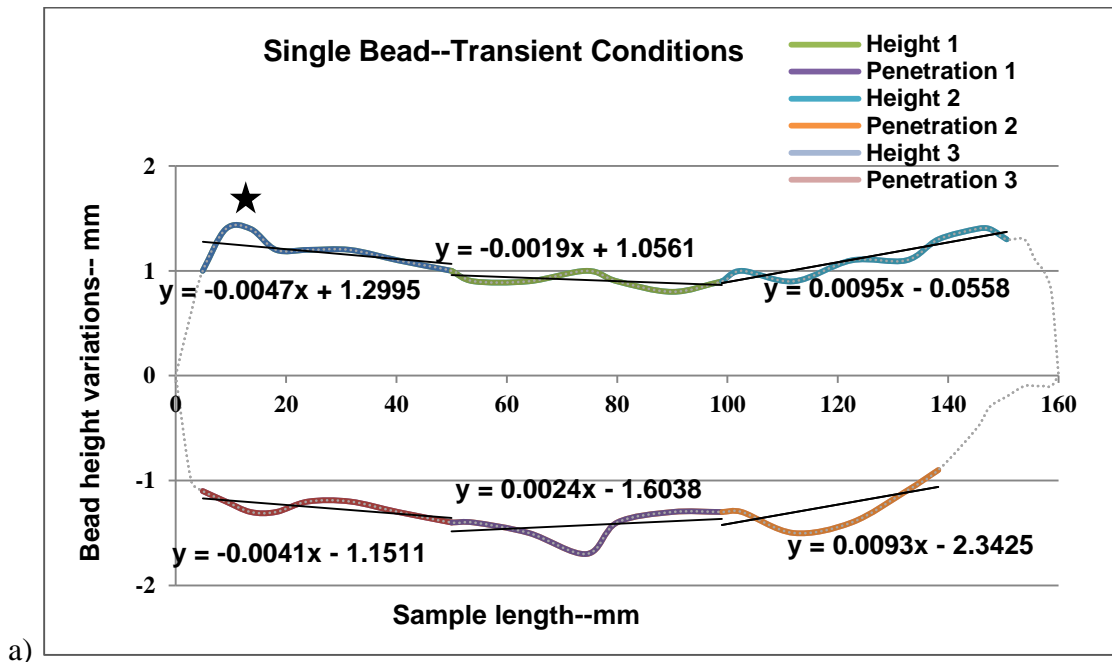


Figure 74. Average bead width for the step intervals, where the overall average width for the 2.6kW level = 2.89 mm, and the average width for the 3.6kW power level = 3.95 mm.

Following the experimental plan (Table 8), the bead height and penetration of the single bead transition (3kW-4kW-3kW) in segments is shown in Figure 75. To understand and find the trend of these variations, it is segmented into three sections (colored lines). The segmented bead width is also shown in different colors.



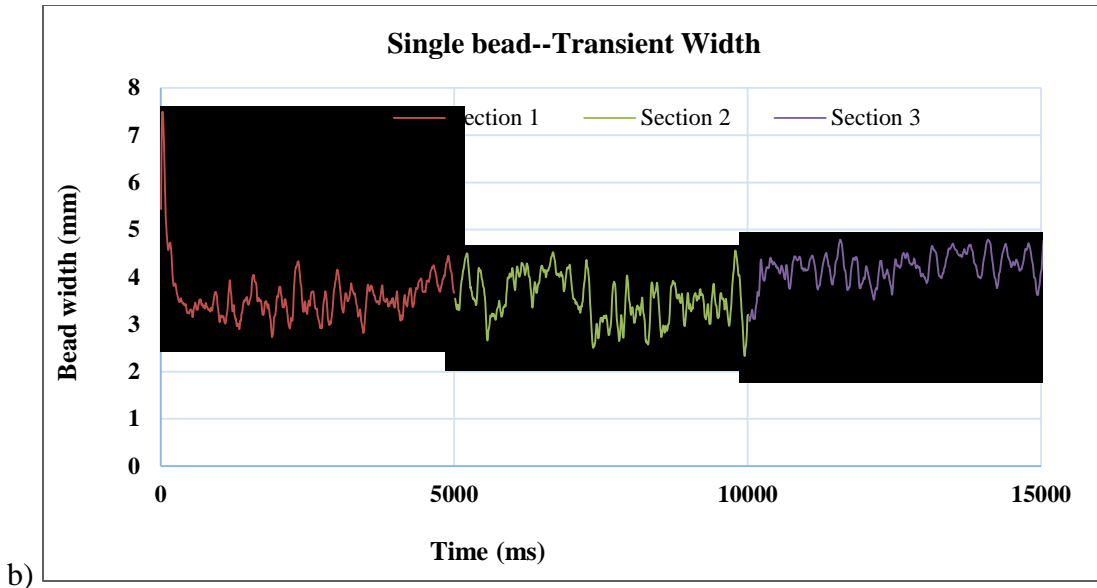


Figure 75. a) Segmented view of the height and penetration of the single bead transient layer b) Segmented bead width in each section.

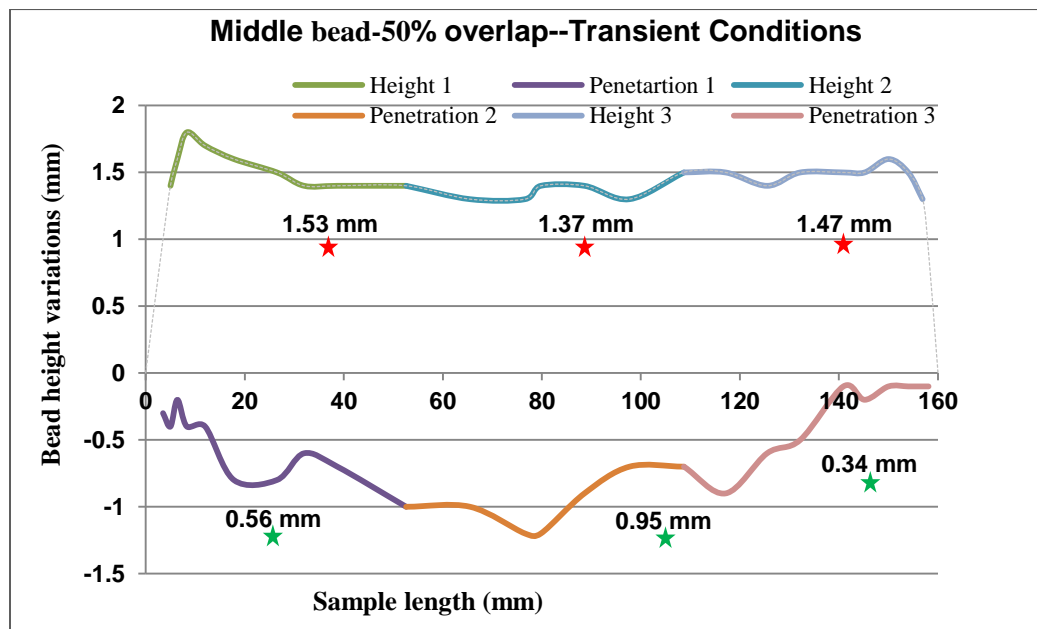
It is seen that the bead achieved the maximum height of 1.4 mm at the starting bead in (shown with a star symbol on Fig.75 a). It settles down, but before a valid steady state point can be definitively determined, the power is increased. There is reduction of height when this occurs. When the power is decreased, the height increases again and the highest point for this section is reached prior to the lead out/stop condition. The maximum penetration depth is observed at 1.7 mm and is found in the central section but this is not stable. It is related to the power levels, as expected, but there are some melt pool dynamics occurring, as the penetration values are oscillating.

For each power level region, the slopes of all geometric values and the differences of slope among sections are calculated (Table 15). It has been observed that the difference in slope height is around 60% less in section 2-1 compared to section 3-2. Similarly it is 75% less in penetration and 85% less in width for section 2-1 respectively. It means that more variation is observed in the last bead section for all responses as the power goes down.

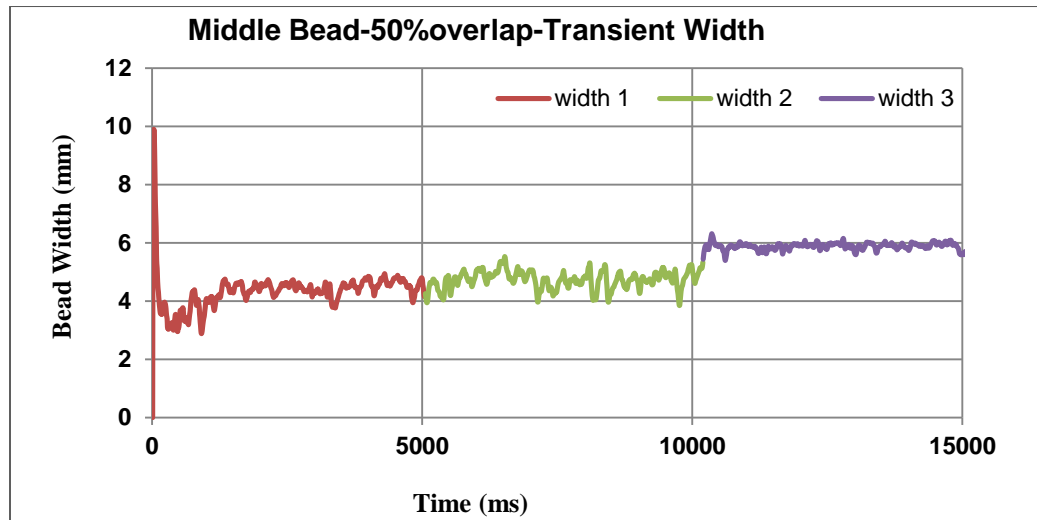
Table 15. Slopes of the single bead shape geometrical values and their differences among their sections

Transient Conditions	Slope	
	Height	Penetration
Section-1 3kW	-0.0047	-0.0041
Section-2 4kW	-0.0019	0.0024
Section-3 3kW	0.0095	0.0093
Slope Difference		
Δ Section 2-1	0.0028	0.0017
Δ Section 3-2	0.0076	0.0069

The bead geometry for the one layer, (50% overlapping condition middle bead) is shown in Figure 76. The trend in the heights and penetrations is similar in both the situations of single and overlap beads, but the magnitude vary. The maximum height and penetration are found to be 1.8 mm and 1.2 mm respectively. The average heights and penetrations in each section are shown with the red and green star symbols respectively. Previous research by Urbanic et al. 2016 [1] has shown that the penetration reduces with bead overlapping conditions, so this reduction in penetration is expected. The minimum variation in bead width is seen in last section (Fig. 76 b- purple line).



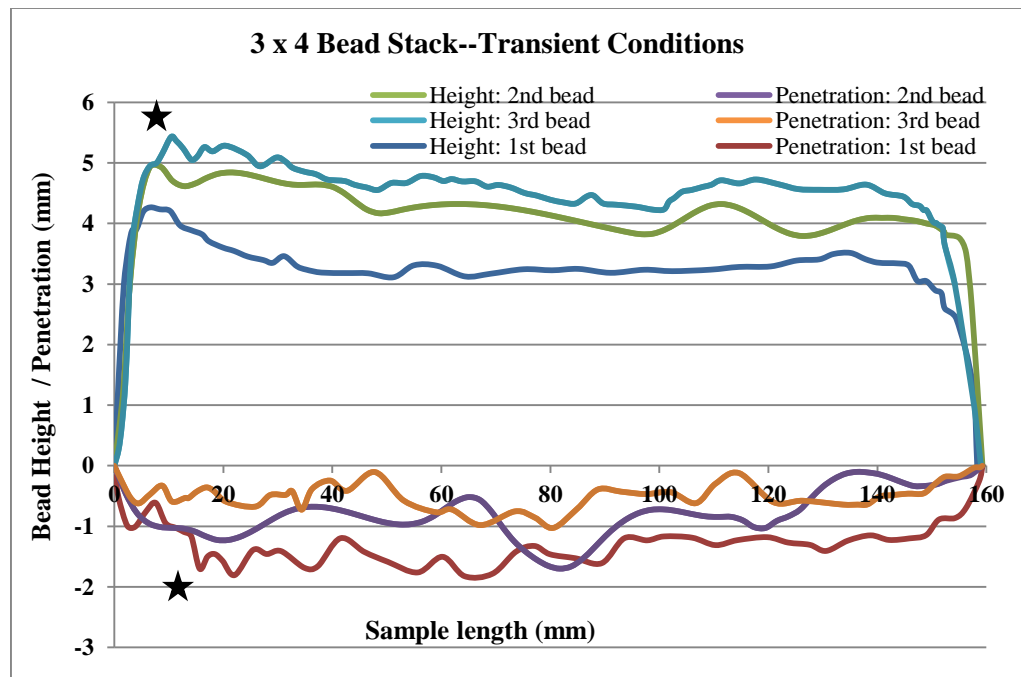
a)



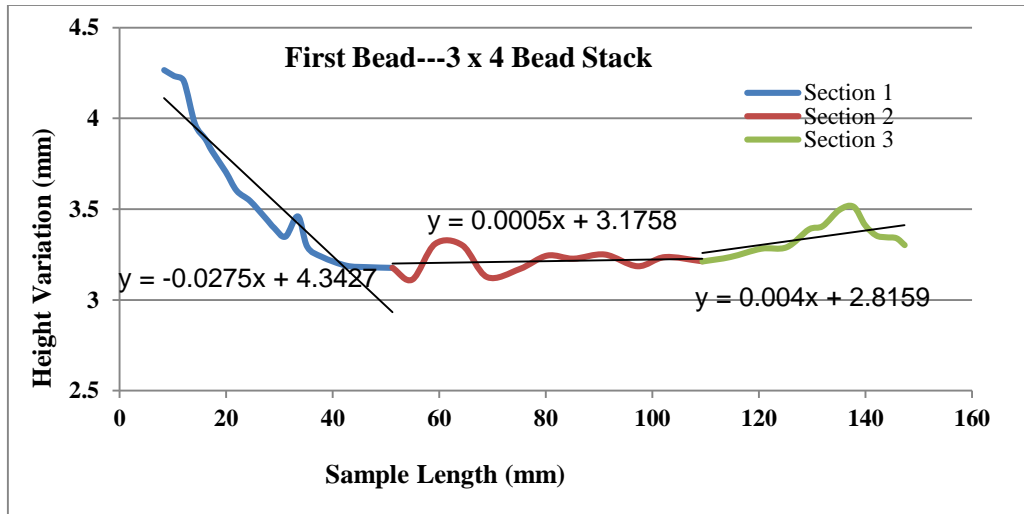
b)

Figure 76. a) Longitudinal transition sample show the variations in height and penetration in sections, star symbols indicates the average height and penetration in each section b) Segmented bead width.

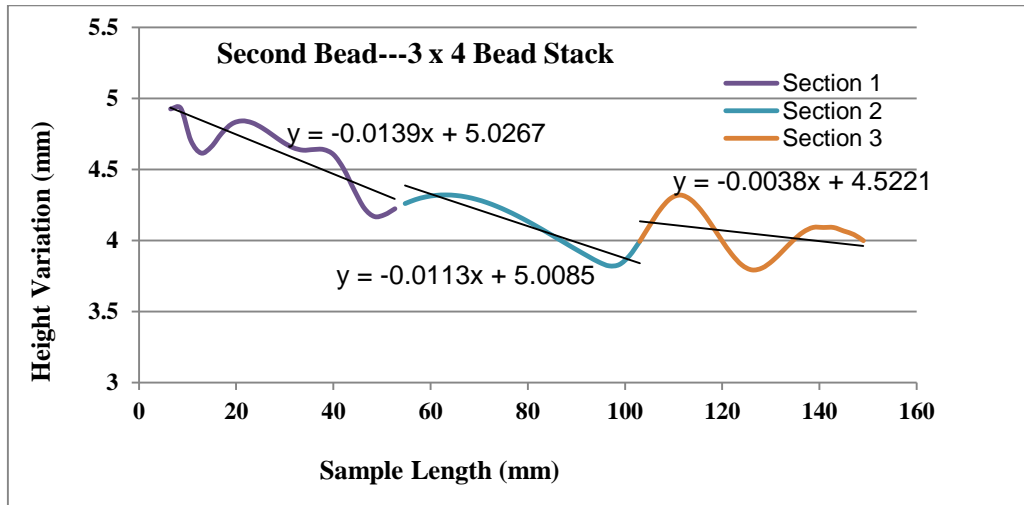
The results for the four bead stack are illustrated in Figure. 77. Sectioning is performed along the center of all three beads. The influences of the transients are evident. The maximum height observed 5.36 mm in the 3rd bead but the deepest penetration is found to be 1.82 mm in the 1st bead (identified with the star symbol). The minimum height and minimum penetration is found in 1st bead and 3rd bead respectively.



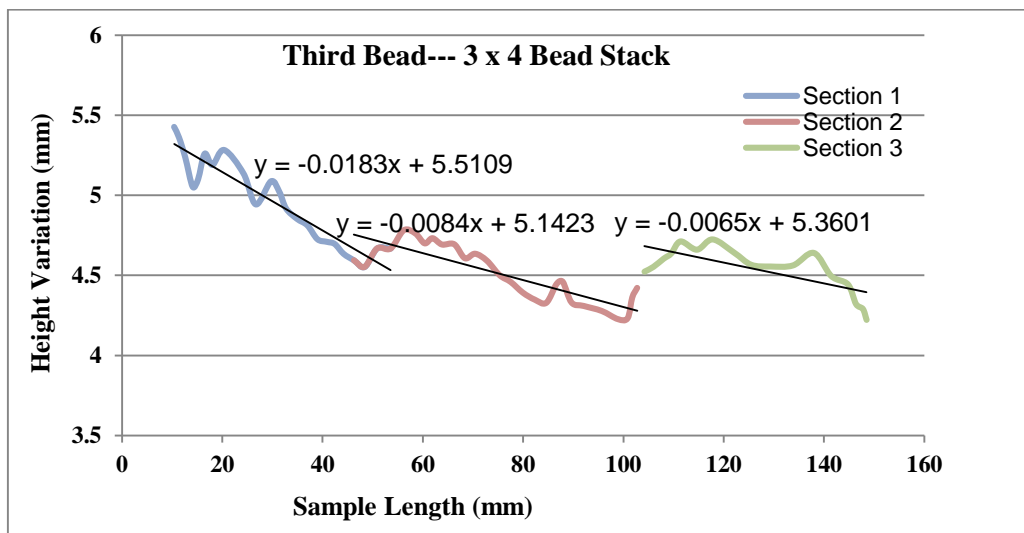
a)



i.)



ii.)



iii.)

b)

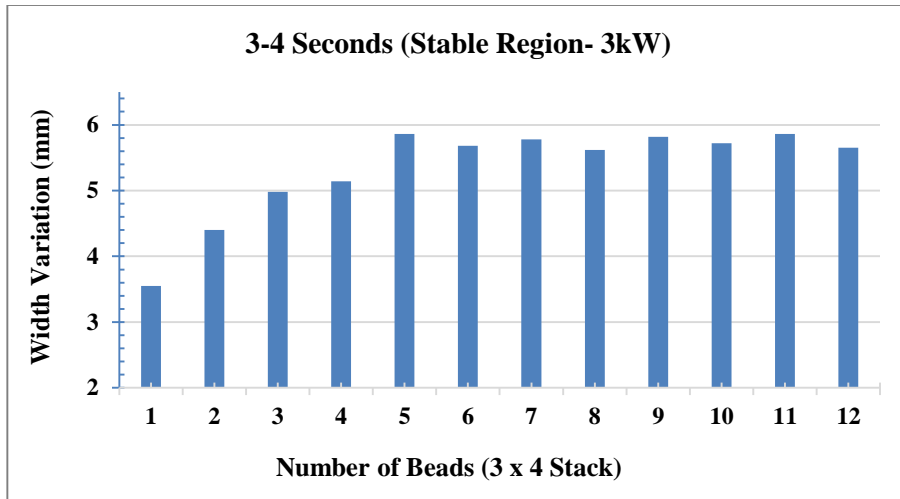
Figure 77. a) Transition sample of 3x4 stack shows the variations in height and penetration b) Segmented views of the i) First bead ii) Second bead and iii) Third bead of the 3 x 4 bead stack.

The average slope of the individual bead height is calculated (Table 16) and found maximum in section 1 and minimum in section 3 (bolded values) among all three sections which means that the bead height decreases in 1st section regardless of the bead sequence and then it is seen stable in section 2 with the transient condition. Similarly the maximum and minimum slope height differences are found in 1st bead and 3rd bead respectively (italicized values) among all three beads over the transient period (Table 16).

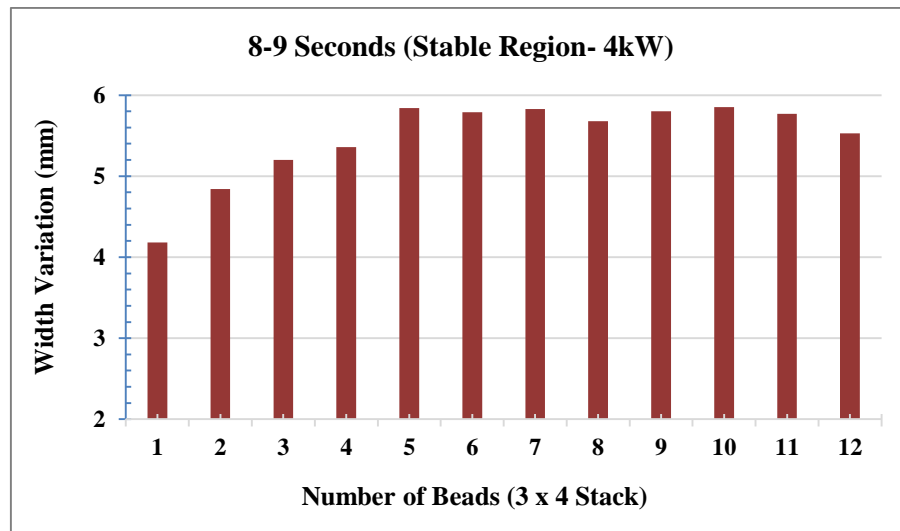
Table 16. Slopes of the bead heights in 3x4 stacks and their differences among their sections.

Transient Heat Conditions (3x4 stack)	Slope			
	1st bead	2nd Bead	3rd Bead	Av Slope height (section wise)
	Height 1	Height 2	Height 3	
Section-1 (3 kW)	-0.0275	-0.0139	-0.0183	0.0199
Section-2 (4 kW)	0.0005	-0.0113	-0.0084	0.0067
Section-3 (3 kW)	0.0040	-0.0038	0.0065	0.0047
Slope Difference				
Section 2-1	<i>0.027</i>	0.0026	0.010	
Section 3-2	0.0035	0.0075	<i>0.0019</i>	

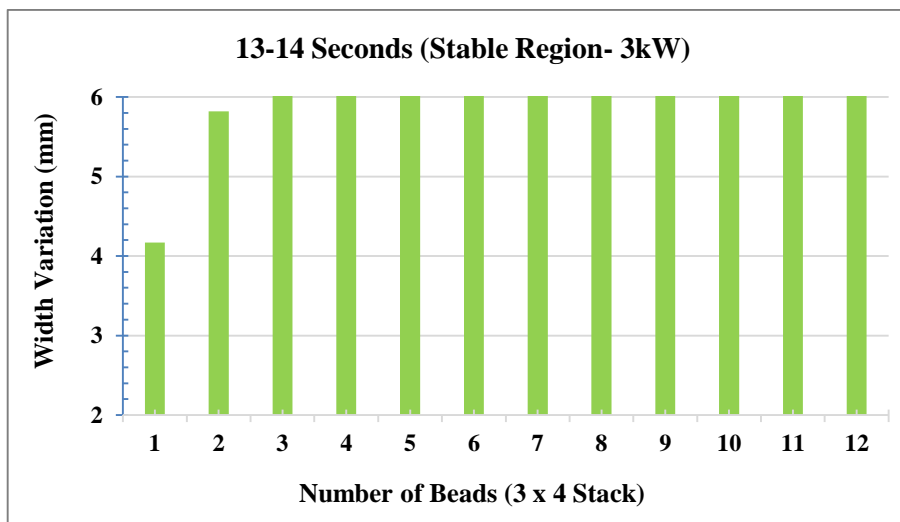
For the 3x4 bead stack sample performed with 3kW- 4kW-3kW, the real time width data in each stable region for all 12 beads are shown in Figure 78, where the power varies in 5 seconds interval for the total of 15 seconds. It can be seen that the melt pool width changes are synchronized with the power level changes. Regardless of the stable region; the bead width trend is similar in all 12 beads.



a)



b)



c)

Figure 78 . Bead width is shown for 12 beads (3x4 stack) in different stable regions

The first three beads of 3 x 4 stacks are compared with the 3-beads of 50% overlapping sample to see if there is any consistency in the bead width. The width data is taken at the mid of each region such as 3-sec, 8 sec and 13 sec time interval. It is seen that, in the first region (3sec), the width of the first and the third bead of 50% overlap sample is more than the width of the corresponding beads of 3x4 stack, as shown in Figure 79. The trend in the bead width of section 1 and section 3 is similar but the magnitude varies.

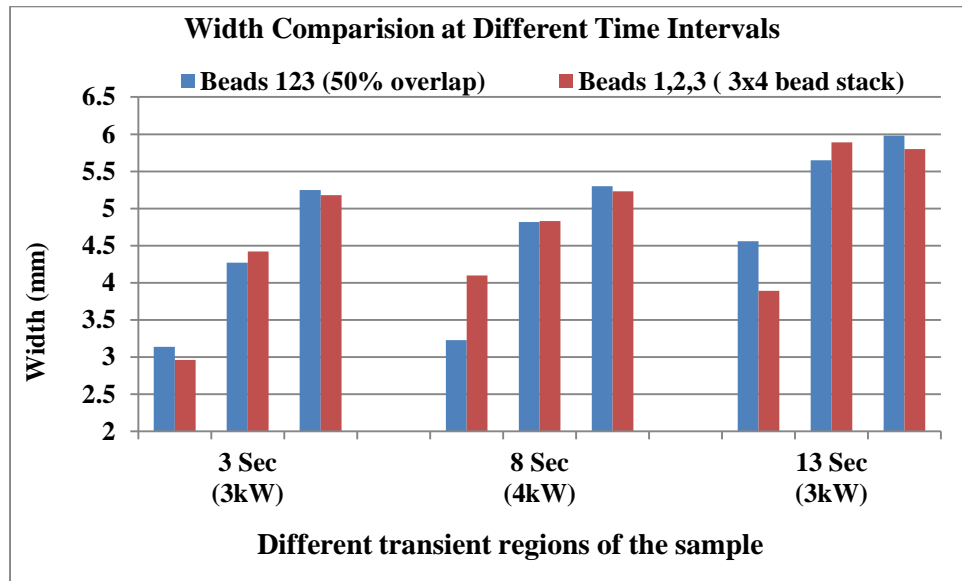


Figure 79. Width comparison of 50% overlap beads and 3x4 bead stack

The height of the single bead at selected transient region is 1.1, 0.9, and 1.2 mm so the theoretical height for 4-layers would be 4.4, 3.6, and 4.8 mm respectively. This theoretical height is compared with the 4-heights of 3x4 bead stack in each section. The height difference is marked with the red line in Figure 80. It is evident that the actual height of section 2 and 3 is 6% more than the theoretical height in 3-4 sec region, similarly it is also 14 % more in 8-9 sec region but it is seen 11 % less than the theoretical height in last 13-14 sec region. The height of the section1 is much below than the theoretical height in all regions.

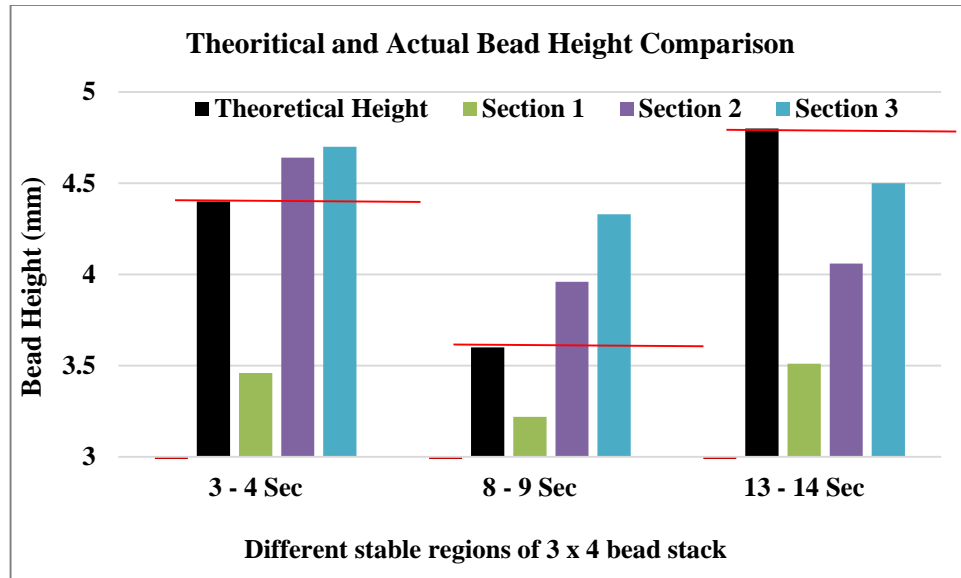


Figure 80. Height comparison between theoretical and actual bead heights

5.6 Standard Process Transient Condition Analysis

5.6.1 Bead Corners Configurations Analysis

The corner configuration samples (Fig. 37) were cut at three different joints and the bead height, width and penetration were measured (Appendix D) for all three corner types of each configuration and graphed, as shown in Figure 81.

It is evident from the graph that the bead height is found to be keep on increasing from 1st bend to the 3rd bend in acute configuration as the deposition progresses in one direction and also it has reached the maximum in 3rd bend among all types of configurations whereas the lowest height is seen in 2nd bend of right angled configuration. Similarly bead width is also found maximum in acute angled configurations where as it is almost consistent in all bends of obtuse configuration. The depth or penetration is the deepest in right angled configuration but also significant in first two bends of acute angled configuration.

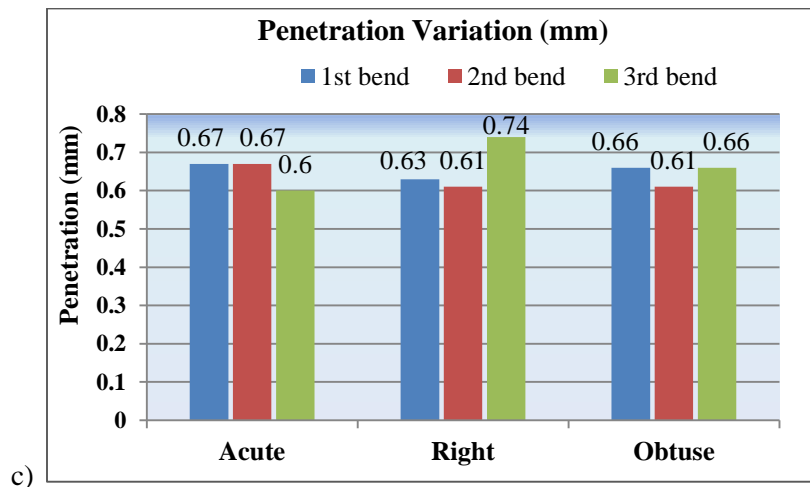
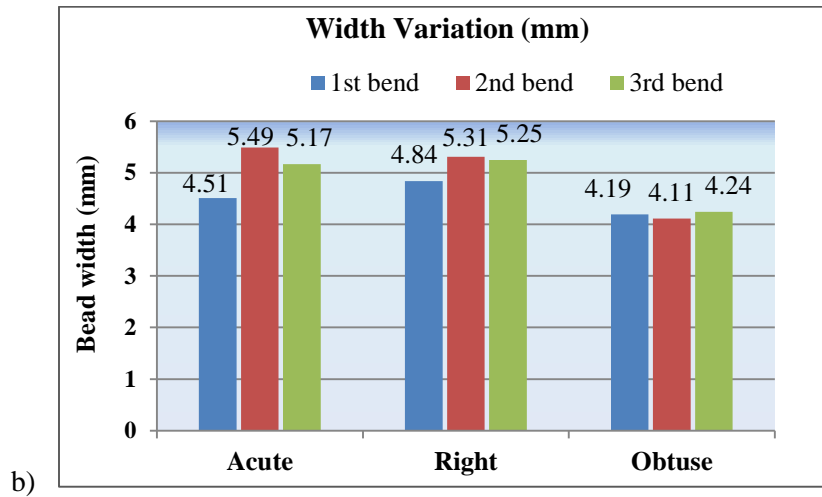
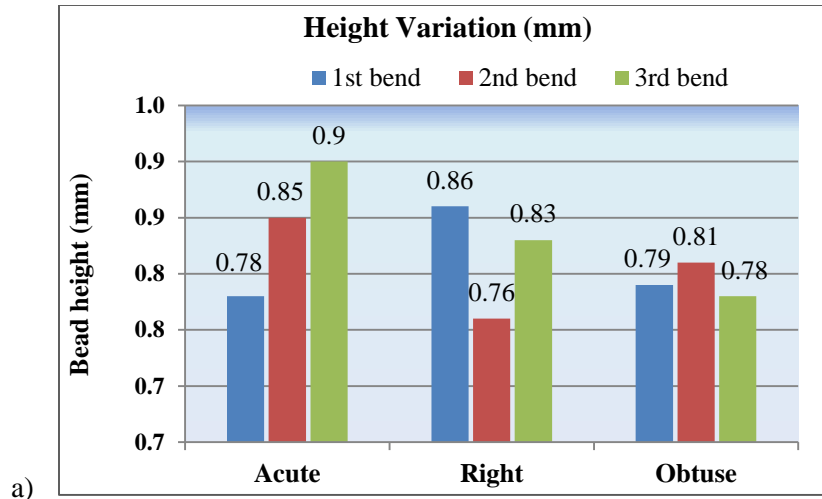


Figure 81. The bead geometry variations a) height b) width and c) penetration) based on the bead deposition flow direction and different cornering configurations

It is also noticed that the height measured at different points before and after the bends appeared to be lesser than the height measured at the bends. It looks like laser nozzle pauses for a second while depositing powder material at corners, accumulates a little bit more material at the bends resulting an increased height at the corners. The highest and lowest standard deviations of the bead height are found to be in acute and obtuse angled configurations respectively (Fig. 82). Although the height variation is small, but still influences the contact tip to work piece distance (CTWD) for overlapping scenarios.

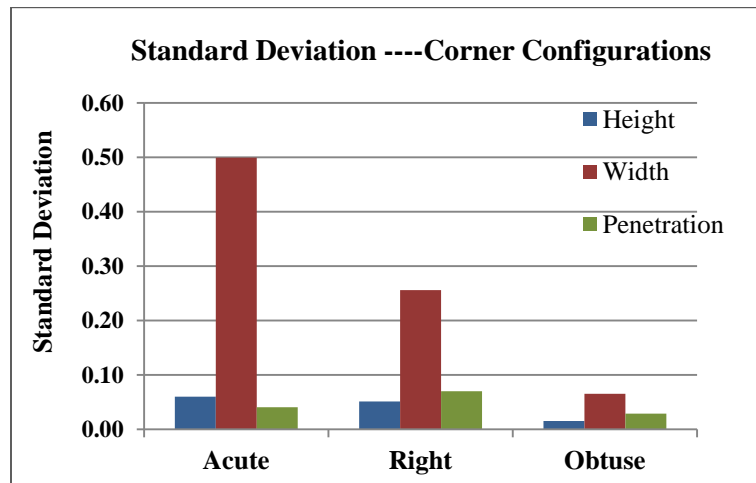


Figure 82. Standard deviations in single bead height, width and penetration are shown

5.6.2 Lead-in and Lead-out Situation Analysis

The laser cladding is a robust process which leads to the formation of continuous coating. When initiating the bead deposition, there is a transition zone prior to establishing the steady state geometry. This is lead-in condition; whereas, the lead-out condition occurs when the process is stopped. Regardless of the conditions; imperfections may be occurred in clad geometry when a continuous cladding is performed. Sometimes the cladding on the edge of flanges is required, where not only the side overlapping of single track is needed but also the start of the track has an overlap with the ending of the track is observed. The understanding and the defect elimination in lead-in and lead-out zones is required especially when cladding is performed in a closed loop manner.

It is also clear from the graph (Figure 83 ---arrow indicates the direction of the deposition) that lead-in and lead-out conditions differ. The clad height is appeared to be increased in the zone which leads to the problem of increased height and microstructural defects as well if continuous coating is desired.

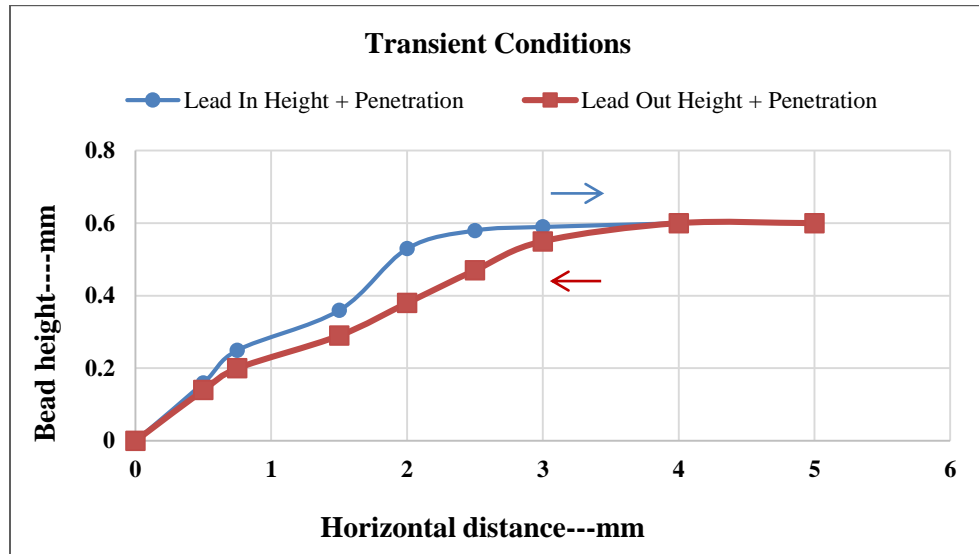
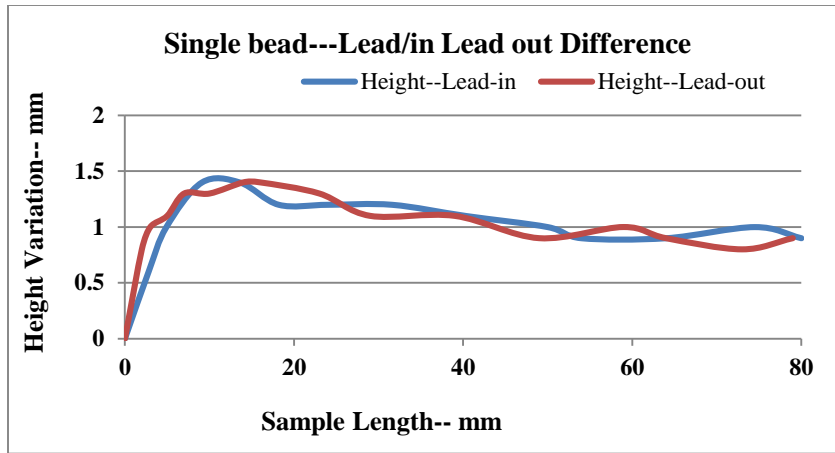


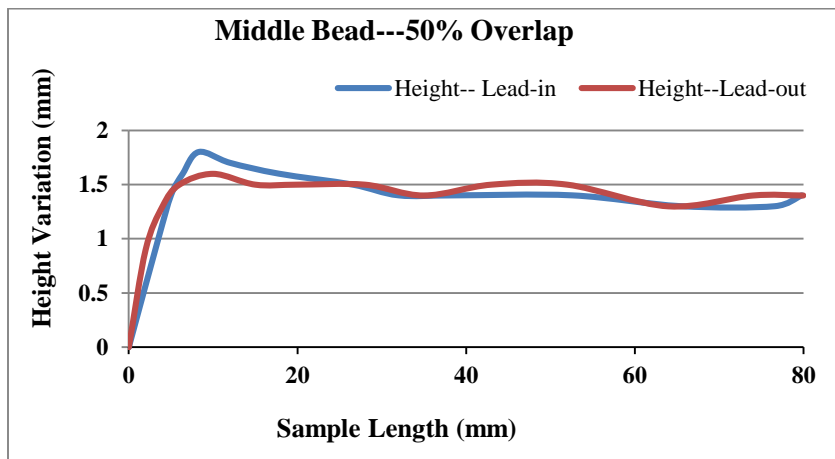
Figure 83. Deposited bead profile in the beginning (lead-in) and in the end (lead-out) of a single track

The bead geometry is seen stable at the 3 mm mark in lead-in condition at a 10 mm/sec deposition speed, this is equivalent to 0.3 seconds but in the lead-out scenario, the transient geometry is approximately 5 mm distance (0.5 seconds). An understanding of this time/distance relationship enables planners to design their deposition strategies. This information would be helpful from the process planning point of view that the planners would address lead-in and lead-out situations while generating the tool path for a multiple bead deposition.

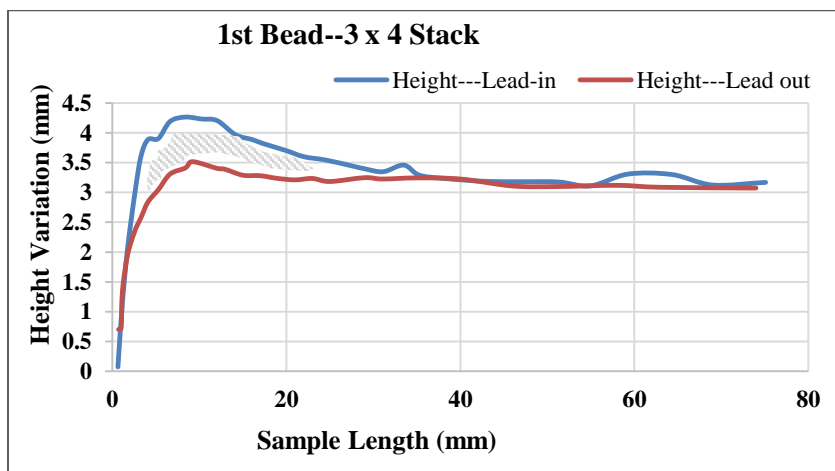
It is necessary to understand and put into consideration that how the bead height does vary in lead-in and lead-out condition either in a single layer or multiple layer depositions (transient conditions). The data collected in these conditions was then mirrored at the midpoint to understand the trend in bead height, is thus shown in Figure 84.



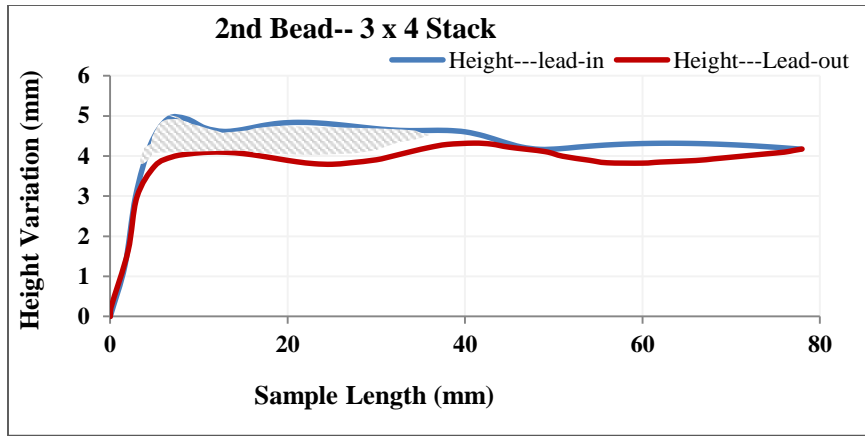
a)



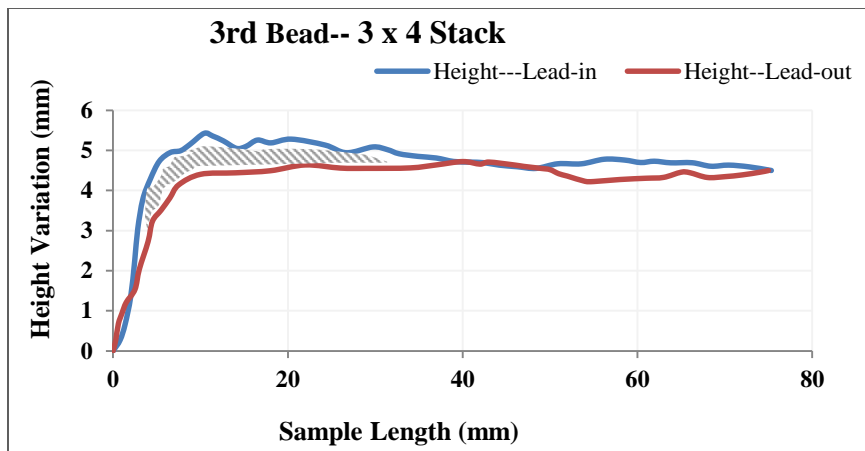
b)



c)



d)



e)

Figure 84. Bead heights varies in lead-in and lead-out situations a) Single bead b) overlap bead c) 1st bead section of 3x4 stack d) 2nd bead section of 3x4 stack and e) 3rd bead section of 3x4 stack.

From this experiment set, it can be seen that there is a difference in slopes, peak values and settling times between the start – stop / lead in – lead out conditions. The difference in the lead-in and lead-out for the height is not significant in single and multiple bead but it is significant in stack up conditions and can easily be seen in Figure 84 c, d, e. (the gap is filled with gray hatch lines). Designers must adjust the process setting in order to minimize the gap between the heights. Using experimentation techniques of making single and multiple beads in different scenarios and evaluate the data will provide a foundation for process planning travel path development as lead-in transient is different from the lead out transient in stack ups.

5.6.3 Analysis of CT Scanned Models

The cladded model mentioned in section 4.8 is CT scanned and the wall thickness of the hollow cone and the parabolic shape models are measured. Results are graphed in Figure 85. Similarly the ranges and standard deviation are shown in Table 17.

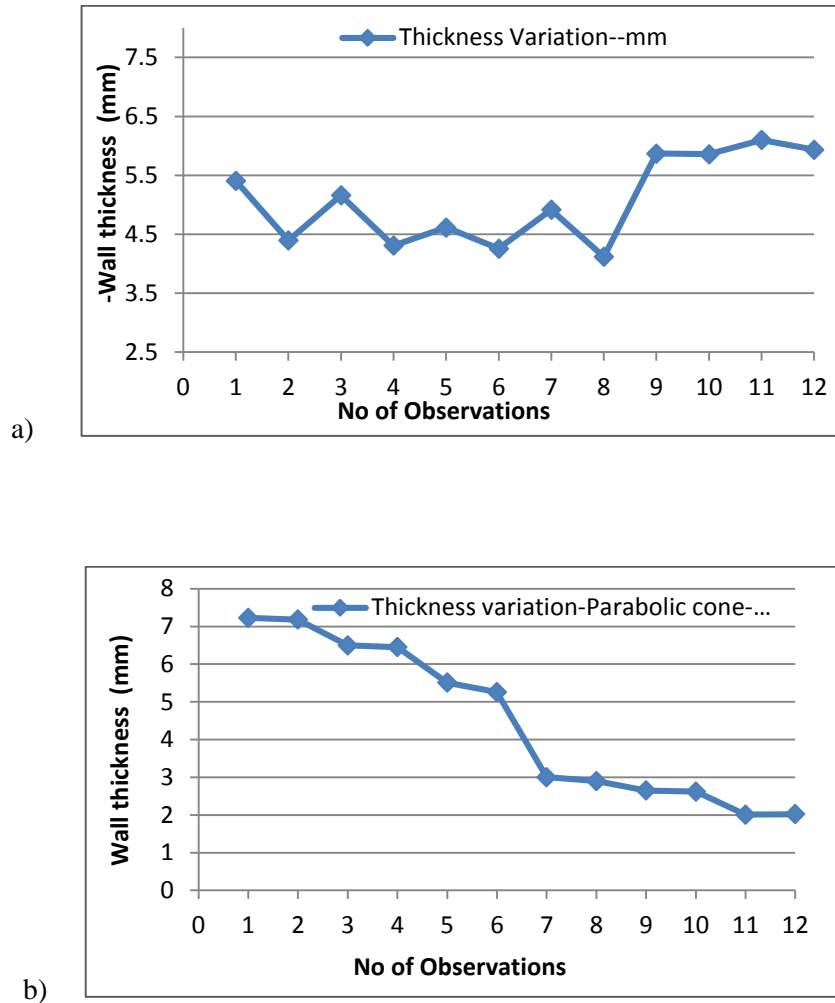


Figure 85. Thickness variation (bottom to top) for a) The cone and b) The parabolic model is shown

Table 17. Ranges and Standard Deviations are shown for thickness data

Cladded Models	Range	Standard Deviation
Hollow Cone	1.98	0.740
Parabolic Cone	5.22	2.002

Then these cladded models are compared with the original CAD data and are shown in Table 18.

Table 18. Comparison in geometry between CAD model and cladded models

Models	CAD Model		Cladded Model		Difference	
	Height	Base diameter	Height	Base diameter	Height	Base diameter
Hollow Cone	40	40	36.31	32.75	-3.69	-7.25
Thin Shell (Parabolic)	115	60	118	55	+3.0	-5.0

Note: All dimensions are in mm. Positive sign indicates that the cladded dimensions are more than the CAD dimensions

It is challenging to maintain the height, diameter and thickness of these models during the cladding since on each layer, geometry is being changed. Once a robust methodology is established for one scenario, additional experimental and calibrated simulation models can be effectively derived for alternative scenarios (i.e., different materials and laser spot size, etc.) to develop an extensible materials-systems database, which is required to develop a comprehensive process-planning module.

Chapter 6

Process Planning and Associated Challenges

The laser cladding (LC) environment is complex, as evident by the reported results. It is challenging to develop robust bead geometry to process parameter model due to noise, non-linearity and coupling. It becomes more challenging when multiple or stacked layers are deposited for making a 3D structure. Since cladding involves melting of metal and then the solidification that causes the deposited layer height unpredictable and adjustment in process parameters becomes essential to accommodate this phenomenon. The cladded models (cone and parabolic) are made in layers, as illustrated in Figure 86. The work bench was set at 0 degree; means the nozzle was orthogonal with the work piece all the time.

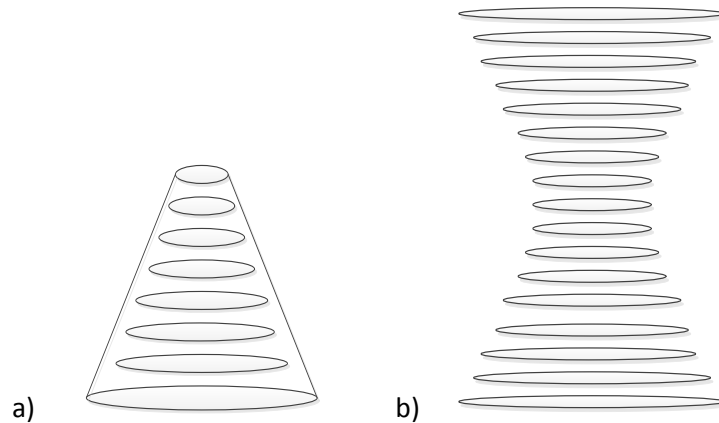


Figure 86. Cladded models made with layer by layers

These are the symmetric shell models, since the geometry of both the models are converging in shape in the beginning, every other layer needs to be set at a reduced diameter not only to keep maintaining the overall model width but also the wall thickness as well. Similarly in the parabolic model, when it is getting diverging shape after half of the way, and the diameter is getting bigger; the challenges continue such as the parameter of each layer needs to adjust. This is not trivial; the systems response time is not fast enough for some of the parameters such as powder flow and adjustment in focal length cannot be made instantly.

To maintain the wall thickness either in converging or diverging area; an option is to wait and let the deposited layer gets cool down and then laid down the other layer with some adjustment but this will affect the travel path planning and increase the build time. Insertion of camera control is an option which may overcome the problem arises with convergent/divergent shape shell model.

6.1 Process Planning in Additive and Subtractive Manufacturing (Machining)

For the additive manufacturing (AM); process planning tasks are trivial and involve decisions related to the slice thicknesses, the position in the build envelope, the part orientation, build time, support structure type (if required) and the fill strategy. Depending on the AM process, support material is required for overhanging geometry, such as undercuts or overhanging structures. If the model is made through layered manufacturing, the time required to build the part is related to the volume of material to be added.

Typically, the CAD model (which must be watertight) is converted into standard triangulation language format (STL), which is then processed using the original equipment manufacturer's (OEM) process planning software to create the build files. The processing steps, their flow and comparison between planning of the additive and subtractive manufacturing (SM) processes is shown in Figure 87. The fused deposition modeling (FDM) process and its process planning software (Insight 8.1 ®) is considered for the representation.

Usually the process planning interaction is minimal in all AM processes; some STL file repairs may be required, and the designer must select some basic location and slice parameters. Some post processing is generally required for curing or removing support materials.

Unlike additive manufacturing process, process planning and its associated machine time is high in subtractive manufacturing (SM) or machining process, especially when any complex component needs to be machined. To form complex geometry from block of stock material, it may be required that material to be removed from multiple orientations, or from different set ups, machines and cutting tools. This leads to longer manufacturing times and high level of process planning skills are required. When a component is designed, all detailed information with respect to the shape, tolerances, surface finish and engineering specifics are used as the foundation for developing a process plan.

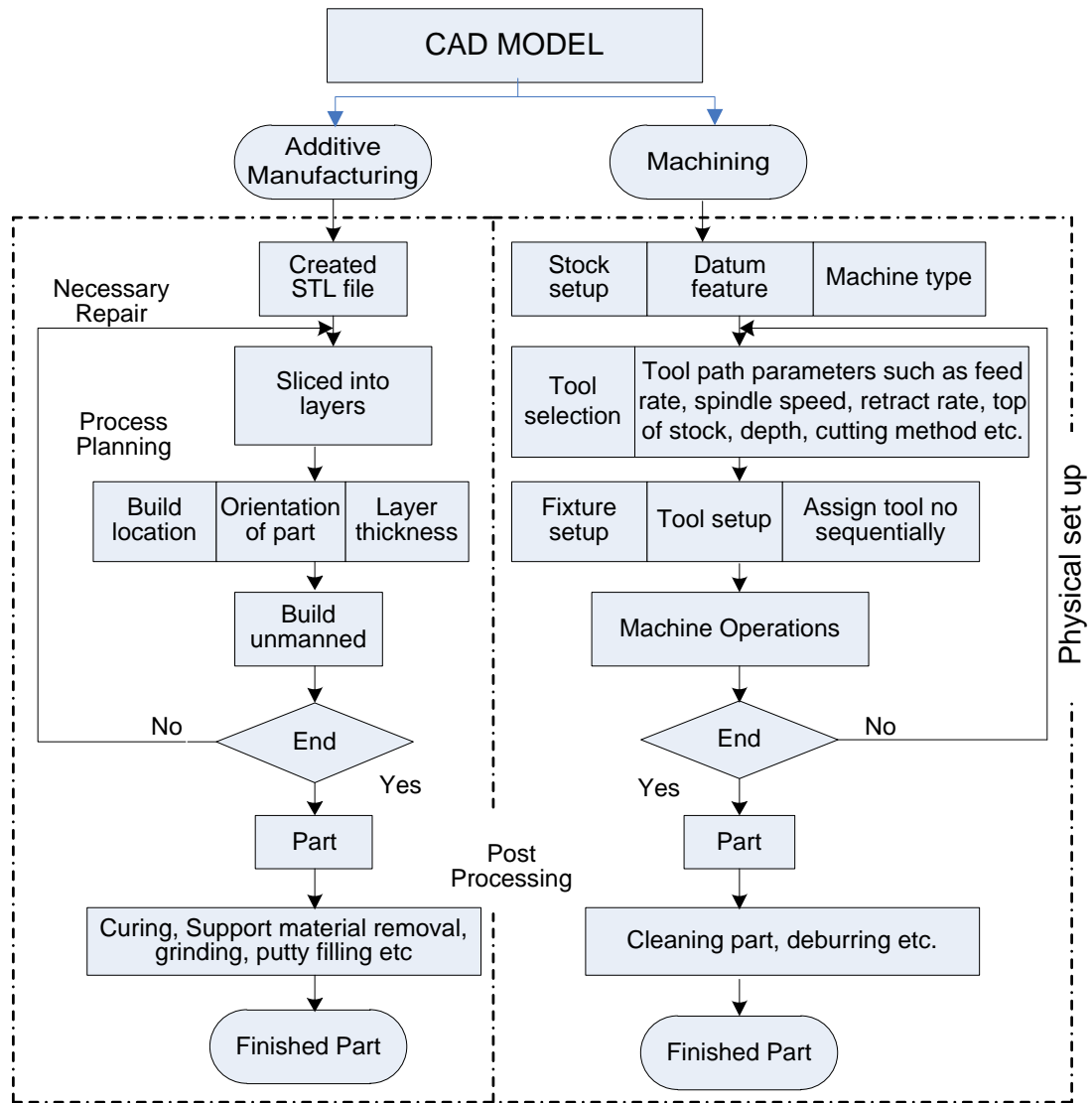


Figure 87. Flow of the additive and subtractive manufacturing processes

Tight tolerances and high quality surface finishes can be achieved with machining. The planning time can be long as fixtures need to be designed for various in-process orientations, tools selection, and decisions with respect the travel path type, step over, lead in/lead out, stock removal per pass, usage of coolant, etc. is required. At each orientation, a tool is required that can reach to the last surface for machining without colliding with any previously machined surface or the stock material. To ensure collision free machining, validation using simulation methods needs to be performed. Most CAM systems have the option for viewing the tool cutting the stock and

simulating a machine tool. Back plot is a verification tool that allows the users to observe tool motion. The travel path and tools can be optimized for any operation, i.e., roughing strategies can be employed for rapid material removal.

To get the understanding of the processing time required in subtractive vs. additive manufacturing, a model is designed in CAD software as illustrated in Figure 88. Nine different setups or operations are performed to get the desired geometry and the total time required to make this model is 2 hrs- 22 min. Multiple setups and changing of tools have caused the excessive time to make this model. A novel idea of path generation for additive manufacturing is introduced. An additive manufacturing (AM) module or add-on feature is integrated with in contemporary CAD/CAM system and virtually the same part is built in layers. A stack of 2 dimensional (2D) planer sections utilized to create the final 3 dimensional (3D) component is shown in Figure 89.

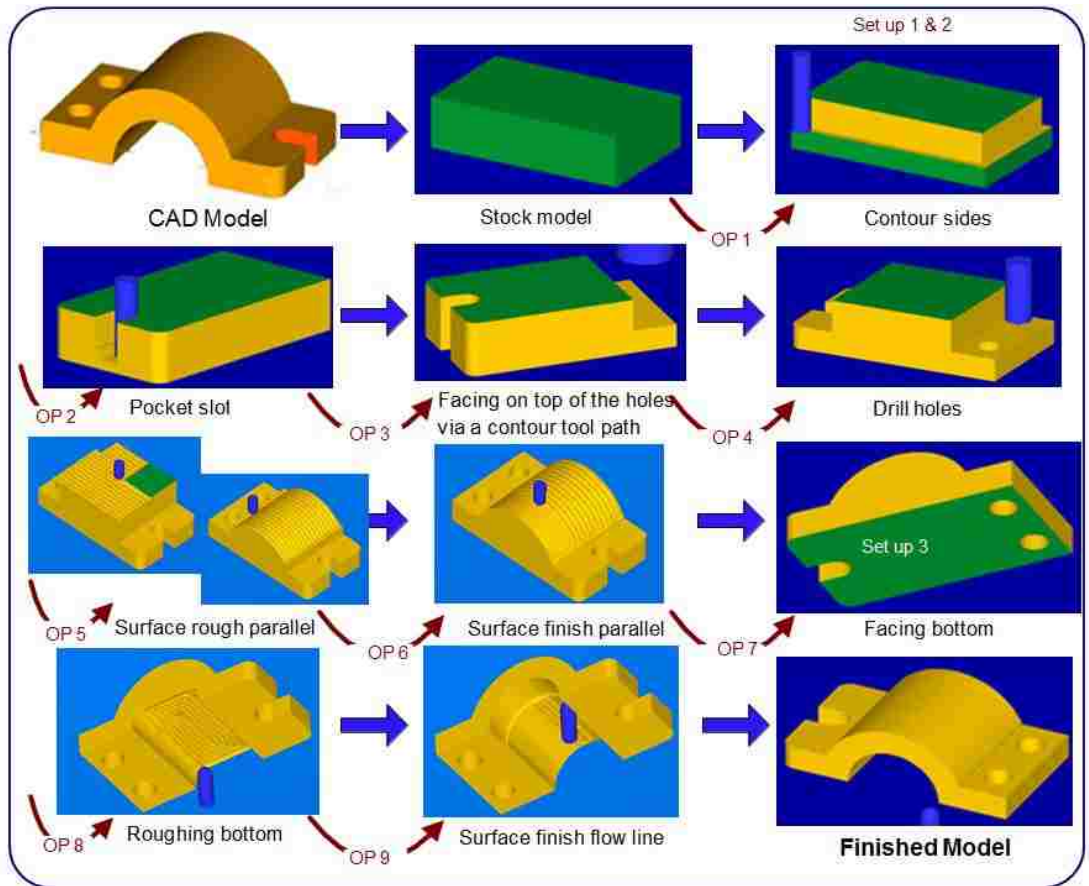


Figure 88. Subtractive manufacturing process and associated machining operations are shown on a CAD model (2 hr-22 min)



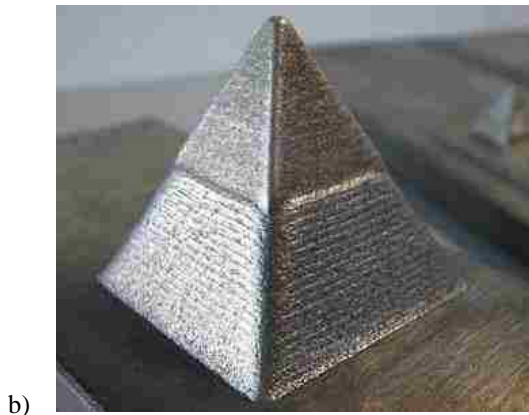
Figure 89. A stack of 2D is shown for CAD model (shown in Fig. 88)

Essentially for a process planning model it can be assumed that each layer has a perimeter contour, a raster scan type of travel path used to fill in the contour boundaries, and process parameters are constant throughout the build process. If the laser cladding process is chosen as an AM process, the bead width is controlled by the laser spot size, but can vary around this amount by adjusting the travel speed, powder feed rate, power levels etc. The processing steps of this model and comparison are shown in next section.

6.2 Process Planning in Hybrid Manufacturing

The effective combination of AM and SM (machining) technologies could bring about a new hybrid manufacturing approach that completely meets the requirements of the next generation of production systems, especially for short run production. Additive manufacturing strategies reduce the material usage, process planning time and machine interactions even for complex structures. The AM components can be fabricated to ‘near net shape’ (Fig.90) and machining employed to meet the component specifications.





b)



c)

Figure 90. a) b) Models made using metal bead deposition process [128-129] c) A cladded component with half machined

For the laser cladding process, determination of the fill volume for the ‘near net shape’ and the appropriate fill rate is the primary challenge. Tool paths are generated for every material deposition process. Regardless of the material type, it is deposited or melted by following a predetermined path and each layer (combination of beads) is laid on the previous one to create some 3D solid structure. The bead geometry is overlapped to eliminate voids. For the CAD model (Figure 88), if it is made in layers, set up 5 and set up 8 are not required in this bead deposition method, as shown in Figure 91.



 <p>a) Isometric view</p>	<p>Required machining operations:</p> <ol style="list-style-type: none"> 1- Contour sides 2- Pocket slot 3- Facing top of the holes via contour tool path 4- Drill holes 6- Surface finish parallel 7- Facing bottom 9- Surface finish flow line
<p>b) <u>Front view</u></p>  <p>Total M/C Time: 44 min 35 sec</p>	<p>Operations NOT required:</p> <ol style="list-style-type: none"> 5-Surface rough parallel 8-Surface roughing bottom

Figure 91. CAD model shown (in extruded layers) using commercial CAD program

These two processes (AM and SM) complement each other; therefore the idea of the hybrid approach has potential to build prototypes or even functional parts in the field of 3D fabrication. By identifying the significant factors that impact dimensional quality and achieving the optimization level in the laser cladding process, hybrid manufacturing method can be made an alternate manufacturing process. Using an appropriately designed near net shape model with finishing machining operations can lead to potential savings, as roughing operations are not required, and material usage is optimized.

6.3 Tool Path Planning in Laser Cladding Process

Unlike the other AM processes, which have original equipment manufacturer (OEM) software with process planning modules defined, no comprehensive process planning software exists for a ‘generic’ bead deposition process such as laser cladding. There are many processes in which a bead of material is deposited on to a substrate to build up a part, which is the focus of this research. Distinct from machining, where the depth of cut is independent from the tool diameter

and width of the tool engagement, the laser cladding bead width, penetration depth, height, and the bead cross sectional area are all interlinked. [1]

Prior research has been performed to be able to select process parameters with confidence that will generate the desired bead geometry for a single bead. However, to facilitate process planning, the process parameters that have the most influence on each geometry parameter need to be determined. Some of them have described and discussed in results section. The general process planning flow for the laser cladding process is illustrated in Figure 92.

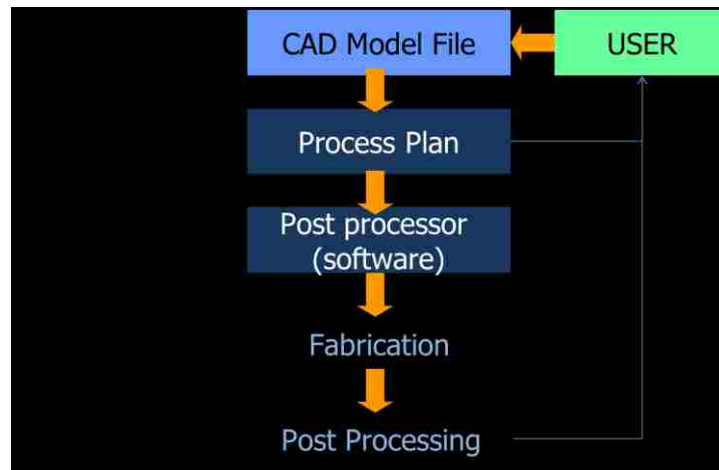


Figure 92. Process planning process flow for laser cladding process [1]

The clad bead shape characteristics are linked with the process parameters mainly due to heat buildup and bead shape changes when bead stacking and overlapping occurs (Fig. 93). This bead deposition process is basically an open loop process especially with a start-stop position; some excess material is deposited or overlapped, somehow which could be adjusted by ramping the heat but flow of the deposited powder cannot be stopped instantly. In other words, the bead geometry does not maintain its shape while depositing layers for solid models. This non-linear phenomenon creates challenges to the process planners and subsequently affects the travel path planning and build time.

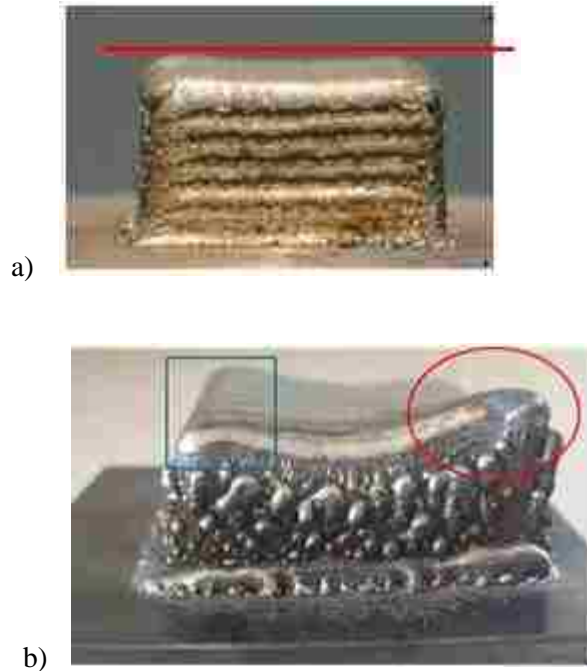


Figure 93. a) A rectangular block is built up with bottom up layers, Note the ‘dish’ in the center region. b) Start-stop phenomenon encircled and cornering condition boxed in the clad model [6]

The raster based fill pattern is used for the solid block with 50% overlap but waviness is seen at the corners because of the excessive heat. The bead geometry is impacted by the surrounding beads (Fig. 93) in stacking conditions, since the created bead is non-cylindrical in shape; tool path generation would be complex in this situation. Deposition at some angle may be helpful to eliminate or minimize the problem of cornering build ups. However, the conditions need to be recognized and address this issue. Adaptive bead widths and heights can be introduced by varying the process parameters appropriately [6]. Therefore, the selection and optimum setting of the process parameters becomes a critical step since the process is highly sensitive to them.

To understand this heat buildup phenomenon, a tool path is generated in CAM environment (Master Cam) for a CAD model and then clad in layers, as illustrated in Figure 94.

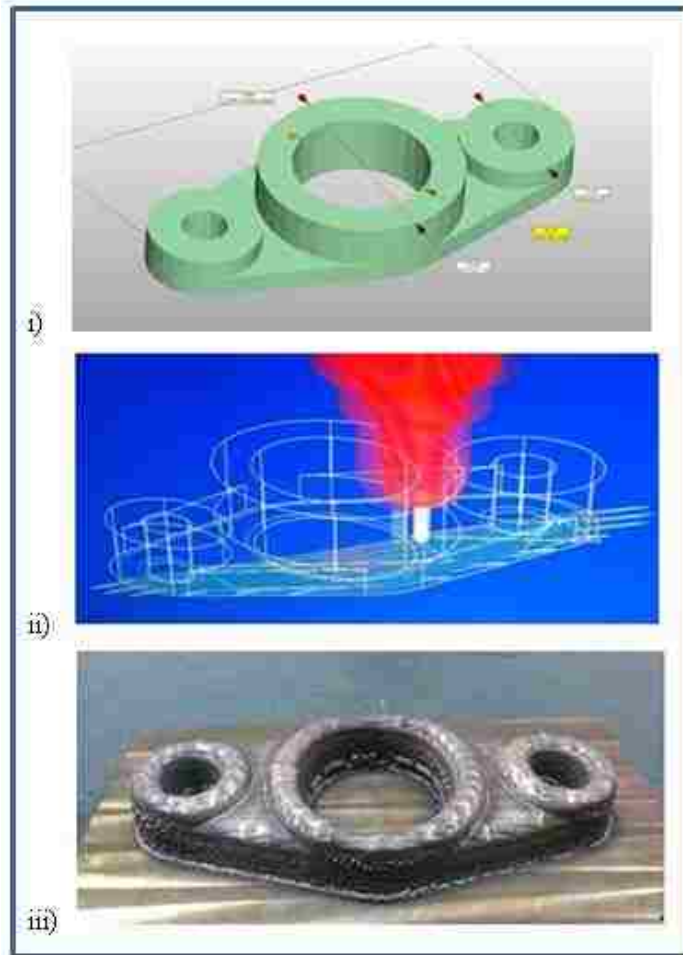


Figure 94. i) A CAD model ii) Tool path is being generated iii) The Cladded model

The desired surface finish and tolerance could be achieved by machining. The metallurgical characteristics such a microstructure and bead surface hardness may also get impacted with this technique that needs to be explored. The cladded model is reverse engineered and the measured dimensions are compared with CAD model (Table 19).

Table 19. Comparison of CAD model and the cladded model

Description	CAD Dimensions (mm)	Cladded Model Dimensions (mm)	Differences
Model length	200.00	202.00	-2.0
Outer diameter of big hole	90.0	91.8	-1.8
Inner diameter of big hole	60.0	63.2	-3.2
Outer diameter of small hole	50.0	50.6	-0.6
Inner diameter of small hole	20	21.5	-1.5
Base plate thickness	10	12.4	-2.4

Note: Negative values mean cladded dimensions are more than expected values

Tool path planning for this model is not trivial, since the model has circular geometric features. While build this geometry, the laser starts and stop many times to maintain the required thickness and that leads to a situation of lead in and lead out. It is observed that the cladded dimensions differ from the CAD values; parameters may require adjustment for each layer based on the local travel path geometry. Investigation of different test scenarios, such as lead-in and lead-out and cornering configurations, for non-steady state conditions would provide help in developing travel path strategies in CAM tools.

Chapter 7

Summary and Conclusion

7.1 Summary

Laser cladding is one of the material additive manufacturing processes used to produce a metallurgically well-bonded deposition layer and now it has been integrated into the industrial manufacturing lines to create a quality surface. To obtain a high-quality resulting part, a deep understanding of the process mechanisms is required since it is a multiple-parameter-dependent process and feedback control is critical for the process stabilization. Small disturbance from one or more of these parameters, from the environmental factors or from the laser-material interaction itself may result in defects in the manufactured parts. The laser cladding (LC) environment is complex, and it is challenging to develop robust bead geometry to process parameter model due to the noise, non-linearity, and coupling.

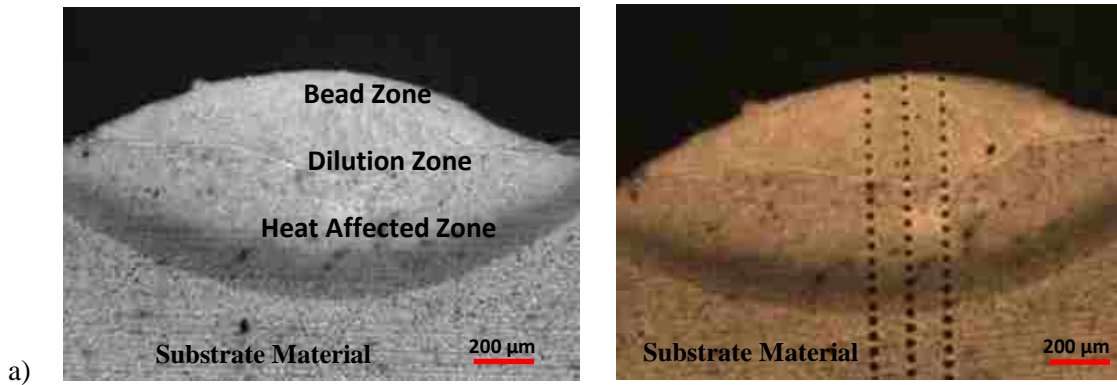
The research scope for this work targets only the coaxial laser cladding process specifically for 420 stainless steel clad powder using a fiber optic laser with a 4.3 mm spot size. In the first phase, single bead and 3-beads overlapping (40%, 50% and 60 %) experiments were performed and then it was extended to multiple beads, stacking and transient conditions to develop the understanding in these scenarios and get the confidence in the process. In the last, experiments of single bead with different cornering configurations (acute, right and obtuse angled) along with lead-in and lead-out situations were also conducted.

This work mainly focuses on experimentation; through which understanding of bead geometry in single and multiple beads is developed. To establish an experimental approach for data collection that minimizes the number of experiments, it is determined that the RSM with a CCD matrix provides the required information. The analysis of variance (ANOVA) is performed on the collected data to develop models for the bead height, bead width and the penetration. A second order model is introduced; the ANOVA based bead geometry models have a good R^2 . Introducing data transformations (log 10) improved the goodness of fit and the resulting predictive models have R^2 which are competitive to other modeling approaches.

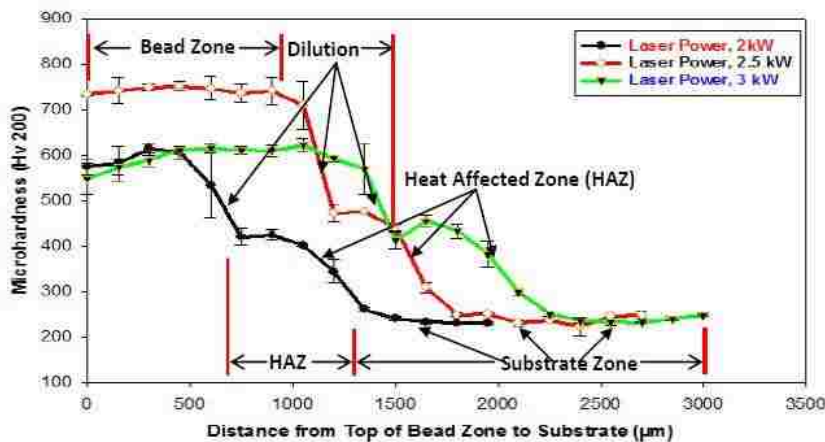
The complexity of the interaction of the many process variables makes this research the main challenge. This requires a quantitative understanding of the influence of the process parameters

such as laser power, laser scanning speed, and powder feed rate etc. on the clad geometry, hardness and microstructure of the resulting part. Developing a bead shape to process parameter model is challenging due to non-linear and dynamic nature of the laser cladding environment. This introduces unique predictive modeling challenges for both single bead and overlapping bead configurations. In this work, some mathematical models are developed using the generalized reduced gradient (GRG) techniques. The presented research proves effective and illustrates good predictive models and in-depth bead analysis in a steady and a non-steady state conditions; an area not investigated by the researchers.

Some preliminary work is performed along with another research fellow (Mr. K. Alam) on the deposited bead hardness in its different zones. As laser power varies from 2.0 kW to 4 kW during the experiments, it is observed that the power affects the micro hardness and the microstructure of the deposited bead [130]. One of the cladded samples is chosen and a load of 200 gm. is applied in all four zones of the clad to see the effect on the micro hardness in respective areas, as illustrated in Figure 95.



a)



b)

Figure 95. a) Measurement of micro hardness of a bead b) Variation in micro hardness in four different zones of the bead with three power levels [130]

Further exploration of micro hardness and other metallurgical properties of the deposited bead are under consideration with different materials and will be performed in the near future.

7.2 Conclusion

The laser cladding process and its associated process parameters play an important role in defining the geometry of the clad bead. Many process parameters influence the bead geometrical shape, and the bead characteristics are varying for single bead and overlap bead conditions. This hypothesis was set in the beginning of the research and proved to be true that the process parameters do affect the bead geometry significantly and in a nonlinear manner.

It has been observed that the average standard deviation for the width was the greatest whereas the penetration values were found to be lowest. The effects of the focal length and the contact tip to work piece distances are typically not investigated by the researchers; however, it was found and proved that these process parameters influence the bead geometry nonlinearly. The CTWD has a significant influence on the bead height, penetration, and positive area, whereas the effect of the focal length influences the bead width more. The laser travel speed to the Area_p relationship is found inversely proportional.

An interesting phenomenon with respect to the material feed rate (FR) and its relation to the bead width illustrates that the width reaches the maximum height of 5.13 mm at 20 gm./min powder feed setting. Similarly when the bead height is observed against the laser power, it indicates that the relationship has an inverted parabolic pattern and maximum height of 1.5 mm was achieved at 2.5 kW settings.

The results for the 3-beads overlap geometry also indicate that a single bead predictive model is not adequate for surface cladding process plans, and that rules for geometry adjustments or unique models for the 1st to 3rd beads must be derived for the overlapping conditions. It was also observed that the penetration values decreases as the overlap percentage increases but the observed standard deviations and ranges were found very close in values to the single bead deposition scenarios. The bead height standard deviations and ranges are very noisy as compared

to single bead configurations. More research needs to be performed with different materials and experimental conditions to be able to determine whether these observed influences are universal.

The multiple bead experiments (10 beads) have shown that the bead geometry is not the direct multiples of single deposited bead because of heat transfer and solidification phenomenon. The CTWD was not able to maintain the distance after each deposition instead this distance got bigger and bigger as the deposition progresses. When building a solid model where hundreds of layers are being deposited, it is a challenge to find and maintain the exact value of CTWD for the model.

It is proved that the transient conditions influenced the bead geometry. In the single bead transient sample, the maximum height of 1.4 mm is seen in the beginning then it settles down but when the power is increased the reduction of height occurs. The maximum penetration depth was observed at 1.7mm and found in the central section of the sample but was not stable. It is related to the power levels, as expected but there are some melt pool dynamics occurring, as the penetration values are oscillating. Similarly, in the overlapping condition, the trend in the values of height and penetration is similar with the single bead but the magnitude varies. The system dynamics must be investigated to be able to develop robust control strategies.

In the 3x4 bead transient sample, it is seen that the melt pool width changes are synchronized with the power level changes. Regardless of the transient region; the bead width trend is similar in all 12 beads. The actual measured height (4-beads) was found to be greater than the theoretical height and vice versa in different sections of the sample. It is also observed that the height and depth of the first section is different than that of height and depth of the other sections.

Different deposition scenarios were tested. The transient condition such as lead-in and lead-out indicates that the height geometry is not the same in these situations regardless of the single bead or multiple bead deposition. If multiple passes are required to coat a surface; the start-stop zone/condition overlays each other in the meeting zone, the clad height was appeared to be increased in the zone which leads to the problem of increased height and microstructural defects as well if continuous coating is performed.

Similarly for the corner configuration samples, the highest and lowest standard deviations of the bead height are found to be in acute and obtuse angled configurations respectively. Although the height variation is small, but still influences the contact tip to work piece distance. These transient conditions analysis would be helpful from the process planning point of view that the

planners would address lead-in/ lead-out and corner configuration scenarios while generating the tool path for a multiple bead deposition.

The laser cladding system dynamics was determined by varying the power. During the deposition process, the bead widths were recorded for the single, overlapping and 3x4 beads stack. The results illustrate that changing in the power level impacts the real time melt pool width and this hypothesis came true. Although the width traces data is found to be noisy and no oscillation patterns are evident. Some data transformation technique may be used in future to extract the process dynamics of melt pool region.

One of the research objectives (secondary) was to plan the experiments in a structured manner that not only provides enough data to develop some understanding of this complex process rather able to generate some predictive models as well with the available data set. The central composite design (CCD) was used to reduce the number of experiments and the aim was to reduce the time and cost of these experiments. This design is one of the types of response surface design or methodology (RSM) and is used in evaluating the significance of large number of factors and their interactions, as well as obtaining a simple relationship that defines the response as a function of these factors. This technique provided enough baseline information and the relationship between the process parameters and the bead geometry with the limited number of experiments.

Once the characterization of the cladding process was determined, then the challenge is to fill the near net shape components by generating the optimized tool path. By identifying and controlling the significant factors, hybrid manufacturing can be introduced; for example, the model developed in layers, shown in Figure 90. Since the model is made virtually in layers but in reality each layer may consists of hundreds of beads. Here the challenge is to search for a build direction along which either the build time is minimized or the part's surface quality is maximized. The first task is setting the orientation of the part relative to the deposition table. The second task is the estimation of a new build direction in the event a part cannot be deposited completely along one direction. The change in build direction is realized by re-orienting the part using a multi-axis deposition table or by moving the nozzle assembly orthogonal to the surface which leads to the 5-axis deposition method.

An adaptive layering approach could be introduced here with some adjustment of power or other parameters when needed. It is a decision making process; at this stage, machining

operations may also be introduced after some initial beads deposition which will lead to potential savings as material usage is optimized.

A solid 3D block is cladded with the start-stop/lead in-lead out phenomena, there is a difference in slopes, peak values and setting time is observed between them. This observation will help designers to adjust the process setting in order to minimize the gap between the heights. Although the stop-start condition can be readily addressed, the cornering issues are evident for multiple layered fabrications (Fig. 96). As cornering builds up materials (angle dependent), a smoothing “laser power only” pass may be necessary, or an adjustment to the process parameters to accommodate the cornering conditions could be implemented.



Figure 96. A cladded solid block, note the sloped corners

For the multi-layer block shown in Figure 96, another process transient condition is evident: sloped walls; however, for this set of process conditions, it can be seen to slope inward at approximately 10° . To determine the effect of introducing 5 axis tool paths, some samples are created by tilting the work piece at different angles (10° , 20° , 30° and 40°) while the deposition nozzle was not kept orthogonal with the substrate (Fig. 97). The impact of an angled slope is evident on the bead deposition. The bead shape changes can be leveraged using a 5 axis tool path approach to ‘straighten’ the vertical surfaces. A set of solid blocks are fabricated (40 x 40x 35 mm high) (Fig. 98) using these angles and a 5 axis tool path approach. There is a distinct improvement in the final results.

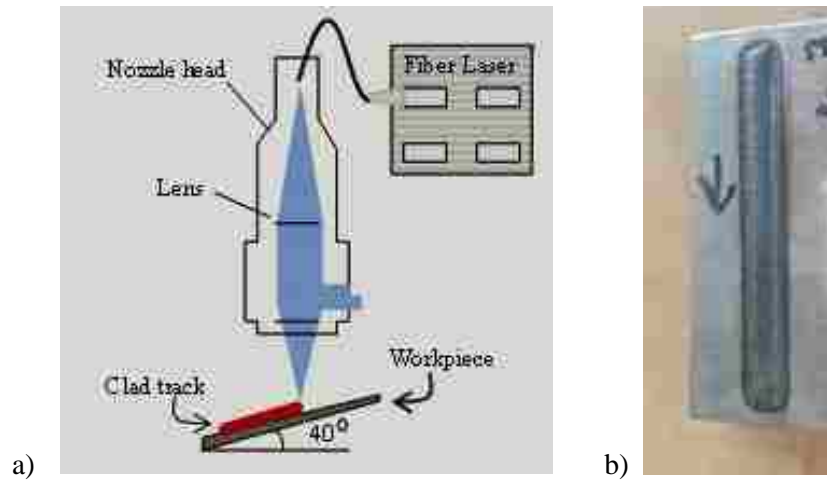


Figure 97. a) Schematic view of 40 degree angular deposition b) A sample made with 40 degree tilt



Figure 98. Four different cladded models with angular deposition

To conclude, changes in the bead geometry are inherent when depositing material. Consequently, real time adjustments for the process settings such as the laser power and / or the contact tip to work piece distance are required, but this introduces system dynamics. More research is required to understand the impact of these system dynamics to develop effective process planning solutions.

Chapter 8

Future Work

This is an experimental based thesis and all the results, outputs and predictive models drawn from it are mainly achieved through experimentation. This research has used 420 stainless steel powder, a low carbon steel, for all types of samples preparation. Some other kind of powder steel (high carbon) such as H13 and non-ferrous material such as tungsten carbide be considered for single and overlapping bead experiments to see effect of the process parameters on bead geometry are consistent.

This research helps in determining the correlation between the process parameters and the bead shape characteristics. Dilution is also a key factor, and exists between the additive material and the base metal, which allows strong metallurgical bond to form. The mechanical properties of the clad layer get affected by the percentage dilution, which in turn is developed due to the process parameters. So additional research topic such as assessing the microstructure evolutions, analysis of hardness of the deposited coating, tensile and compressive strength etc. are the areas that need to be explored in the future. This work will be continued for multiple beads; layering experiments are presently being conducted to determine whether the trends observed at the bead and overlap levels are consistent when there are stacking conditions. Another area which can be explored is to investigate the approaches to vary the bead width while maintaining a fixed height in order to reduce clad surface waviness and voids for complex shapes, and minimize the dilution percentages. Simulation of the single and overlapping beads need to be performed to understand the effect of heat and the bead's physical mass on the bead geometry, if multiple layers are deposited.

In future, the effect of the power levels on the melt pool width would be further explored. A transient sample was created with 2.6kW-3.6kW-2.6kW power intervals and variation in width is plotted (Fig. 73), which does not show any oscillation pattern. The fast Fourier transforms (FFTs) technique can be employed to extract process related dynamics. FFT is a mathematical tool that provides a means of transforming information from the time domain to the frequency domain, and vice versa. It is particularly efficient when evaluating periodic signals and can detect irregularities of the profile. In Figure 99, it can be seen that here are oscillations occurring at 0.23, 0.69, and 1.22 Hz. The 0.23 Hz or 4.35 sec. peak has amplitude of 0.6 mm. Identification of these

oscillation values will help to understand the variation in bead width with respect to the deposition time and laser power may be adjusted to get the desired geometry.

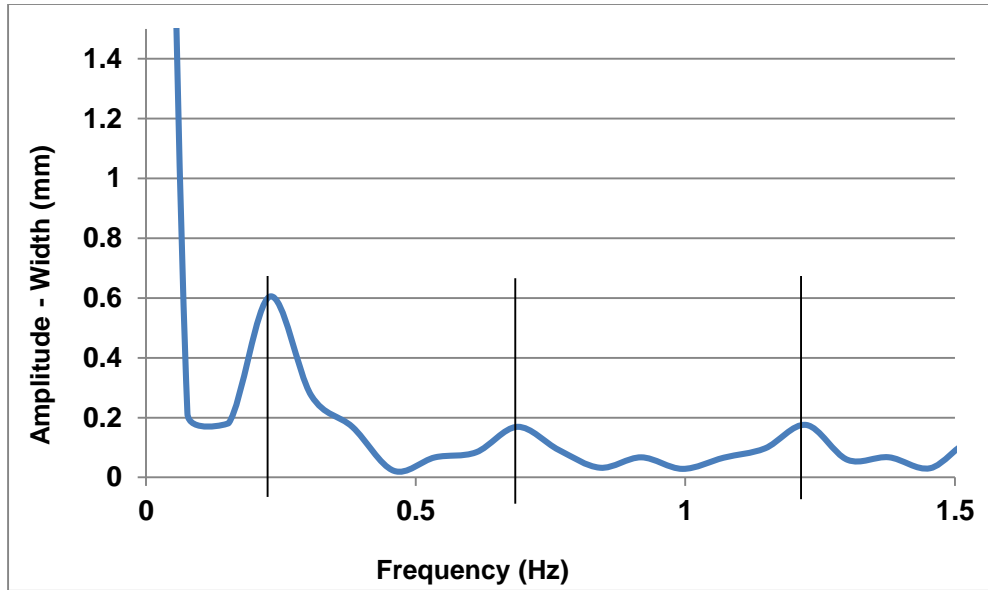


Figure 99. FFT for the single bead, 2 sec. step intervals, showing dominate frequencies at 0.23, 0.69, and 1.22 Hz or 4.35, 1.45, and 0.82 sec., respectively. The mean value is recorded at the 0 Hz point

Since laser cladding (LC) process has potential to make 3D components; determination of the fill volume for the ‘near net shape’ and the appropriate fill rate is the primary challenge. Although the layering approach reduces many issues related to process planning, there are still issues related to accuracy, surface finish, and build time that require improvement. Some laser clad shapes (Fig. 100) are created and different filling strategies are employed to get the desired geometry. Later on, the experimental results will include microstructure and hardness analyses for these buildups.

As the long term goal of this research is to develop a robust and adaptable framework for AM bead deposition process planning, a database needs to be developed to contain this information along with relevant process planning rules for different cladding scenarios. The future work is to conduct more experiments with multi beads, stack ups and some angular deposition in order to understand the effect of laser heat on the geometric shapes of the buildup or solid models. However, the experimental scope has increased, a 5-axis tool paths should be considered when addressing 3D component fabrication.

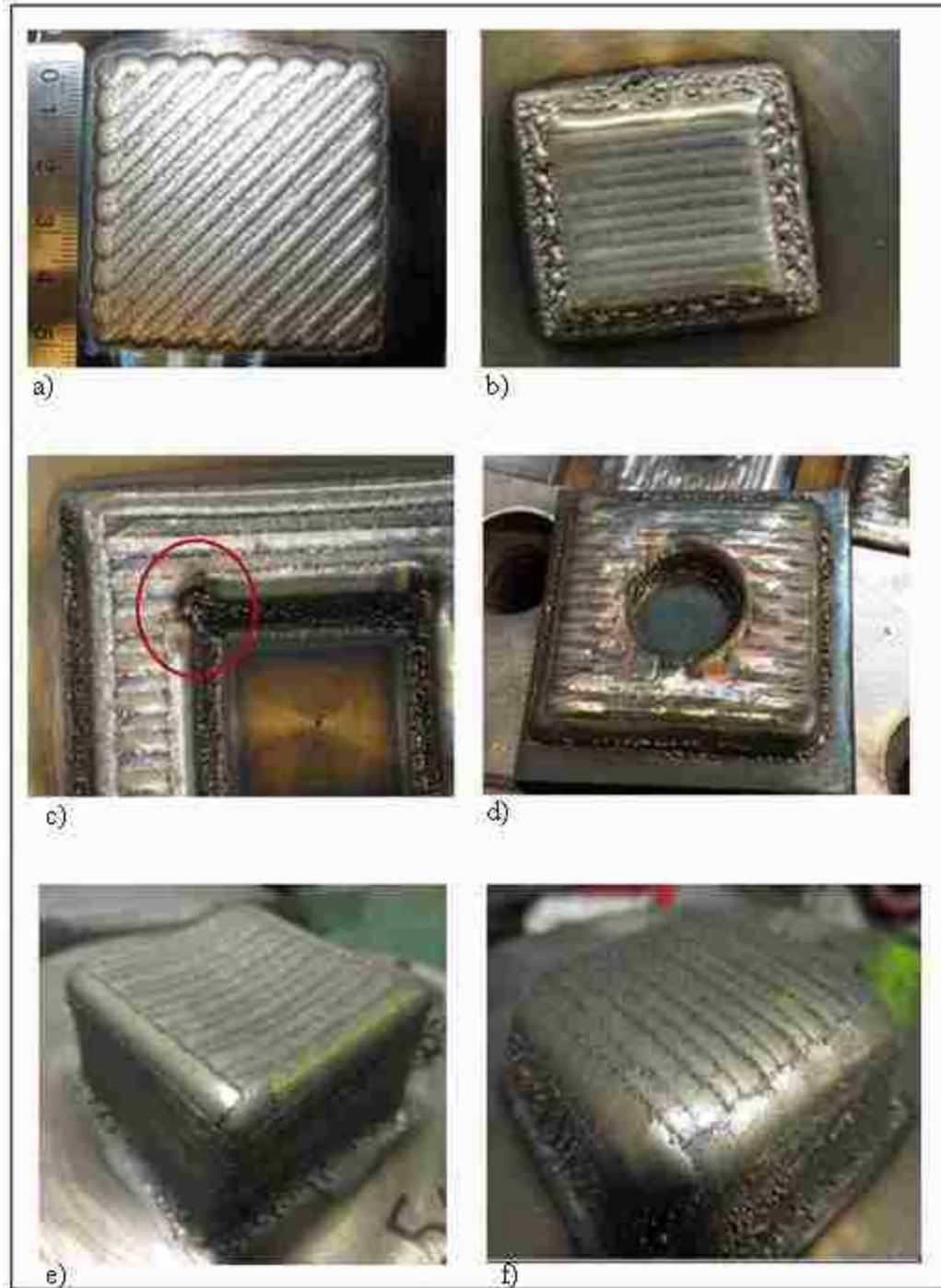


Figure 100. Laser clad models with different filling strategies a) Raster type filling with no contour b) Contour the square and then filling with 50% overlap c) A small square in a big square, contour and filling. The problematic corner is encircled d) Filling with 50% overlap and e) f) Solid clad blocks, bulging is visible

REFERENCES

- [1] Urbanic. R.J, Saqib. S and Aggarwal. K., 2016, “Using predictive modeling and classification methods for single and overlapping bead laser cladding to understand bead geometry to process parameter relationships.” *J. Manuf. Sci. Eng.*, vol. 138, issue 5.
- [2] Aggarwal. K., Urbanic. J., Saqib. S., 2014, “Identifying relative importance of input parameters in developing predictive model for laser cladding process.” *International Mechanical Engineering Congress and Exposition-ASME.*, November 14-20, Montreal, Canada, pp. 1–9.
- [3] Jichang. L and Lijun. L., 2005., “Study on cross section clad profile in coaxial single pass cladding with a low-power optics and laser technology.” *Opt. laser Technol.*, vol. 37, pp. 478–482.
- [4] Lee. H-K., 2008., “Effects of the cladding parameters on the deposition efficiency in pulsed Nd:YAG laser cladding.” *J. Mater. Process. Technol.*, vol. 202, no. 1–3, pp. 321–327.
- [5] Y. Sun and M. Hao., 2012, “Statistical analysis and optimization of process parameters in Ti6Al4V laser cladding using Nd:YAG laser.” *Opt. Lasers Eng.*, vol. 50, no. 7, pp. 985–995.
- [6] Hedrick. R. W, Urbanic. R.J and Burford. C., 2015, “Development considerations for an additive manufacturing CAM System.” *IFAC Conference.* vol. 48, issue 3, pp. 2327-2332.
- [7] Rosochowski and A. Matuszak., 2000, “Rapid tooling: the state of the art.” *Journal of Materials Processing Technology*, vol. 106, no. 1-3, pp. 191-198.
- [8] Saqib. S and Urbanic. J., “An experimental study to determine geometric and dimensional accuracy impact factors for fused deposition modeled parts.” *Proceedings of the 4th International Conference on Changeable, Agile, Reconfigurable and virtual production (CARV 2011)*, Montreal, Canada, 2-5 Oct 2014. pp. 293-298.
- [9] Toyserkani, E., Khajepour, A. and Corbin, S., 2002, “Application of experimental-based modeling to laser cladding.” *J. of Laser Applications*, vol. 14, pp. 165-173.
- [10] Komvopoulos, K., and Nagarathnam, K., 1990, “Processing and Characterization of laser-cladded coating Materials.” *Engineering Material Technology*, vol. 112, pp. 131–143.
- [11] Laser bond extending machinery life with advanced surface engineering available at http://www.laserbond.com.au/laser_cladding.shtml, (accessed on November 2014)
- [12] Jonathan Hoffman., 2009, “Development of an observation and control system for Industrial laser cladding.” PhD thesis, University of Twente, Enschede, The Netherland.

- [13] <http://www.hardchrome.com.au/technologies//laser-cladding/>, accessed on July,2015.
- [14] <http://www.precitec.de/en/applications/joining-technology/laser-cladding/>, accessed on Feb 20, 2015.
- [15] Toyserkani. E and Khajepour. A., 2005, “Laser Cladding” CRC Press, LLC, Boca Raton, Florida, pages 280.
- [16] Taberbero. I, Lamikiz. A and Ukar. E., 2014, “Modeling of the geometry built-up by coaxial laser material deposition process.” *Int. J. of Advanced Manuf Technology*, vol.70, pp. 843-851.
- [17] Ermurat, M., Arslan, A., Erzincanli, F and Uzman, I., 2013, “Process parameters investigation of a laser-generated single clad for minimum size using design of experiments.” *Rapid Prototype J.*, vol.9, pp. 452–462.
- [18] Dasgupta. B and Mukherjee. S., 2013, “Optimization of Weld Bead Parameters of Nickel Based Overlay Deposited By Plasma Transferred Arc Surfacing,” *International Journal of Modern Engineering Research (IJMER)*, vol. 3, no. 3, pp. 1330-1335.
- [19] Gruel M, Pintat T, Greulich. M., 1995, “Rapid Prototyping of Functional Metallic parts.” *Computers in Industry*, vol 28, no. 1, pp. 23-28.
- [20] Blackwell P, Wisbey. A., 2005, “Laser aided manufacturing technologies; their application to the near-net shape forming of high strength titanium alloy.” *Journal of Materials Processing Tech*, vol. 170,pp. 268-276.
- [21] Horii T, Kirihara. S, Miyamoto Y., 2008, “Freedom fabrication of Ti-Al alloys by 3D micro-welding.” *Inter metallics* , vol. 16, pp. 1245-1249.
- [22] Narendra. D., 1998, “Lasers in Surface Engineering.” *ASM International, Surface Engineering Series Vol. 1*, chapter 4, Page 153. ISBN: 0-87170-665-2.
- [23] Klingbeil NW, Beuth JL, China. R. K., 2002, “Residual stress induced warping in direct metal solid freeform fabrication.” *International journal of Mechanical Sciences*, vol. 44, pp. 57-77.
- [24] Mazumder J, Dutta D, Kikuchi N, Ghosh. A., 2000, “Closed loop direct metal deposition: art to part.” *Optics and Lasers in Engineering*, vol. 34, pp. 397–414.
- [25] Hu D, Mei H, Kovacevic. R., 2002, “Improving solid freeform fabrication by laser-based additive manufacturing.” *Proceedings of the Institution of Mechanical Engineers, Part B: Journal of Engineering Manufacture*, vol. 216, pp. 1253–1264.
- [26] Rannar LE, Glad A, Gustafson. CG., 2007, “Efficient cooling with tool inserts manufactured by electron beam melting.” *Rapid Prototyping Journal*, vol. 13, no. 3, pp. 128–135.

- [27] Song Y, Park S., 2006, "Experimental investigations into rapid prototyping of composites by novel hybrid deposition process." *Journal of Materials Processing Tech*, vol. 171, pp. 35–40.
- [28] Xiong X, Zhang H, Wang G., 2009, "Metal direct prototyping by using hybrid plasma deposition and milling." *Journal of Materials Processing Technology*, vol. 209, pp. 124–130.
- [29] Hur J, Lee K, Zhu-hu, Kim J., 2002, "Hybrid rapid prototyping system using machining and deposition." *Computer-Aided Design*, vol.34, pp. 741–754.
- [30] Karunakaran. K. P, Suryakumar. S, Pushpa. V, Akula. S., 2010, "Low cost integration of additive and subtractive processes for hybrid layered manufacturing." *Journal of Robotics and Computer-integrated Manufacturing*, vol. 26, pp. 490-499.
- [31] Kovacevic. R, and Dongming. Hu., 2003, "Sensing, modeling and control for laser-based additive manufacturing." *Int J of Machine Tools and Manufacture*, vol. 43, pp. 51-60.
- [32] Merz. R, Prinz. F. B AND Ramaswami. K., 1994. "Shape deposition manufacturing." *Proceedings of the Solid Freeform Fabrication Symposium, Austin, Texas, Aug 8-10.*
- [33] Dickens. PM, Spencer. JD and Wykes. CM., 1998, "Rapid Prototyping of metal parts by three dimensional welding. » *Proceedings of the Institution of Mechanical Engineers, Part B*, vol. 212, no. 3, pp. 175-182.
- [34] Li. Y, Huang. X, Peng. H, and Azer. M, 2005, "Laser net shape manufacturing of metallic matallic materials with CO₂and fiber laser." In 24th Int. Congress on Application of Lasers and Electro-optics (ICALEO), Laser institute of America, Miami, USA, pp. 320-325.
- [35] Qi. H, Azer. M, and Deaton. J, 2005, "Development of transfer functions for controlling fabrication of components by laser net shape manufacturing (LNSM)." In 24th Int. Congress on Application of Lasers and Electro-optics (ICALEO), Miami, USA. pp. 869-877.
- [36] Huan Qi, Magdi. A and Prabhjot. S., 2007, "Laser net shape manufacturing using an adaptive tool path deposition method". 26th International congress on Applications of lasers and electro-optics, ICALEO 2007-Congress Proceedings, paper 104. pp. 40-45.
- [37] Oliveira U, Oceli'k V, De Hosson J., 2005, "Analysis of coaxial laser cladding processing conditions." *Surface & Coatings Technology*, vol. 197, pp. 127–136.
- [38] Kathuria K., 1997, "Laser-cladding process: a study using stationary and scanning CO₂ laser beams." *Surface & Coatings Technology*, vol. 97, pp. 442–447.
- [39] Kai Z, Weijun L, Xiaofeng S., 2006, "Research on the processing experiments of laser metal deposition." *Optics & Laser Technology*, vol. 39, no. 3, pp. 549-557.
- [40] Liu J, Li L., 2005, "Study on cross-section clad profile in coaxial single-pass cladding with a low-power laser." *Optics & Laser Technology*, vol. 37, pp. 478–482.

- [41] Davim JP, Oliveira CR, Cardoso. A., 2008, "Predicting geometric form of clad in Laser cladding by powder using multiple regression analysis (MRA)." *Materials & Design*, vol.29, no. 2, pp. 554-557.
- [42] Onwubolu. G. C, Davim. J. P, Oliveira. C and Cardoso. A, 2007, "Prediction of clad angle in laser cladding by powder using response surface methodology and scatter search." *J. of Optics & Laser Tech*, vol. 39, pp.130-1134.
- [43] Xinghong. X, Zhang. H, Guilan. W and Wang. G., 2010, "-Hybrid plasma deposition and milling for an aeroengine double helix integral impeller made of super alloy." *Robotics and Computer-integrated Manufacturing*, vol. 26, pp. 291-295.
- [44] Sreeraj. P, Kannan. T and Maji. S., 2013, "Genetic algorithm for optimization of welding variables for percentage of dilution and application of ANN for prediction of weld bead geometry in GMAW process." *J. Mechanical Confab*, vol. 2, no. 1, pp. 1-16.
- [45] Chande. T, Mazumder. J., 1985, "Two-dimensional, transient model for mass transport in laser surface alloying." *J. Appl Physics*, vol. 57, no. 6, pp. 2226–2232.
- [46] Jouvard. JM, Grevey. DF, Lemoine F, and Vannes. AB., 1997, "Continuous wave Nd: YAG laser cladding modeling: a physical study of track creation during low power processing." *J. Laser Appl*, vol. 9, issue 43, pp. 43–50.
- [47] Picasso. M, Marsdan. CF, Wangniere. JD, Frenk A, and Rappaz. M., 1994, "A simple but realistic model for laser cladding." *Metall Mater Trans B*, vol. 25, no. 2, pp. 281–91.
- [48] Kim. JD and Peng. Y., 2000, "Melt pool shape and dilution of laser cladding with wire feeding." *J. Mater Process Tech*, vol. 104, pp. 284–93.
- [49] Kar. A, and Mazumder. J., 1987, "One dimensional diffusion model for extended solid solution in laser cladding." *J. Appl Physics*, vol. 61, no. 7, pp. 2645-2655.
- [50] Hoadley. AFA and Rappaz. M., 1992, "A thermal model of laser cladding by powder injection." *Metall Trans B*, vol. 23B, no. 1, pp. 631–642.
- [51] Amara, E. H., Achab, L. and Boumia, O., 2005, "Numerical modelling of the laser cladding process using a dynamic mesh approach in advanced optoelectronics and lasers." *J. Achievement in Materials and Manufacturing Engineering*, vol. 15, no. 1-2, pp.100-106.
- [52] Toyserkani, E., Khajepour, A. and Corbin, S., 2004, "3-D finite element modeling of laser cladding by powder injection: Effects of laser pulse shaping on the process." *Optics and Lasers in Engineering*, vol. 41, pp. 849-867.
- [53] Davim, J. P., Oliveira, C. and Cardoso, A., 2008, "Predicting the geometric form of clad in laser cladding by powder using multiple regression analysis (MRA)." *J. of Materials and Design*, vol. 29, pp. 554-557.
- [54] Song, Yong-AK, Park, S. and Chae Soo-Won., 2005, "3D welding and milling: part II---

- optimization of the 3D welding process using an experimental design approach.”
International Journal of Machine Tools and Manufacture, vol. 15, pp. 1063-1069.
- [55] Zeinali, M. and Khajepour, A., 2010, “Development of an adaptive fuzzy logic-based inverse dynamic model for laser cladding process.” Engineering Applications of Artificial Intelligence, vol. 23, pp. 1408-1419.
- [56] Liu, J.C., Ni, L.B., 2012, “Prediction of laser clad parameters based on neural network.” J. of Materials Technology, vol. 27, pp. 11-14.
- [57] Mahapatra, M.M., and Li, L., 2008, “Prediction of pulsed-laser powder deposits’ shape profiles using a back-propagation artificial neural network.” Proceedings of the Institution of Mechanical Engineers, Part B (Journal of Engineering Manufacture), vol. 222, pp. 1567-1576.
- [58] Song, C.Y., Park, Y.W., Kim, H.R, Lee, K.Y. and Lee, J., 2008, “The use of Taguchi and approximation methods to optimize the laser hybrid welding of a 5052-H32 aluminum alloy plate.” Proceedings of the Institution of Mechanical Engineers, Part B: Journal of Engineering Manufacture, vol. 222, pp. 507-518.
- [59] Liu Chang-Yi and Jehnming. L., 2003, “Thermal processes of a powder particle in coaxial laser cladding.” J. of Optics and Laser Tech, vol. 35, no. 2, pp 81-86.
- [60] Picasso. M and Rappaz. M., 1994, “Laser-powder material interactions in the laser cladding process.” J. of Physics IV, vol. 4, pp 27-33.
- [61] Han. L, Liou. F and Phatak. K.M, 2004, “Modeling of laser cladding with powder injection.” Metallurgical and Materials Transactions B, vol. 35 B, pp. 1139-1150.
- [62] Maropoulos, P. G., 1999, “Review of research in tooling technology, process modeling and process planning, Part 2: Process planning.” Computer Integrated Manufacturing Systems, vol. 8, pp.13–20.
- [63] Kiritsis, D., 1995, “A review of knowledge-based expert systems for process planning. Methods and problems.” The International Journal of Advanced Manufacturing Technology, vol. 10, no. 4, pp. 240–262.
- [64] ElMaraghy. H. A., 1993., “Evaluation and future perspective of Capp”. CIRP Annals, vol. 1, 42, pp. 739-751.
- [65] Azab. Ismail. A., 2008., “Reconfigurable process plans: A mathematical programming approach.” PhD thesis, University of Windsor, Windsor, Canada.
- [66] Azab. Aand ElMaraghy. H., 2007., “ Mathematical modeling for reconfigurable process planning.” Annals of CIRP, vol. 56, issue 1. pp. 467-472.
- [67] Koulmans, C., 1993, “Operation sequencing and machining economics.” International Journal of Production Research, vol. 31, no. 4, pp. 957–975.

- [68] Vancza, J. and Markus, A., 1991, "Genetic algorithm in process planning." *Computers in Industry*, vol. 17, pp. 181–194.
- [69] Usher, J. M. and Bowden, R. O., 1996, "The application of genetic algorithms to operation sequencing for use in computer-aided process planning." *Computers and Industrial Engineering*, vol. 30, pp. 999–1013.
- [70] Ma, G.H., Zhang, Y. F. and Nee, A. C. Y., 2000, "A simulated annealing-based optimization algorithm for process planning." *International Journal of Production Research*, vol. 38, pp. 2671–2687.
- [71] Kim, Y. S., Wang, E. and Rho, H. M., 2001, "Geometry based machining precedence reasoning for feature-based process planning." *International Journal of Production Research*, vol. 39, pp. 2077–2103.
- [72] Limaiem, A. and ElMaraghy, H. A., 1995, "An integrated resource selection and operation sequencing method." *Proceedings of 27th CIRP International Seminar on Manufacturing Systems*, Ann Arbor, MI, USA.
- [73] Yut, G. and Chang, T. C., 1995, "Hierarchical operation sequencing using a heuristic grouping algorithm." *Proceedings of 27th CIRP International Seminar on Manufacturing Systems*, Ann Arbor, MI, USA.
- [74] Irani, S. A, Koo, H. Y. and Raman, S., 1995, "Feature-based operation sequence generation in CAPP." *International Journal of Production Research*, vol. 33, pp. 17–39.
- [75] Yip-Hoi, D. and Dutta, D., 1996, "A genetic algorithm for sequencing operations in process planning for parallel machining." *IIE Transactions*, vol. 28, no.1, pp. 55–68.
- [76] Morad, N. and Zazala, A., 1999, "Genetic algorithms in integrated process planning and Scheduling." *International Journal of Intelligent Manufacturing*, vol. 10, pp. 169–197.
- [77] Sun, G, Carlo, H, and Wright, P, 2001, "Operation decomposition for freeform surface features in process planning." *Computer aided design*, vol. 33, no. 9, pp. 621-636.
- [78] Gupta, D.P, Gopalakrishan, B, Chaudhari, S.A and Jalali, S, 2011, "Development of an integrated model for process planning and parameter selection for machining processes." *Intl. J. of Production Research*, vol. 49, no. 21, pp. 6301-6319.
- [79] Spence, A, D, Sawula, A, Stone, J.R, and Lin, Y.P., 2014, "In-Situ measurements and distributed computing for adjustable CNC machining." *Computer-Aided Design and Applications*, vol. 11, no. 6, pp. 659-669.
- [80] Ocelik, V, Hemmati, M.E., and De Hossan, J, 2012, "Elimination of Start/Stop defects in laser cladding." *Surface and Coating Tech.*, vol. 206, pp. 2403-2409.

- [81] Zheng, X., Qiao-bin, Z. & Xiao-yan, Z., 2011, “ Effects of Process Parameters of Laser Cladding on the Deformation.” 2011 Fourth International Conference on Intelligent Computation Technology and Automation, (i), pp.1089–1092.
- [82] Benyounis, K.Y. & Olabi, a. G., 2008, “ Optimization of different welding processes using statistical and numerical approaches.” A reference guide. *Advances in Engineering Software*, vol. 9, no. 6, pp.483–496.
- [83] Dey. V, Dilip Kumar. P and Datta. G.L, 2008, “ Prediction of weld bead profile using neuralnetwork.” First Intl. Conference on Emerging Trends in Engineering and Technology, IEEE, pp. 581-586.
- [84] Liao, H.-T. & Shie, J.-R., 2007, “ Optimization on selective laser sintering of metallic powder via design of experiments method. *Rapid Prototyping Journal*, vol. 13, no. 3, pp.156–162.
- [85] Giuliani, V. et al., 2008, “ Particle velocity detection in laser deposition processing.” *Rapid Prototyping Journal*, vol. 14, no. 3, pp.141–148.
- [86] Gangxian. Z, Anfeng. Z and Dichen Li, 2011, “ Numerical simulation of thermal behaviour during laser metal direct deposition.” *Int J Adv Manuf Technol*, vol. 55, pp. 945-954.
- [87] Pinkerton, A.J. & Li, L., 2004, “The significance of deposition point standoff variations in multiple-layer coaxial laser cladding (coaxial cladding standoff effects).” *International Journal of Machine Tools and Manufacture*, vol. 44, no. 6, pp.573–584.
- [88] Alireza. F, Ehsan. T , Khajepour. A, Durali. M, 2006, “ Prediction of melt pool depth and dilution in laser powder depostion.” *Journal of Physics D: Applied Physics*, vol. 39, no. 12, pp.
- [89] Mondal, S. Paul. C.P, Kukreja.L.M., 2013, “ Application of Taguchi-based gray relational analysis for evaluating the optimal laser cladding parameters for AISI1040 steel plane surface.” *The Int J Adv Manuf Technol*, vol. 66, no.1-4, pp.91–96.
- [90] Xinghong. X, Zhang. H, Wang. G and Guoxian. W, 2010, “ Hybrid plasma deposition and milling for an aeroengine double helix integral impeller made of superalloy.” *Robotics and Computer-integarted Manufacturing*, vol. 26, pp. 291-295.
- [91] Edoardo. C and Barbara. P., 2006, “The influence of operator skills, process parameters and materials on clad shape in repair using laser cladding by wire.” *Journal of Materials Processing Technology*, vol. 174, no. 1-3, pp. 223-232.
- [92] Benjamin. G, Stefen. A, Rethmeier. M., 2013, “Design of experiments for laser metal deposition in maintenance, repair, and overhaul applications.” 2nd Intl Through-life Engineering Services Conference, *Procedia CIRP*, vol. 11, pp. 245-248.
- [93] Kaunakaran. K.P, Suryakumar. Sand Pushpa. V., 2009, “Retrofitment of a CNC machine for hybrid layered manufacturing.” *Int J Adv Manuf Technol*, vol. 45, pp. 690-703.

- [94] Jeng. J-Y, Peng, S-C and Chou. C-J., 2000, “Metal Rapid Prototype Fabrication Using Selective Laser Cladding Technology.” *Int J Adv Manuf Technol*, vol. 16, pp. 681-687.
- [95] Lalas. C, Tsirbas. K and Cryssolouris., 2007, “ An analytical model of the laser clad geometry.” *Int J Adv Manuf Technol*, vol. 32, pp. 34-41.
- [96] Vijay. P and Choudhary. Deepak. K, 2013, “Application of two-level half factorial design technique for developing mathematical models of bead penetration and bead reinforcement in SAW process.” *Int J of Innovative Research in Science, Engineering and Tech*, vol. 2, no. 6, pp. 2011-23.
- [97] Glardon. R, Karapatis. N and Romano. V, 2001, “Influence of Nd:YAG parameters on the selective laser sintering of metallic powders.” *J of Manuf Tech*, vol 50, no. 1, pp. 133-136.
- [98] Mazumder. J, X He and Yu G., 2010, “Temperature and composition profile during double-track laser cladding of H13 tool steel.” *J of Physics: Applied Physics*, vol. 43, 9 pp.
- [99] Levy N.G, Schindel. Rand Kruth. J.P., 2003, “Rapid manufacturing and rapid tooling with layer manufacturing technologies, State of the art and future perspectives.” *CIRP Annals Manufacturing Technology*, vol. 52, no. 2, pp. 589-609.
- [100] Shepelva. , Medres. B, Kaplan. WD, and Wesisheit. A., 2000, “Laser cladding of turbine blades.” *Surface coating technology*, vol. 125, pp. 45-48.
- [101] Suryakumar. S, Karunakaran. K.P, Bernard. A, Chandrasekhar. U and Sharma. D., 2011, “Weld bead modeling and process optimization in hybrid layered manufacturing.” *Computer-aided design*, vol. 43, pp. 331-344.
- [102] Griffith.M, Keicher. M, Romero. J and Green. H., 1996, “ Free form fabrication of metallic components using laser engineered net shaping (LENS).” *Proceedings of the solid freeform fabrication symposium*, pp. 125-132.
- [103] Yuwen. S and Mingzhong. H., 2012, “Statistical analysis and optimization of process parameters in Ti6Al4V cladding using Nd:YAG laser.” *Optics and lasers in Engineering*, vol. 50, pp. 985-995.
- [104] Hoffman. JT, Lange. D, and Meijer. J., 2011 “FEM modeling and experimental verification for dilution control in laser cladding.” *Journal of Materials Processing Tech*, vol. 211, pp. 187-196.
- [105] Kim. I.S, Son. J.S, Park. C. E and Kim. H .H, 2005 “An investigation in to an intelligent system for predicting bead geometry in GMA welding process.” *Journal of Materials Processing Technology*, vol. 159, pp. 113-118.
- [106] Nagesh. D. S and Datta. G. L., 2002 “Prediction of weld bead geometry and penetration in shielded metal-arc welding using artificial neural networks.” *Journal of Materials Processing Technology*, vol. 123, pp. 303–312.

- [107] Jendrzewski . R, Sliwi_nski. G, Krawczuk. M and Ostachowicz. W., 2004
 “Temperature and stress fields induced during laser cladding.” Computers and Structures, vol. 82, pp. 653-658.
- [108] Paul. C.P and Khajepour. A., 2008 “Automated laser fabrication of cemented carbide components.” Optics & Laser Technology, vol. 40, pp. 735-741.
- [109] Ding. D, Pan. Z Cuiuri. Dand Li. H., 2015 “A multi bead overlapping model for robotic wire and arc additive manufacturing.” Robotics and Computer-integrated Manufacturing, vol. 31, pp. 101-110.
- [110] Xing. J, Guangjun. Z, Gao. H and Wu. L., 2013 “Modeling of bead section profile and overlapping beads with experimental validation for robotic GMAW-based rapid manufacturing.” Robotics and Computer-integrated Manufacturing, vol. 29, pp. 417-423.
- [111] Aiyiti. W, Zhao. W, Lu. B and Yiping. T., 2006 “Investigation of the overlapping parameters of MPAW-based rapid prototyping.” Rapid prototyping Journal, vol. 12, no. 3,pp. 165-172.
- [112] Zoran L, Simon. K, Jose. Band Miran.B., 2015., “Modeling and design of experiments of laser cladding process by genetic programming and non-dominated sorting.” J. Material and manufacturing processes, vol. 30, pp. 458-463.(desktop)
- [113] Gangxian. Z, Dichen.L, Anfeng. Z,Gang. P and Yiping. T., 2011 “The influence of standoff variations on the forming accuracy in laser direct metal deposition.” Rapid prototyping Journal, vol. 17, no. 2, pp. 98-106.
- [114] Shojjin. S, Yvonne. D and Brandt. M., 2004 “Correlation between melt pool temperature and clad formation in pulsed and continuous wave ND:YAG laser cladding of Stellite6.” Proceedings of the 1st Pacific Int Conference on Application of Lasers and Optics,
- [115] Victor. D and Alberto. C., 2008 “Computational simulation of shaped metal deposition.” Association of Argentina, *Mechanica Computacional* , vol.27, pp. 1531-1543, 10-13 November.
- [116] Bi. G, Sun. C.N, Gasser.A., 2013., “ Study on influential factors for process monitoring and control in laser aided additive manufacturing.” *Journal of Materials Processing Tech*, vol. 213, pp. 463-468.
- [117] Cheikh. H.EI, Courant. B, Hascoet.J, Guillen. R., 2012, “Prediction and analytical description of the single laser track geometry in direct laser fabrication from process parameters and energy balance reasoning.” *Journal of Material Processing Tech*, vol. 212, pp. 1832-1839.
- [118] Sneider. M., 1998., “Laser Cladding with Powder.” PhD thesis, Univeristy of Twente, Enschede, The Netherland. ISBN: 90 365 1098 8.

- [119] Salehi. D.S., 2005., “ Sensing and control of Nd:YAG laser cladding process.” PhD thesis, Swinburne University of Technology, Melbourne, Australia.
- [120] Gedda. H., 2000, “Laser surface cladding, a literature survey.” Technical report, Lulea Tekniska Universitet.
- [121] Torims, T., 2013, “Application of laser cladding to mechanical component repair, renovation and regeneration.” DAAAM International Scientific Book, chap 32, pp. 587-608.
- [122] http://en.wikipedia.org/wiki/Selective_laser_Sintering, accessed on March 2015.
- [123] Montgomery. Douglas. C., 1997, “Design and Analysis of Experiments.” Fifth Edition, John Wiley and Sons, Inc, New York. USA, ISBN: 0-471-31649-0.
- [124] Mazumder. J, and Steen. W. M., 1980, “Heat transfer model for cw laser material processing.” Journal of applied physics, vol. 51, no. 2, pp. 941-947.
- [125] Samarasinghe. S., 2006., “ Neural Networks for applied sciences and engineering- from fundamentals to complex pattern re-cognition.” Boca Raton, New York: Auerbach Publications- Taylor & Francis Group, LLC.
- [126] Aggarwal. K., Urbanic. J., Saqib. S., 2014 “Development of predictive models for effective process parameter selection for single and overlapping laser clad bead geometry,” Rapid Prototyp. J., RPJ-04-2016-0059 (Submitted)
- [127] S. Saqib, R. J. Urbanic and K. Aggarwal., “Analysis of laser cladding bead morphology for developing additive manufacturing travel paths.” Proceedings of the 47th CIRP conference on Manufacturing Systems. vol. 17, 2014, pp.824-829.
- [128] www.dmgmori.com/webspecial/journal_2014/lasertec-65.html, accessed on Jan 2016.
- [129] www.afas.org.au/vic/events/2007/laser.html, accessed on Jan 2016.
- [130] Mohammad. A, Urbanic. J, Saqib. S and Edrisy. A., 2015. “ Effect of process parameters on the microstructural evaluations of laser clad 420 martensitic stainless steel.” Proceedings on Material Science & Technology (MS&T, 2015), Oct 4-8, OH, USA

APPENDICES

Appendix A: Published/submitted papers—Acceptance/Permission Letter from Publisher

Conference Paper ---- Permission from the Publisher

Title: "Analysis of laser cladding bead morphology for developing additive manufacturing travel paths".

Procedia CIRP 47th CMS Conference 2014, (17), pp 824-829.

Dear Syed Mohammad

Please note that as one of the Authors of this article, **you retain the right to include the journal article, in full or in part, in a thesis or dissertation.** You do not require permission to do so.

For full details of your rights as a Journal Author, please visit: <http://www.elsevier.com/wps/find/authorsview.authors/copyright#whatrights>

Your retained rights allow you to submit your article in electronic format and to post this Elsevier article online if it is embedded within your thesis. You are also permitted to post your Author Accepted Manuscript online; however posting of the final published article is prohibited.

Please refer to Elsevier's Posting Policy for further information:

<http://www.elsevier.com/wps/find/authors.authors/postingpolicy>

Feel free to contact me if you have any queries.

Regards

Lakshmi Priya

Global Rights Department

Elsevier

(A division of Reed Elsevier India Pvt. Ltd.)

International Tech Park | Crest – 12th Floor | Taramani Road | Taramani | Chennai 600 113 | India

ASME Paper: MANU-14-1721 for the Journal of Manufacturing Science and Engineering.

Title: “Using Predictive Modeling and Classification Methods for Single and Overlapping Bead Laser Cladding to Understand Bead Geometry to Process Parameter Relationships”.

Dear Prof. Saqib:

It is our pleasure to grant you permission to use **all or any part** of the ASME paper “Using Predictive Modeling and Classification Methods for Single and Overlapping Bead Laser Cladding to Understand Bead Geometry to Process Parameter Relationships,” by R. J. Urbanic, S. M. Saqib and K. Aggarwal, J. Manuf. Sci. Eng 138(5), 2016, cited in your letter for inclusion in a dissertation entitled Experimental Investigation of Laser Cladding Bead Morphology and Process Parameter Relationship for Additive Manufacturing Process Planning to be published by University of Windsor.

Permission is granted for the specific use as stated herein and does not permit further use of the materials without proper authorization.

As is customary, we request that you ensure full acknowledgment of this material, the author(s), source and ASME as original publisher. Acknowledgment must be retained on all pages printed and distributed.

Many thanks for your interest in ASME publications.

Sincerely,



Beth Darchi

Publishing Administrator-
ASME

2 Park Avenue, 6th Floor

New York, NY 10016-5990

Tel [1.212.591.7700](tel:1.212.591.7700)

darchib@asme.org

ASME Paper: MANU- 16- 1168 for the Journal of Manufacturing Science and Engineering.

Title: “**Investigation of the Transient Characteristics for laser cladding beads using 420 Stainless Steel Powder.**”

Dear Syed M,

Thank you for submitting your Research Paper to the *Journal of Manufacturing Science and Engineering*.

Paper Number: MANU-16-1168

Paper Title: “Investigation of the Transient Characteristics for Laser Cladding Beads using 420 Stainless Steel Powder”.

The number assigned to your work is MANU-16-1168. This number will be used for any further activity for this paper (including final submission). It will also be used to identify your manuscript on the web site and in any further communication with the editorial staff.

For more information about Journal Submission Types and Publication Charges please see <http://journaltool.asme.org/Help/AuthorHelp/WebHelp/JournalsHelp.htm>

Thank you for choosing the ASME, Journal of Manufacturing Science and Engineering to submit your work.

Appendix B: Response Variables (bead parameters) measured against five process parameters

Std Order	Design Matrix					Run Order	Bead Parameters					
	FR	PW	FL	LS	CTD		W (mm)	RH (mm)	P (mm)	Area (Positive bead)	Area (negative bead)	D (%)
1	-1	-1	-1	-1	1	1	3.91	0.67	0.47	1.809	0.713	28.27
						Replicate 2	3.88	0.72	0.44	1.932	0.674	25.86
						Replicate 3	4.15	0.68	0.48	1.842	0.759	29.18
18	2	0	0	0	0	2	4.13	1.17	0.24	3.360	0.216	6.04
						Replicate 2	5.08	1.36	0.09	4.236	0.163	3.71
						Replicate 3	3.65	1.2	0.17	3.304	0.178	5.11
4	1	1	-1	-1	1	3	4.06	0.66	0.49	1.841	0.732	28.45
						Replicate 2	3.77	0.65	0.52	1.775	0.727	29.06
						Replicate 3	4.06	0.61	0.38	1.652	0.599	26.61
25	0	0	0	0	-2	4	4.05	0.93	0.4	2.453	0.530	17.77
						Replicate 2	4.27	0.92	0.38	2.431	0.497	16.97
						Replicate 3	4.08	0.86	0.41	2.348	0.644	21.52
2	1	-1	-1	-1	-1	5	3.71	1.27	0.16	3.367	0.144	4.10
						Replicate 2	3.84	1.2	0.15	3.205	0.162	4.81
						Replicate 3	3.93	1.3	0.16	3.466	0.163	4.49
12	1	1	-1	1	-1	6	4.35	0.88	0.42	2.541	0.724	22.17
						Replicate 2	3.9	0.88	0.41	2.513	0.634	20.15
						Replicate 3	3.9	0.85	0.51	2.454	0.812	24.86
9	-1	-1	-1	1	-1	7	3.75	0.51	0.21	1.240	0.166	11.81
						Replicate 2	3.59	0.53	0.14	1.323	0.124	8.57
						Replicate 3	3.79	0.49	0.11	1.151	0.114	9.01
7	-1	1	1	-1	1	8	4.9	0.75	0.84	2.632	1.988	43.03
						Replicate 2	4.7	0.78	0.8	2.488	1.907	43.39
						Replicate 3	4.36	0.74	0.93	2.303	2.112	47.84
26	0	0	0	0	2	9	4.45	0.78	0.49	2.106	0.746	26.16
						Replicate 2	4.02	0.76	0.41	2.077	0.667	24.31
						Replicate 3	4.23	0.77	0.42	2.167	0.686	24.04
23	0	0	0	-2	0	11	5.16	1.51	0.71	5.306	1.341	20.17
						Replicate 2	5.19	1.45	0.71	4.954	1.397	22.00
						Replicate 3	5.2	1.46	0.68	5.294	1.391	20.81
14	1	-1	1	1	-1	12	3.72	0.8	0.06	1.815	0.035	1.89
						Replicate 2	3.19	0.77	0.04	1.751	0.027	1.52

						Replicate 3	3.41	0.73	0.09	1.698	0.052	2.97
28	0	0	0	0	0	13	4.48	0.85	0.43	2.589	0.632	19.62
						Replicate 2	4.58	0.88	0.39	2.590	0.600	18.81
						Replicate 3	4.32	0.9	0.42	2.630	0.581	18.09
16	1	1	1	1	1	14	4.54	0.77	0.39	2.389	0.636	21.02
						Replicate 2	4.15	0.77	0.38	2.383	0.578	19.52
						Replicate 3	4.07	0.84	0.32	2.308	0.520	18.39
20	0	2	0	0	0	15	4.88	0.85	1.06	3.113	2.560	45.13
						Replicate 2	5.04	0.91	0.87	3.157	2.602	45.18
						Replicate 3	4.97	0.88	0.84	3.100	2.316	42.76
13	-1	-1	1	1	1	16	3.79	0.43	0.23	1.163	0.162	12.23
						Replicate 2	3.73	0.49	0.28	1.224	0.218	15.12
						Replicate 3	3.63	0.47	0.22	1.070	0.175	14.06
27	0	0	0	0	0	17	4.03	0.93	0.61	2.778	0.600	17.76
						Replicate 2	3.73	0.98	0.42	2.683	0.549	16.99
						Replicate 3	3.9	0.97	0.3	2.734	0.527	16.16
10	1	-1	-1	1	1	18	3.82	0.74	0.04	1.811	0.045	2.42
						Replicate 2	3.51	0.77	0.02	1.779	0.020	1.11
						Replicate 3	3.03	0.76	0.06	1.745	0.028	1.58
8	1	1	1	-1	-1	19	5.13	1.21	0.76	4.393	1.408	24.27
						Replicate 2	4.91	1.22	0.79	4.306	1.503	25.87
						Replicate 3	4.79	1.27	0.75	4.092	1.476	26.51
17	-2	0	0	0	0	20	4.03	0.54	0.62	1.357	1.168	46.26
						Replicate 2	4	0.43	0.6	1.324	1.105	45.49
						Replicate 3	4.52	0.49	0.61	1.321	1.108	45.62
5	-1	-1	1	-1	-1	21	3.8	0.83	0.51	2.248	0.766	25.41
						Replicate 2	4	0.78	0.49	2.071	0.779	27.33
						Replicate 3	3.84	0.74	0.45	2.025	0.738	26.71
30	0	0	0	0	0	22	3.7	1.03	0.34	2.893	0.471	14.00
						Replicate 2	4.12	1.16	0.33	3.019	0.472	13.52
						Replicate 3	4.35	0.91	0.39	2.745	0.492	15.20
29	0	0	0	0	0	23	4.19	1.02	0.38	2.800	0.486	14.79
						Replicate 2	3.8	1.05	0.33	2.784	0.444	13.75
						Replicate 3	4.17	1.06	0.29	2.947	0.405	12.08
31	0	0	0	0	0	24	3.98	1.05	0.36	2.944	0.507	14.69
						Replicate 2	4.06	1.05	0.29	3.307	0.426	11.41
						Replicate 3	4.19	1.04	0.35	2.977	0.493	14.21

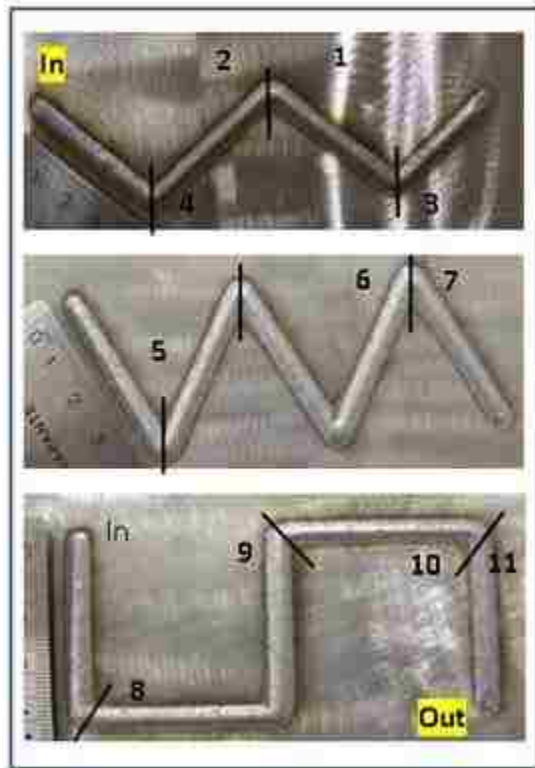
15	-1	1	1	1	-1	25	4.58	0.56	0.65	1.784	1.179	39.79
						Replicate 2	4.35	0.56	0.6	1.731	1.170	40.33
						Replicate 3	4.38	0.51	0.62	1.657	1.207	42.14
3	-1	1	-1	-1	-1	26	4.35	0.83	1.06	2.665	2.414	47.53
						Replicate 2	4.34	0.84	0.99	2.632	2.399	47.68
						Replicate 3	4.37	0.84	0.93	2.758	2.426	46.80
11	-1	1	-1	1	1	27	4.23	0.53	0.66	1.592	1.354	45.96
						Replicate 2	4.39	0.46	0.65	1.487	1.355	47.68
						Replicate 3	4.22	0.49	0.68	1.509	1.425	48.57
6	1	-1	1	-1	1	28	4.01	1.25	0.12	3.288	0.149	4.34
						Replicate 2	3.93	0.94	0.31	2.767	0.100	3.49
						Replicate 3	4.03	1.15	0.1	3.460	0.104	2.92
32	0	0	0	0	0	29	4.35	1.13	0.36	3.110	0.422	11.95
						Replicate 2	4.19	1.04	0.32	3.008	0.407	11.92
						Replicate 3	4.12	1.12	0.3	3.082	0.347	10.12
24	0	0	0	2	0	30	3.89	0.63	0.28	1.625	0.363	18.26
						Replicate 2	3.96	0.64	0.16	1.464	0.223	13.22
						Replicate 3	3.69	0.61	0.26	1.535	0.355	18.78
22	0	0	2	0	0	31	4.18	1.16	0.1	3.344	0.500	13.01
						Replicate 2	4.39	0.92	0.25	2.614	0.435	14.27
						Replicate 3	4.22	0.89	0.31	2.741	0.421	13.31

Appendix C: Experimental design matrix of 50 % overlap bead configuration (40 % and 60% are exactly the same as this one)

50 % overlap					
Runs	FR	PW	FL	LS	CTD
1	15	2	390	7.5	24
Replicate	15	2	390	7.5	24
2	30	2.5	400	10	23
Replicate	30	2.5	400	10	23
3	25	3	390	7.5	24
Replicate	25	3	390	7.5	24
4	20	2.5	400	10	21
Replicate	20	2.5	400	10	21
5	25	2	390	7.5	22
Replicate	25	2	390	7.5	22
6	25	3	390	12.5	22
Replicate	25	3	390	12.5	22
7	15	2	390	12.5	22
Replicate	15	2	390	12.5	22
8	15	3	410	7.5	24
Replicate	15	3	410	7.5	24
9	20	2.5	400	10	25
Replicate	20	2.5	400	10	25
11	20	2.5	400	5	23
Replicate	20	2.5	400	5	23
12	25	2	410	12.5	22
Replicate	25	2	410	12.5	22
13	20	2.5	400	10	23
Replicate	20	2.5	400	10	23
14	25	3	410	12.5	24
Replicate	25	3	410	12.5	24
15	20	4	400	10	23
Replicate	20	4	400	10	23
16	15	2	410	12.5	24
Replicate	15	2	410	12.5	24
17	20	2.5	400	10	23
Replicate	20	2.5	400	10	23
18	25	2	390	12.5	24
Replicate	25	2	390	12.5	24
19	25	3	410	7.5	22
Replicate	25	3	410	7.5	22

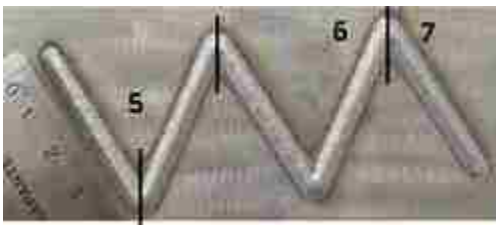
	20	10	2.5	400	10	23
Replicate		10	2.5	400	10	23
	21	15	2	410	7.5	22
Replicate		15	2	410	7.5	22
	22	20	2.5	400	10	23
Replicate		20	2.5	400	10	23
	23	20	2.5	400	10	23
Replicate		20	2.5	400	10	23
	24	20	2.5	400	10	23
Replicate		20	2.5	400	10	23
	25	15	3	410	12.5	22
Replicate		15	3	410	12.5	22
	26	15	3	390	7.5	22
Replicate		15	3	390	7.5	22
	27	15	3	390	12.5	24
Replicate		15	3	390	12.5	24
	28	25	2	410	7.5	24
Replicate		25	2	410	7.5	24
	29	20	2.5	400	10	23
Replicate		20	2.5	400	10	23
	30	20	2.5	400	15	23
Replicate		20	2.5	400	15	23
	31	20	2.5	420	10	23
Replicate		20	2.5	420	10	23
	32	20	1	400	10	23
Replicate		20	1	400	10	23

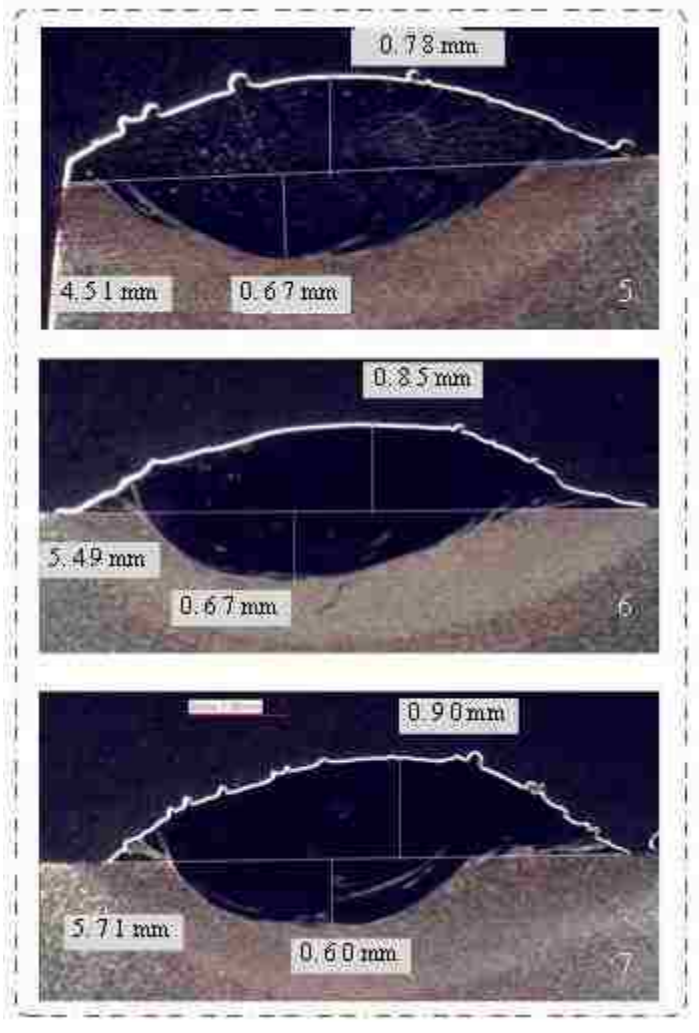
Appendix D: Different Cornering Configurations with numbers shown on them



Note: The numbers mentioned on the above figure are from 1 to 11, and the same numbers are used on all beads cross sections below

Acute Angled Configuration

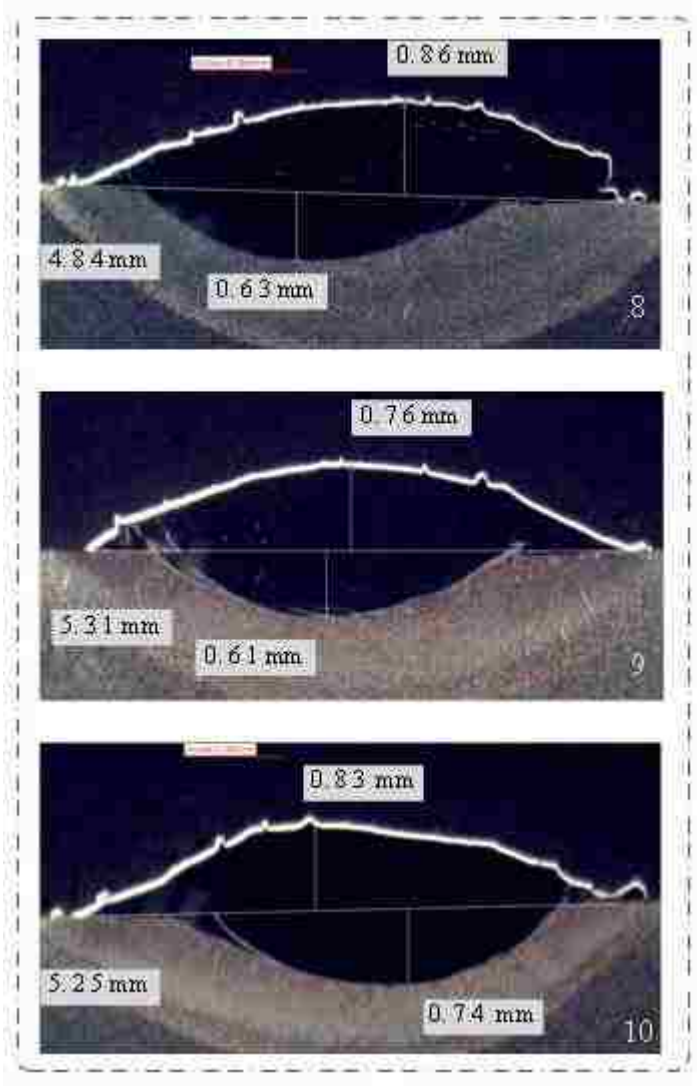




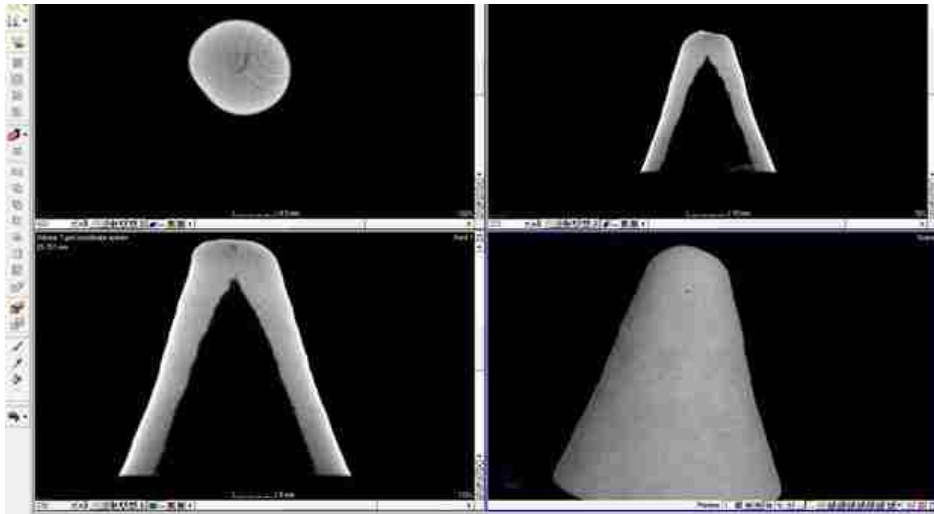
	Acute			Right			Obtuse		
	H	W	P	H	W	P	H	W	P
1st bend	0.78	4.51	0.67	0.86	4.84	0.63	0.79	4.19	0.66
2nd bend	0.85	5.49	0.67	0.76	5.31	0.61	0.81	4.11	0.61
3rd bend	0.9	5.17	0.6	0.83	5.25	0.74	0.78	4.24	0.66
Stdev	0.06	0.50	0.04	0.05	0.26	0.07	0.02	0.07	0.03

Note: H=bead height, W= Bead width, P= Bead penetration----- All values are in millimeter

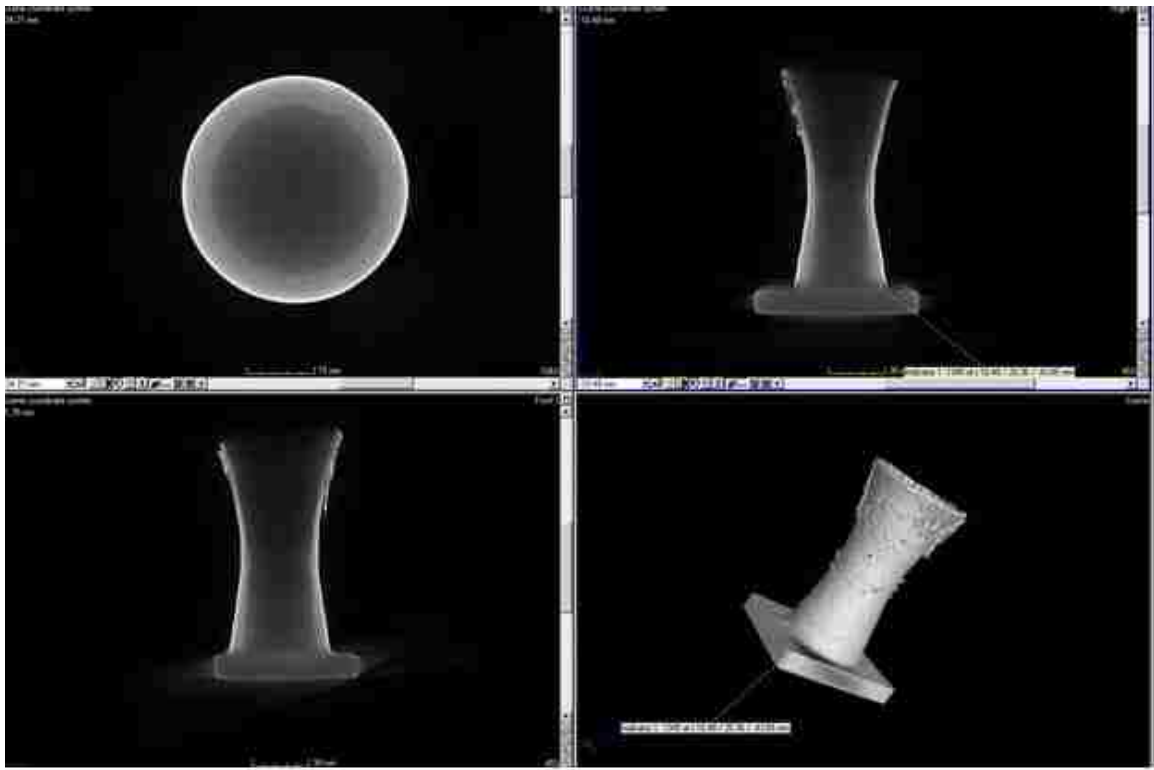
Right Angled Configuration



Appendix E: Screen shot of the hollow cone (CT Scanned view)



Appendix F: Screen shot of hollow parabolic cone (CT Scanned view)



Appendix G: Single Bead Experiments--- No Overlaps

Output Results (with 30 x 3 rep = 90 experiments)

W---Bead width results

Summary of Model

S = 0.267419 R-Sq = 71.38% R-Sq (adj) = 63.08%

Analysis of Variance

Source	DF	Seq SS	Adj SS	Adj MS	F	P
Regression	20	12.3057	12.3057	0.61528	8.6038	0.000000
FR	1	0.0975	0.0975	0.09753	1.3639	0.246886
PW	1	6.4685	5.5623	5.56234	77.7811	0.000000
FL	1	0.5735	0.8469	0.84690	11.8427	0.000987
LS	1	3.0299	3.0299	3.02990	42.3687	0.000000
TWD	1	0.0028	0.0028	0.00281	0.0393	0.843382
FR*FR	1	0.0112	0.0013	0.00134	0.0187	0.891715
PW*PW	1	0.0399	0.0062	0.00618	0.0865	0.769607
FL*FL	1	0.3301	0.3393	0.33934	4.7451	0.032801
LS*LS	1	0.3936	0.3599	0.35989	5.0325	0.028089
TWD*TWD	1	0.0237	0.0237	0.02371	0.3315	0.566624
FR*PW	1	0.0008	0.0008	0.00075	0.0105	0.918617
FR*FL	1	0.1764	0.1764	0.17642	2.4670	0.120838
FR*LS	1	0.1210	0.1210	0.12100	1.6920	0.197660
FR*TWD	1	0.1355	0.1355	0.13547	1.8943	0.173165
PW*FL	1	0.4701	0.4701	0.47005	6.5730	0.012536
PW*LS	1	0.0403	0.0403	0.04025	0.5629	0.455659
PW*TWD	1	0.1576	0.1576	0.15755	2.2031	0.142285
FL*LS	1	0.1838	0.1838	0.18377	2.5697	0.113494
FL*TWD	1	0.0059	0.0059	0.00585	0.0818	0.775686
LS*TWD	1	0.0438	0.0438	0.04380	0.6125	0.436523
Error	69	4.9344	4.9344	0.07151		
Lack-of-Fit	4	1.3252	1.3252	0.33130	5.9666	0.000375
Pure Error	65	3.6092	3.6092	0.05553		
Total	89	17.2400				

H ---Bead height results

Summary of Model

S = 0.0900632 R-Sq = 90.52% R-Sq(adj) = 87.77%

Analysis of Variance

Source	DF	Seq SS	Adj SS	Adj MS	F	P
Regression	20	5.34355	5.34355	0.26718	32.939	0.00000
FR	1	1.86889	1.86889	1.86889	230.403	0.00000

PW	1	0.00306	0.00000	0.00000	0.000	0.98568
FL	1	0.06379	0.06560	0.06560	8.087	0.00586
LS	1	1.81134	1.81134	1.81134	223.308	0.00000
TWD	1	0.23120	0.23120	0.23120	28.503	0.00000
FR*FR	1	0.17261	0.21384	0.21384	26.363	0.00000
PW*PW	1	0.24496	0.15859	0.15859	19.552	0.00004
FL*FL	1	0.11787	0.11073	0.11073	13.651	0.00044
LS*LS	1	0.00100	0.00176	0.00176	0.217	0.64310
TWD*TWD	1	0.27755	0.27755	0.27755	34.217	0.00000
FR*PW	1	0.05468	0.05468	0.05468	6.741	0.01151
FR*FL	1	0.02521	0.02521	0.02521	3.108	0.08235
FR*LS	1	0.00000	0.00000	0.00000	0.000	1.00000
FR*TWD	1	0.05741	0.05741	0.05741	7.078	0.00970
PW*FL	1	0.06163	0.06163	0.06163	7.598	0.00747
PW*LS	1	0.06308	0.06307	0.06307	7.776	0.00684
PW*TWD	1	0.04813	0.04813	0.04813	5.934	0.01744
FL*LS	1	0.05201	0.05201	0.05201	6.412	0.01362
FL*TWD	1	0.09013	0.09013	0.09013	11.112	0.00138
LS*TWD	1	0.09901	0.09901	0.09901	12.206	0.00084
Error	69	0.55969	0.55969	0.00811		
Lack-of-Fit	4	0.27066	0.27066	0.06766	15.217	0.00000
Pure Error	65	0.28903	0.28903	0.00445		
Total	89	5.90323				

P ---- Bead penetration results

Summary of Model

S = 0.0647132 R-Sq = 94.82% R-Sq(adj) = 93.32%

Analysis of Variance

Source	DF	Seq SS	Adj SS	Adj MS	F	P
Regression	20	5.29329	5.29329	0.26466	63.199	0.000000
FR	1	1.04401	1.04401	1.04401	249.298	0.000000
PW	1	2.90580	2.20185	2.20185	525.778	0.000000
FL	1	0.00548	0.00402	0.00402	0.961	0.330407
LS	1	0.90900	0.90900	0.90900	217.059	0.000000
TWD	1	0.01361	0.01361	0.01361	3.251	0.075768
FR*FR	1	0.00154	0.00787	0.00787	1.880	0.174820
PW*PW	1	0.06546	0.08393	0.08393	20.042	0.000029
FL*FL	1	0.04872	0.05217	0.05217	12.458	0.000746
LS*LS	1	0.06120	0.07117	0.07117	16.994	0.000103
TWD*TWD	1	0.02462	0.02462	0.02462	5.879	0.017942
FR*PW	1	0.00677	0.00677	0.00677	1.616	0.207877
FR*FL	1	0.02042	0.02042	0.02042	4.876	0.030562
FR*LS	1	0.04025	0.04025	0.04025	9.612	0.002799
FR*TWD	1	0.02475	0.02475	0.02475	5.911	0.017653
PW*FL	1	0.00227	0.00227	0.00227	0.542	0.464202
PW*LS	1	0.00775	0.00775	0.00775	1.851	0.178082
PW*TWD	1	0.05672	0.05672	0.05672	13.544	0.000458
FL*LS	1	0.00880	0.00880	0.00880	2.102	0.151652
FL*TWD	1	0.00585	0.00585	0.00585	1.397	0.241215
LS*TWD	1	0.04025	0.04025	0.04025	9.612	0.002799

Error	69	0.28896	0.28896	0.00419		
Lack-of-Fit	4	0.03693	0.03693	0.00923	2.381	0.060540
Pure Error	65	0.25203	0.25203	0.00388		
<u>Total</u>	<u>89</u>	<u>5.58225</u>				

% D ---Dilution results

Summary of Model

S = 2.21628 R-Sq = 98.05% R-Sq (adj) = 97.49%

Analysis of Variance

Source	DF	Seq SS	Adj SS	Adj MS	F	P
Regression	20	17049.5	17049.5	852.48	173.55	0.000000
FR	1	6743.3	6743.3	6743.25	1372.84	0.000000
PW	1	8122.5	6715.4	6715.37	1367.16	0.000000
FL	1	106.3	37.2	37.21	7.58	0.007550
LS	1	432.8	432.8	432.77	88.11	0.000000
TWD	1	49.7	49.7	49.71	10.12	0.002197
FR*FR	1	514.4	642.7	642.66	130.84	0.000000
PW*PW	1	201.6	161.7	161.67	32.91	0.000000
FL*FL	1	8.5	5.8	5.81	1.18	0.280439
LS*LS	1	68.4	112.0	111.99	22.80	0.000010
TWD*TWD	1	296.7	296.7	296.72	60.41	0.000000
FR*PW	1	65.2	65.2	65.18	13.27	0.000518
FR*FL	1	0.1	0.1	0.12	0.03	0.874696
FR*LS	1	66.5	66.5	66.46	13.53	0.000461
FR*TWD	1	22.4	22.4	22.38	4.56	0.036357
PW*FL	1	52.4	52.4	52.43	10.67	0.001695
PW*LS	1	70.5	70.5	70.53	14.36	0.000320
PW*TWD	1	0.0	0.0	0.01	0.00	0.972002
FL*LS	1	1.0	1.0	0.97	0.20	0.658105
FL*TWD	1	217.6	217.6	217.58	44.30	0.000000
LS*TWD	1	9.7	9.7	9.66	1.97	0.165264
Error	69	338.9	338.9	4.91		
Lack-of-Fit	4	106.0	106.0	26.51	7.40	0.000056
Pure Error	65	232.9	232.9	3.58		
<u>Total</u>	<u>89</u>	<u>17388.4</u>				

Any P-value less than 0.05 means that factor or interactions are significant

Appendix H: Response output---40 % overlap

Runs	L1	L2	L3	L4	L5	L6	L7	L8	L9	L10	L11
1	3.14	2.33	3.89	0.60	0.49	0.36	0.98	1.01	0.91	0.80	0.84
	3.10	2.27	3.85	0.62	0.41	0.33	0.95	1.05	0.95	0.83	0.80
2	3.33	2.93	2.83	0.35	0.29	0.30	1.24	1.36	1.39	1.21	1.10
	3.36	2.90	2.85	0.37	0.32	0.31	1.20	1.35	1.41	1.18	1.07
3	3.19	2.66	3.85	0.67	0.47	0.69	2.13	1.91	1.52	1.76	1.37
	3.17	2.60	3.81	0.59	0.44	0.63	2.18	1.99	1.55	1.74	1.36
4	3.64	2.48	3.16	0.37	0.31	0.38	1.20	1.30	1.30	1.07	1.12
	3.98	2.43	3.02	0.26	0.28	0.46	1.25	1.41	1.28	1.12	1.18
5	2.78	2.24	3.90	0.00	0.00	0.00	2.02	1.91	1.73	1.70	1.47
	2.63	2.92	3.26	0.00	0.00	0.00	2.05	1.92	1.67	1.71	1.52
6	2.88	2.64	3.30	0.68	0.57	0.43	1.12	1.26	1.08	0.97	0.99
	3.49	2.46	3.18	0.34	0.40	0.51	1.14	1.27	1.32	1.05	1.08
7	2.94	2.74	3.00	0.19	0.26	0.36	0.70	0.75	0.73	0.57	0.60
	3.23	2.92	2.85	0.13	0.32	0.37	0.60	0.68	0.68	0.52	0.52
8	3.54	2.60	3.73	1.34	1.15	1.07	1.33	1.21	0.99	1.09	0.95
	3.64	2.76	3.63	1.25	1.12	1.04	1.33	1.22	1.02	1.14	0.96
9	3.44	2.83	3.03	0.36	0.40	0.51	0.94	1.16	1.15	0.91	1.07
	3.45	2.76	3.27	0.21	0.36	0.59	1.09	1.24	1.16	1.05	1.08
10	Parameters are not feasible to generate any bead										
11	3.89	2.78	3.04	0.71	0.52	0.43	2.00	2.27	2.78	1.97	2.20
	3.81	2.72	3.06	0.75	0.50	0.42	1.97	2.26	2.81	2.00	2.21
12	3.62	2.70	2.66	0.00	0.00	0.00	1.13	1.21	1.17	0.97	0.80
	3.65	2.73	2.70	0.00	0.00	0.00	1.15	2.20	1.18	1.01	0.82
13	3.43	2.54	3.13	0.40	0.45	0.47	1.06	1.20	1.21	1.02	0.95
	3.44	2.81	2.96	0.27	0.29	0.40	1.10	1.21	1.27	1.04	1.06
14	3.13	2.00	2.91	0.33	0.26	0.47	0.87	1.46	1.56	0.89	1.45
	3.61	2.76	3.05	0.38	0.42	0.56	1.05	1.24	1.24	1.00	1.12
15	3.42	2.79	3.49	0.92	0.84	1.19	1.24	1.54	1.67	1.20	1.44
	3.50	2.40	3.84	1.27	0.92	0.97	1.52	1.46	1.12	1.33	1.08
16	3.30	2.75	3.05	0.28	0.32	0.33	0.53	0.65	0.65	0.48	0.55
	2.92	2.89	3.10	0.49	0.34	0.25	0.62	0.65	0.62	0.54	0.55
17	3.53	2.48	3.28	0.41	0.29	0.29	1.30	1.36	1.14	1.06	1.08
	3.64	2.81	2.82	0.45	0.49	0.50	1.00	1.11	1.19	0.84	0.91

18	3.01	2.77	2.87	0.02	0.08	0.07	0.97	0.96	1.00	0.86	0.70
	3.00	2.58	3.50	0.11	0.02	0.03	0.97	1.06	0.98	0.83	0.84
19	4.08	2.84	3.06	0.67	0.56	0.54	1.40	1.91	2.01	1.41	1.79
	4.20	2.61	3.01	0.52	0.53	0.48	1.51	1.89	2.17	1.51	1.80
20	3.32	2.58	3.29	0.93	0.77	0.55	0.77	0.77	0.67	0.61	0.53
	3.25	2.88	3.07	0.65	0.76	0.90	0.53	0.64	0.70	0.46	0.52
21	3.40	2.88	2.87	0.31	0.39	0.40	1.00	1.23	1.27	0.92	1.11
	3.49	2.77	3.08	0.15	0.35	0.43	1.19	1.27	1.20	1.06	1.12
22	3.29	2.85	3.05	0.34	0.40	0.45	1.17	1.33	1.28	1.08	1.06
	3.47	2.73	2.97	0.34	0.42	0.51	1.17	1.26	1.38	1.07	1.04
23	3.35	2.75	3.30	0.27	0.33	0.31	1.11	1.29	1.26	1.06	1.09
	3.36	2.93	3.08	0.21	0.37	0.35	1.17	1.31	1.37	1.08	1.14
24	3.67	2.79	2.63	0.24	0.38	0.46	1.06	1.23	1.26	0.98	1.08
	3.77	2.56	2.73	0.32	0.31	0.43	1.10	1.26	1.31	1.00	1.12
25	3.51	2.73	3.25	0.51	0.76	0.84	0.69	0.81	0.87	0.66	0.70
	3.59	2.84	3.02	0.57	0.73	0.80	0.78	0.88	0.89	0.74	0.81
26	3.45	3.10	3.07	0.31	0.37	0.42	1.09	1.29	1.33	1.03	1.14
	3.58	2.65	3.05	0.23	0.16	0.38	1.60	1.32	1.02	1.28	0.96
27	3.02	2.80	3.03	0.11	0.24	0.32	0.75	0.81	0.79	0.60	0.61
	3.06	2.81	2.97	0.12	0.20	0.34	0.77	0.85	0.82	0.71	0.66
28	3.98	2.95	2.01	0.04	0.04	0.04	1.82	1.78	1.49	1.55	1.39
	3.95	2.98	1.99	0.06	0.06	0.06	1.80	1.84	1.53	1.52	1.41
29	3.95	2.75	2.87	0.25	0.33	0.42	1.23	1.38	1.28	1.13	1.19
	3.45	2.58	3.50	0.31	0.26	0.35	1.24	1.32	1.08	1.18	1.05
30	3.40	2.78	2.95	0.16	0.28	0.31	0.82	0.80	0.85	0.73	0.57
	3.14	2.71	2.94	0.13	0.28	0.37	0.81	0.77	0.84	0.67	0.59
31	3.64	2.66	2.83	0.15	0.23	0.29	1.20	1.38	1.39	1.17	1.26
	3.66	2.62	2.89	0.22	0.29	0.38	1.17	1.34	1.36	1.14	1.21
32	Parameters are not feasible to generate any bead										

Appendix I: Response output---50 % overlap

Runs	L1	L2	L3	L4	L5	L6	L7	L8	L9	L10	L11
1	3.14	2.33	3.89	0.60	0.49	0.56	0.98	1.01	0.91	0.84	0.84
	3.03	2.45	2.75	0.32	0.37	0.46	0.96	1.21	1.27	0.89	1.14
2	3.57	2.23	2.70	0.00	0.00	0.00	1.57	1.97	2.25	1.48	1.88
	3.51	2.27	2.62	0.00	0.00	0.00	1.52	2.03	2.21	1.52	1.90
3	3.56	2.25	3.08	0.63	0.46	0.32	1.35	2.16	2.44	1.57	2.09
	3.50	2.21	3.15	0.55	0.38	0.25	1.40	2.19	2.31	1.63	2.00
4	2.86	1.92	3.35	0.12	0.10	0.33	1.48	1.57	1.16	1.48	1.12
	2.27	2.38	3.51	0.23	0.19	0.27	1.59	1.57	1.18	1.46	1.13
5	2.09	2.17	3.49	0.00	0.00	0.00	2.40	2.12	1.70	2.06	1.66
	2.20	2.55	3.60	0.00	0.00	0.00	2.32	2.13	1.65	2.04	1.59
6	3.28	1.95	3.40	0.42	0.33	0.26	1.51	1.41	1.11	1.30	1.11
	2.72	2.35	3.33	0.43	0.35	0.38	1.54	1.33	1.07	1.24	1.02
7	2.99	2.32	2.66	0.24	0.31	0.31	0.66	0.78	0.79	0.68	0.72
	2.73	2.37	2.81	0.27	0.31	0.14	0.82	0.77	0.63	0.71	0.65
8	3.48	1.92	3.66	1.17	1.05	1.06	1.59	1.36	0.92	1.35	0.90
	3.30	2.36	3.37	1.06	1.00	0.95	1.62	1.30	0.86	1.34	0.89
9	2.76	2.19	3.14	0.42	0.31	0.26	1.43	1.32	1.01	1.26	0.99
	2.87	2.33	3.35	0.40	0.32	0.22	1.35	1.36	1.17	1.29	1.14
10	Parameters are not feasible to generate the bead										
11	4.14	2.53	3.17	0.75	0.62	0.60	1.67	2.18	2.45	1.64	2.10
	3.82	2.24	3.07	0.70	0.39	0.40	1.73	2.49	2.97	1.71	2.46
12	4.18	1.96	2.01	0.00	0.00	0.00	1.15	1.36	1.39	1.10	1.17
	3.55	2.41	2.27	0.00	0.00	0.00	1.09	1.38	1.35	1.04	1.16
13	2.88	2.37	3.24	0.33	0.21	0.20	1.49	1.45	1.18	1.38	1.20
	2.58	2.34	3.29	0.34	0.34	0.28	1.48	1.31	1.02	1.33	1.02
14	3.19	2.44	2.73	0.27	0.36	0.40	0.91	1.24	1.41	0.92	1.25
	3.33	2.35	2.79	0.30	0.37	0.41	0.98	1.30	1.47	0.97	1.25
15	3.34	2.13	3.43	0.97	0.79	0.91	1.91	1.67	1.13	1.62	1.09
	3.40	2.11	3.29	0.95	0.82	0.74	1.80	1.60	1.10	1.56	1.12
16	2.98	2.21	2.84	0.24	0.26	0.30	0.53	0.71	0.76	0.55	0.68
	2.97	2.28	2.66	0.19	0.25	0.37	0.69	0.79	0.79	0.68	0.70
17	3.55	1.94	3.14	0.33	0.20	0.32	1.60	1.51	1.09	1.41	1.03
	3.23	2.27	2.59	0.37	0.30	0.35	1.39	1.27	1.04	1.19	0.98
18	3.03	2.36	2.34	0.00	0.00	0.00	1.04	1.17	1.15	1.04	1.00
	2.90	2.76	2.25	0.00	0.00	0.00	1.19	1.25	1.00	1.08	1.00

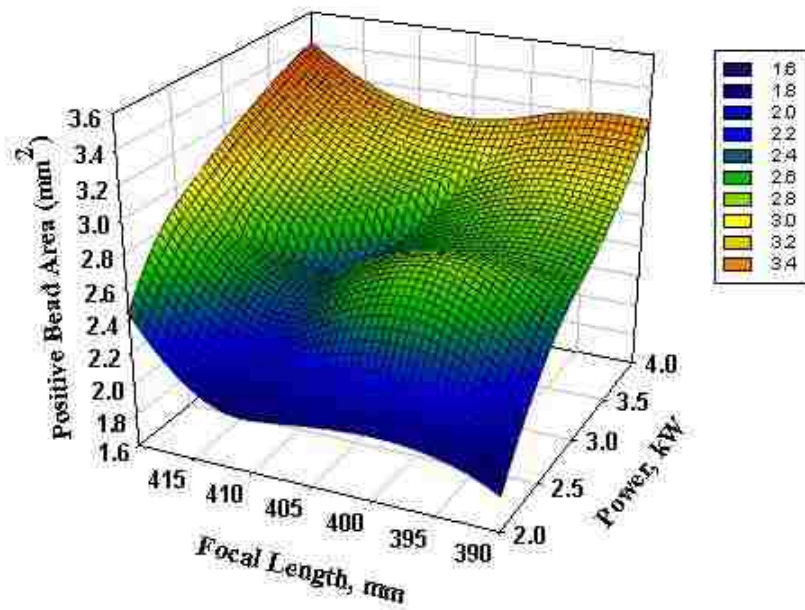
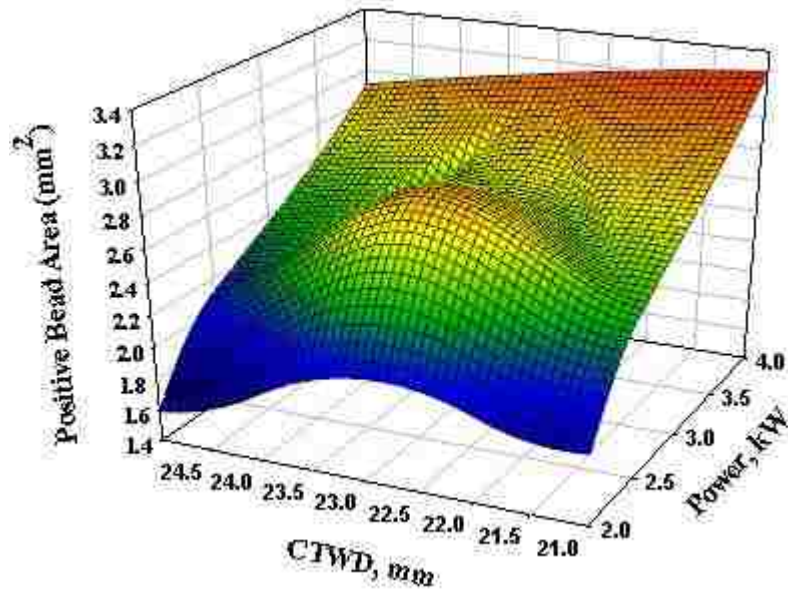
19	4.26	2.39	3.06	0.57	0.35	0.25	1.60	2.16	2.59	1.60	2.19
	4.20	2.35	2.98	0.59	0.36	0.22	1.69	2.19	2.63	1.54	2.23
20	3.00	2.38	3.11	0.77	0.69	0.58	0.90	0.86	0.62	0.75	0.58
	3.05	2.40	3.14	0.78	0.65	0.59	0.93	0.87	0.59	0.71	0.56
21	2.65	2.39	3.20	0.32	0.32	0.19	1.44	1.35	1.03	1.31	1.00
	2.67	2.19	3.31	0.30	0.27	0.27	1.45	1.33	0.96	1.27	0.96
22	2.92	2.46	2.62	0.39	0.31	0.35	0.88	1.27	1.53	1.02	1.26
	3.10	2.49	2.55	0.40	0.28	0.34	0.90	1.32	1.46	0.97	1.23
23	3.18	2.23	2.25	0.37	0.18	0.20	1.12	1.43	1.80	1.10	1.49
	3.16	2.10	2.41	0.25	0.21	0.13	1.08	1.60	1.87	1.05	1.57
24	3.10	2.31	2.87	0.29	0.21	0.16	1.02	1.44	1.55	1.07	1.38
	3.09	2.36	2.94	0.32	0.25	0.19	0.98	1.40	1.57	1.01	1.46
25	3.33	2.32	3.04	0.55	0.61	0.77	0.80	0.89	0.96	0.73	0.84
	3.34	2.35	3.00	0.61	0.70	0.82	0.84	0.85	1.02	0.70	0.86
26	3.51	2.46	2.51	0.22	0.30	0.30	1.17	1.48	1.53	1.12	1.38
	3.41	2.17	2.98	0.22	0.13	0.26	1.12	1.56	1.63	1.12	1.48
27	3.01	2.42	2.67	0.28	0.36	0.36	0.70	0.78	0.82	0.69	0.77
	2.99	2.51	2.74	0.25	0.37	0.38	0.68	0.73	0.81	0.70	0.79
28	3.44	2.29	2.77	0.02	0.02	0.02	1.51	1.95	2.15	1.51	1.90
	3.63	2.22	3.01	0.02	0.02	0.02	1.43	2.02	2.17	1.43	1.97
29	2.71	2.22	3.70	0.35	0.28	0.25	1.52	1.44	1.14	1.36	1.13
	2.69	2.20	3.56	0.30	0.25	0.25	1.56	1.40	1.10	1.40	1.10
30	3.05	2.37	2.85	0.22	0.26	0.17	0.93	0.89	0.73	0.84	0.70
	3.04	2.23	2.77	0.14	0.21	0.28	0.74	1.00	1.02	0.70	0.82
31	3.65	2.26	2.86	0.23	0.20	0.21	1.11	1.43	1.60	1.12	1.39
	3.54	2.07	2.86	0.19	0.17	0.24	1.28	1.53	1.59	1.26	1.46
32	Parameters are not feasible to generate the bead										

Appendix J: Response output---60 % overlap

Runs	L1	L2	L3	L4	L5	L6	L7	L8	L9	L10	L11
1	3.27	1.66	2.55	0.42	0.40	0.37	0.81	1.24	1.46	0.80	1.21
	3.20	1.58	2.59	0.50	0.44	0.41	0.85	1.21	1.32	0.89	1.19
2	3.22	2.12	2.20	0.02	0.02	0.04	1.60	2.02	2.31	1.57	1.96
	3.23	2.00	2.26	0.02	0.02	0.04	1.58	2.09	2.36	1.59	1.87
3	3.58	1.89	2.74	0.69	0.41	0.26	1.28	2.19	2.66	1.39	2.21
	3.56	1.90	2.68	0.74	0.48	0.22	1.35	2.25	2.64	1.41	2.26
4	3.25	1.93	2.26	0.24	0.15	0.17	1.14	1.67	1.87	1.18	1.67
	3.30	2.00	2.27	0.28	0.17	0.19	1.19	1.60	1.93	1.24	1.73
5	3.48	1.98	1.47	0.00	0.00	0.00	1.72	2.29	2.66	1.68	2.27
	3.30	1.91	2.00	0.00	0.00	0.00	1.55	2.19	2.57	1.53	2.15
6	3.00	1.80	2.68	0.35	0.21	0.38	1.00	1.46	1.78	1.01	1.54
	3.41	1.70	2.29	0.20	0.22	0.26	1.08	1.64	1.80	1.10	1.59
7	2.95	1.74	2.37	0.25	0.13	0.24	0.72	0.92	0.98	0.73	0.91
	2.74	1.72	2.64	0.24	0.21	0.24	0.75	0.87	0.93	0.75	0.90
8	2.97	1.91	3.21	1.00	0.87	1.02	0.88	1.45	1.78	0.88	1.44
	3.03	2.09	3.26	0.96	0.85	0.97	0.83	1.44	1.74	0.88	1.43
9	3.02	1.68	3.05	0.32	0.19	0.24	0.91	1.44	1.64	0.87	1.44
	3.51	1.51	2.44	0.25	0.18	0.22	1.00	1.45	1.64	0.99	1.44
10	Parameters are not feasible to generate any bead										
11	3.83	2.27	2.54	0.71	0.40	0.10	1.66	2.50	3.29	1.68	2.49
	3.78	2.35	2.52	0.73	0.42	0.15	1.70	2.58	3.36	1.71	2.51
12	4.04	2.07	1.51	0.00	0.00	0.00	1.07	1.47	1.66	1.04	1.41
	3.40	1.87	1.84	0.00	0.00	0.00	1.15	1.57	1.66	1.11	1.41
13	3.07	1.35	2.74	0.23	0.13	0.17	1.09	1.60	1.79	1.11	1.58
	2.92	1.86	2.26	0.37	0.25	0.25	0.91	1.48	1.73	0.94	1.46
14	3.21	2.46	2.88	0.25	0.37	0.44	1.08	1.16	1.20	0.93	0.95
	3.67	2.62	2.92	0.26	0.42	0.48	1.02	1.12	1.22	0.96	1.01
15	3.10	1.79	3.26	0.82	0.83	0.78	1.09	1.73	2.13	1.09	1.68
	3.18	1.65	3.32	0.89	0.73	0.74	1.14	1.76	2.02	1.13	1.74
16	2.53	1.86	2.69	0.12	0.15	0.23	0.60	0.84	0.92	0.61	0.82
	2.47	1.86	2.74	0.27	0.23	0.15	0.88	0.86	0.47	0.80	0.49
17	2.72	2.07	2.63	0.25	0.07	0.08	0.99	1.63	1.89	1.01	1.58
	3.16	1.83	2.28	0.30	0.19	0.18	1.04	1.49	1.64	1.03	1.46
18	2.92	2.06	2.23	0.00	0.00	0.00	0.93	1.31	1.42	0.93	1.28
	3.02	2.01	2.24	0.00	0.00	0.00	1.00	1.31	1.45	1.05	1.26
19	4.02	1.51	2.41	0.46	0.22	0.05	1.57	2.40	2.92	1.55	2.42

	3.94	1.47	2.54	0.33	0.18	0.04	1.52	2.35	3.80	1.59	2.41
20	2.98	1.91	2.76	0.65	0.50	0.54	1.13	0.99	0.58	0.97	0.58
	2.96	1.84	2.66	0.64	0.47	0.61	1.18	1.04	0.62	1.03	0.51
21	3.22	1.68	2.39	0.20	0.16	0.15	1.09	1.56	1.75	1.02	1.53
	3.15	1.73	2.55	0.24	0.24	0.21	1.05	1.44	1.63	1.03	1.48
22	2.70	1.74	2.67	0.32	0.07	0.17	1.19	1.61	1.89	1.17	1.60
	2.85	1.86	2.43	0.30	0.27	0.26	0.99	1.38	1.75	1.04	1.46
23	4.08	2.31	2.61	0.26	0.27	0.24	1.13	1.43	1.59	1.10	1.37
	4.13	2.36	2.57	0.24	0.29	0.31	1.16	1.52	1.64	1.05	1.46
24	3.30	1.65	2.21	0.28	0.20	0.16	1.08	1.61	1.86	1.12	1.57
	3.32	1.54	2.16	0.26	0.18	0.18	1.05	1.57	1.93	1.16	1.51
25	3.26	1.59	2.96	0.65	0.69	0.68	0.68	1.02	1.10	0.66	0.99
	3.28	1.67	3.00	0.69	0.74	0.65	0.76	1.06	1.15	0.73	0.98
26	3.46	1.91	2.48	0.12	0.16	0.06	1.10	1.60	1.92	1.08	1.60
	2.95	2.02	2.57	0.23	0.04	0.15	1.13	1.69	1.84	1.13	1.67
27	2.97	1.82	2.41	0.22	0.15	0.29	0.77	0.98	1.01	0.75	0.89
	2.99	1.86	2.37	0.25	0.17	0.33	0.75	0.97	0.99	0.76	0.92
28	2.98	1.92	2.49	0.04	0.04	0.04	2.51	2.19	1.38	2.18	1.34
	3.00	1.89	2.56	0.03	0.03	0.03	0.03	2.15	1.36	2.25	1.38
29	3.62	2.10	2.25	0.24	0.19	0.15	1.08	1.56	1.85	1.09	1.52
	3.46	1.87	2.74	0.23	0.08	0.06	1.08	1.67	1.85	1.05	1.63
30	2.82	1.90	2.46	0.11	0.04	0.06	0.75	1.01	1.05	0.69	0.96
	2.76	1.88	2.59	0.17	0.03	0.09	0.77	0.97	1.03	0.71	0.99
31	2.87	1.82	2.86	0.56	0.53	0.55	1.14	1.07	0.68	1.03	0.65
	2.95	1.75	2.71	0.64	0.62	0.54	1.25	1.07	0.74	0.95	0.64
32	Parameters are not feasible to generate any bead										

Appendix K: The 3D representation shows the effect on the positive bead area by varying the laser power, CTWD and the focal length while the other factors were remained constant



VITA AUCTORIS

NAME: Syed Mohammad Saqib

PLACE OF BIRTH: Karachi, Pakistan

YEAR OF BIRTH: February, 1967

EDUCATION: NED University of Engineering and Technology,
B.Sc., Mechanical Engineering, Karachi, Pakistan
1989

University of Ottawa, ON, Canada, 2005
Masters in Engineering Management Program

University of Windsor, ON, Canada 2016
PhD, Industrial and Manufacturing Systems
Engineering (IMSE)